



**UNIVERSITÀ DI PARMA**

# UNIVERSITA' DEGLI STUDI DI PARMA

DOTTORATO DI RICERCA IN  
"INGEGNERIA INDUSTRIALE"

CICLO XXXV

---

## **RFID in complex production and logistics processes in the automotive industry**

---

Coordinatore:

Chiar.mo Prof. Ing. Gianni ROYER CARFAGNI

Tutore:

Chiar.mo Prof. Ing. Giovanni ROMAGNOLI

Prof. Dr.-Ing. Dieter UCKELMANN

Dottorando: Henriette Adriana KNAPP

Anni Accademici 2019/2020 – 2021/2022

# Abstract

RFID (Radio Frequency Identification) is used in production and logistics in the automotive industry to automate and optimise processes, as RFID has some advantages over barcodes, e.g., no line of sight is needed and RFID transponders can be read in a bulk. When introducing a new RFID application into a company, a pilot is usually carried out first, to test the feasibility. If the pilot is successful, the application is then transferred to series operation in a production area. If the series operation of the RFID application works reliably, the RFID application is rolled out in other production areas, halls, and plants, so that they can also benefit from the advantages of RFID, such as time savings in newly automated processes.

However, the rollout and operation of RFID applications pose major challenges. During rollout, for example, the antennas of an RFID gate must be aligned in the best possible way because the positioning and orientation between RFID transponders and antennas influence the detection rate. Due to the many possible mounting heights and angles of the antennas of an RFID gate, their optimal alignment is a major challenge. Currently, the most common methods for doing so are exemplary guidelines based on expert knowledge and the trial-and-error principle, but so far no algorithm has been published that systematically determines the optimal antenna orientation to increase the detection rate, to the best of the author's knowledge. Therefore, in this work, a new algorithm for optimal antenna alignment was developed and tested with the objective of improving the detection rate compared to the approach based on expert knowledge and the trial-and-error principle.

During a rollout, the RFID installation is set up and put into operation in a new environment. The different environmental influences lead to different sources of interference, which have a negative effect on the detection rate. Due to the lack of application experience, it is a challenge to systematically identify and reduce these sources of interference, because there are no test procedures or guidelines for this activity. Therefore, in this work, a new test procedure was developed for the identification and reduction of sources of interference. The verification shows that the application of this test procedure eliminated all simulated sources of interference and thus significantly improved the performance, such as the detection rate.

During operation, the data generated by RFID installations are not used for further analyses and insights to optimise material flow, which could help to solve a common and often reiterated problem, the low-cost efficiency of RFID. Therefore, a model for a digital twin of the RFID-enabled material flow in real time was developed in this work, and then implemented in a practical case study to prove its feasibility. A simulative profitability analysis shows the potential cost savings through this digital twin. An additional user survey confirms that the digital twin of the RFID-enabled material flow in real time could be very helpful and needed to optimise the material flow.

**Keywords:** RFID, logistics, production, automotive industry, RFID gates, sources of interference, digital twin

# Acknowledgements

I would like to thank the people for their great support, who made the success of my Ph.D. thesis possible.

In particular, I would like to thank my supervisors Professor Giovanni Romagnoli from the University of Parma and Professor Dieter Uckelmann from the HFT Stuttgart for their support, guidance, and outstanding feedback throughout this research project.

This Ph.D. was done in cooperation with the IT department of Mercedes-Benz AG in Sindelfingen, Germany. Therefore, I would like to thank Mercedes-Benz AG for the funding of my Ph.D. position and the opportunity to research this highly interesting topic in practise.

# Table of Contents

<b>Abbreviations .....</b>	<b>vi</b>
<b>List of figures.....</b>	<b>viii</b>
<b>List of tables.....</b>	<b>xi</b>
<b>1 Introduction.....</b>	<b>1</b>
1.1 Motivation for the study .....	1
1.2 Research aim .....	3
1.3 Research methodology and methods.....	5
1.4 Structure of this thesis .....	6
<b>2 Background.....</b>	<b>9</b>
2.1 RFID technology .....	9
2.2 RFID applications in the automotive industry.....	22
2.3 Rollout of RFID applications .....	29
2.4 RFID gate parameters and guidelines.....	30
<b>3 RFID network planning algorithm for RFID gates.....</b>	<b>33</b>
3.1 Literature review on RFID network planning algorithms .....	33
3.2 Methodology and implementation of the RFID network planning algorithm for RFID gates .....	37
3.3 Verification of the RFID network planning algorithm for RFID gates .....	39
3.4 Discussion of the RFID network planning algorithm for RFID gates.....	41
<b>4 Algorithm for optimal alignment of the antennas of the RFID gate.....</b>	<b>42</b>
4.1 Methodology of the rule-based algorithm for optimal antenna alignment .....	42
4.2 Implementation of the rule-based algorithm for optimal antenna alignment .....	51
4.3 Verification of the rule-based algorithm for optimal antenna alignment .....	54
4.4 Discussion of the rule-based algorithm for optimal antenna alignment.....	56
4.5 Comparison of the three approaches to align antennas of the RFID gate .....	56
<b>5 Test procedure to identify and reduce sources of interference .....</b>	<b>58</b>
5.1 Literature review on RFID test procedures .....	58
5.2 Literature review on sources of interference and proposed solutions .....	62
5.3 Test procedure to identify and reduce sources of interference .....	64
5.4 Verification of the test procedure and tests .....	67
5.5 Discussion of the test procedure.....	76

<b>6</b>	<b>Digital twin of the RFID-enabled material flow in real time.....</b>	<b>77</b>
6.1	Definition and objectives of the digital twin of the RFID-enabled material flow in real time.....	77
6.2	Requirements of the digital twin of the RFID-enabled material flow in real time.....	78
6.3	Literature review on digital twin and big data architectures .....	82
6.4	Architecture of the digital twin of the RFID-enabled material flow in real time.....	86
6.5	Technologies for implementation of the architecture of the digital twin of the RFID-enabled material flow in real time .....	87
6.6	Implementation of the digital twin of the RFID-enabled material flow in real time by means of a case study.....	88
<b>7</b>	<b>Simulation of the RFID-enabled material flow and verification of the digital twin of the RFID-enabled material flow in real time.....</b>	<b>94</b>
7.1	Methodology and implementation of the simulation.....	94
7.2	Results of the digital twin of the RFID-enabled material flow in real time .....	104
7.3	Evaluation of the requirements of the digital twin of the RFID-enabled material flow in real time .....	110
7.4	Simulative profitability analysis and user survey.....	112
7.5	Discussion of the digital twin of the RFID-enabled material flow in real time.....	120
<b>8</b>	<b>Conclusions and outlook.....</b>	<b>122</b>
<b>9</b>	<b>References .....</b>	<b>124</b>
<b>10</b>	<b>Appendix .....</b>	<b>132</b>
10.1	User interface of the algorithm for the optimal alignment of the antennas of the RFID gate .....	132
10.2	Entity relationship diagram of the tables from the logistics back end system.....	138

## Abbreviations

<b>ABC</b>	Artificial Bee Colony
<b>ACK</b>	Acknowledge
<b>AFI</b>	Application Family Identifier
<b>ASCII</b>	American Standard Code for Information Interchange
<b>ASK</b>	Amplitude Shift Keying
<b>CAGR</b>	Compound Annual Growth Rate
<b>CA-RNP</b>	Curling Algorithm for RFID Network Planning
<b>CIN</b>	Company Identification Number
<b>CS</b>	Cuckoo Search
<b>CSMA</b>	Carrier-Sense Multiple Access
<b>CSV</b>	Comma-Separated Values
<b>DI</b>	Data Identifier
<b>DSB-ASK</b>	Double-Side Band Amplitude Shift Keying
<b>DTRMF</b>	Digital Twin of the RFID-enabled Material Flow
<b>EPC</b>	Electronic Product Code
<b>ESD</b>	Electrostatic Discharge
<b>FDMA</b>	Frequency-Division Multiple Access
<b>GA</b>	Genetic Algorithm
<b>FWA</b>	Guided Fireworks Algorithm
<b>GID</b>	General Identifier
<b>HF</b>	High Frequency
<b>HTTP</b>	Hypertext Transfer Protocol
<b>IAC</b>	Issuing Agency Code
<b>I-MOBCA</b>	Indicator-Based Multi-Objective Bacterial Colony Foraging Algorithm
<b>IoT</b>	Internet of Things
<b>JIT</b>	Just In Time
<b>JSON</b>	JavaScript Object Notation
<b>KPI</b>	Key Performance Indicator
<b>LF</b>	Low Frequency
<b>LNG</b>	Liquefied Natural Gas
<b>LoRa</b>	Long Range
<b>LoRaWAN</b>	Long Range Wide Area Network
<b>MBO</b>	Monarch Butterfly Optimisation
<b>MOFA</b>	Multi-Objective Firefly Algorithm
<b>MOPSO</b>	Multi-Objective Particle Swarm Optimisation
<b>NP</b>	Non-Polynomial
<b>NSGA</b>	Non-dominated Sorting Genetic Algorithm
<b>OARG Algorithm</b>	Optimal Alignment of RFID Gates Algorithm
<b>OT</b>	Object Type
<b>PIE</b>	Pulse-Interval Encoding
<b>PLC</b>	Programmable Logic Controller
<b>PR-ASK</b>	Phase-Reversal Amplitude Shift Keying
<b>PSK</b>	Phase Shift Keying
<b>PSO</b>	Particle Swarm Optimisation
<b>QA</b>	Q-Algorithm
<b>REST</b>	Representational State Transfer
<b>RF</b>	Radio Frequency
<b>RFID</b>	Radio Frequency Identification

<b>RGNP Algorithm</b>	RFID Gate Network Planning Algorithm
<b>RNP</b>	RFID Network Planning
<b>RPLN</b>	Ring Probabilistic Logic Neuron
<b>RSSI</b>	Received Signal Strength Indication
<b>SACS</b>	Self Adaptive Cuckoo Search
<b>SGTIN</b>	Serialised Global Trade Item Number
<b>SHF</b>	Super High Frequency
<b>SN</b>	Serial Number
<b>SPEA</b>	Strength Pareto Evolutionary Algorithm
<b>SQL</b>	Structured Query Language
<b>SSB-ASK</b>	Single-Sideband Amplitude Shift Keying
<b>SSCC</b>	Serial Shipping Container Code
<b>TDMA</b>	Time-Division Multiple Access
<b>TID</b>	Transponder ID
<b>UHF</b>	Ultra High Frequency
<b>UII</b>	Unique Item Identifier
<b>UML</b>	Unified Modelling Language

## List of figures

Figure 1	Identified research problems, objectives, questions, and hypotheses .....	4
Figure 2	Design science research cycles, according to Hevner and Chatterjee (2010); Hevner et al. (2004) .....	6
Figure 3	Outline and structure of this thesis.....	8
Figure 4	Structure of an RFID system, according to Finkenzeller (2015); Fleisch and Mattern (2005); Knapp and Uckelmann (2022); Tamm and Tribowski (2010); Wagner (2009).....	9
Figure 5	Different types of constructions and antenna designs.....	10
Figure 6	RFID gate with stationary reader and four external antennas.....	11
Figure 7	Mobile RFID reader with integrated antenna: RFID handheld (left) and RFID cuff (right) .....	11
Figure 8	Communication between RFID reader and transponder through backscattering, according to Finkenzeller (2015); Lechner (2020) .....	13
Figure 9	Radiation diagram of an isotropic emitter and of a dipole, according to Finkenzeller (2015).....	14
Figure 10	Aperture angle of a dipole antenna, according to Lechner (2020).....	14
Figure 11	Influence of position and orientation between reader and transponder, according to Lechner (2020).....	15
Figure 12	Linearly (left) and circularly (right) polarised electromagnetic waves, source: ©universaldenker.org.....	16
Figure 13	Effect of antenna polarisation and transponder orientation on readability, according to Kleist (2004); Wagner (2009).....	16
Figure 14	Measurement results of transmitted power of different transponder orientations .....	17
Figure 15	Overview of the channels of the lower band, according to ETSI (2020).....	18
Figure 16	Overview of the channels of the upper band, according to ETSI (2020).....	18
Figure 17	Factors influencing the detection rate, according to Hur et al. (2009); Kleist (2004); Knapp and Uckelmann (2022).....	22
Figure 18	Typical areas of use of RFID in the automotive industry .....	23
Figure 19	Automatic goods receipt process with RFID .....	25
Figure 20	Shelf with RFID reader and antennas for automatic material retrieval .....	27
Figure 21	RFID reader and antennas on the shelf.....	27
Figure 22	Automatic material retrieval process with RFID .....	28
Figure 23	Plausibility check process at the body shop construction station .....	29
Figure 24	Side view of the RFID gate.....	31
Figure 25	Top view of the RFID gate .....	31
Figure 26	RFID gate installed according to guideline 2 .....	32
Figure 27	Top view of the RFID gate according to guideline 2.....	32
Figure 28	Modelling of the antenna field, according to Knapp and Romagnoli (2021) .....	38
Figure 29	RFID gate at the goods receipt at the automatic small parts warehouse.....	40
Figure 30	Golden sample for verification of the RFID network planning algorithm.....	40



Figure 31	Application and methodology of the OARG algorithm.....	43
Figure 32	Part of a golden sample CSV file.....	43
Figure 33	Part of the CSV file with the readings of the RFID transponders.....	43
Figure 34	Procedure of the algorithm for optimal alignment of the antennas.....	44
Figure 35	Antenna heights and simulated antenna field of an RFID gate.....	46
Figure 36	Flowchart of the algorithm to determine new antenna heights and vertical angles .....	47
Figure 37	Flowchart of the algorithm to determine new horizontal angles .....	49
Figure 38	Exemplary gate passage forwards.....	50
Figure 39	Exemplary gate passage backwards.....	50
Figure 40	Flowchart of the algorithm to determine the new power .....	51
Figure 41	Architecture for the algorithm for optimal antenna alignment .....	51
Figure 42	Entity relationship diagram of the algorithm for optimal antenna configuration .....	52
Figure 43	Forklift with golden sample for verification.....	55
Figure 44	Passage through the RFID gate with the golden sample.....	55
Figure 45	Test procedure to identify sources of interference, according to Knapp and Uckelmann (2022) .....	65
Figure 46	Setup of the RFID installation for the verification of the absorption test .....	70
Figure 47	RFID transponders in an ESD load carrier with lid (left) and without lid (right).....	70
Figure 48	Setup of the RFID installation for the verification of the interference test.....	72
Figure 49	Frequency sweep measurement with simulated source of interference by LoRa .....	73
Figure 50	Frequency sweep measurement without simulated source of interference.....	73
Figure 51	Setup of the RFID installation for the verification of the reader-to-transponder signal collision test.....	74
Figure 52	Setup of the RFID installation for the verification of the environmental impact test.....	76
Figure 53	RFID transponder with simulated source of interference (water).....	76
Figure 54	DTRMF architecture, according to Knapp et al. (2022).....	87
Figure 55	Entity relationship diagram of the DTRMF – part 1.....	91
Figure 56	Entity relationship diagram of the DTRMF – part 2.....	92
Figure 57	Flowchart of the simulation of logistics back end system and load carrier management system.....	94
Figure 58	Dashboard of use case 1 – part 1 .....	105
Figure 59	Dashboard of use case 1 – part 2 .....	105
Figure 60	Dashboard of use case 2, according to Knapp et al. (2023).....	106
Figure 61	Dashboard of use case 3, according to Knapp et al. (2022).....	107
Figure 62	Dashboard of use case 4.....	107
Figure 63	Dashboard of use case 5 without exceeded lead time.....	108
Figure 64	Dashboard of use case 5 with exceeded lead time.....	108
Figure 65	Databricks completed runs.....	110
Figure 66	Questionnaire of the user survey.....	118

Figure 67	Results of question 1 of the user survey (n = 11) .....	119
Figure 68	Results of question 2 of the user survey (n = 11) .....	119
Figure 69	Results of question 3 of the user survey (n = 11) .....	120
Figure 70	User interface to create a golden sample .....	132
Figure 71	User interface to create a test – part 1 .....	133
Figure 72	User interface to create a test – part 2 .....	133
Figure 73	User interface to create a test – part 3 .....	134
Figure 74	User interface to upload data with RFID readings .....	134
Figure 75	User interface to show the test results – part 1 .....	135
Figure 76	User interface to show the test results – part 2 .....	135
Figure 77	User interface to show the test results – part 3 .....	136
Figure 78	User interface to show the test results – part 4 .....	136
Figure 79	User interface to show the test results – part 5 .....	137
Figure 80	User interface to show the test results – part 6 .....	137
Figure 81	Entity relationship diagram of the logistics back end system – part 1 .....	138
Figure 82	Entity relationship diagram of the logistics back end system – part 2 .....	139

## List of tables

Table 1	Research methods used in this thesis .....	6
Table 2	Frequency ranges and their characteristics, according to Bundesnetzagentur (n.d.); Lechner (2020); Tamm and Tribowski (2010); Wagner (2009) .....	12
Table 3	Sessions and their properties, according to ISO/IEC (2015); Kathrein Solutions GmbH (2017) .....	19
Table 4	Data structure for special load carriers with multi-use RFID transponders, according to VDA (2016) .....	21
Table 5	Data structure for universal load carriers with single-use RFID transponders, according to VDA (2022) .....	21
Table 6	RFID gate guideline 1 .....	31
Table 7	RFID gate guideline 2 .....	32
Table 8	Overview of RFID network planning algorithms .....	33
Table 9	Results of the RFID network planning algorithm for the case study, according to Knapp and Romagnoli (2021) .....	40
Table 10	Reader parameters for verification of the RFID network planning algorithm .....	40
Table 11	Results of the verification of the RGNP algorithm .....	41
Table 12	Notation definition .....	44
Table 13	Determination of the new antenna height depending on top worse, middle worse, and bottom worse .....	47
Table 14	Endpoints of the REST web service .....	53
Table 15	Reader parameters for verification of algorithm for antenna alignment .....	55
Table 16	Results of the verification of the algorithm for optimal antenna alignment – detection rates .....	55
Table 17	Results of the verification of the algorithm for optimal antenna alignment – antenna configurations .....	55
Table 18	Comparison of the three approaches to determine antenna configuration .....	57
Table 19	Overview and evaluation of RFID test procedures .....	58
Table 20	Overview of sources of interference, according to Knapp and Uckelmann (2022) .....	62
Table 21	Reader parameters for the verification of the absorption test .....	70
Table 22	Comparison of the average detection rates of the absorption test .....	71
Table 23	Reader parameters for the verification of the interference test .....	72
Table 24	Reading rate with and without LoRa signals .....	72
Table 25	Reader parameters for the verification of the reader-to-transponder signal collision test .....	75
Table 26	Reading rate with and without both reader and shielding .....	75
Table 27	Reader parameters for the verification of the environmental impact test .....	76
Table 28	Use case 1: analysis of process times and transports between a source and a sink .....	78
Table 29	Use case 2: analysis of the inventory of special load carriers with multi-use RFID transponders .....	79

Table 30	Use case 3: analysis of the best-before date for adhesive parts for a certain period of time .....	79
Table 31	Use case 4: analysis to determine the delayed material, the actual stock, and the expected deliveries.....	80
Table 32	Use case 5: analysis to identify open transfer orders and exceeding of the lead time .....	81
Table 33	Evaluation of the architectures from the literature review.....	83
Table 34	Required tables for the case study from logistics back end system .....	88
Table 35	Exemplary representation of the configuration file .....	95
Table 36	Exemplary representation of the stocks per storage location, material number, batch, and load carrier .....	103
Table 37	Exemplary representation of the prepared stocks per storage location, material number, batch, and load carrier.....	103
Table 38	Exemplary representation of the stocks per storage location, and material number.....	103
Table 39	Exemplary representation of the stocks per storage location, material number, and batches .....	103
Table 40	Execution times of pre-processing.....	109
Table 41	Execution times of dashboard update .....	110
Table 42	Costs for the DTRMF, load carriers and production downtime .....	114
Table 43	Costs and savings of different scenarios .....	116

# 1 Introduction

## 1.1 Motivation for the study

RFID (Radio Frequency Identification) is an important technology for the Internet of Things (IoT), because objects can be identified automatically by means of RFID (Uckelmann et al., 2011). RFID belongs to the “*most widely used auto-ID technologies*” (Chen & Chen, 2016). The advantages of RFID compared to the automatic identification procedure (auto-ID) barcodes are the contactless reading of the data without line of sight, reading transponders in a bulk, and rewritable storage (Finkenzeller, 2015; Fleisch & Mattern, 2005). Because of these advantages, RFID is used in different sectors such as production and logistics, fashion and apparel retail, food industry, or healthcare (Esposito et al., 2015; Franke & Dangelmaier, 2006; Kirch et al., 2017; Richter, 2013; Zhu et al., 2012). The use of RFID technology offers the potential for many improvements, such as reducing costs, automating and simplifying processes, increasing accuracy, reducing errors, and improving information quality (Fleisch & Mattern, 2005; Uckelmann, 2012; Zhu et al., 2012). The importance of RFID technology and future growth is shown by Allied Market Research's report, where the global market size of RFID is estimated to reach \$25.47 billion in 2030 and a compound annual growth rate of 9.6 % from 2021 to 2030 is forecasted (Sachan et al., 2021). The significance of RFID in the future is also shown by the study from the EHI Retail Institute, where 97 retail companies in Germany, Austria, and Switzerland were interviewed. This study revealed that 19 % are using RFID, 15 % have concrete plans, and 41 % are interested in the technology in the future (EHI Retail Institute, 2021). These studies and forecasts should be interpreted with caution, as an analysis of previous forecasts of RFID market development shows that “*expectations about market growth had to be revised downwards*” (Uckelmann, 2012).

In the automotive industry, RFID is used in various places for process optimisation (Richter, 2013). An application in the container / load carrier identification area is automatic goods receipt posting using RFID gates. If a new RFID application is introduced in a company, then a process analysis, as well as a profitability analysis and a feasibility test are typically carried out first. If the feasibility test is successful, the RFID application is first tested in a pilot operation in an area in the real environment. If this pilot is successful, the RFID application is transferred to series operation. In order to use the RFID application comprehensively in other areas, it is then rolled out to other areas, halls, and plants. (Bartneck et al., 2008)

Although the beginnings of RFID technology date back to the 1940s, the rollout of RFID applications poses a major challenge (Schmidt et al., 2011; Tamm & Tribowski, 2010; van Hoek, 2019). Between the years 2003 and 2006, there was a hype about RFID technology (Günthner et al., 2010). However, expectations regarding the use and diffusion of RFID in the logistics of the manufacturing industry (especially the automotive industry) were not met (Schmidt et al., 2011). Dwight Klappich from Gartner said in an interview in June 2018:

*“There is hype around how blockchain is going to solve world hunger, create world peace. No technology can live up to all that hype. It relates to what we saw around RFID in 2004-2005. It was a technology with clear potential and opportunity but the hype became so overzealous. I remember being at an event where it was claimed that soon we would have refrigerators with RFID readers that would auto-replenish. I don't think we have that yet today, we did not replace the barcode, we still have work to do on RFID and there is still more potential for its roll out.”*  
(van Hoek, 2019)

This statement shows that despite the initial hype surrounding RFID technology, there is still a need to optimise the rollout of RFID installations. Optimising the rollout of RFID applications is important

because “*the complexity of large-scale RFID rollout projects is a barrier for widespread adoption and diffusion of RFID*” (Schmidt et al., 2011). However, only a few companies publish anything about their failed RFID projects (Uckelmann, 2012). Insufficient reading reliability is considered by the study from Günthner et al. (2010) to be the second most relevant reason for deciding against the introduction of RFID after insufficient cost-effectiveness (Lechner, 2020). Low read rate is also mentioned in Ebrahimi-Asl et al. (2017) as a main challenge for passive RFID technology.

The focus of this thesis is on the rollout and operation of RFID applications at an automotive manufacturer. There, the rollout is carried out in the four phases: (i) planning, (ii) implementation, (iii) commissioning, and (iv) operation (see Section 2.3). These phases entail various problems as described in the following.

The number of RFID readers and antennas required must be planned in the first phase of the rollout. The number of antennas of an RFID installation and their positioning define the size of the reading field in which a transponder can be identified. In addition to the reading field, the orientation between the RFID transponder and the RFID reader antenna also influences the readability of the RFID transponder (see Section 2.1) and thus the detection rate. In the second phase of the rollout, the hardware must be installed and realigned if needed during the commissioning (third phase). Widely used are applications that use RFID gates, such as automatic goods receipt posting. With RFID gates, the antennas are mounted on two sides and can vary in number, height, and vertical and horizontal mounting angles. Due to these many possible parameters, optimal alignment of the antennas of an RFID gate is a major challenge. Currently, there is only an exemplary guideline based on expert knowledge and the trial-and-error principle, but no algorithm that systematically determines the optimal alignment of the antennas of RFID gates to increase the detection rate. (Knapp & Romagnoli, 2021; Salayong et al., 2019)

Another problem are the sources of interference that occur during a rollout, as the RFID installation is set up and put into operation in a new environment. Each RFID installation is exposed to different environmental influences during a rollout, which can have a negative impact on the detection rate. For example, a metallic environment or interference from other electrical devices will disrupt communication between the reader and transponder of an RFID installation (Brunner et al., 2015; Ciftler et al., 2015; Costa et al., 2017; VDI/AIM, 2008; Windmann et al., 2017). However, also during the operation of an RFID installation, the environment can change. This change can cause a new source of interference, for example, when another radio system is implemented nearby. The term sources of interference is defined in this thesis as follows:

*“[Sources of interference are] influences, which negatively affect the electromagnetic field of the reader or the backscatter signal of the tag and thus the communication between the RFID reader and tag, resulting in a lower read rate, read frequency per second or reading range. In addition, environmental influences that can affect the tag and thus have a negative impact on communication are referred to as sources of interference.”* (Knapp & Uckelmann, 2022)

Sources of interference belong to the main challenges of RFID installations and can lead to insufficient process quality, which could result in manual rework and additional costs (Ebrahimi-Asl et al., 2017; Knapp & Uckelmann, 2022; Luh & Liu, 2011). For this reason, it is important to identify and eliminate existing sources of interference during commissioning and operation. However, due to the well-known problem of lack of experience and technical skills, this is a major challenge, as there is no existing test procedure for systematic identification and reduction of sources of interference (Abugabah et al., 2020; Costa et al., 2017; Knapp & Romagnoli, 2021).

During operation, the RFID installations continuously generate new data. However, these data are only used for the automation of individual processes and not for analyses to optimise the material flow. The

use of the data could be a way to solve the known problem of low-cost efficiency of the RFID technology (Abugabah et al., 2020; Costa et al., 2017; Moretti et al., 2019); because big data analyses offer enormous potential and can be used, for example, to reduce inventory costs (Amerland, 2015; Klein et al., 2013). Currently, there is no infrastructure and application to program and execute RFID-based material flow data analyses, but companies should adjust their IT-infrastructure for big data solutions to remain competitive (Uckelmann et al., 2018). For linking the data from the RFID installation with other data and using them for further analyses, the digital twin concept is suitable, because it can simplify the provision of different data (Lietaert et al., 2021). In general, a digital twin is defined as the image of a real object or process and offers many advantages such as higher robustness, more predictable production processes, and the opportunity to proactively manage supply chain risks (Greis et al., 2021; Jamwal et al., 2021; Lietaert et al., 2021; Tao et al., 2019).

### 1.2 Research aim

These problems lead to the research aim, which is to make the rollout of RFID applications more efficient by increasing the detection rate of RFID installations and to benefit more from the data generated by the RFID installations through the optimisation of the material flow. To realise this aim, the following three objectives must be achieved:

- **O1:** The first objective is to develop one or more new approaches to determine the number of antennas, the heights, and mounting angles of the antennas of an RFID gate and compare these approaches with the exemplary guideline to find out which approach is the best to increase the detection rate.
- **O2:** The second objective is to develop a test procedure to identify and reduce sources of interference. This includes the research of existing test procedures, sources of interference, and proposed solutions.
- **O3:** The third objective is to develop a digital twin, and big data analyses to manage, and use the data generated by single RFID installations.

The research question that arises from the research aim is: “How can the rollout of RFID applications be optimised through the development and use of new algorithms and test procedures, and how can the data generated by RFID installations be used to optimise material flow?”. In this thesis, the research question is divided into three subquestions, which are related to the three research problems and objectives, as shown in Figure 1.

- **RQ1:** What is the best approach to plan the number of antennas for an RFID installation and to optimally position and align the antennas of an RFID gate to improve the detection rate?
- **RQ2:** How can sources of interference in RFID installations be identified and reduced to improve performance?
- **RQ3:** How can the data generated by RFID installations be used in a digital twin for additional analyses and optimisation of the material flow?

The underlying research hypotheses are as follows:

- **H1:** There is a better approach to align the antennas than using expert knowledge or the trial-and-error principle by using scientific theories as a basis for alignment of the antennas.
- **H2:** With a test procedure, it is possible to systematically identify and eliminate the sources of interference for RFID installations.
- **H3:** By means of a digital twin, the data of the RFID-based material flow can be used for further analyses and findings to optimise the material flow.

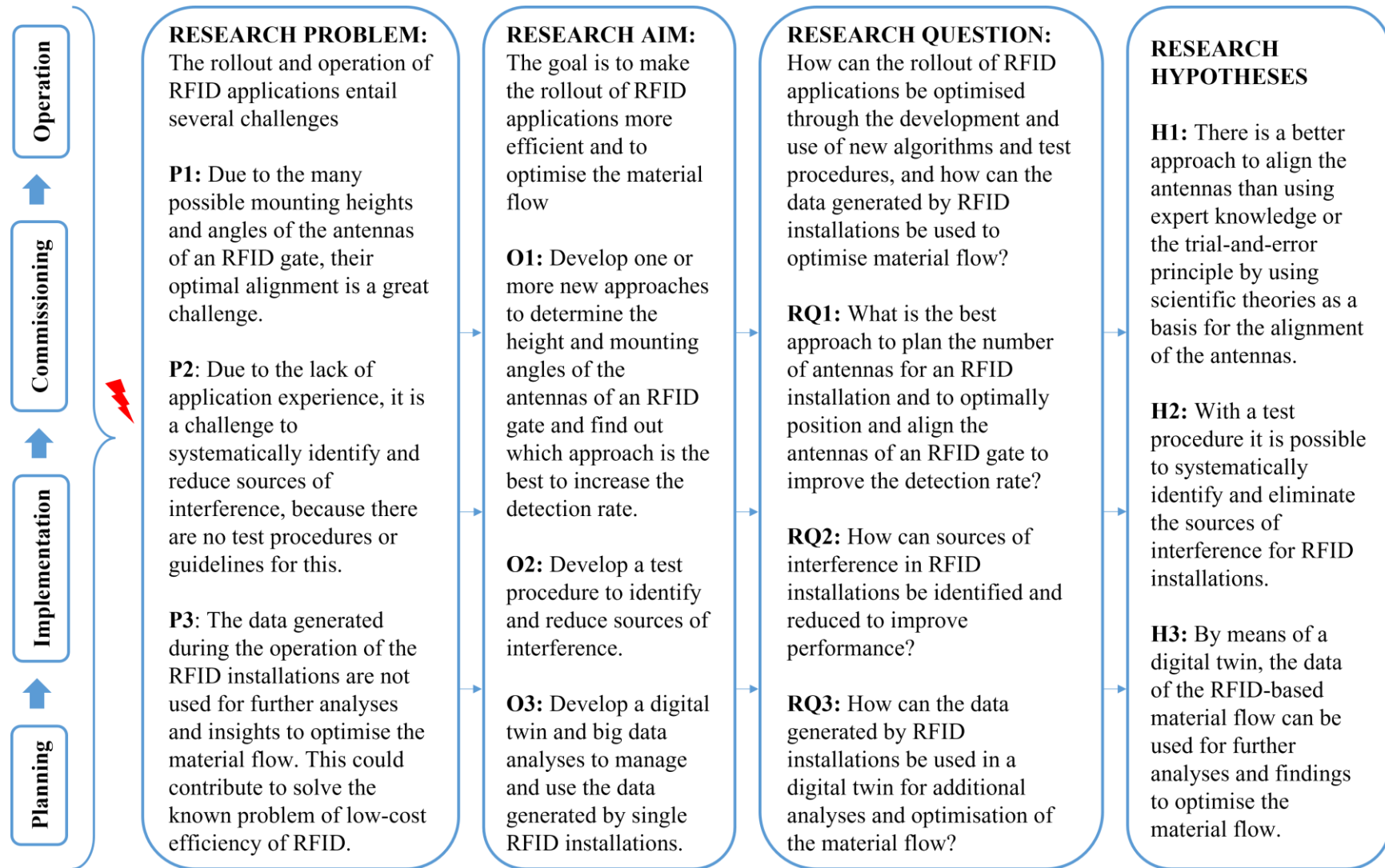


Figure 1 Identified research problems, objectives, questions, and hypotheses



### 1.3 Research methodology and methods

In this thesis, the design science research methodology according to Hevner (Hevner & Chatterjee, 2010; Hevner et al., 2004) is used to answer the three research questions to ensure that the results of this thesis meet scientific standards.

Therefore, the following seven guidelines are followed:

- 1) **Design as an artifact:** “Design-science research must produce a viable artifact in the form of a construct, a model, a method, or an instantiation.” (Hevner et al., 2004)
- 2) **Problem relevance:** “The objective of design-science research is to develop technology-based solutions to important and relevant business problems.” (Hevner et al., 2004)
- 3) **Design evaluation:** “The utility, quality, and efficacy of a design artifact must be rigorously demonstrated via well-executed evaluation methods.” (Hevner et al., 2004)
- 4) **Research contributions:** “Effective design-science research must provide clear and verifiable contributions in the areas of the design artifact, design foundations, and/or design methodologies.” (Hevner et al., 2004)
- 5) **Research rigour:** “Design-science research relies upon the application of rigorous methods in both the construction and evaluation of the design artifact.” (Hevner et al., 2004)
- 6) **Design as a search process:** “The search for an effective artifact requires utilizing available means to reach desired ends while satisfying laws in the problem environment.” (Hevner et al., 2004)
- 7) **Communication of research:** “Design-science research must be presented effectively both to technology-oriented as well as management-oriented audiences.” (Hevner et al., 2004)

The design science research methodology contains the three research cycles: (i) relevance cycle, (ii) design cycle, and (iii) rigour cycle (see Figure 2) as described below according to Hevner and Chatterjee (2010).

The purpose of the **relevance cycle** is to define the application domain, which consists of people, organisational systems, and technical systems, as well as the problems and opportunities for a particular environment that should be improved. In the relevance cycle, the requirements for the research are defined, but also the acceptance criteria for the evaluation of the research results. In the end, the developed artifact should be tested in the field. An additional iteration of the relevance cycle is necessary if, for example, the newly developed artifact has deficiencies or the requirements set at the beginning were incorrect or incomplete.

In the **rigour cycle**, the knowledge base for design science research is created, which consists of foundations (scientific theories and engineering methods), experience, and expertise as well as meta-artifacts (design products and design processes). This knowledge base is required to ensure research innovation and “*to guarantee that the designs produced are research contributions and not routine designs*” (Hevner & Chatterjee, 2010). The findings and results of the research, in turn, also contribute to the knowledge base.

The **design cycle** is dependent on the other two cycles and it “*is the heart of any design science research project*” (Hevner & Chatterjee, 2010). The inputs are the requirements and acceptance criteria from the relevance cycle and “*the design and evaluation theories and methods are drawn from the rigor cycle*” (Hevner & Chatterjee, 2010). In the design cycle, multiple iterations are performed, where the artifacts are developed and tested, for example, in case studies, experiments, and simulations before they are tested in the field.

In addition to the methodology described here, the research methods listed in Table 1 are used in this thesis.

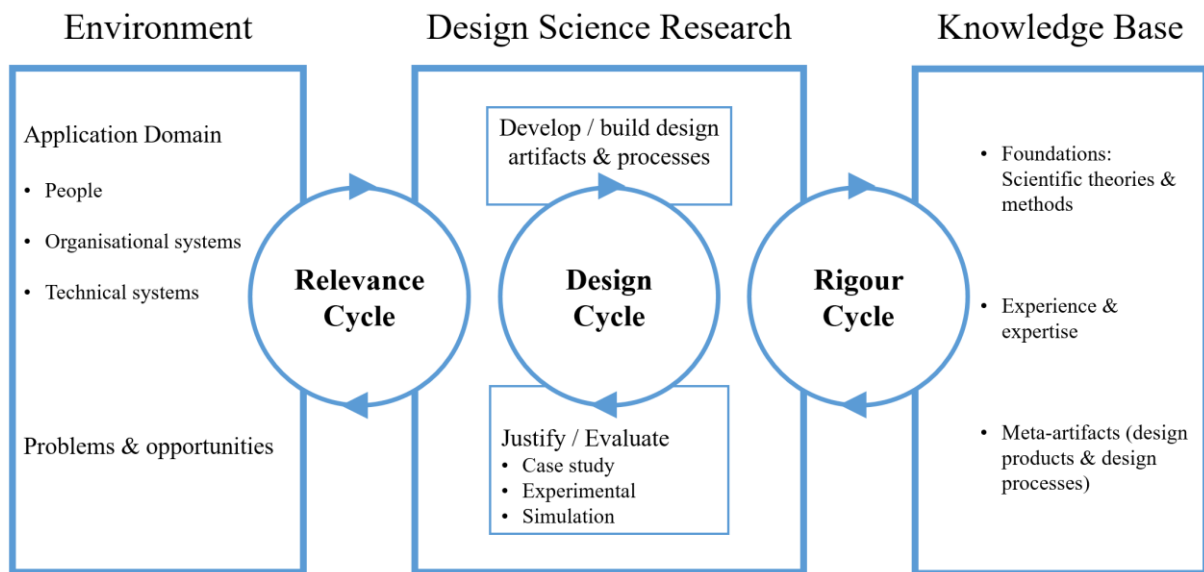


Figure 2 Design science research cycles, according to Hevner and Chatterjee (2010); Hevner et al. (2004)

Table 1 Research methods used in this thesis

Method used	Section
Literature reviews	
RFID network planning algorithms	3.1
RFID test procedures	5.1
Sources of interference and proposed solutions	5.2
Digital twin and big data architectures	6.3
Case studies with prototype solutions	
RFID network planning algorithm for RFID gates	3.2 & 3.3
Algorithm for optimal antenna alignment of RFID gates	4.2 & 4.3
Digital twin of the RFID-enabled material flow	6.6
Verification by simulating sources of interference	5.4
Simulative profitability analysis	7.4.1
User survey	7.4.2

#### 1.4 Structure of this thesis

Figure 3 shows the outline and structure of this thesis. Chapter 1, the introduction, describes the motivation and research goals, which are derived from the background chapter but also the methodology of this thesis, and thereby describes the environment (relevance cycle).

Chapter 2 summarises the background to this thesis, which consists of the fundamentals of RFID technology, RFID applications in the automotive industry, and the rollout of RFID applications and thus forms the general knowledge base (rigour cycle).

In the core part of this thesis, the design science research methodology according to Hevner (Hevner & Chatterjee, 2010; Hevner et al., 2004) is applied to answer the three research questions. In Chapter 3, a

new RFID network planning algorithm is presented. First, a literature review on RFID network planning algorithms is conducted to research the current state and expand the knowledge base (rigour cycle). Then a new RFID network planning algorithm is developed, implemented, and verified (design cycle). Furthermore, the results were critically reviewed in the discussion.

In a further iteration of the design cycle, a new algorithm is proposed, implemented, and verified for optimal alignment of the antennas of the RFID gate as described in Chapter 4. In the discussion, the results of the algorithm are evaluated. At the end of this chapter, all three approaches for aligning antennas of an RFID gate are compared to answer RQ1.

Chapter 5 has the aim of answering RQ2 and contains two literature reviews, one on RFID test procedures and one on sources of interference and proposed solutions for RFID installations which contribute to the knowledge base (rigour cycle). Then a new test procedure to identify and reduce sources of interference is presented and this is verified by simulation of different sources of interference (design cycle). At the end of this chapter follows the discussion.

At the beginning of Chapter 6, the term digital twin is defined for this thesis, and the requirements of the digital twin of the RFID-enabled material flow are determined based on expert discussions with future users (relevance cycle). Then, the state of the art of digital twin and big data architectures is researched to extend the knowledge base (rigour cycle). Subsequently, a new architecture for the digital twin of the RFID-enabled material flow in real time and suitable technologies for implementation are proposed. This architecture is implemented by means of a case study (design cycle).

Chapter 7 serves to verify the architecture of the digital twin of the RFID-enabled material flow in real time. Therefore, a simulation of the material flow in real time is developed and implemented. Then the results of the digital twin are presented by using this simulation. At the end of this chapter, an evaluation of functional and qualitative requirements is done, and a simulative profitability analysis and user survey are conducted (design & relevance cycle).

Chapter 8 summarises the results of this thesis and provides an outlook for future research.

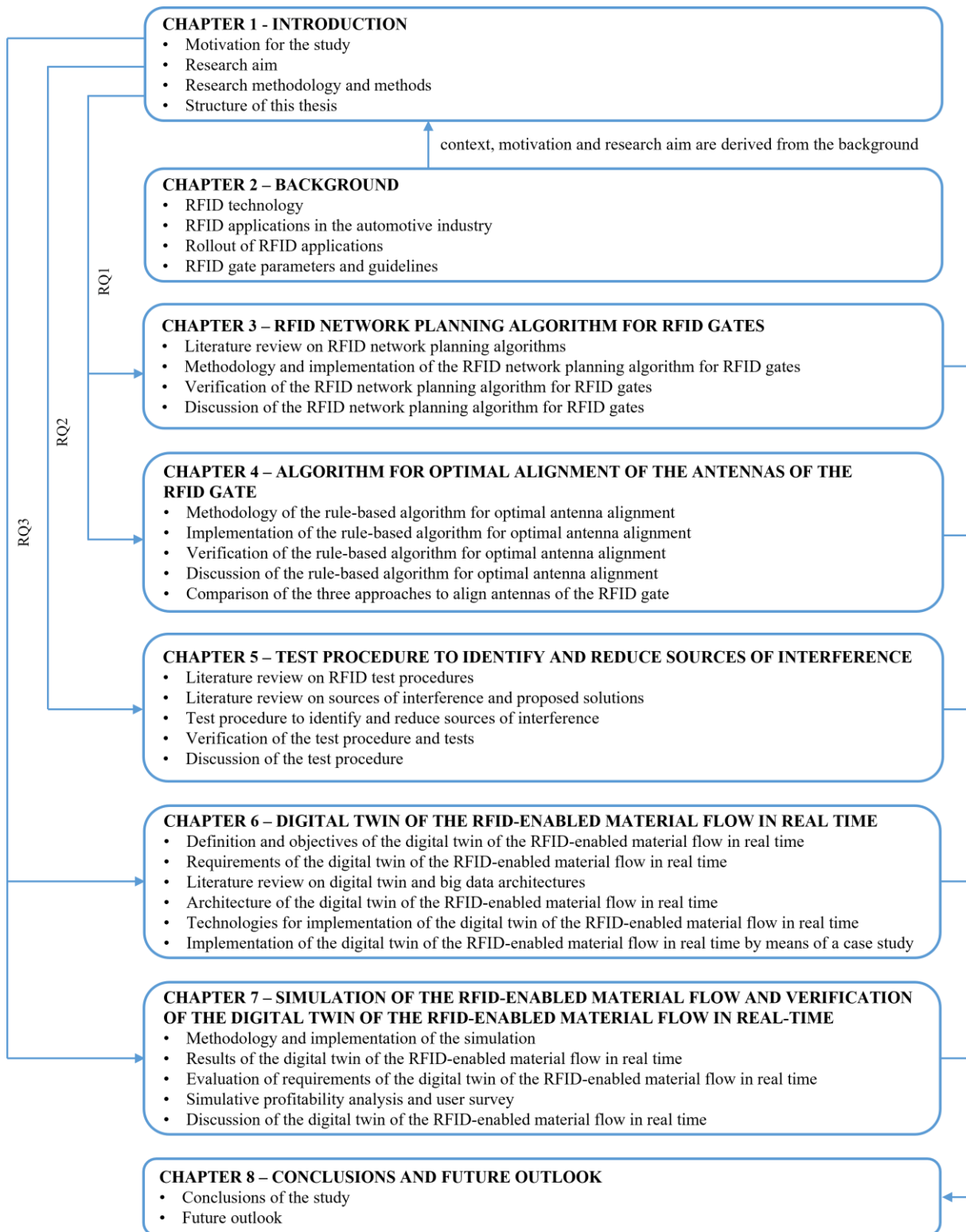


Figure 3 Outline and structure of this thesis

## 2 Background

The background chapter forms the knowledge base and thus the basis for the developments in the core part of this thesis.

### 2.1 RFID technology

Since this thesis is about RFID, the basics of this technology are explained first.

#### 2.1.1 Components of an RFID system

An RFID system typically consists of a write / read device, a transponder, and an application, as shown in Figure 4. The write / read device (also known as an interrogator) contains a coupling unit (coil or antenna) and is referred to as reader in this thesis. The transponder is attached to the object to be identified. The data on the transponders are read and written by the RFID readers over the air interface. In passive RFID systems, the reader supplies the transponder with energy. The application controls the reader and processes the received data. (Finkenzeller, 2015; Fleisch & Mattern, 2005; Tamm & Tribowski, 2010)

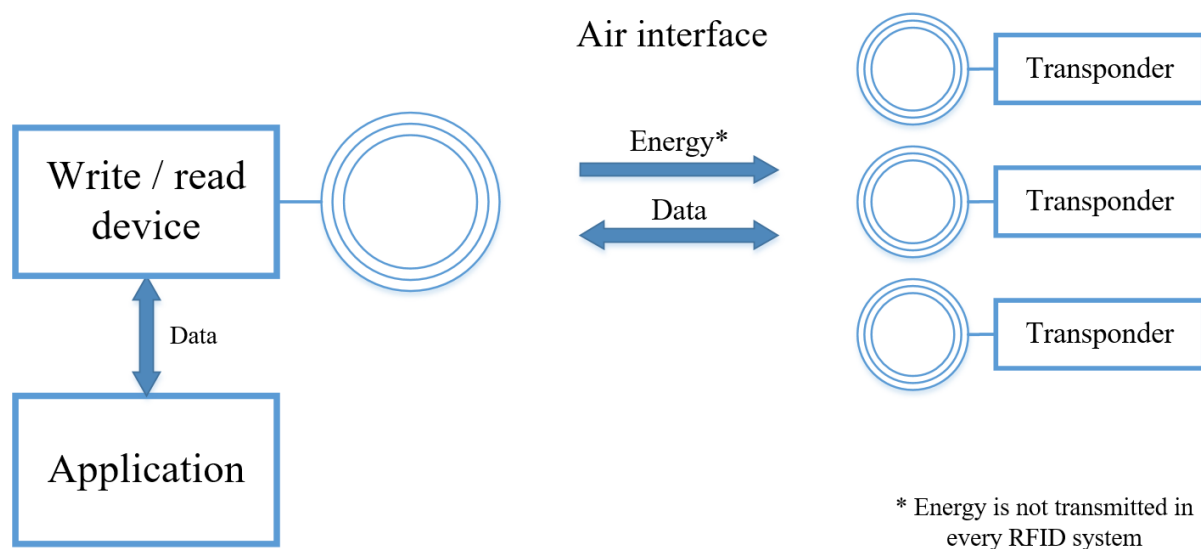


Figure 4 Structure of an RFID system, according to Finkenzeller (2015); Fleisch and Mattern (2005); Knapp and Uckelmann (2022); Tamm and Tribowski (2010); Wagner (2009)

##### 2.1.1.1 RFID transponder

The name transponder is composed of the terms “*transmit*” and “*response*” (Bartneck et al., 2008). The term tag is used synonymously with transponder. The transponder consists of a coupling element and a microchip and is the data carrier of the RFID system (Finkenzeller, 2015).

There are various technical characteristics of RFID transponders. A distinction is made between active, semi-active, and passive transponders. An active transponder has a battery for the power supply of the microchip and for sending data. The semi-active transponder also has a battery, but this is only used to supply power to the microchip, but it is not used to send data, instead the energy from the field of the reader is used. A passive transponder does not have a battery and uses only the energy of the reader to supply power to the microchip and to send data (Tamm & Tribowski, 2010). The advantage of active or semi-active transponders over passive ones is that greater read ranges can be realised. However, active

transponders are not as small as passive transponders due to the battery, and the battery lifetime is limited. The advantage of passive transponders is that they can be manufactured at low-cost due to their simpler design without a battery (Franke & Dangelmaier, 2006).

Transponders are available in a wide variety of construction formats and antenna designs, as shown in Figure 5. The transponders can, for example, be incorporated into so-called smart labels, which can be printed on the outside, e.g., with a barcode, and can also be self-adhesive. Another option is to use plastic housings, which protect the transponders from external environmental influences such as dirt or acids (Fleisch & Mattern, 2005; Franke & Dangelmaier, 2006). However, manufacturing costs are higher when the transponder is placed in a housing instead of in a smart label (Wagner, 2009).

The choice of construction and antenna design depends on the application. If a transponder is used only once and is then discarded, it is referred to as a single-use label or single-use transponder. However, if a transponder is used several times, it is called a multi-use transponder (VDI, 2006).

The transponder is attached directly to the object to be identified by gluing, riveting, or another method. Certain carrier materials, such as metal, influence the communication between the transponder and the reader. For this reason, there are transponders specially designed for the different carrier materials, for example the so-called on-metal transponders (Tamm & Tribowski, 2010).

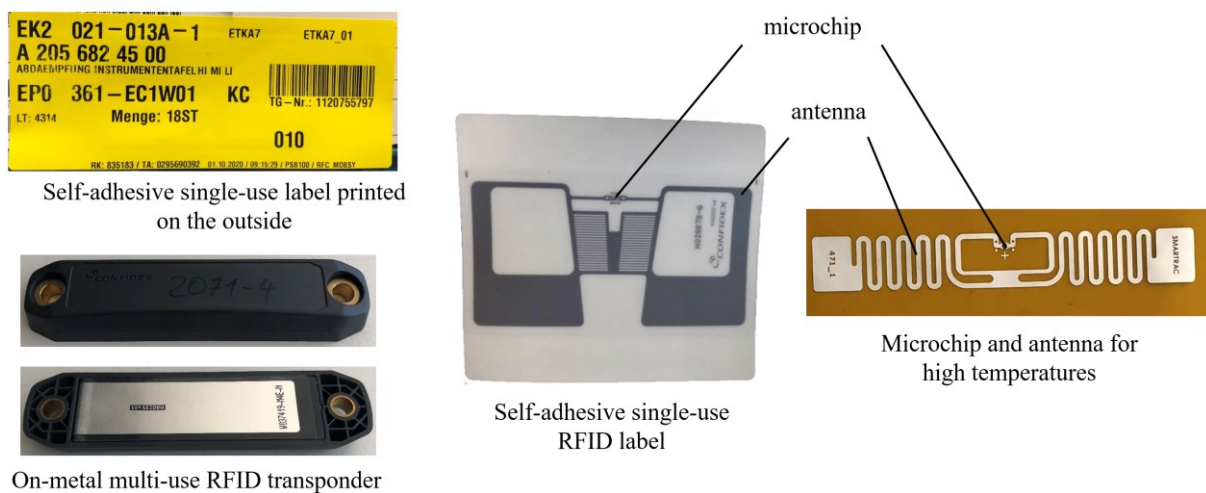
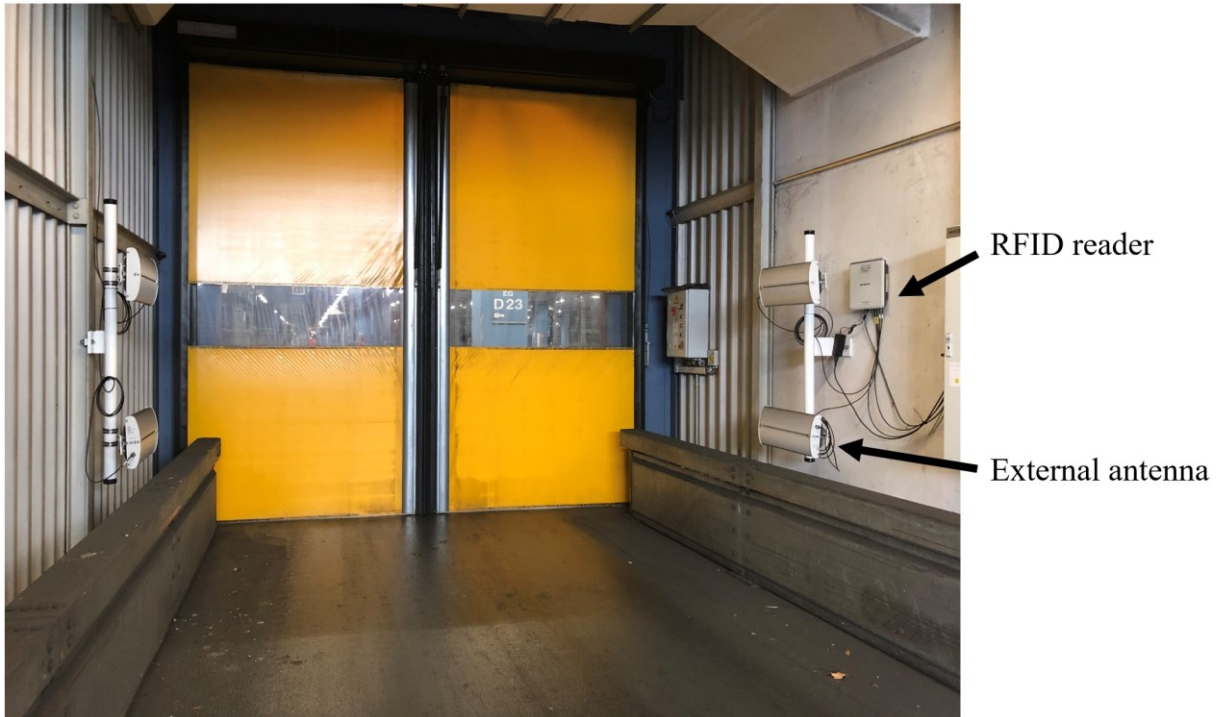


Figure 5 Different types of constructions and antenna designs

### 2.1.1.2 RFID reader

The RFID reader has an internal antenna, external antenna(s) to extend the reading field, or both (Azizi, 2019). RFID readers are also divided into stationary readers, which are supplied with power via a power cable or Power over Ethernet (PoE), and mobile readers, such as an RFID handheld or an RFID cuff, which are battery powered (Tamm & Tribowski, 2010). Figure 6 shows an RFID gate with a stationary reader and four external antennas where the reader is supplied via a power cable and connected via Ethernet to the application. Figure 7 shows an RFID handheld and an RFID cuff, which are both mobile readers with integrated antenna.



*Figure 6 RFID gate with stationary reader and four external antennas*



*Figure 7 Mobile RFID reader with integrated antenna: RFID handheld (left) and RFID cuff (right)*

### **2.1.2 Frequency ranges**

In RFID, a basic distinction is made between the four frequency ranges (i) Low Frequency (LF), (ii) High Frequency (HF), (iii) Ultra High Frequency (UHF), and (iv) Super High Frequency (SHF). Each frequency range has different characteristics and this results in different application areas, as shown in Table 2. (Tamm & Tribowski, 2010)

When selecting the operating frequency, legal requirements must be taken into account because each country has its own laws regarding permitted frequencies and permitted transmission power. There are no internationally uniform frequency standards for the frequency range UHF. In Europe, 865 – 868 MHz and in North America 902 – 928 MHz is used, for example. (Finkenzeller, 2015; GS1, 2022b; Wagner, 2009)

Table 2 Frequency ranges and their characteristics, according to Bundesnetzagentur (n.d.); Lechner (2020); Tamm and Tribowski (2010); Wagner (2009)

	LF	HF	UHF	SHF
<b>Operating frequency</b>	125 kHz	13.56 MHz	865 – 868 MHz (EU)	2.45 GHz, 5.8 GHz
<b>Type of coupling</b>	inductive	inductive	electromagnetic	electromagnetic
<b>Typical reading range</b>	0.2 m	1.5 m	10 m (passive) 100 m (active)	3 m (passive) 300 m (active)
<b>Bulk capability</b>	no	yes	yes	yes
<b>Data transfer rates</b>	low	high	very high	very high
<b>Transponder costs*</b>	1 – 5 €	0.50 – 5 €	0.07 (passive) – 5 € (active)	20 (passive) – 150 € (active)
<b>Influence of metal</b>	very low	low	high	very high
<b>Influence of liquids</b>	low	low	high	very high
<b>Application examples</b>	animal identification	access control, time recording, theft protection	warehouse, logistics	vehicle identification, toll collection, container logistics

\* Transponder costs depend on the characteristics of the microchip, for example storage size, but also on the housing and the number of transponders that are purchased.

### 2.1.3 Backscattering communication

The so-called backscattering is used for communication between RFID reader and transponder in passive UHF systems, as simplified shown in Figure 8. The RFID reader generates a high-frequency signal with the power  $P_{Reader}$ , which is fed into the antenna via a cable. Due to the attenuation of the cable, the power fed into the antenna  $P_{Antenna_{in}}$  is lower than  $P_{Reader}$ . The antenna emits the power as an electromagnetic wave. The power emitted by the antenna  $P_{Radiated}$  differs from the power  $P_{Antenna_{in}}$  due to the antenna gain. The power arriving at the transponder  $P_{Radiated}'$  is significantly less than  $P_{Radiated}$  due to free space attenuation. If the incoming power  $P_T$  is sufficient to supply the microchip with energy, the transponder is activated. The transponder reflects a part of the received power. To transmit data, the amplitude shift keying (ASK) modulation method is used, where the reflected power  $P_{Reflected}$  is modulated by switching a load resistor connected in parallel to the antenna on and off in time with the data stream. The power reflected  $P_{Reflected}$  from the transponder is reduced by the free space attenuation, so that the power  $P_{Reflected}'$  arrives at the antenna of the reader. If the power  $P_{Received}$  is strong enough, the reader can detect and decode the received signal. (Finkenzeller, 2015; Lechner, 2020)

To indicate the signal strength of the signal reflected from the transponder, the received signal strength indication (RSSI) value is used, which is given in dBm in the Kathrein ReaderStart software. The factor provides information about how well a transponder is read and is often used to determine the distance between the reader antenna and the transponder. However, the RSSI is dependent on environmental factors, such as reflections, and therefore the RSSI value cannot always be used to infer the distance between the transponder and the reader antenna. To compare different transponders with each other, however, the RSSI value can be determined in an anechoic measurement chamber, for example. (Russell, 2018; Whitney et al., 2014)



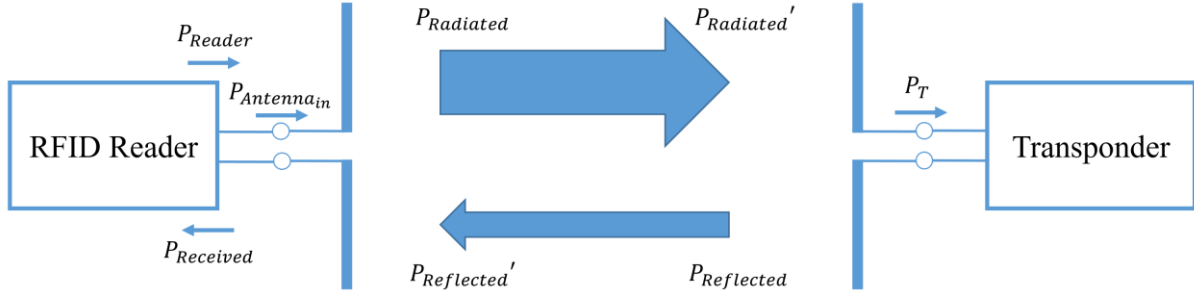


Figure 8 Communication between RFID reader and transponder through backscattering, according to Finkenzeller (2015); Lechner (2020)

### 2.1.3.1 Antenna gain and directional effect

As mentioned already, the antenna gain affects the radiated power  $P_{Radiated}$ . For an isotropic emitter, the radiation is uniform in all directions. In a real antenna, however, for example, a dipole, the antenna does not radiate uniformly in all directions, as shown in Figure 9. The antenna gain  $G_i$  indicates the factor by which the radiance is amplified compared to an isotropic emitter. The effective isotropic radiated power  $P_{EIRP}$  is calculated by the power fed into the antenna times the antenna gain (cf. Eq. 1).

However, the power can also be given in terms of a dipole antenna as the effective radiated power  $P_{ERP}$ . The power in ERP can be converted to a power in EIRP using the gain of the dipole antenna ( $G_i = 1.64$ ) as shown in Eq. 2. (Finkenzeller, 2015; Lechner, 2020)

The radiated power of real antennas is concentrated on a part of the space and thus on one main direction. Therefore, antennas have an aperture angle, indicating at which points the directional gain has decreased by half compared to the main direction, which means the power is decreased by 3 dB (see Figure 10). Due to directional radiation, the optimal alignment between two antennas is when their main beam directions point towards each other as shown in Figure 11. A change in position or orientation of the transponder leads to a reduced directional gain that results in a lower theoretically read range (see Figure 11). (Lechner, 2020)

$$P_{EIRP} = P_{Radiated} = P_{Antenna_{in}} * G_i \quad Eq. 1$$

$$P_{EIRP} = P_{ERP} * 1.64 \quad Eq. 2$$

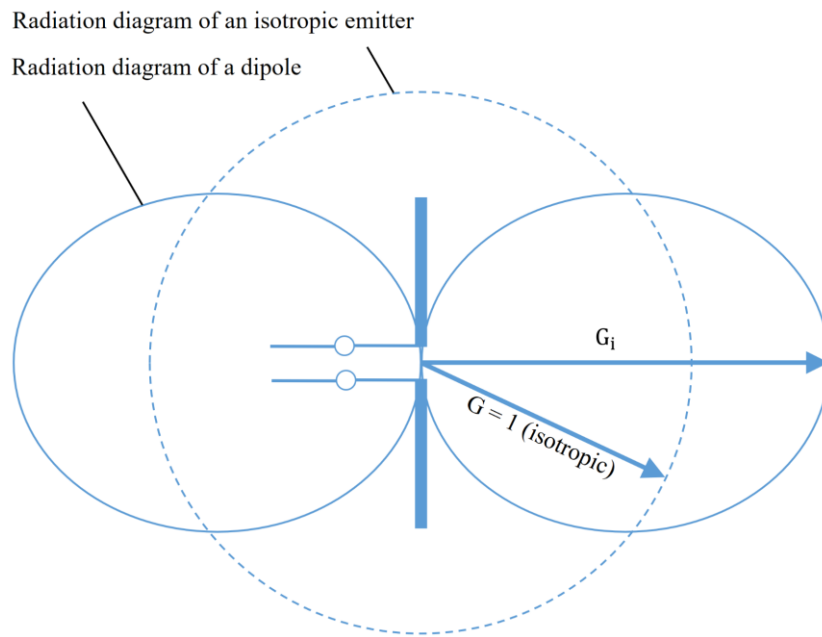


Figure 9 Radiation diagram of an isotropic emitter and of a dipole, according to Finkenzeller (2015)

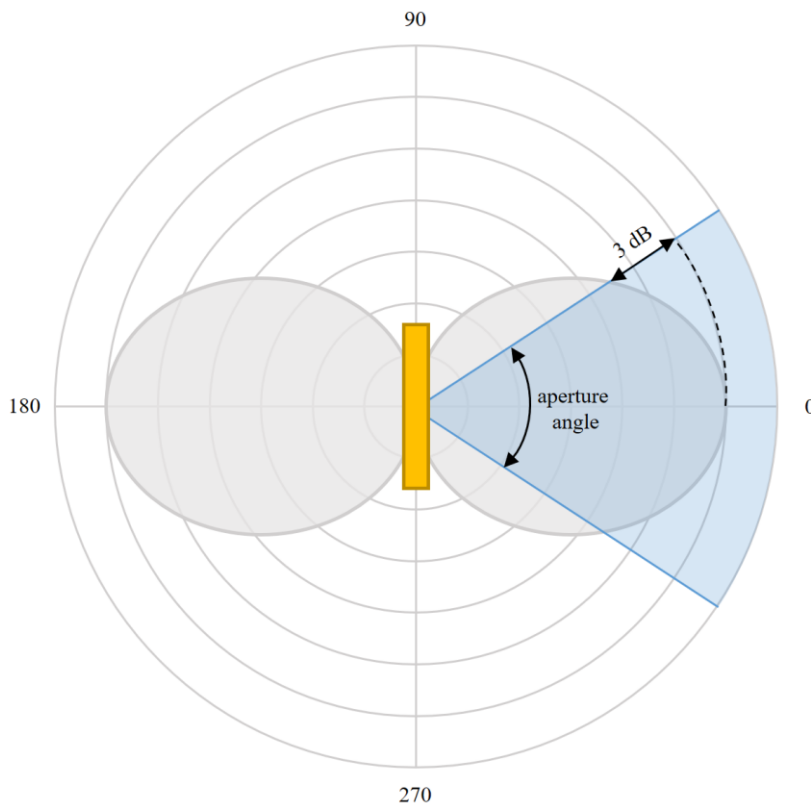


Figure 10 Aperture angle of a dipole antenna, according to Lechner (2020)

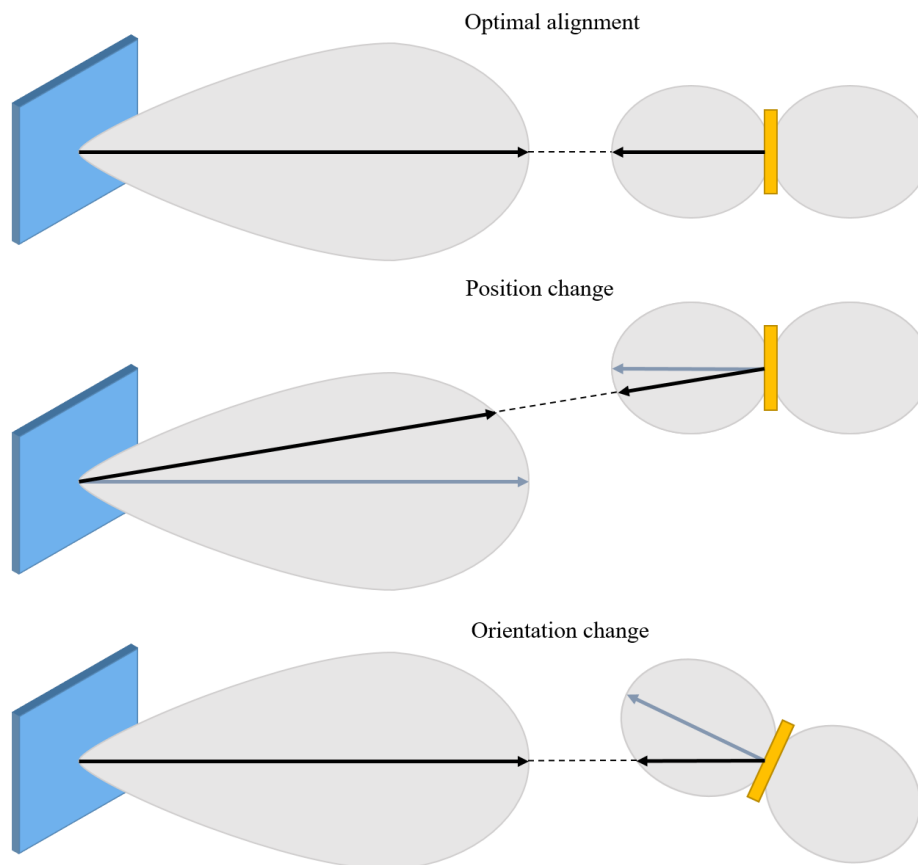


Figure 11 Influence of position and orientation between reader and transponder, according to Lechner (2020)

### 2.1.3.2 Antenna polarisation

Another property of antennas that affects the communication between the reader and the transponder is the antenna polarisation. A distinction is made between linearly and circularly polarised antennas. The electromagnetic field of the linearly polarised antennas propagates in one direction, as shown in Figure 12 on the left. A distinction is also made between horizontal polarisation, where the electric field lines run parallel to the earth's surface, and vertical polarisation, where the field lines run at right angles to the earth's surface. The energy transmission is optimal when the polarisation of the reader and transponder antennas are the same. If the polarisation between reader and transponder is rotated by  $90^\circ$  or  $270^\circ$  to each other, then the energy transmission is the lowest. In this case, a power loss of 20 dB is expected, which means that only 1/100 of the power can be absorbed by the receiving antenna.

The effect of polarisation and orientation on the reading behaviour of the transponder can be determined, for example, in a shielded measurement chamber by performing threshold measurements. In a threshold measurement, the power is increased step by step until the RFID transponder is detected or the maximum power is reached. Figures 13 and 14 show the results of threshold measurements of six different transponder positions. These were performed in the shielded measurement chamber of the HFT Stuttgart and the software Tagformance from Voyantic was used. The measurement chamber contains a linearly polarised antenna. The RFID single-use Confidex eKanban transponder used for the measurements is also linearly polarised. The measurements showed that the positions “horizontal, parallel” and “horizontal, lying” are optimal. The position “vertical, lying” is good and the position “vertical, parallel” is bad. In the positions “vertical, orthogonal” and “horizontal, orthogonal”, the transponder was not detected at all and therefore these are very bad.

When using mobile RFID readers, the alignment between reader and transponder is often unpredictable. To solve this problem, circularly polarised reader antennas can be used. With circularly polarised antennas, the electromagnetic field rotates once through 360°, as can be seen in Figure 12 on the right. A distinction is made between counter-clockwise and clockwise rotation. However, the disadvantage of circularly polarised antennas compared to linearly polarised antennas is that a polarisation loss of 3 dB is expected. (Finkenzeller, 2015)

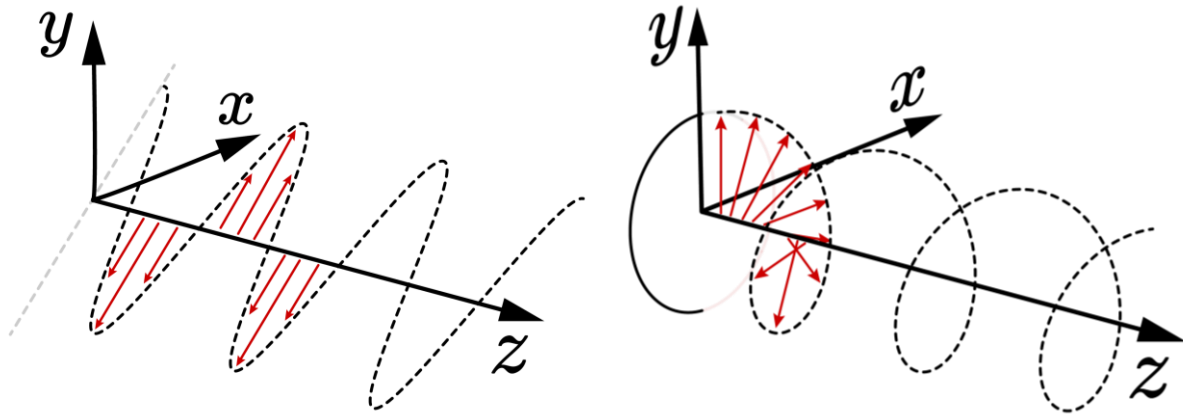


Figure 12 Linearly (left) and circularly (right) polarised electromagnetic waves, source: ©universaldenker.org

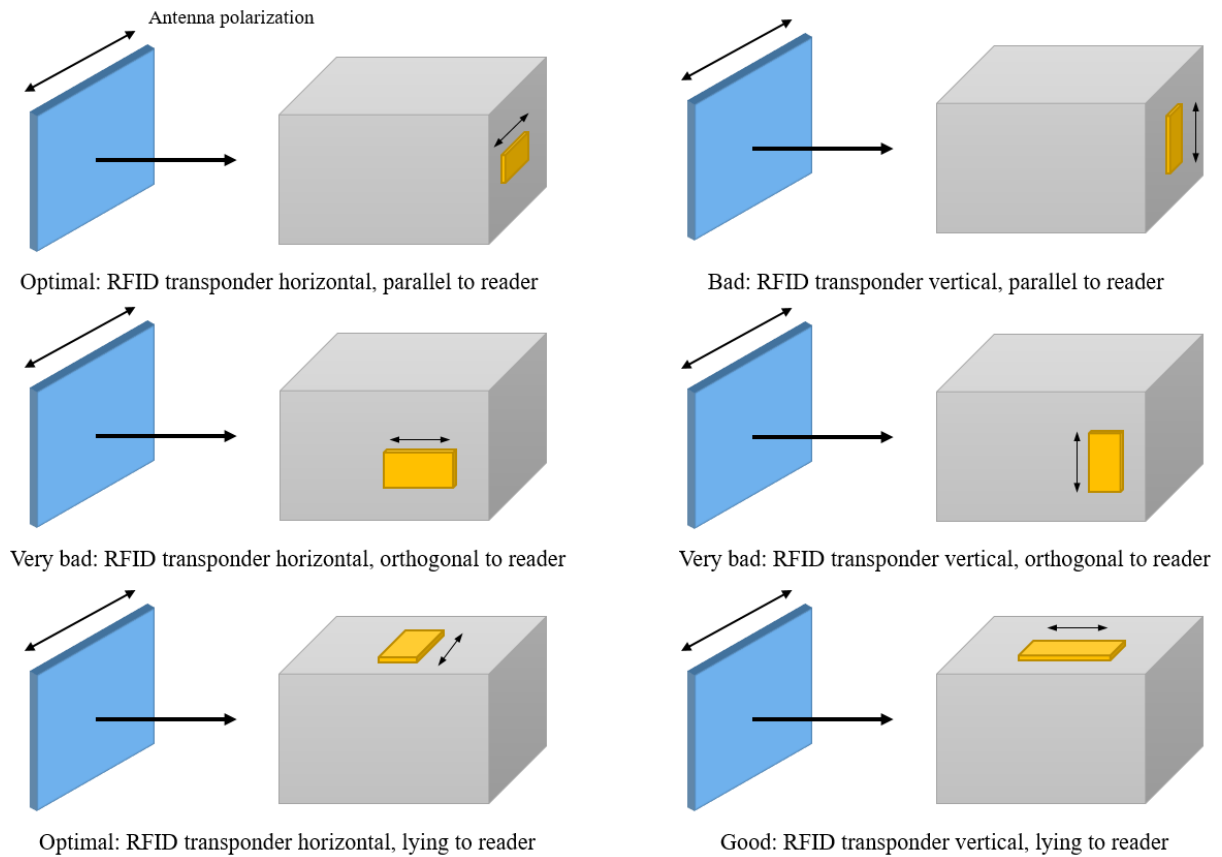


Figure 13 Effect of antenna polarisation and transponder orientation on readability, according to Kleist (2004); Wagner (2009)

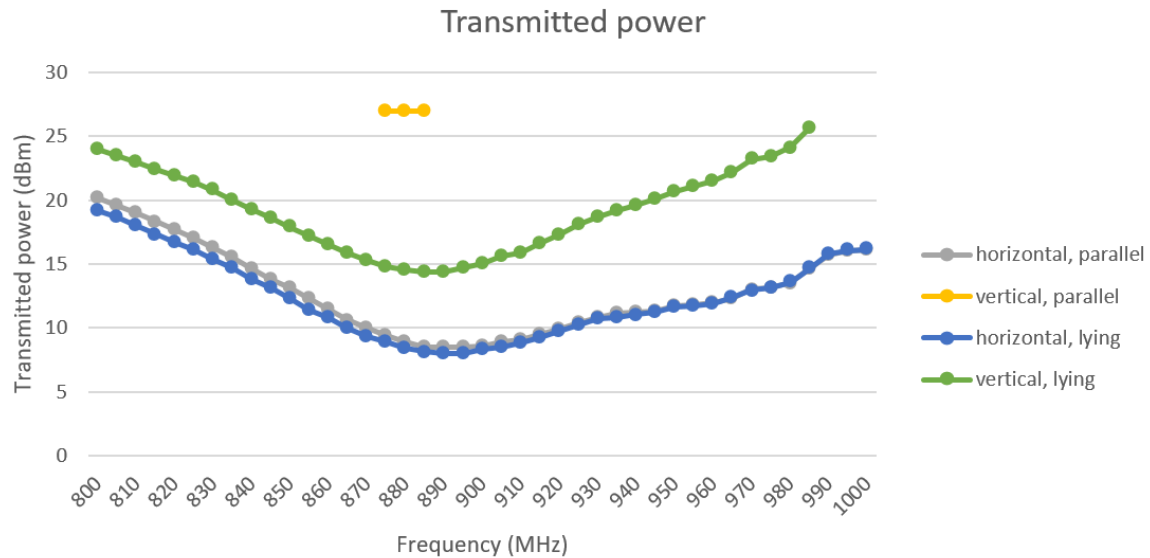


Figure 14 Measurement results of transmitted power of different transponder orientations

#### 2.1.4 RFID standards for communication

For successful communication between readers and transponders, standards are required to clearly regulate parameters such as the used frequencies, modulation, or anticollision algorithm (Wagner, 2009).

##### 2.1.4.1 Radio regulations

In the UHF frequency range, there are no uniform international frequency standards (Wagner, 2009). In Europe, ETSI (European Telecommunications Standards Institute) is responsible for the development of radio regulations in the sector of information and communication technologies. The EN 302 208 standard describes the use of passive transponders in the UHF frequency band. The standard EN 302 208 (ETSI, 2020) describes the lower band (865 MHz – 868 MHz) and the upper band (915 – 921 MHz). In the lower band, a maximum reader power of max. 2 W and in the upper band of max. 4 W is permitted. The overview of the channels allowed in the lower and upper bands is shown in Figures 15 and 16. The channel plan of the standard contains the channels 4, 7, 10 and 13 in the lower band and channels 3, 6, 9 and 12 in the upper band, but “EU member states are requested to implement only Interrogator Transmit channel 3 (916,1 MHz to 916,5 MHz), Interrogator Transmit channel 6 (917,3 MHz to 917,7 MHz) and Interrogator Transmit channel 9 (918,5 MHz to 918,9 MHz)” (ETSI, 2020). Due to the double channel bandwidth of 400 kHz within the upper band compared to the lower band, double data rates are possible there. In addition, the increased transmitting power of maximum 4 W allows higher ranges to be achieved. However, the use of the upper band is not allowed in every country, such as Germany. Here, the frequencies 915 – 918 MHz are reserved for military use and the frequencies 918 – 921 MHz for the Extended Railways Global System for Mobile communication. The radiated power of the transponder should not be greater than  $-20$  dBm which is equivalent to  $10 \mu\text{W}$  in the lower band, and not be greater than  $-10$  dBm ( $= 10 \mu\text{W}$ ) in the upper band. (ETSI, 2020; Ident, 2022)

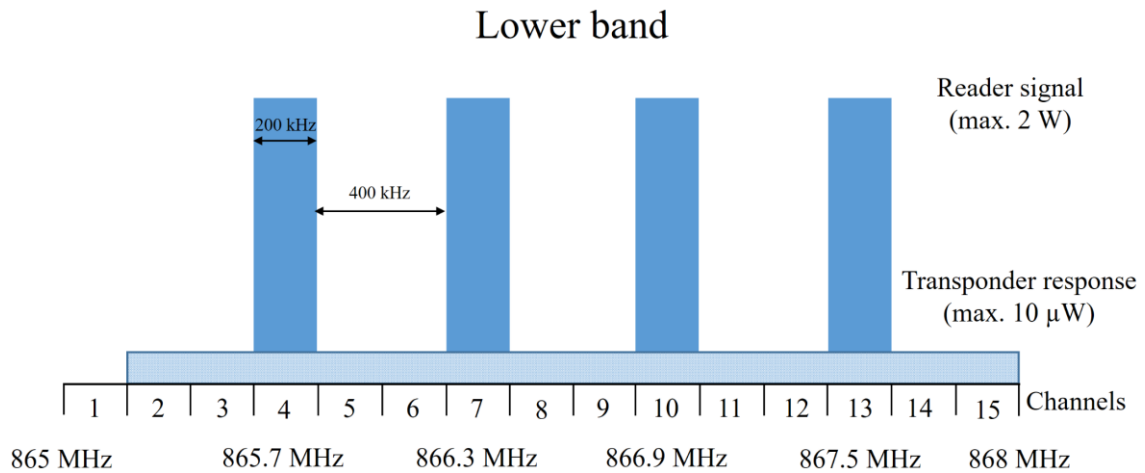


Figure 15 Overview of the channels of the lower band, according to ETSI (2020)

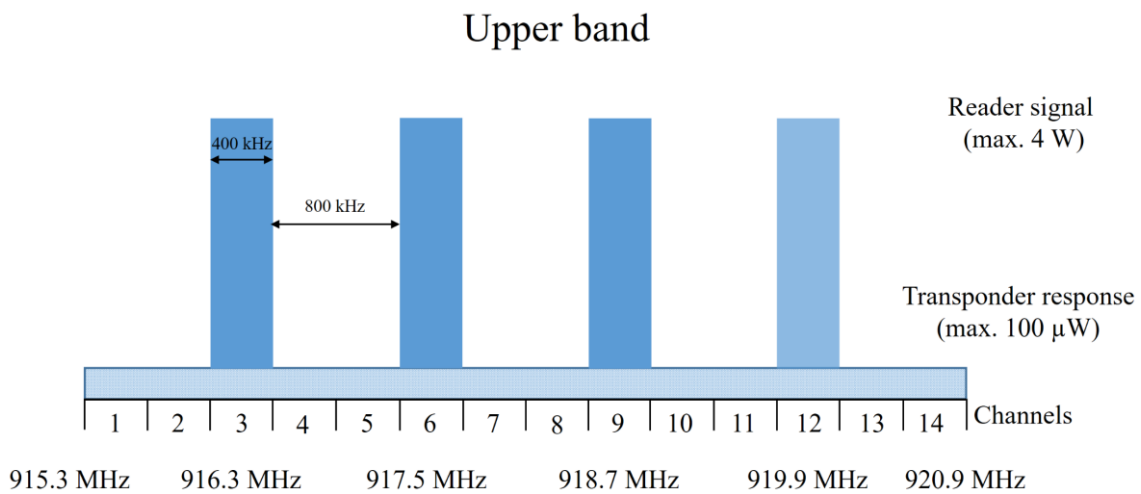


Figure 16 Overview of the channels of the upper band, according to ETSI (2020)

#### 2.1.4.2 Modulation and encoding

For communication between the reader and the transponder, the data must be modulated and encoded. The specifications for modulation and encoding are described in the ISO/IEC 18000-63 standard (ISO/IEC, 2015). This standard also contains additional parameters for the air interface communication in the frequency range of 860 MHz to 960 MHz and is fully compatible with the EPC global UHF Generation 2 Air Interface Protocol (Ident, 2022). According to this standard, the reader can use double-sideband amplitude shift keying (DSB-ASK), single-sideband amplitude shift keying (SSB-ASK), or phase-reversal amplitude shift keying (PR-ASK) for modulating an RF carrier. The encoding is done by using a pulse-interval encoding (PIE). The modulations amplitude shift keying or phase shift keying (PSK) can be used for transponder-to-reader communication. The reader determines the data encoding which is FM0 or Miller and must be used by the transponder. In addition, the reader specifies the data rates. Miller encoding is more robust against counter noise and interference than FM0. (ISO/IEC, 2015; Wang, 2017)

#### 2.1.4.3 Anticollision algorithm

Also important for the communication between RFID reader and transponders is the anticollision algorithm because in RFID applications, there are usually several transponders in the field of a reader at the same time and if two or more transponders respond to the reader simultaneously, collisions occur. These collisions lead to the reader not being able to distinguish the signals of the transponders and thus

not being able to identify the transponders. Anticollision algorithms are used to avoid this. The Q-Algorithm (QA), which is based on the ALOHA algorithm, is anchored in the EPCglobal Class1 Gen-2 standard and proceeds as follows.

- 1) The identification takes place in several cycles, and the reader initiates the identification cycle by sending a *Query* command, which contains the four bit binary variable  $Q$  in range of  $[0, 15]$ .
- 2) Then, each active transponder calculates a slot counter  $q$  in range of  $[0, 2^Q - 1]$ .
- 3) If the slot counter is zero, the transponder answers the reader with a 16-bit long random number. The reader checks how many transponders have sent a random number.
- 4) If only one transponder has responded, the reader sends an acknowledge (ACK) command that contains the random number received from the transponder. The transponder checks if it matches the one it sent and then sends its id / EPC (Electronic Product Code). After the successful activation, the reader sends the *QueryRep* command.
- 5) If multiple transponders respond to the reader (collision) or no transponder responds, the reader sends a *QueryRep* or *QueryAdjust* command.
- 6) If the unidentified transponders accept the *QueryRep*, they reduce their slot counter by one and the process is continued from step 3.
- 7) If the reader sends the *QueryAdjust* command, a new cycle begins. (ISO/IEC, 2015; Wang et al., 2019)

#### 2.1.4.4 Session

The use of an appropriate session can save time in the anticollision procedure because transponders that have already been detected do not have to be identified again. The session is specified by the reader during an inventory round and specifies how long a transponder remembers that the reader identified it during an inventory process. A distinction is made between the state in which the transponder is permanently supplied with energy and the state in which it is not supplied with energy, which can occur due to reading holes, for example. Table 3 shows the four sessions and their properties. (Finkenzeller, 2015; ISO/IEC, 2015; Kathrein Solutions GmbH, 2017)

Table 3 Sessions and their properties, according to ISO/IEC (2015); Kathrein Solutions GmbH (2017)

Session	Transponder energised	Transponder not energised
S0	Indefinite persistence	No persistence
S1	Persistence > 500 milliseconds, but < 5 seconds	Persistence > 500 milliseconds, but < 5 seconds
S2	Indefinite persistence	Persistence > 2 seconds
S3	Indefinite persistence	Persistence > 2 seconds

#### 2.1.4.5 Transponder memory

Once a transponder has been successfully identified, its storage can be read or written to. The transponder memory is divided into the following four memory banks according to ISO/IEC 18000-63 (ISO/IEC, 2015).

- 1) **Bank 00 (RESERVED)** contains the reserved memory, which are the kill and / or access passwords.
- 2) **Bank 01 (UII)** contains the UII (unique item identifier) memory. This consists of header information and the UII (e.g., EPC) itself. The header contains a toggle bit to indicate if the UII is encoded after GS1 (= 0) or ISO/IEC (= 1). If the UII is encoded after ISO/IEC, then the application family identifier (AFI) is specified, otherwise this is set to zero. The AFI describes the type of object to be identified, e.g., component or returnable container. The AFI is A2 for transport units (ISO 17365) and A3 for returnable transport item (ISO 17364) in the supply chain applications of RFID. (VDA, 2015b, 2016, 2022)
- 3) **Bank 10 (TID)** contains the TID (transponder id) memory, which includes manufacturer-specific data.
- 4) **Bank 11 (USER)** contains the user memory, and this is optional.

### 2.1.4.6 Unique item identifier

The UII is used to uniquely identify objects equipped with an RFID transponder. There are different coding schemes to create the UII. A distinction is made between UII for GS1 EPCglobal Applications and for ISO Applications. (ISO/IEC, 2015)

The EPC (electronic product code) is defined in the EPC tag data standard (GS1, 2019). The EPC supports various coding schemes, such as the SGTIN (serialised global trade item number), GID (general identifier), or SSCC (serial shipping container code). Basically, the EPC consists of a header and several data fields which are specified by the header. An EPC can have a total length of 64 bits and 96 bits. (Finkenzeller, 2015)

For the automotive sector, the general principles for ISO/IEC-based object identification are described in VDA 5500 (VDA, 2015b). The technical requirements for the use of RFID in container management and for packages are described in VDA 5501 (VDA, 2016) and VDA 4994 (VDA, 2022). In the logistics of Mercedes-Benz AG, Sindelfingen, VDA 5501 is used for the identification of multi-use RFID transponders on special load carriers and VDA 4994 for single-use transponders on universal load carriers.

The container id according to VDA 5501 consists of a data identifier (DI), issuing agency code (IAC), company identification number (CIN), object type (OT), separator, and serial number (SN) as shown in Table 4. The data identifier indicates the container type, such as 27B for large load carriers. The issuing agency code indicates the issuing agency of the CIN, such as UN for Dun & Bradstreet or OD for Odette Europe. The CIN is assigned by the issuing agency and ensures the unique identification of the company or organisation, which are primarily the owners of the containers, such as 498999044 for Daimler AG. This is followed by the object type, which indicates the container type, such as 23478. Then a separator (+) and the serial number follow.

The structure of the package id according to VDA 4994 is similar and also contains a DI, such as 1J for the package id of the innermost packaging level (single-use label), then an IAC and CIN, as well as the SN but without OT (see Table 5).



Table 4 Data structure for special load carriers with multi-use RFID transponders, according to VDA (2016)

DI	IAC	CIN	OT	+	SN
Data Identifier	Issuing Agency Code	Company Identification Number	Object Type	Separator	Serial Number
26B – 29B	UN or OD	Variable	Variable	Fix	Variable
27B	UN	498999044 (Daimler AG)	23478	+	1221592

Table 5 Data structure for universal load carriers with single-use RFID transponders, according to VDA (2022)

DI	IAC	CIN	SN
Data Identifier	Issuing Agency Code	Company Identification Number	Serial Number
1J – 6J	UN or OD	Variable	Variable
1J	UN	498999044 (Daimler AG)	TG1108980106

#### 2.1.4.7 Detection rate

An important KPI (key performance indicator) to measure the communication of RFID installations is the read rate. The read rate is defined in AIM 4472 Part 10 (VDI/AIM, 2008) as in Eq. 3.

$$Read\ rate = \frac{Number\ of\ positive\ events}{Total\ number\ of\ positive\ events} \quad Eq. 3$$

In this thesis the terms read rate, reading rate, and detection rate are used synonymously.

#### 2.1.5 Factors influencing the detection rate

In the previous sections, some factors that influence the detection rate have already been explained, such as antenna gain. However, there are more factors that influence the detection rate, which are summarised in the Ishikawa diagram in Figure 17. These influencing factors can be divided into the categories (i) reader, (ii) reader antenna, (iii) transponder, (iv) setup, and (v) location.

The set reader power determines the size of the reading field. The higher the reader power, the greater the reading range. However, high power in metallic environments can lead to more reflections and thus to reading holes. Other adjustable parameters of the reader are the modulation, encoding, session, and the frequency used, which can affect the communication between reader and transponder. In addition, interferences, which are generated by the reader itself, can have an effect on the communication. Therefore, there are readers that have a self-jammer cancelation hardware to suppress these signals (Kathrein Solutions GmbH, 2017). The sensitivity of the reader describes the sensitivity in the detection of transponder signals, and thus can have an effect on the detection rate. Another influencing factor is the anticollision algorithm used.

As described in Section 2.1.3, the gain, polarisation, and aperture angle of the reader antenna affect the readability of transponders. The antenna cable, which is used for readers with external antennas, has an attenuation and thus reduces the power radiated at the reader port.

The antenna design of the transponder also has an influence on readability. The antenna design can, for example, take into account the surface, as is the case with on-metal transponders, whose antenna design is designed for metallic objects. However, the size of the antenna also plays a role. The polarisation and gain of the transponder antenna can also have an influence. As with the reader, encoding and modulation are further influencing factors. The microchip is an essential part of the transponder and therefore a

possible influencing factor. The sensitivity of the transponder describes the energy needed to activate the transponder, which might influence the detection rate. The housing serves to protect the transponder and its antenna from environmental influences to ensure that it is not destroyed.

In addition to the individual components of an RFID system, the setup of the RFID installation has an influence on the readability of the transponders. The speed of the transponders that are moved past the reader is an influencing factor here. A very high number of transponders can mean that not all of them can be read in a certain time span. The distance between the reader and the transponders is also crucial for readability. The orientation between the reader antenna and the transponder also has a major influence (see Section 2.1.3). (Finkenzeller, 2015; Günther et al., 2011; Lechner, 2020; VDI/AIM, 2008; Wagner, 2009)

Location-related influencing factors are referred to as sources of interference in this thesis and were identified through a systematic literature review as described in Section 5.2.

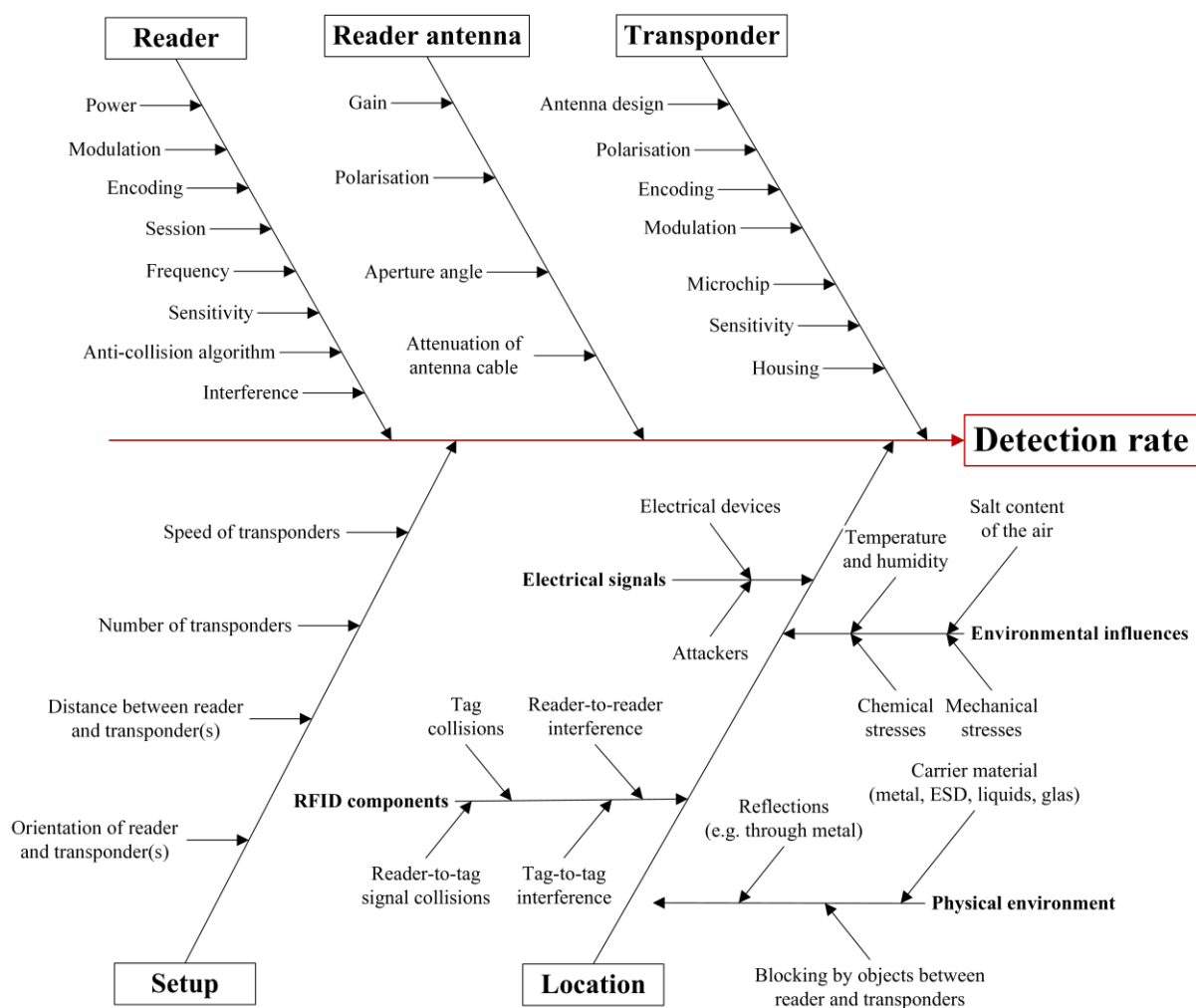
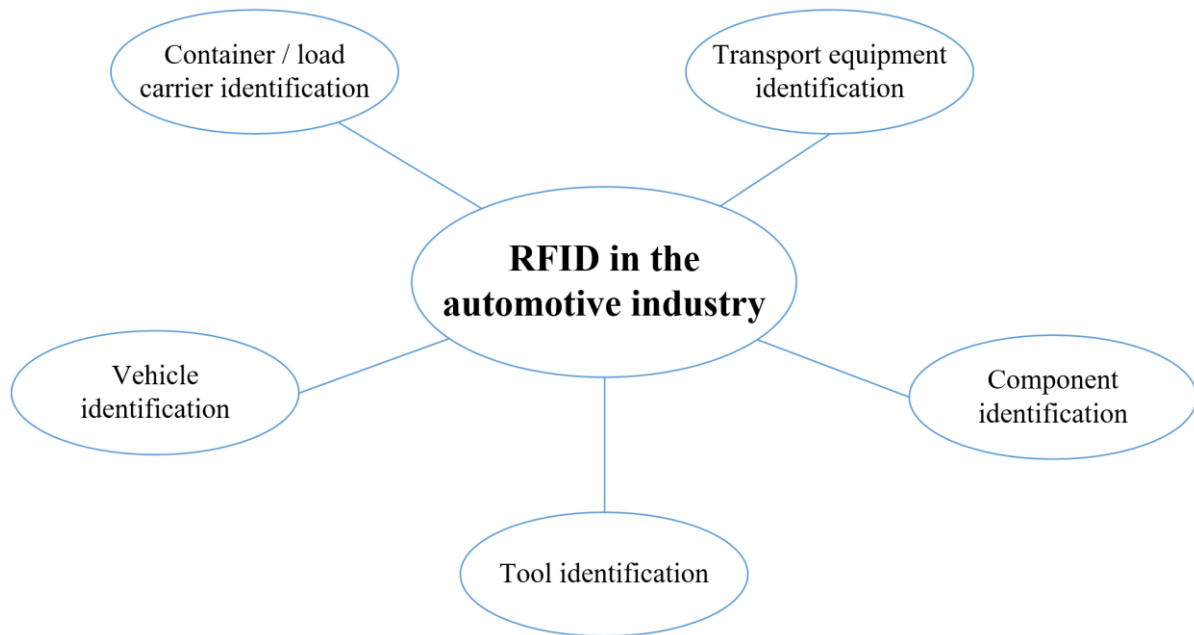


Figure 17 Factors influencing the detection rate, according to Hur et al. (2009); Kleist (2004); Knapp and Uckelmann (2022)

## 2.2 RFID applications in the automotive industry

The RFID technology described above is used in the automotive industry in the areas of container / load carrier identification, vehicle identification, tool identification, component identification, and transport equipment identification, as shown in Figure 18. The focus of this work is on the identification of

container / load carrier in complex logistics and production processes. In the following, three RFID applications used at Mercedes-Benz AG are described. For all applications, the load carriers are equipped with an RFID transponder. All special load carriers that circulate only between one supplier and the car manufacturer have multi-use RFID transponders. Universal load carriers, which come from a pool and are used by many different companies, are affixed with single-use RFID transponders. RFID transponders are coded with a UII according to the standards VDA 5501 (VDA, 2016) and VDA 4994 (VDA, 2022), and all other information about the load carrier and material contained in it, is stored in the logistics back end system.



*Figure 18 Typical areas of use of RFID in the automotive industry*

### **2.2.1 Automatic goods receipt posting with RFID gates**

The goods required for production are delivered by the suppliers and booked at goods receipt. All load carriers must be equipped with an RFID transponder to automatically book the material delivered at the goods receipt. Furthermore, this application requires an RFID gate at goods receipt, which typically consists of a reader and four external antennas (see Figure 6 on page 11). RFID gates are used not only at incoming goods, but also inside the production for automatic transport order acknowledgement. Alternatively, there are also applications where ceiling readers are used instead of gates. In the following, the automatic goods receipt process using RFID gate is described (see Figure 19):

- 1) The supplier notifies the delivery and sends the notification electronically to the logistics back end system of the automotive manufacturer (Mercedes-Benz AG), where it is stored.
- 2) A carrier transports the goods on a truck to the plant of the automotive manufacturer.
- 3) The truck is driven to the unloading point inside the plant and parked there.
- 4) Then a forklift driver unloads the material and drives through the RFID gate and places the material on the handling area.
- 5) The RFID reader reads the UIIs of the transponders attached to the load carriers, which are encoded in hexadecimal format and converts them to ASCII (American standard code for

information interchange). The UIIs are then sent to the logistics back end system with a timestamp, reader name, and gate id (determines that it is a goods receipt gate) via an interface.

- 6) Incoming goods inspection is performed in the logistics back end system. Here, the data transmitted by the reader is compared with the notified delivery and it is checked whether the set lucky shot quota has been reached. The lucky shot quota indicates the percentage of transponders that must be detected, e.g., 80 %, i.e. the detection rate for one pass, since it can happen that not all transponders are read due to sources of interference such as ESD (electrostatic discharge) load carriers.
- 7) If the incoming goods inspection was successful, the goods receipt posting is automatically carried out in the logistics back end system, and the goods are ready for further transport to the warehouse or directly to the production supply area. Otherwise, the clearing must be performed first manually.

The advantages compared to the use of barcodes at goods receipt are:

- The use of RFID leads to time savings, as no barcodes must be scanned manually.
- RFID enables greater transparency due to automatic structure check. This checks, for example, whether the number of small load carriers is correct or whether the correct small load carriers are in a container. This structure check is only carried out to a limited extent when barcodes are used.

However, there are also disadvantages due to the use of RFID at goods receipt:

- Due to sources of interference, the lucky shot quota may not be reached, and the material then has to be manually scanned and booked during clearing.
- Suppliers must convert their IT systems to correctly encode RFID transponders and must notify the shipment differently than they would with barcodes.
- If the suppliers encode the RFID transponders incorrectly or notify the delivery incorrectly, there is an effort in the goods receipt to perform the clearing.

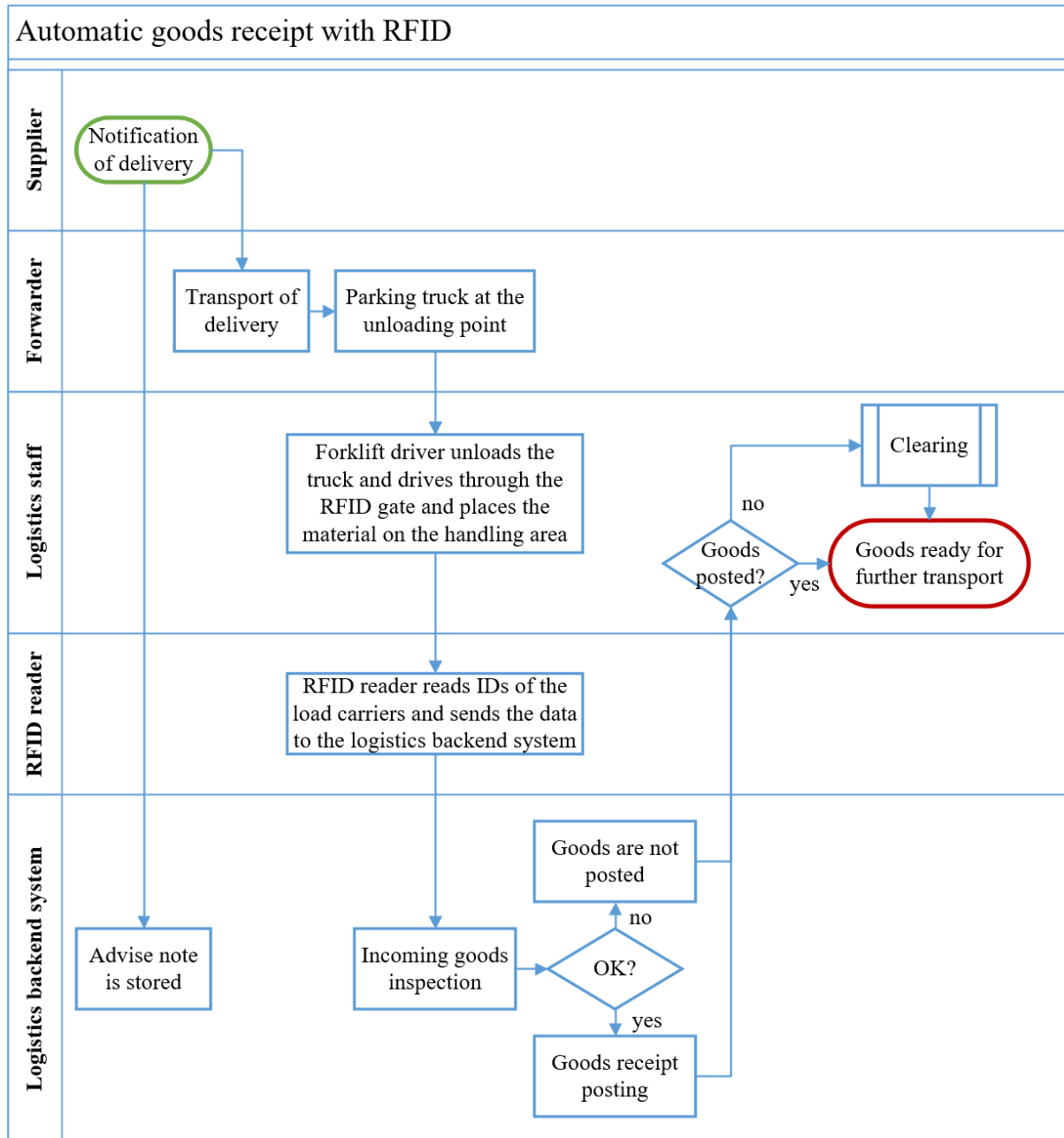


Figure 19 Automatic goods receipt process with RFID

### 2.2.2 Automatic material retrieval with RFID reader on the shelf

Another application used in the assembly is the automatic material retrieval with RFID reader on the shelf. For this application, the shelves on which the small load carriers are provided on the assembly line are equipped with RFID readers and antennas as shown in Figures 20 and 21. The number of antennas depends on the width of the shelf, and also RFID readers with an integrated antenna can be used. Small load carriers are equipped with RFID transponders. As soon as the empty small load carrier is placed on the empty container track, the RFID transponder is read, and the required material is automatically reordered. To ensure that only the RFID transponders of the load carriers on the empty container track are read, shielding material is used on the sides and underneath the empty container track. This is important because material that is reordered too early would lead to excess stock on the shelf at the assembly line and thus to extra work for the employees. In the following, the automatic material retrieval with an RFID reader on the shelf is described (see the process diagram in Figure 22):

- 1) The tour driver places the full load carrier on the full container track on the shelf at the assembly line.
- 2) The conveyor employee removes the material and installs it in the vehicle.
- 3) The employee then returns the empty load carrier to the empty container track.
- 4) RFID reader reads the UID of transponder, prepares data (analogous to the automatic goods receipt), and sends it to logistics back end system.
- 5) The logistics back end system automatically reorders the used material.

Compared to the use of sensors on the shelf, RFID offers several advantages:

- This RFID application provides more flexibility, since no sensors have to be reprogrammed when the shelves are rearranged.
- Furthermore, it also leads to more flexibility, as a load carrier can also be put back on an adjacent rack, and the correct material is still reordered.
- When using this RFID application, there is no need to replace batteries, as it is the case with sensors.
- The RFID reader has no problem with dust, whereas with sensors, dust can lead to the fact that the load carrier is not recognised any more.

However, there are also disadvantages to retrieving via RFID reader on the shelf:

- Single-use RFID transponders can drop out or employees can misuse the load carriers with the RFID transponder for other purposes, for example, as stools, which means that no material is ordered and material is missing at the line. This material has to be reordered manually and possibly moved to the conveyor in a prioritised manner.
- Sources of interference for RFID are not directly visible, and therefore the search after the cause in case of problems is more time-consuming than with sensor polling.
- ESD load carriers are a known source of interference, as the RFID transponders are more difficult to read on these load carriers than on plastic load carriers. One solution is to increase the power of the reader or to use RFID transponders that are especially suitable for ESD.
- Costs for RFID transponders, infrastructure, and hardware costs have to be considered.

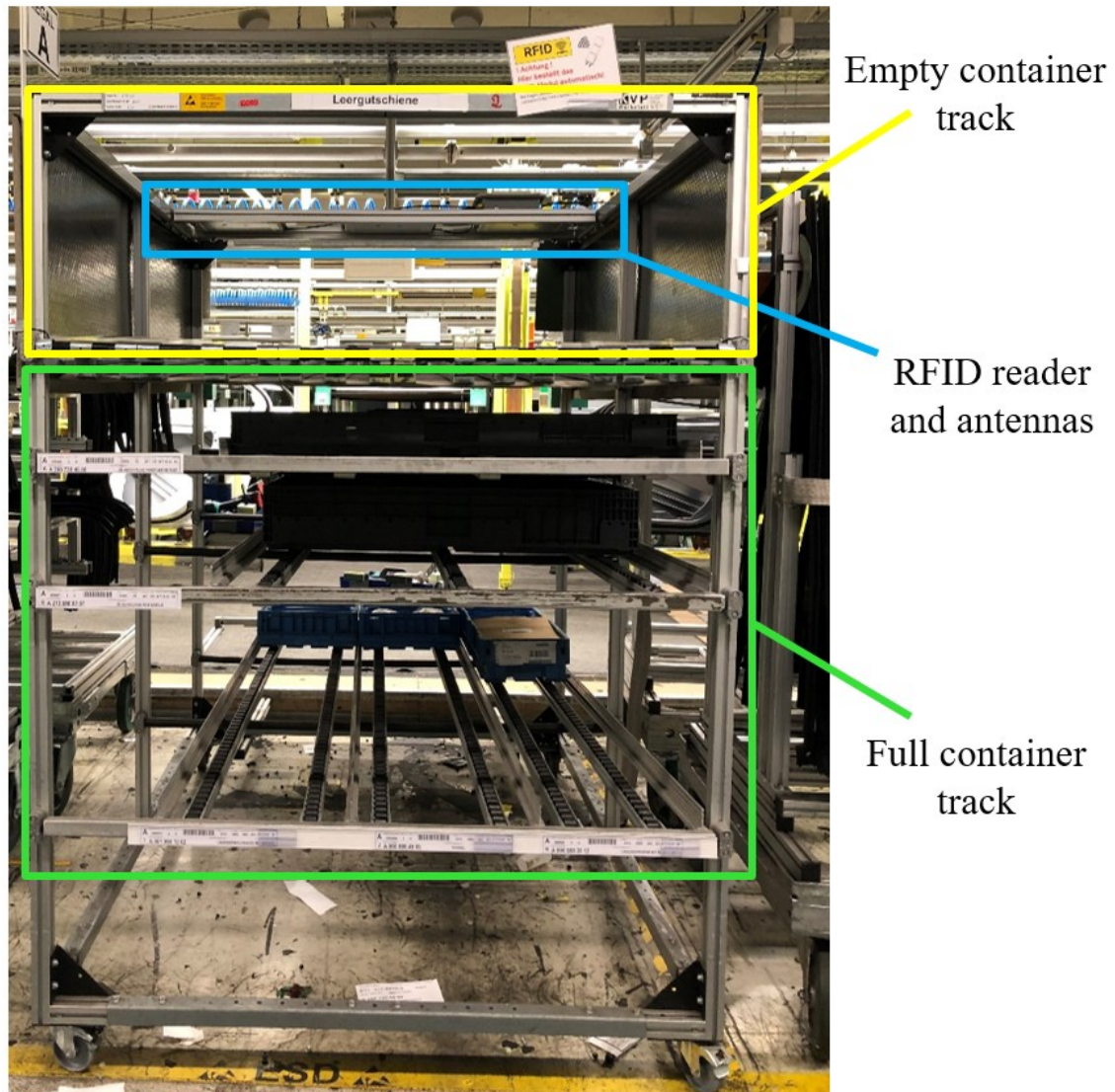


Figure 20 Shelf with RFID reader and antennas for automatic material retrieval

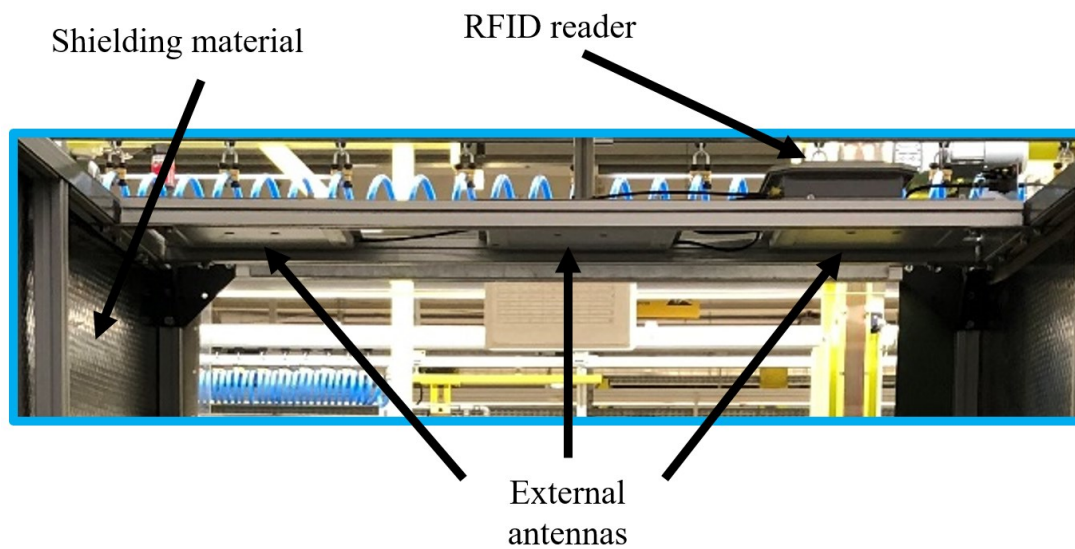


Figure 21 RFID reader and antennas on the shelf

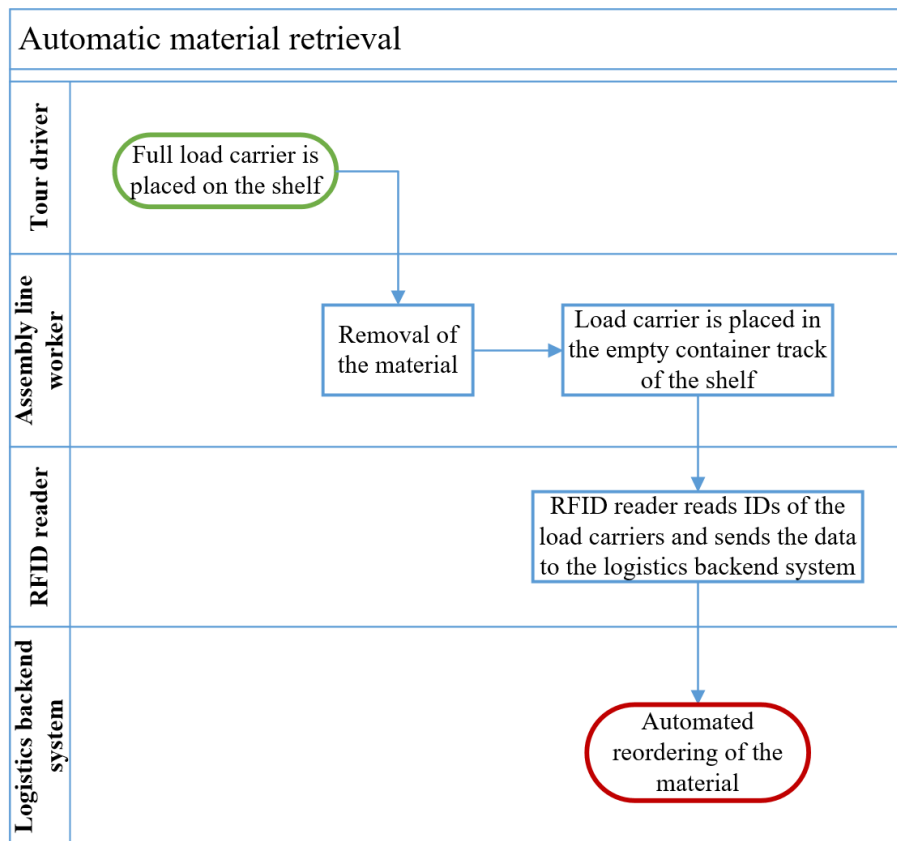


Figure 22 Automatic material retrieval process with RFID

### 2.2.3 Plausibility check at the body shop construction station with RFID

Another application in which the RFID transponders of load carriers are read is the plausibility check at the body shop. Here, an RFID reader is located at the body shop construction station. In the following, the process of the plausibility check at the body shop construction station is described (see Figure 23):

- 1) An employee transports the load carrier to the station using a forklift and places it there.
- 2) The RFID reader reads the UII of the transponder and transmits it to the programmable logic controller (PLC).
- 3) The PLC sends a request to the logistics back end system with the UII and receives information such as material number, quantity, batch, and best-before date.
- 4) Then the PLC checks whether it is the correct material. If it is the correct material, then the open transport order is acknowledged automatically, and the material is ready to be picked up by the robot. If not, the load carrier must be exchanged.

The use of RFID at the body shop construction station has the following advantages:

- The transport order is automatically acknowledged.
- It is not necessary to check with a scanner whether the correct components are in the load carrier (e.g., check for holes in certain places).

However, there is also a disadvantage due to the use of RFID at the body shop construction station:

- If the supplier packs the wrong material in a load carrier, this is not detected during the plausibility check.



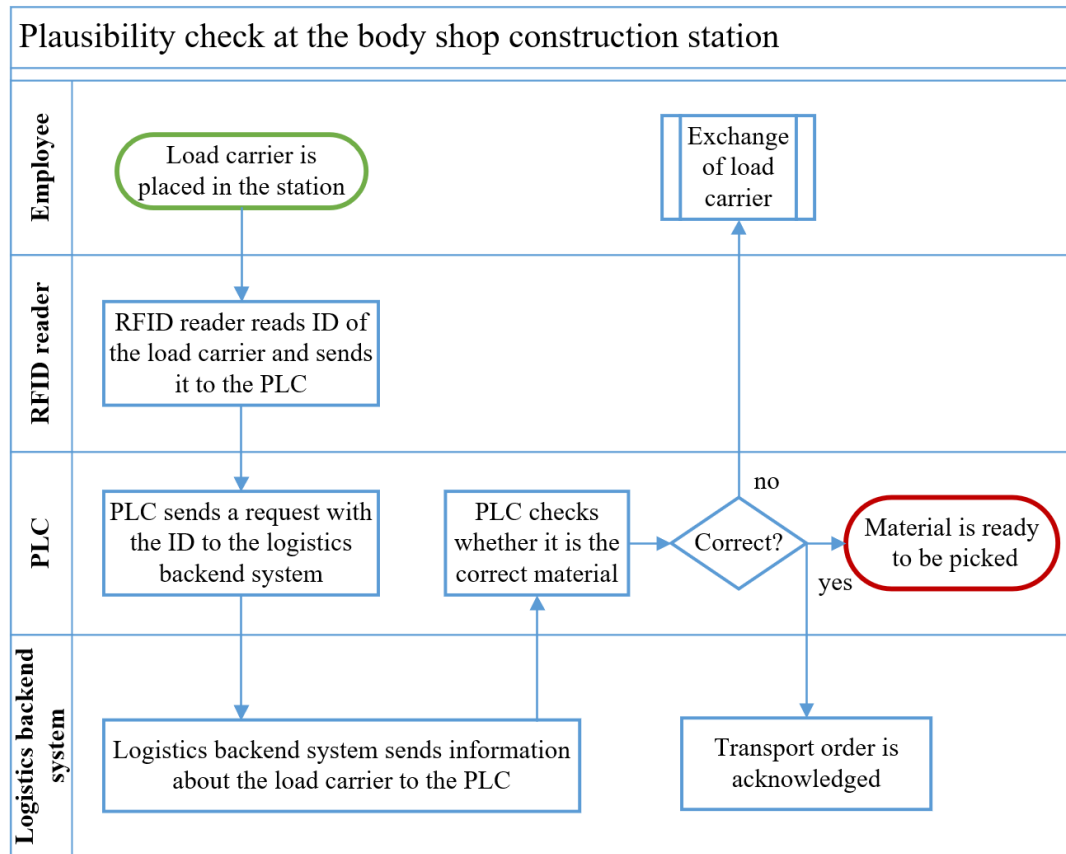


Figure 23 Plausibility check process at the body shop construction station

### 2.3 Rollout of RFID applications

The RFID applications described above have already been developed, piloted, and tested in series production. In order to benefit from RFID also in other areas, halls, and plants, these applications must be rolled out. In the following, the four basic phases of the rollout of RFID applications are described, which are derived from the readiness check of Mercedes-Benz AG, Sindelfingen (Mercedes-Benz AG, 2019).

#### Planning

The first step is the initialisation of the project for a rollout at a kick-off event with all project participants. In addition, a project overview is created and a process analysis of the actual process without and the target process with RFID is carried out. Furthermore, the scope of the rollout is defined, i.e., which RFID applications should be rolled out in which halls or plants, and the milestones are planned. The next step is to determine the quantity structure of the required RFID hardware. For each RFID application, there is standardised hardware and a standardised number of RFID readers and antennas. After that, the hardware procurement must be planned and the supplier connection must be planned so that the suppliers of the materials can equip the load carriers with RFID transponders and code them correctly. Furthermore, a potential assessment and budget planning is carried out in the planning phase, and a schedule is created.

#### Implementation

After the planning is done, the implementation continues. In this phase, the RFID hardware purchased is installed in the hall. Setup of the respective RFID application is done according to the respective guideline. There are two guidelines for RFID gates without direction recognition (see Section 2.4). In addition, RFID hardware is connected to IT systems. Furthermore, key users must be trained in this

phase. In this phase, the suppliers must equip the load carriers with RFID transponders, and the type of notification must be communicated.

### **Commissioning**

In the third phase, commissioning, a composite test is performed to ensure functionality from reading the transponder to the software application. In addition, an acceptance test of the RFID installations is performed to verify the functionality and detection rate. This is done only with RFID gates. The RFID gate acceptance process starts with the definition of a golden sample. A golden sample describes the set of different containers and load carriers, as well as the RFID transponders attached to them, which are used to determine the detection rate. Then the required or expected detection rate for this golden sample is defined, for example, 80 %. Now, the test to determine the detection rate is prepared. In the test, at least ten passes are made with the golden sample through the centre of the gate, and then the average detection rate is calculated. Finally, the results must be documented. If necessary, the orientation of the antennas is adjusted or other measures are taken by experts to improve the detection rate. If all tests are successful, the RFID installation is accepted, and operation can begin.

### **Operation**

During operation, the RFID installations are in use and continuously generate new data. During operation, stabilisation takes place, where the detection rates are continuously checked and adjustments are made to the RFID installation if necessary.

## **2.4 RFID gate parameters and guidelines**

In the following, the two exemplary RFID gate guidelines from the automotive industry used during the rollout of the application automatic goods receipt posting in the assembly are described. In both guidelines, each RFID gate has one RFID reader with four external directional antennas of the type WIRA 30 from Kathrein (Kathrein Solutions GmbH, 2011) as well as standardised cables, adapters, cold-device plugs, brackets, and a collision guard. The antennas have an aperture angle of  $30^\circ$  horizontal and  $70^\circ$  vertical if mounted as in Figure 24. The adjustable parameters for the alignment of the antennas of RFID gates are the height  $h_i$ , the mounting angles vertically  $\gamma_i$  and horizontally  $\partial_i$  for each antenna  $i$  as shown in Figures 24 and 25. In Figure 24 of the side view of an RFID gate, the antennas 2 and 4 have the vertical angle  $\gamma_{2,4} = 0^\circ$ , antenna 1  $\gamma_1 = 30^\circ$  and antenna 3  $\gamma_3 = -30^\circ$ . The horizontal angle of antenna 1 in Figure 25 is  $\partial_1 = -20^\circ$  and of antenna 3  $\partial_3 = 20^\circ$ . In this figure, the horizontal angles of antennas 2 and 4 are not drawn for clarity.

The parameters of the two exemplary RFID gate guidelines are shown in Table 6 (guideline 1) and Table 7 (guideline 2). In both guidelines, the vertical mounting angles are  $0^\circ$  and the lower antennas are at a height of approximately 115 cm. What differs is the height of the upper antennas, which is 210 cm for guideline 1 and 180 cm for guideline 2. In addition, guideline 1 has horizontal angles of  $0^\circ$ . In guideline 2, the antennas on the left side are aligned parallel to those on the right side, so that the larger distance between the outside of the antenna and the antenna holder is about 20 cm, as shown in Figure 27 and Figure 26. The reader's power is 28 dBm or 30 dBm according to the guideline, but users also can change this individually.

These two exemplary guidelines were developed on the basis of empirical knowledge and the trial-and-error principle but were not systematically compared or tested. Furthermore, there is no manual for the selection of one of the two guidelines. This must be decided during planning, implementation, or commissioning. Furthermore, no distinction is made according to the direction of travel of the forklift, the width of the gate, or the height of the load carriers that should be transported through the RFID gate.

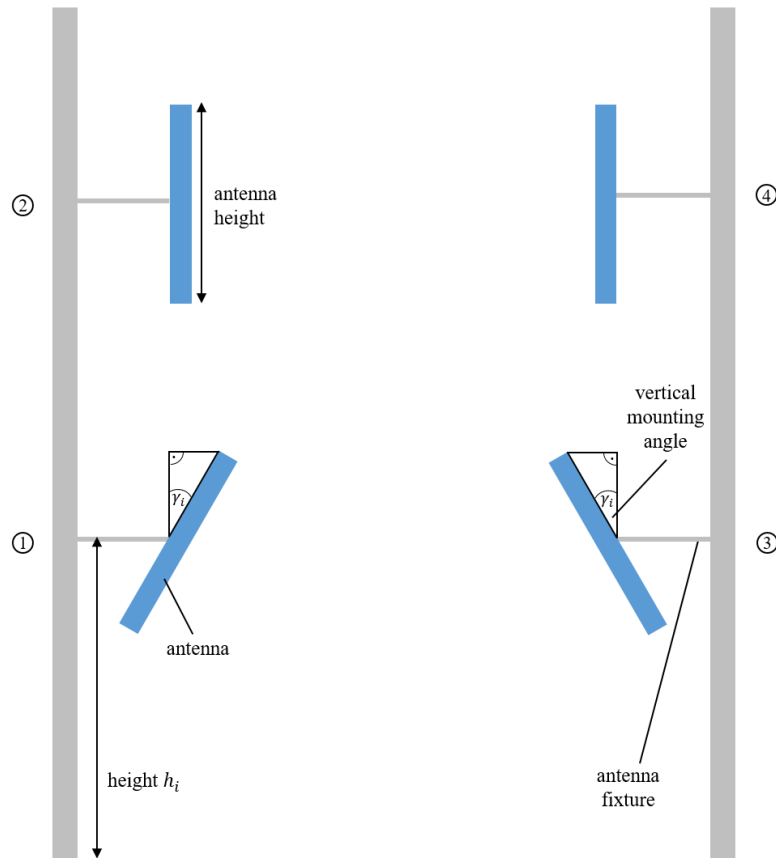


Figure 24 Side view of the RFID gate

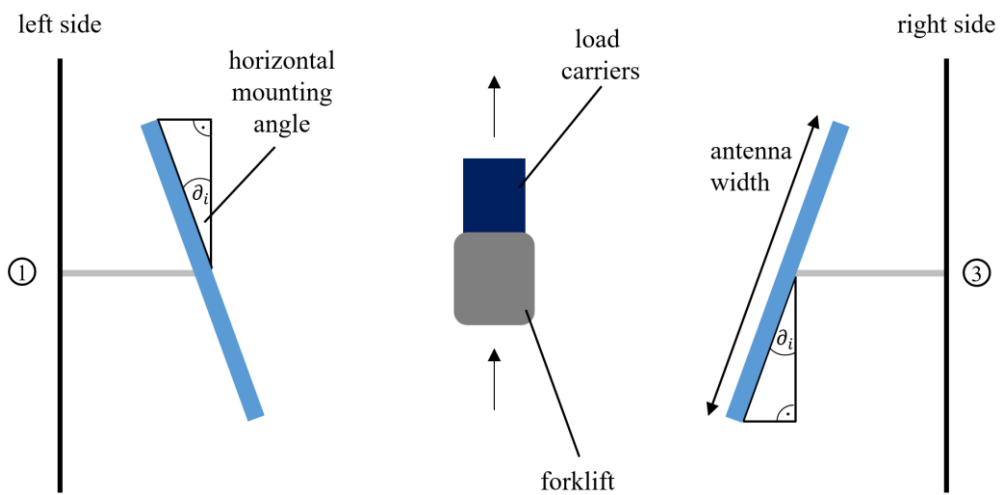


Figure 25 Top view of the RFID gate

Table 6 RFID gate guideline 1

Antenna	Position	Height	Vertical angle	Horizontal angle
1	Left bottom	115 cm	0°	0°
2	Left top	210 cm	0°	0°
3	Right bottom	115 cm	0°	0°
4	Right top	210 cm	0°	0°

## 2 Background

Table 7 RFID gate guideline 2

Antenna	Position	Height	Vertical angle	Horizontal angle
1	Left bottom	115 cm	0°	The antennas on the left side are parallel to the antennas on the right side of the RFID gate, as shown in Figures 27 and 28.
2	Left top	180 cm	0°	
3	Right bottom	115 cm	0°	
4	Right top	180 cm	0°	



Figure 26 RFID gate installed according to guideline 2

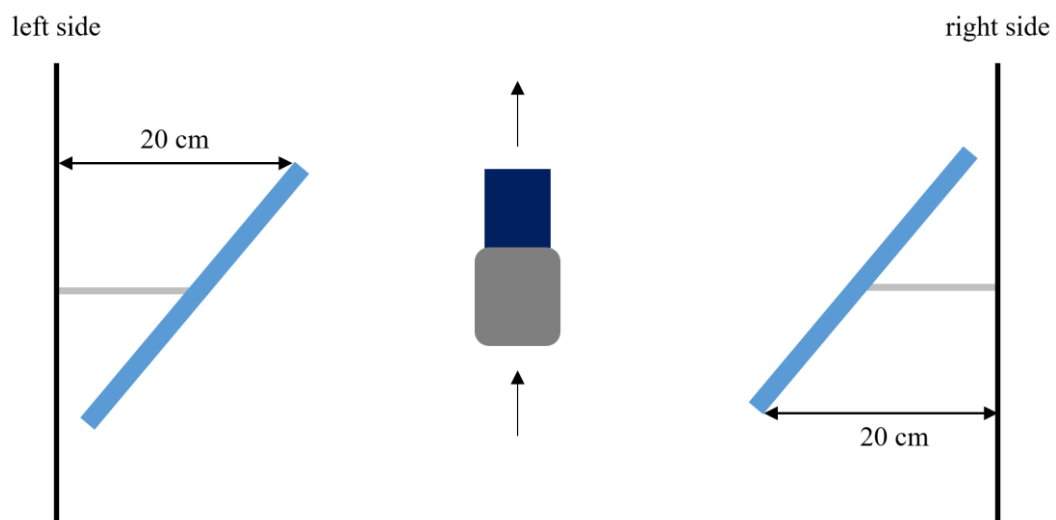


Figure 27 Top view of the RFID gate according to guideline 2

### 3 RFID network planning algorithm for RFID gates

In this chapter, a new approach is presented for the alignment of the antennas of an RFID gate.

#### 3.1 Literature review on RFID network planning algorithms

In order to find a better approach for determining the alignment of the antennas of an RFID gate than according to the previously described exemplary guidelines, which are based on expert knowledge and the trial-and-error principle, a systematic literature review is first carried out and the knowledge base is thereby expanded. In the literature, the problem of determining the required number of antennas / readers, their positioning, and partly also their power in RFID applications, taking into account various objectives, is solved by RFID network planning (RNP) algorithms. The most important objective is usually to achieve maximum transponder coverage so that as many transponders as possible are covered by the reading field of the antennas / readers. However, this objective contradicts the idea that the number of antennas or readers should be minimised in order to save costs. If the reading fields of two readers overlap, this can lead to collisions, which are also referred to as reader interference in this section, and to transponders being read more poorly. Therefore, preventing reader interference is often a goal in contrast to maximising coverage of all transponders. The minimisation of power can lead to the minimisation of reader interferences and serves to minimise power consumption, which must be taken into account in the total cost of an RFID network. Another objective is to optimise load balance, because “*a network with a homogeneous distribution of tags between readers can give a better performance than an unbalanced configuration*” (Jaballah & Meddeb, 2019). The RFID network planning problem is referred to as NP (non-polynomial) hard. (Jaballah & Meddeb, 2019; Strumberger et al., 2018b; Tuba et al., 2017; Zhao et al., 2017)

In the conducted literature review, the search term “*RFID network planning algorithm*” was used. Only publications since 2015 were taken into account to consider only current algorithms. The literature found was filtered by title, abstract, and thematic relevance. Therefore, the focus was placed on literature for RFID applications with UHF and passive transponders, as these are often used in industrial applications in the automotive industry. Table 8 shows an overview of the algorithms of the literature review and their partially contradictory objectives.

Table 8 Overview of RFID network planning algorithms

Algorithm	Year	Objectives
Guided Fireworks Algorithm (GFWA) (Tuba et al., 2017)	2017	- Maximisation of transponder coverage - Minimisation of the number of readers - Minimisation of reader collisions - Minimisation of reader power
Multi-Objective Firefly Algorithm (Zhao et al., 2017)	2017	- Maximisation of transponder coverage - Minimisation of the number of readers - Minimisation of reader interferences
Self Adaptive Cuckoo Search (Jaballah & Meddeb, 2019)	2019	- Maximisation of transponder coverage - Minimisation of the number of readers - Minimisation of reader interferences - Optimisation of load balance - Minimisation of power loss

Indicator-Based Multi-Objective Bacterial Colony Foraging Algorithm (Yuan et al., 2019)	2019	<ul style="list-style-type: none"> <li>- Maximisation of transponder coverage</li> <li>- Minimisation of reader interferences</li> <li>- Optimisation of load balance</li> <li>- Optimisation of efficiency</li> </ul>
Artificial Bee Colony (ABC) Algorithm (Bacanin et al., 2015)	2015	<ul style="list-style-type: none"> <li>- Maximisation of transponder coverage</li> <li>- Minimisation of the number of readers</li> <li>- Minimisation of reader interferences</li> <li>- Minimisation of reader power</li> </ul>
Optimizing radio frequency identification network planning through ring probabilistic logic neurons (Azizi et al., 2016)	2016	<ul style="list-style-type: none"> <li>- Maximisation of transponder coverage</li> <li>- Minimisation of the number of readers</li> <li>- Minimisation of antenna interferences</li> </ul>
Modified Monarch Butterfly Optimization (Strumberger et al., 2018b)	2018	<ul style="list-style-type: none"> <li>- Maximisation of transponder coverage</li> <li>- Minimisation of the number of readers</li> <li>- Minimisation of signal interferences</li> </ul>
Curling Algorithm for RNP (Zhang & Liu, 2017)	2017	<ul style="list-style-type: none"> <li>- Maximisation of transponder coverage</li> <li>- Minimisation of the number of readers</li> <li>- Minimisation of reader interferences</li> <li>- Minimisation of reader power</li> <li>- Optimisation of load balance</li> </ul>

The fireworks algorithm has already been used to solve numerous optimisation problems in different variants, such as spam detection or image compression (Li & Tan, 2020). The fireworks algorithm has also been used in various variants to solve the RFID network planning problem (Strumberger et al., 2018a; Tuba et al., 2015). One variant is the Guided Fireworks Algorithm (GFWA) described by Tuba et al. (2017), where guided sparks lead to a faster convergence of the algorithm. This variant pursues the four objectives: (i) to achieve high transponder coverage, (ii) to avoid reader collisions, (iii) to minimise the number of readers, and (iv) to minimise power of the reader. How well these objectives are achieved is determined by the fitness value, which is a weighted sum of transponder coverage and power. The number of readers is not represented by the fitness value due to the large impact on results. Therefore, a minimum and maximum number of readers is defined and the GFWA is run once for each possibility in order to have enough time to approach the optimal solution. The transponder coverage by the readers is calculated by a probabilistic coverage model, which takes into account uncertainties due to the environment and represents the detection field by a circle whose radius depends on the set power and indicates the range of the reader. It would also be possible to use a three-dimensional transponder coverage model, but the two-dimensional one was chosen for comparability with other RFID network planning algorithms. At the beginning of the algorithm, the population is initialised by generating  $n$  random fireworks within the search space. Each of these fireworks represents a potential solution to the RFID network planning problem, and for each firework the fitness value is calculated. Subsequently, the following steps are performed until the termination criterion of the GFWA is reached. First, the number of sparks  $n_{sp}$  and the explosion amplitude are calculated. Within the explosion amplitude,  $n_{sp}$  sparks are generated for each firework and new solutions are found in the search space. In addition, the guided sparks are generated for each firework, and the fitness value is calculated for all new solutions. From this set, the best solution and additional  $n-1$  individuals are transferred to the next generation. In the end, the result is the position and power of the individual with the best fitness value. The comparison with the other algorithms GPSO (traditional PSO (Particle Swarm Optimisation) with global topology), VNPSO (traditional PSO with the von Neuman topology), GPSO-RNP, VNPSO-RNP with Tentative Reader Elimination (TRE), and mutations shows the advantage of the GFWA. With a

smaller number of readers, a transponder coverage of 100 % could be achieved in different scenarios, and therefore hardware costs of the readers can be saved. (Tuba et al., 2017)

In the paper “Decomposition-based multi-objective firefly algorithm for RFID network planning with uncertainty” from Zhao et al. (2017), the use of the firefly algorithm to solve the RFID network planning problem is presented and the three objectives are to maximise transponder coverage, minimise the number of readers, and reduce reader interference. The detection field of the readers is modelled by a circle, and if a transponder is within this detection field, it can be read. The coverage model takes into account reader power, transponder and reader antenna gain, wavelength, backscatter transmission loss, and a variable to simulate ambient noise and thermal noise of the electronic components. In this algorithm, each firefly represents a possible solution to the optimisation problem, and each firefly contains for each reader the x and y coordinate, the power of the reader, and a variable, which indicates whether this reader is used or not. The firefly follows the three basic rules when determining a solution: (i) a firefly is attracted by other fireflies, the gender does not matter, (ii) the attractiveness is proportionally dependent on the brightness, i.e. the brighter the more attractive (for a maximisation problem) and inversely proportional to the distance between two fireflies, and (iii) the fitness determines the brightness of a firefly. At the beginning of the algorithm, a population of n fireflies is initialised, and each firefly is placed in a different area, thus creating good conditions for finding the global optimum. The Tchebycheff approach with a weight vector is used to divide the pareto front into evenly distributed quantities. After initialisation, each firefly is moved by the attraction of another brighter firefly. If the firefly is not attracted by a lighter one, the random walk with the virtual force algorithm is used to move the firefly. The random walk uses a mutation operator to ensure that a new reader is added randomly with a low probability. If this new firefly dominates individuals in the neighbourhood, then these are updated. After that, the population is updated, and for each newly created firefly, the individuals that are dominated by it are identified. All individuals dominated by this firefly are deleted from the population and the new dominant ones are added. The steps described above are repeated until the stopping criterion of the Multi-Objective Firefly Algorithm (MOFA) is met. The output of the algorithm is the set of pareto-optimal solutions. This algorithm (MOFA) was compared with the three algorithms NSGA (Non-dominated Sorting Genetic Algorithm), MOPSO (Multi-Objective Particle Swarm Optimisation), and NSGA-II. The MOFA algorithm provided better quality metrics and better generational distance. Furthermore, the algorithm developed was used in a practical application. The goal was to equip the training centre for liquefied petroleum gas with RFID readers so that transponders on machines, employees, and LNG (liquefied natural gas) components can be read with it. The goal is to track movements and progress. The RFID network planning algorithm has shown that the training centre requires eight RFID readers with different positions and powers. (Zhao et al., 2017)

The Self Adaptive Cuckoo Search (SACS) algorithm described in Jaballah and Meddeb (2019) is a further development of the Cuckoo Search (CS) algorithm, which was applied to the RFID network planning problem based on promising benchmark tests and has the following objectives: maximise transponder coverage, minimise the number of readers, minimise reader interference, optimise load balance and minimise power loss. Optimising transponder coverage is the top priority. The load balance is also taken into account so that all readers read the same number of transponders. This is especially important for battery-powered readers since readers that cover more transponders than others will also drain the battery faster. Furthermore, the aim is to minimise power loss outside the working range because this can interfere with other RFID networks in the immediate vicinity, and minimising power loss also saves energy. Transponder coverage is calculated based on the power of the reader, the gain of the transponder and reader antennas, the distance and the wavelength, and it is checked if the reader can still read the backscatter signal from the transponder. With the Self Adaptive Cuckoo Search algorithm, the step size and discovery probability are adjusted during execution and therefore do not need to be determined during initialisation. The step size is needed to generate new solutions and is influenced by

the distance between a cuckoo and the one with the best fitness, the rank of the fitness, and the current iteration. As a fitness function, a weighted sum with the rating functions is used. The discovery probability determines the probability that a bird will detect the foreign egg in the nest and throw it out. In each iteration, new solutions are calculated and evaluated based on the fitness, and the best nests are transferred to the next generation until the abort criterion is reached. The ultimate objective is to achieve a high transponder coverage, therefore starting with a number of readers that enable a transponder coverage of 100 %. To minimise the number of readers, the tentative reader elimination operator is used, which deletes the reader that has the least transponder coverage. If within the following generations the coverage rate does not go back to 100 %, the reader is added again. Comparisons with the original CS, the four adaptive CS variants, the GA (Genetic Algorithm) and the PSO showed “*that only the SACS algorithm guarantees full tag coverage with a smaller number of deployed readers*” (Jaballah & Meddeb, 2019). The algorithm was not only compared to others, but was also used as a practical example for the planning of the research laboratories at the National Engineering School of Sousse. The goal is to track how long students stay in the labs, see the availability of instruments, automatically detect if a lab is empty, and then intelligently control the lights and air conditioning. The optimal result of the algorithm determined that eight readers are needed. (Jaballah & Meddeb, 2019)

The Indicator-Based Multi-Objective Bacterial Colony Foraging Algorithm (I-MOBFA) presented in Yuan et al. (2019) pursues the following objectives: maximise transponder coverage, minimise interference, find optimal load balance and improve overall efficiency. The overall efficiency should be emphasised in the desired objectives because this objective is not taken into account by the other RFID network planning algorithms presented here. This means that readers should be placed near the centre of a transponder cluster due to “*the stochastic noise, multi-path effect, and attenuation in the propagation channel*” (Yuan et al., 2019). Therefore, a K-Mean cluster algorithm is used to identify the transponder clusters and then the distance of the centre to the reader can be calculated. The algorithm is a further development of the Bacterial Foraging Optimisation (BFO), which optimises the bacteria's search for food by using a self-adaptive search and “*bacterial cell-to-cell communication mechanism at colony level*” (Yuan et al., 2019). The Indicator-Based Multi-Objective Bacterial Colony Foraging algorithm was compared with the NSGAII and the SPEA2 (Strength Pareto Evolutionary Algorithm) in benchmark tests and this showed that the I-MOBFA strength Pareto “*finds the best computational results in terms of mean, best and standard deviation on most test instances*” (Yuan et al., 2019).

The objectives of the Artificial Bee Colony (ABC) algorithm described in Bacanin et al. (2015) are to maximise transponder coverage, minimise the number of readers, minimise interference, and minimise reader power. The order in which the objectives are listed reflects their priorities, i.e., the most important objective is to maximise transponder coverage, and the least important is to minimise reader power. The first step of the algorithm is to determine the number of readers and their approximate position. The second step is to optimise transponder coverage, reader interference, and reader power using the ABC algorithm. The ABC algorithm simulates the foraging of bees. The ABC algorithm was benchmarked against GPSO (traditional PSO with the global topology), VNPSO (traditional PSO with the von Neumann topology), GPSO-RNP, and VNPSO-RNP. In all tests, the ABC algorithm achieved 100 % coverage with a lower number of readers. (Bacanin et al., 2015)

The Ring Probabilistic Logic Neuron Algorithm proposed in Azizi et al. (2016) pursues the typical objectives: maximising coverage rate, minimising number of antennas, and minimising antenna collisions. The algorithm is divided into several parts. First, the number of antennas is set equal to the number of transponders distributed in the workspace. Then the Redundant Antenna Elimination (RAE) function calculates how many of these antennas are redundant. This is done by eliminating one antenna after the other, and if the coverage deteriorates as a result, it is added again. Then the optimisation of the objectives is performed and for comparison, the three variants GA, PSO and RPLN (Ring



Probabilistic Logic Neuron) were implemented. The GA and PSO work similarly, because both start with a population, which is changed in several iterations, taking into account the fitness. However, the PSO does not have evolution operators like mutation or recombination. Fitness depends on transponder coverage and interferences. In the RPLN, as in the GA and PSO, a population is initialised first and for each individual a PLN with random input and output values is assigned to each gene. The PLNs are trained using purely random searches, taking fitness into account. The comparison of GA, PSO and RPLN showed that the RPLN algorithm requires fewer antennas and achieves less interference. Furthermore, the algorithm converges faster and requires fewer iterations. (Azizi et al., 2016)

In Strumberger et al. (2018b) the swarm based Monarch Butterfly Optimisation (MBO) algorithm is used to solve the RFID network planning problem with the objectives: maximising transponder coverage, minimising reader interference, and minimising the number of readers. In this algorithm, the power of the readers is constantly set to 2 W. A weighted fitness function of transponder coverage, interference, and number of readers is used to determine how well each objective is met. The transponder coverage is the most important factor. The MBO algorithm includes two mechanisms that are used in the search for new solutions: the migration operator and the butterfly adjusting operator. Furthermore, a hybrid approach is used in the last 10 % of iterations by using the recombination operator known from the GA. Because of that it is assumed that in the last iterations the right part of the search space is already found, and therefore only around the best solutions improvement takes place. In comparison with the GA and PSO the MBO algorithm performed better, because with the same number of readers more transponders could be covered and a better fitness could be achieved. (Strumberger et al., 2018b)

The Curling Algorithm for RNP (CA-RNP) described in Zhang and Liu (2017) is a new algorithm for solving the RFID network planning problem and pursues the following five objectives: high coverage rate, minimisation of readers, minimisation of reader interference, reduction of power, and optimisation of load balance. Each reader is represented by a curling whose size is determined by its power. The working area where the transponders are located is the ice rink and each transponder placed on the ice surface has a part of the frictional force and slows down the curling (reader). At the beginning of the algorithm, new readers are gradually distributed on the ice until the required transponder coverage is reached. The readers that cover the fewest transponders are deleted. To find new solutions, the reader movement operator is used. If the reader reaches the limits of the ice rink or the working area, it bounces back and the reader collision operator is used. The algorithm has been tested on different instances with different workspace and transponder distributions, and it was found that the CA-RNP is efficient and fast, especially for more complex instances. The comparison with the GA and PSO showed that the CA-RNP “*can also get the best solutions*” (Zhang & Liu, 2017).

The algorithms described above assume readers with omni-directional antennas and model the reading field as a circle with a radius. For this reason, existing algorithms cannot be applied to an RFID gate with directional antennas and vertical and horizontal mounting angles. (Knapp & Romagnoli, 2021)

### **3.2 Methodology and implementation of the RFID network planning algorithm for RFID gates**

Since the existing RFID network planning algorithms analysed in the literature review are not designed for RFID gates, a new RFID network planning algorithm is developed, which is called the RGNP (RFID Gate Network Planning) algorithm.

The goal of the RGNP algorithm is to determine the number of required antennas, their heights, vertical mounting angles, and horizontal mounting angles, while minimising the number of antennas to save

costs, achieving maximum transponder coverage, and keeping the overlap of the antenna fields as small as possible.

Since directional antennas with a vertical and a horizontal aperture angle are typically used for RFID gates, the antenna field must first be modelled. The antenna field is therefore modelled two-dimensionally, once to represent the vertical and once to represent the horizontal aperture angle. The field is defined by two straight lines in a Cartesian coordinate system with a gradient depending on the aperture angle but also the mounting angle and the read range, as can be seen in Figure 28. An ideal antenna field is assumed, and therefore overreaches or reading holes are not considered when modelling the antenna field.

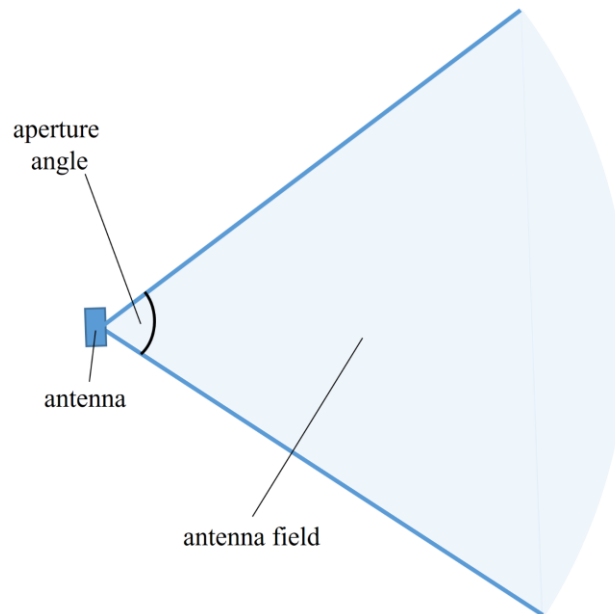


*Figure 28 Modelling of the antenna field, according to Knapp and Romagnoli (2021)*

Within an RFID gate, the transponders can be located in many different places, for example, according to the height of the load carriers. Therefore, an area is specified in which transponders can be located. The minimum and maximum possible height in the RFID gate and the width and passage length in the horizontal plane where a transponder can be placed determine this area.

To reduce complexity, the RFID gate is only considered in two dimensions, once from the side view and once from the top view. Therefore, the first part of the algorithm determines the number of antennas needed, their height, and vertical mounting angles. The number of antennas determined is the input of the second part, which determines the horizontal mounting angles. The number of antennas required is determined in the first part, as the vertical reading field has a greater influence than the horizontal one, as the load carriers and attached RFID transponders pass through the horizontal reading field.

Since the RFID network planning problem is an NP-hard problem, an evolutionary algorithm based on Weicker et al. (2003) is used for both parts, which modifies a population over several generations to determine a good solution. For this algorithm, boundary conditions must be defined to ensure that only valid and practicable solutions for antenna positioning and alignment are generated. The boundary conditions that every possible solution (individual) must ensure are for part 1:

- 1) 99 % transponder coverage,
- 2) no reflections with the ground to avoid reading holes,

- 3) antenna field must be inside the gate area,
- 4) the distance between two antennas must be minimum the antenna height, and
- 5) on both sides, the same number of antennas should be placed.

The boundary condition for part 2 is that the antenna field must be inside the gate area. In this algorithm, the assumption is that if all transponders are covered by the antenna fields, and if reflections with the ground are avoided, the detection rate increases.

The evaluation functions are needed to compare different solutions (individuals) out of the population of the evolutionary algorithm. The evaluation functions for part 1 are:

- 1) minimise the number of antennas (and thereby costs),
- 2) optimise load balance of antenna fields,
- 3) minimise overlapping of the antenna fields.

For part 2, the evaluation functions are:

- 1) maximise coverage rate,
- 2) optimise load balance,
- 3) minimise overlapping of antenna fields.

In both parts, first a population is initialised, which means several possible solutions are generated. Then a repair function is called to ensure that the boundary conditions are met. Subsequently, for every possible solution, the rank is calculated. In each generation, the population is changed. This rank is used to select two parents (individuals). Then these are modified by using directed mutation, random mutation, or recombination to create a new individual. Afterwards it is evaluated, if the new generated individual is included in the population and replaces another one. After the defined number of generations has passed, an individual is selected from the population, which represents the new antenna configuration for the RFID gate. (Knapp & Romagnoli, 2021)

Further details of the methodology and implementation of the RGNP algorithm are described in Knapp and Romagnoli (2021).

### **3.3 Verification of the RFID network planning algorithm for RFID gates**

To verify the algorithm, it is applied to the case study automatic goods receipt posting with RFID gate and compared with the two exemplary guidelines (see Section 2.4). Table 9 shows the antenna configuration according to the RGNP algorithm for this case study (see also Knapp and Romagnoli (2021)). To compare the antenna configuration of the RGNP algorithm with the two exemplary guidelines, three tests are carried out at the RFID gate in the automatic small parts warehouse of Mercedes-Benz AG, Sindelfingen (see Figure 29). For all three tests, the same golden sample is used, which consists of six containers arranged as shown in Figure 30. Four containers of this golden sample consist of ESD small load carriers, and two containers consist of plastic small load carriers. A total of 104 RFID single-use transponders of the type Confidex eKanban are attached to the small load carriers of the containers with adhesive tape. On the lids of the containers and on the forklift itself permanent multi-use RFID transponders are attached. However, these are not taken into account in the three tests for verification because multi-use RFID transponders are typically read better than single-use RFID transponders. For each test, 10 passes are made backwards through the RFID gate and the readings are

recorded with the Kathrein ReaderStart software. The reader settings are the same for all three tests and can be seen in Table 10.

After the three tests were performed, the average detection rates are calculated in Excel. Average detection rates are calculated as in Eq. 4, where  $n$  is the number of passes and  $m$  is the number of RFID transponders. The average detection rate of single-use transponders using guideline 1 is 46.06 %. The detection rate using guideline 2 is 43.27 % and the detection rate using the RGNP algorithm is 34.23 %. The detection rates of the single-use RFID transponders per container can be seen in Table 11.

$$\overline{detection\ rate}_{total} = \frac{1}{n} \frac{1}{m} \sum_{i=1}^n \sum_{j=1}^m x_{ij} \quad Eq. 4$$

Table 9 Results of the RFID network planning algorithm for the case study, according to Knapp and Romagnoli (2021)

Antenna	Position	Height	Vertical angle	Horizontal angle
1	Left bottom	60 cm	-30°	-15°
2	Left top	150 cm	-15°	15°
3	Right bottom	60 cm	-30°	10°
4	Right top	150 cm	-15°	-20°

Table 10 Reader parameters for verification of the RFID network planning algorithm

Parameter	Value
Power	28.00 dBm
Communication profile	8: Tx:80kbps/Rx:320kbps/FM0
Channels	4, 7, 10, 13
Session	1

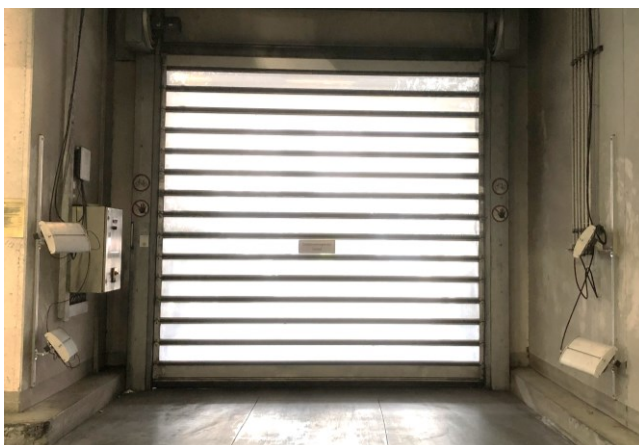


Figure 29 RFID gate at the goods receipt at the automatic small parts warehouse



Figure 30 Golden sample for verification of the RFID network planning algorithm

*Table 11 Results of the verification of the RGNP algorithm*

<b>Average detection rate</b>	<b>Guideline 1</b>	<b>Guideline 2</b>	<b>RGNP algorithm</b>
Total	46.06 %	43.27 %	34.23 %
Container 1	25.33 %	14.00 %	27.33 %
Container 2	26.21 %	29.31 %	5.52 %
Container 3	37.33 %	24.67 %	30.67 %
Container 4	60.67 %	56.00 %	38.67 %
Container 5	70.00 %	71.33 %	56.00 %
Container 6	75.33 %	77.33 %	74.00 %

### 3.4 Discussion of the RFID network planning algorithm for RFID gates

The advantage and contribution of the new RGNP algorithm is that it can be applied to RFID gates, unlike the RFID network planning algorithms identified through the literature review (see Section 3.1), which assume readers with omni-directional antennas. For this purpose, the antenna field of directional antennas, which are often used in RFID gates, was modelled. Furthermore, the new RGNP algorithm ensures a vertical transponder coverage of 99 % and prevents reflections with the ground due to the defined boundary conditions. In addition, the number of antennas is minimised, the load balance is optimised and the overlapping of the antenna fields is minimised by the defined evaluation functions (Knapp & Romagnoli, 2021). The RGNP algorithm has determined that four antennas are needed to cover the transponder area and has confirmed the number of antennas used in the exemplary guidelines.

The total average detection rate of guideline 1 is about 3 % higher than the one of guideline 2. In particular, the two upper containers 1 and 3 are read significantly better with guideline 1, which can be explained by the higher antenna position of the upper antennas compared to guideline 2. The detection rate of the RGNP algorithm is approximately 12 % and 9 % lower compared to the exemplary guideline 1 and 2. Therefore, the verification has shown that this new RGNP algorithm is not suitable to determine a better antenna configuration than the exemplary guidelines. This means that the assumptions of the algorithm, which were followed using the boundary conditions and evaluation functions, could not be confirmed. For example, the orientation between the RFID antenna and transponder was not taken into account, but this has an influence on the reading behaviour (see Section 2.1). Furthermore, the RGNP algorithm does not determine the required power and is based only on the theoretical modelling of the antenna fields but does not take into account the real antenna fields and real detection rates.

## 4 Algorithm for optimal alignment of the antennas of the RFID gate

Since the RGNP algorithm did not meet the requirement to increase the detection rate compared to the exemplary guidelines, a new algorithm to align the antennas of the RFID gate is developed with a different approach, which is called the OARG (Optimal Alignment of RFID Gates) algorithm.

### 4.1 Methodology of the rule-based algorithm for optimal antenna alignment

The RGNP algorithm showed that four antennas are needed to cover the area where RFID transponders can be located inside the RFID gate. Therefore, in this approach, the number of antennas is used as a prerequisite, and the heights, horizontal and vertical angles, and additionally the power of the antennas are determined. The approach of the new OARG algorithm is based on the fact that the positioning and orientation between RFID transponders and antennas affect readability, as described in Section 2.1.3. Furthermore, an existing antenna configuration is used as the initial situation and then optimised by the OARG algorithm. As an initial antenna configuration, the antennas are mounted according to the exemplary guidelines or based on expert knowledge. The prerequisite is that the horizontal mounting angles are  $0^\circ$ . To determine the new antenna configuration, the detection rates and number of readings of several passes through the RFID gate and the positions of the RFID transponders and their orientations to the antennas (parallel or orthogonal) are analysed automatically. The application and methodology of the OARG algorithm are presented in Figure 31. First, all input parameters for the algorithm must be defined, which are the following:

- Minimum possible antenna height of the lower antennas
- Maximum possible antenna height of the upper antennas
- Maximum possible antenna power
- Direction of travel through the RFID gate (backwards or forwards)
- Height of stacked containers
- Initial antenna configuration:
  - Height of the antennas
  - Vertical mounting angle of the antennas
  - Power of the antennas
- CSV (comma-separated values) file with golden sample (see Figure 32):
  - Transponder id (transponder number)
  - UII of the RFID transponders
  - Positions of the RFID transponders (x: width, y: length, z: height)
  - Orientation of the RFID transponders to the antenna (mainly parallel or orthogonal)

Then several passes through the RFID gate must be made with the defined golden sample, and the data with the readings of the RFID transponders from each pass must be stored in a separate CSV file (see Figure 33). This file contains one row for every transponder reading with the length of the UII (EPC), the UII (EPC) itself, the port (which indicates by which antenna the transponder was read), the RSSI, the RSSI in dBm, the time of first and last reading, the cycles, and the used frequency. The algorithm is executed with the input parameters and the CSV files of the readings. The output of the algorithm is the new antenna configuration (height, vertical angles, horizontal angles, and power). If it is different from the previous one, the user must adjust the antennas according to it. Then, in the second iteration, several passes through the RFID gate are made again, the algorithm is executed, and the new antenna configuration has to be applied. This procedure is repeated for so many iterations until the optimal

#### 4 Algorithm for optimal alignment of the antennas of the RFID gate

antenna alignment according to the algorithm has been found, and the algorithm no longer detects any changes in the antenna configuration to improve the detection rate.

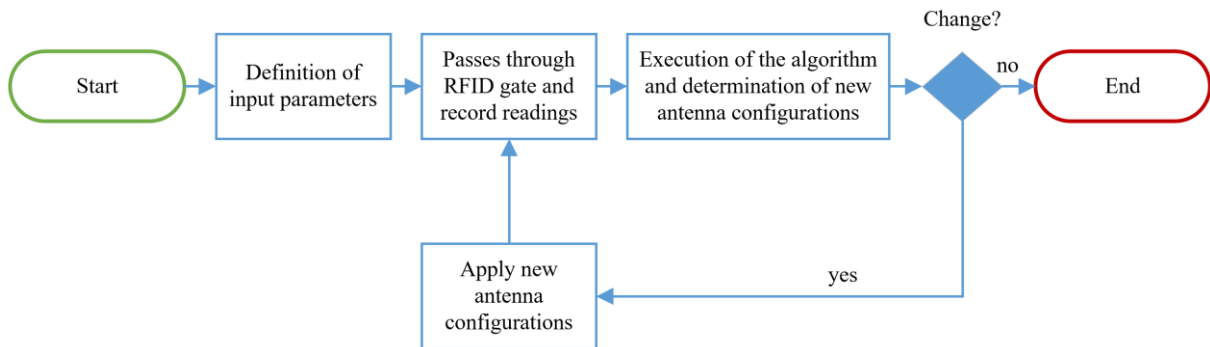


Figure 31 Application and methodology of the OARG algorithm

	A	B	C	D	E	F
1	tag id	uii	x	y	z	orientation
2	1	C4A1D3D39E39E79C34D141F0C30C30C30C618	38	0	23	orthogonal
3	2	C4A1D3D39E39E79C34D141F0C30C30C30C30CA18	38	0	31	orthogonal
4	3	C4A1D3D39E39E79C34D141F0C30C30C30C30CE18	26	0	49.5	orthogonal
5	4	C4A1D3D39E39E79C34D141F0C30C30C30C30D218	26	0	57.5	orthogonal
6	5	C4A1D3D39E39E79C34D141F0C30C30C30C30D618	38	0	75.5	orthogonal
7	6	C4A1D3D39E39E79C34D141F0C30C30C30C30DA18	38	0	83.5	orthogonal
8	7	C4A1D3D39E39E79C34D141F0C30C30C30C30DE18	84	0	23	orthogonal
9	8	C4A1D3D39E39E79C34D141F0C30C30C30C30E218	84	0	31	orthogonal
10	9	C4A1D3D39E39E79C34D141F0C30C30C30C30E618	74	0	49.5	orthogonal
11	10	C4A1D3D39E39E79C34D141F0C30C30C30C31C218	74	0	57.5	orthogonal
12	11	C4A1D3D39E39E79C34D141F0C30C30C30C31C618	84	0	75.5	orthogonal
13	12	C4A1D3D39E39E79C34D141F0C30C30C30C31CA18	84	0	83.5	orthogonal
14	13	C4A1D3D39E39E79C34D141F0C30C30C30C31CE18	100	35	23	parallel
15	14	C4A1D3D39E39E79C34D141F0C30C30C30C31D218	100	35	31	parallel
16	15	C4A1D3D39E39E79C34D141F0C30C30C30C31D618	100	26	49.5	parallel

Figure 32 Part of a golden sample CSV file

	A	B	C	D	E	F	G	H	I	J
1	EPC length	EPC	Port		RSSI	RSSI DBM	First Reading	Last Reading	Cycles	Frequency
2	160	C4A1D3D39E39E79C34D141F0C30C30C30C35D218	1		60	-86,6	2022-03-24T17:18:12.5654004+01:00	2022-03-24T17:18:12.5889852+01:00	120,9	865,7
3	160	C4A1D3D39E39E79C34D141F0C30C30C30C35D218	1		62	-85,3	2022-03-24T17:18:12.5654004+01:00	2022-03-24T17:18:12.7148114+01:00	154,6	867,5
4	160	C4A1D3D39E39E79C34D141F0C30C30C30C35D218	1		62	-85,3	2022-03-24T17:18:12.5654004+01:00	2022-03-24T17:18:12.7656615+01:00	112,5	865,7
5	160	C4A1D3D39E39E79C34D141F0C30C30C30C35D218	1		65	-83,1	2022-03-24T17:18:12.5654004+01:00	2022-03-24T17:18:13.1457508+01:00	101,2	867,5
6	160	C4A1D3D39E39E79C34D141F0C30C30C30C35D218	1		66	-82,2	2022-03-24T17:18:12.5654004+01:00	2022-03-24T17:18:13.2966374+01:00	168,7	866,9
7	160	C4A1D3D39E39E79C34D141F0C30C30C30C35D218	1		66	-82,2	2022-03-24T17:18:12.5654004+01:00	2022-03-24T17:18:13.3906344+01:00	42,1	865,7
8	160	C4A1D3D39E39E79C34D141F0C30C30C30C35E218	1		64	-84,1	2022-03-24T17:18:13.3936296+01:00	2022-03-24T17:18:13.4006259+01:00	112,5	865,7
9	160	C4A1D3D39E39E79C34D141F0C30C30C30C70DA18	1		64	-84,1	2022-03-24T17:18:13.4036278+01:00	2022-03-24T17:18:13.4606971+01:00	84,3	865,7
10	160	C4A1D3D39E39E79C34D141F0C30C30C30C36E218	3		62	-85,3	2022-03-24T17:18:13.4626994+01:00	2022-03-24T17:18:13.5136939+01:00	137,8	865,7
11	160	C4A1D3D39E39E79C34D141F0C30C30C30C70DA18	1		65	-83,1	2022-03-24T17:18:13.4036278+01:00	2022-03-24T17:18:13.5686987+01:00	154,6	866,3
12	160	C4A1D3D39E39E79C34D141F0C30C30C30C35E218	1		65	-83,1	2022-03-24T17:18:13.3936296+01:00	2022-03-24T17:18:13.5707348+01:00	160,3	866,3
13	160	C4A1D3D39E39E79C34D141F0C30C30C30C30DA18	1		65	-83,1	2022-03-24T17:18:13.5726996+01:00	2022-03-24T17:18:13.5747005+01:00	126,5	866,3
14	160	C4A1D3D39E39E79C34D141F0C30C30C30C35D218	1		65	-83,1	2022-03-24T17:18:12.5654004+01:00	2022-03-24T17:18:13.5767038+01:00	81,5	866,3
15	160	C4A1D3D39E39E79C34D141F0C30C30C30C30D618	1		65	-83,1	2022-03-24T17:18:13.5796971+01:00	2022-03-24T17:18:13.6767474+01:00	2,8	866,3

Figure 33 Part of the CSV file with the readings of the RFID transponders

#### 4.1.1 Procedure of the algorithm

The algorithm is based on how well the RFID transponders are read in the different areas bottom, middle, and top. Therefore, each transponder of a golden sample is automatically classified first into one of these three areas before the algorithm is executed. This must be done for every golden sample only once.

Figure 34 shows the procedure of the algorithm. First, the average detection rates and the number of readings are calculated. Then, the new heights or vertical angles are determined. Once the iterations to determine the new heights are completed, the new horizontal angles are calculated. Once the iterations to determine the new horizontal angles are completed, the new power is calculated. The height / vertical angles, the horizontal angles, and the power are not changed at the same time to eliminate interactions.

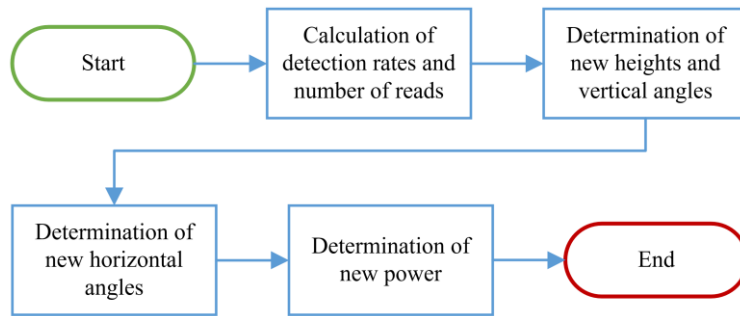


Figure 34 Procedure of the algorithm for optimal alignment of the antennas

#### 4.1.2 Calculation of the average detection rates

First, the average detection rates are calculated. Table 12 shows the notation definition for the calculations. The average detection rates are calculated for all transponders, parallel, orthogonal transponders, and the transponders in the bottom, middle, and top area of the golden sample as shown in Eq. 5 – Eq. 10. Thereby, the detection rate for each passage is calculated first and then the average for all passages. The variable  $x$  is 0 if a transponder was not recognised and 1 if it was identified at least once, as shown in Eq. 11. Furthermore, the average RSSI values in dBm are calculated analogously to visualise them to users, but they are not used in the OARG algorithm. The reason is that when calculating the average RSSI values, only the RSSI values of the transponders read can be taken into account, and therefore the expressiveness of the RSSI values is limited.

Table 12 Notation definition

Symbol	Definition
$n$	Number of passes through the RFID gate
$m$	Number of transponders of the golden sample
$m_{parallel}$	Number of transponders which are parallel to the antennas
$m_{ortho}$	Number of transponders which are orthogonal to the antennas
$m_{bottom}$	Number of transponders which are in the bottom area of the golden sample
$m_{middle}$	Number of transponders which are in the middle area of the golden sample
$m_{top}$	Number of transponders which are in the top area of the golden sample
$p$	Number of readings

Eq. 5



$$\overline{detection\ rate}_{total} = \frac{1}{n} \frac{1}{m} \sum_{i=1}^n \sum_{j=1}^m x_{ij}$$

$$\overline{detection\ rate}_{parallel} = \frac{1}{n} \frac{1}{m_{parallel}} \sum_{i=1}^n \sum_{j=1}^{m_{parallel}} x_{parallel_{ij}} \quad Eq. 6$$

$$\overline{detection\ rate}_{orthogonal} = \frac{1}{n} \frac{1}{m_{ortho}} \sum_{i=1}^n \sum_{j=1}^{m_{ortho}} x_{ortho_{ij}} \quad Eq. 7$$

$$\overline{detection\ rate}_{bottom} = \frac{1}{n} \frac{1}{m_{bottom}} \sum_{i=1}^n \sum_{j=1}^{m_{bottom}} x_{bottom_{ij}} \quad Eq. 8$$

$$\overline{detection\ rate}_{middle} = \frac{1}{n} \frac{1}{m_{middle}} \sum_{i=1}^n \sum_{j=1}^{m_{middle}} x_{middle_{ij}} \quad Eq. 9$$

$$\overline{detection\ rate}_{top} = \frac{1}{n} \frac{1}{m_{top}} \sum_{i=1}^n \sum_{j=1}^{m_{top}} x_{top_{ij}} \quad Eq. 10$$

$$x = \begin{cases} 0, & \text{transponder was not read} \\ 1, & \text{transponder was read at least once} \end{cases} \quad Eq. 11$$

### 4.1.3 Calculation of the number of reads

In addition to the average detection rates, the number of reads is also used to determine the horizontal angles. The number of reads is calculated for the orthogonal transponders as seen in Eq. 12 and analogously for the transponders aligned parallel to the antennas.

$$number\ of\ reads_{ortho} = \frac{1}{n} \frac{1}{m_{ortho}} \sum_{i=1}^n \sum_{j=1}^{m_{ortho}} \sum_{t=1}^p x_{ortho_{ijp}} \quad Eq. 12$$

### 4.1.4 Determination of new antenna heights and vertical angles

The goal of determination of new antenna heights and vertical angles is to cover the transponders of the height areas bottom, middle, and top as equally good as possible with the antenna fields. The algorithm detects if the antennas are placed too high or too low based on how well the bottom, middle, and top transponders were read. Figure 35 for example shows an RFID gate with several containers where it is clearly visible that the transponders located on the uppermost container are not optimally covered by the antenna field because the antennas are placed too low. Vertical angles are only changed if the heights have reached their minimum or maximum possible position because this leads to changes in the orientation between the antennas and transponders, which could influence readability (see Section 2.1.3).

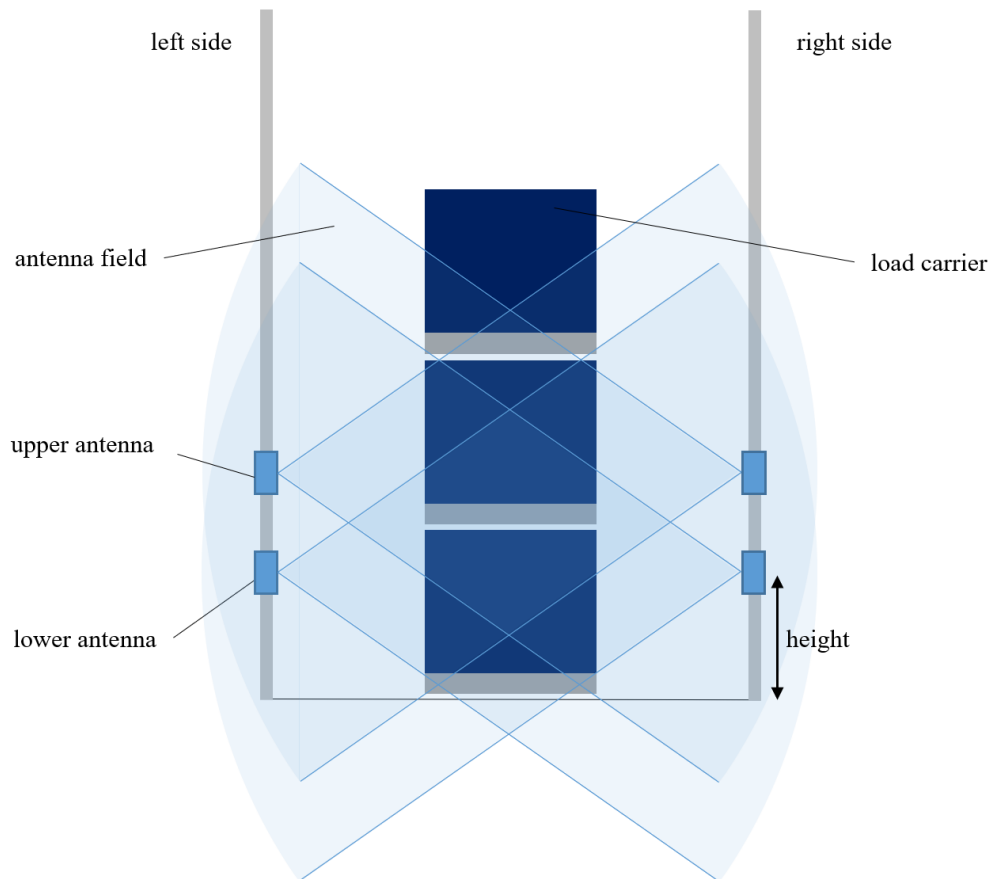


Figure 35 Antenna heights and simulated antenna field of an RFID gate

Figure 36 shows the procedure for determining new heights and vertical angles of the antennas. By means of a flag, it is stored whether the final height has already been determined. First, it is checked by use of this flag if the height determination is finished. If this is true, the heights are not changed any further, and the algorithm continues with the determination of the horizontal angles.

If the determination of the heights is not finished, then it is continued with the next else if statement. If it is not the first iteration or the average total detection rate has not improved, then the last changes of the antenna heights or vertical angles are undone. Additionally, the flag is set to indicate that the determination of new heights or vertical angles is finished. Then the previous iteration is saved as the best iteration.

If it is the first iteration or the overall average detection rate has improved, then it is calculated whether the transponders in the top area are read worse than in the middle or bottom area (top worse). It is also calculated whether the transponders in the middle area are read worse than in the top or bottom area (middle worse) and it is calculated whether the transponders in the bottom area are read worse than in the middle or top area (bottom worse). Depending on this, it is decided whether the upper or lower antennas are moved up or down or not changed in height, as can be seen in Table 13. The degree to which the height is adjusted is defined as a parameter and set to 25 cm. If the height changes exceed the maximum or minimum possible height, then the vertical angle is changed by 20 % instead. If the antenna configuration has not changed as a result, then the flag is set to end the determination of new heights or vertical angles and this iteration is saved as the best one.

#### 4 Algorithm for optimal alignment of the antennas of the RFID gate

Table 13 Determination of the new antenna height depending on top worse, middle worse, and bottom worse

Top worse	Middle worse	Bottom worse	Upper antennas	Lower antennas
true	false	true	move up	move down
true	true	false	move up	move up
true	false	false	move up	no change
false	true	true	move down	move down
false	false	true	no change	move down
false	true	false	move down if upper detection rate is better than bottom	move up if bottom detection rate is better than upper
false	false	false	no change	no change
true	true	true	no change but should not happen	

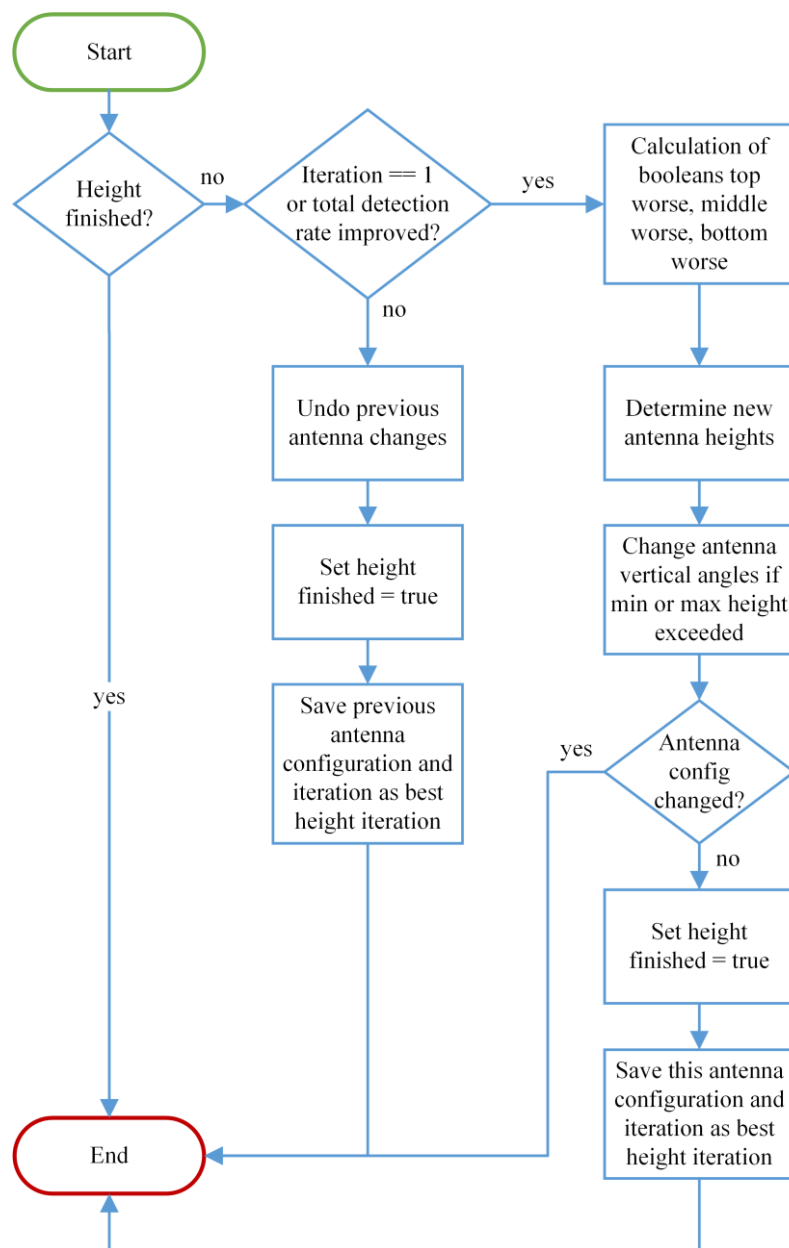


Figure 36 Flowchart of the algorithm to determine new antenna heights and vertical angles

### 4.1.5 Determination of new horizontal angles

After the new heights / vertical angles have been determined, the horizontal angles are changed next.

The scientific basis for the determination of the horizontal angles is that the reading behaviour depends on the angles between the reader antenna and the transponder (see Section 2.1.3). The initial situation is that the horizontal angles are at  $0^\circ$ , which means the parallel transponders are read optimally and the orthogonal transponders poorly. The approach here is to increase or decrease horizontal angles so that the orthogonal transponders are read better. If the total detection rate deteriorates compared to the previous iteration, then the last change is reversed.

The procedure for determining the new horizontal angles is shown in Figure 37. Again, a flag is used to store whether the horizontal angles should be optimised further. If this is true, it is checked if the horizontal angles have not changed compared to the previous iteration, which means that they are changed for the first time or if the detection rate has improved if the horizontal angles have already been changed. If the total detection rate has not improved compared to the previous iteration, then the last changes of the horizontal angles are undone and the flag is set that the determination of the new horizontal angles is finished.

If the detection rate has improved compared to the previous iteration or the angles have not been changed before, then it is checked whether the transponders aligned orthogonally to the antenna are read worse than the transponders aligned parallel. For this purpose, the detection rate of the orthogonal transponders is subtracted from the detection rate of the parallel ones and compared to a threshold value, which is 2 %. It is also checked if the number of reads of the parallel aligned transponders is greater than that of the orthogonal aligned transponders. If the orthogonal transponders are not read better, then the flag is set that the determination of the horizontal angles is finished. Otherwise, the angles are changed depending on the direction of travel. When the driving route is forwards, the horizontal angles of the antennas are increased on the right and decreased on the left side. When driving backwards through the RFID gate, the horizontal angles on the left side are increased and on the right side decreased. Angles are increased and decreased by  $20^\circ$ .

The distinction between the direction of travel is made so that the forklift shields the transponders as little as possible. This is illustrated in Figures 38 and 39, where the forklift drives once forwards and once backwards through a gate, where the horizontal angles have been increased on the left and decreased on the right. When driving backwards through the gate, it can be seen that the signals from the antennas in the middle image are partially shielded by the forklift, which is not the case when driving forwards through the gate.

If the minimum or maximum possible angles are exceeded due to the changes in the horizontal angles, these are set to the minimum or maximum possible angles. If this does not result in any change of the angles, the determination of the horizontal angles is completed and the corresponding flag is set.

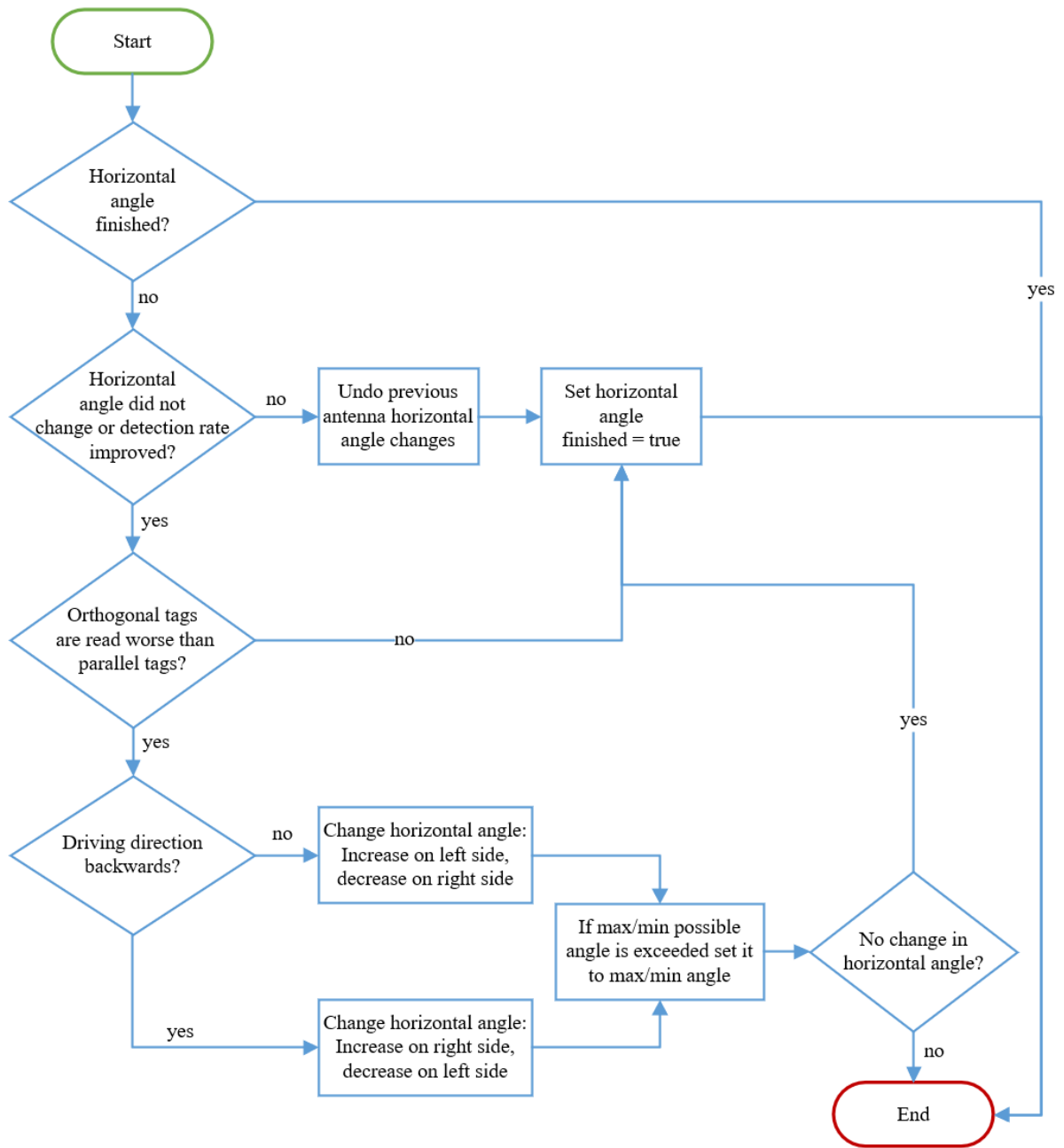


Figure 37 Flowchart of the algorithm to determine new horizontal angles

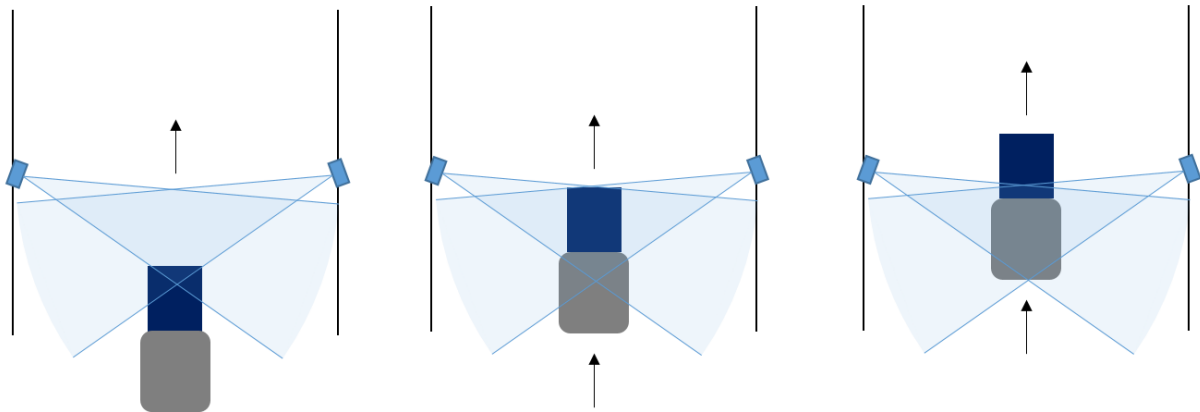


Figure 38 Exemplary gate passage forwards

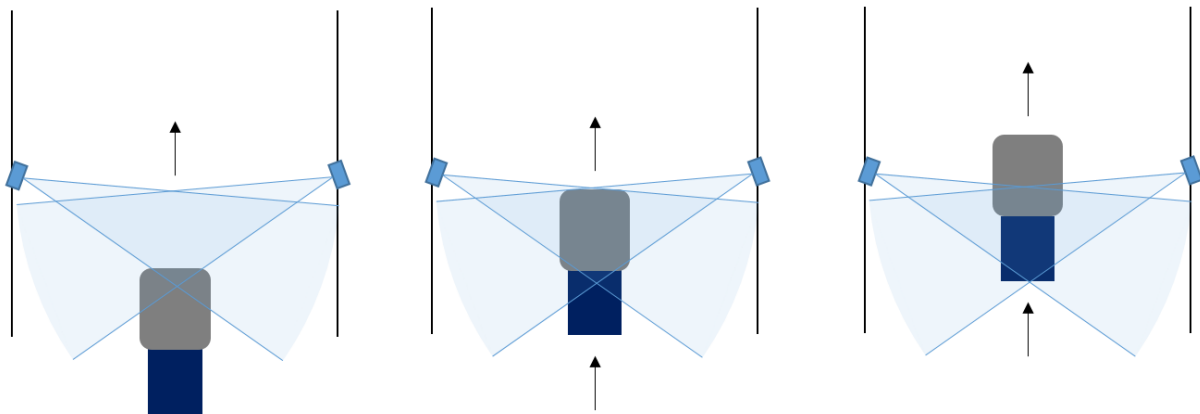


Figure 39 Exemplary gate passage backwards

#### 4.1.6 Determination of new power

Finally, the optimal power is determined. In this approach to align the antennas, it is started with the lowest possible power, as higher powers can lead to more reflections from the environment and unwanted transponders being read. Figure 40 shows the procedure for determining the new power.

The power is increased step by step, and also here a flag is used to store whether the determination of the power is finished. If not, it is checked whether the total detection rate is already at 100 % and if so, the flag is set to true. If the detection rate is not at 100 % it is checked if the power has already been changed. If this is true, then it is checked if the detection rate has improved compared to the previous iteration. If the detection rate has not improved, then the previous change of the power is undone, and the flag is set, which ends the determination of the power.

If the power has not changed yet or the detection rate has improved, then the power is increased by 1 dBm. If the maximum possible power is exceeded as a result, then the power is set to the maximum possible. If this does not change the power, the determination of the power is set to finished.

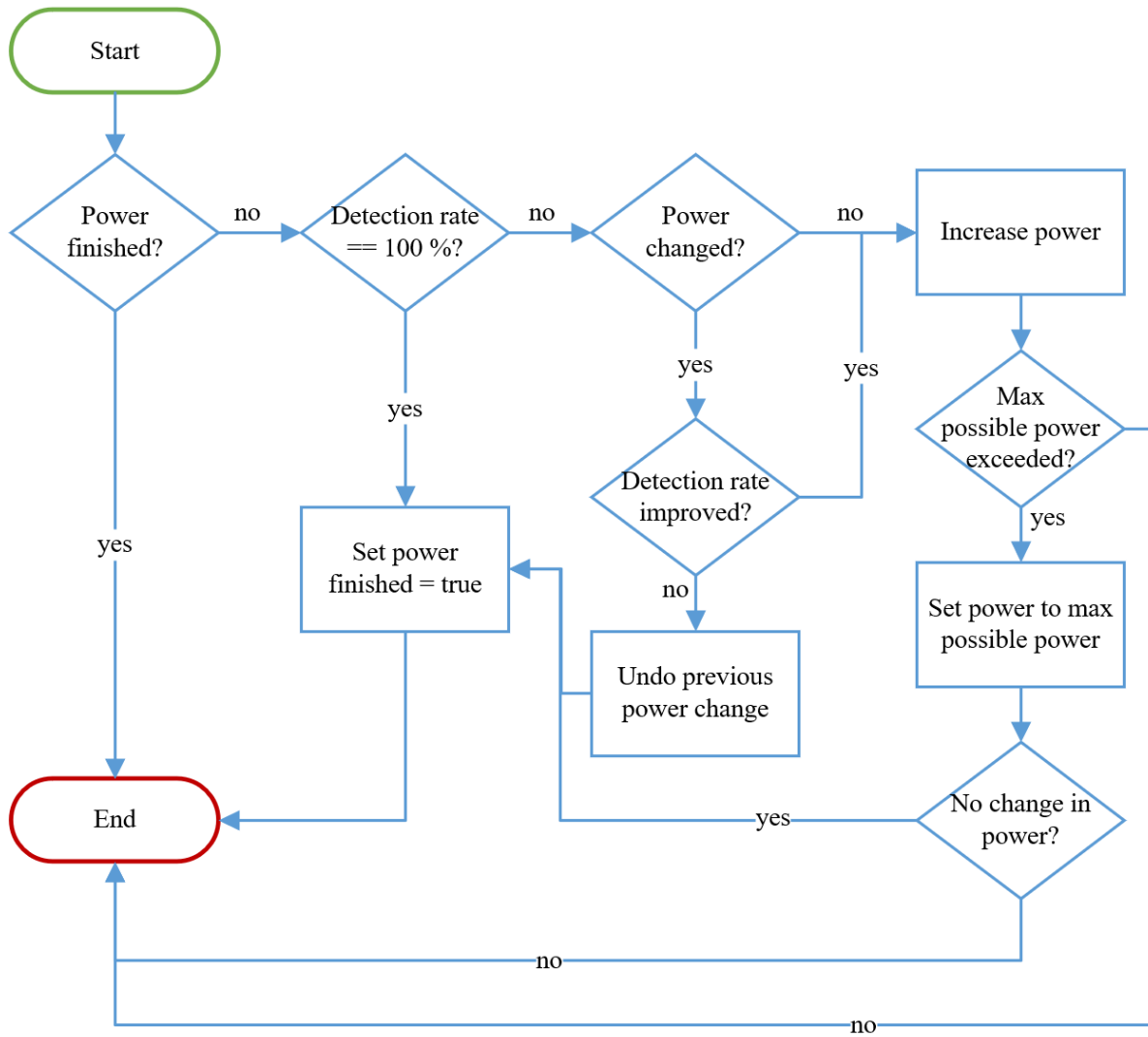


Figure 40 Flowchart of the algorithm to determine the new power

## 4.2 Implementation of the rule-based algorithm for optimal antenna alignment

The algorithm described previously was implemented by using of the architectural pattern layers in order to reduce the dependency relationships and to facilitate the implementation of the individual functions (Goll, 2014). The architecture consists of three layers: data storage layer, processing layer, and presentation layer, as shown in Figure 41.

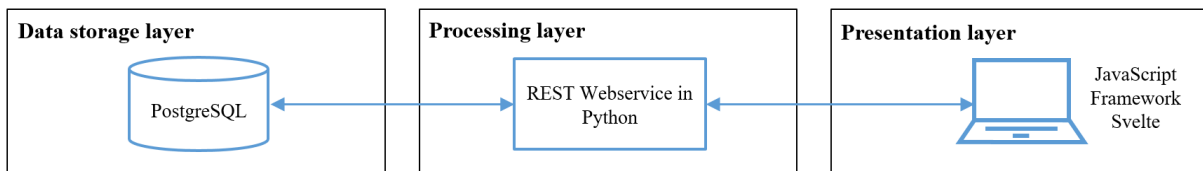


Figure 41 Architecture for the algorithm for optimal antenna alignment

### 4.2.1 Data storage layer

The data storage layer is used to persist not only the input parameters but also the results of the algorithm after each iteration. The relational database PostgreSQL is used for this purpose because the data of the

tests and parameters are structured data. Figure 42 shows the entity relationship diagram of the database. The database consists of six tables. The table *test parameters* contains all information about the test, like name, date, location, but also the input parameters for the algorithm, like minimum possible antenna height or the golden sample id. The *golden samples* table contains information about the golden samples, such as the height of the containers. A golden sample consists of several RFID transponders. These are stored in the table *tag information* with their position (x, y, z), orientation, and mapped area (bottom, middle, top). The antenna configurations are stored for each iteration in the *antenna configuration* table. The RFID transponder readings from the CSV files are stored in the *test data raw* table. The average detection rate, RSSI values in dBm, and number of reads for each run per iteration are stored in the *test results* table.

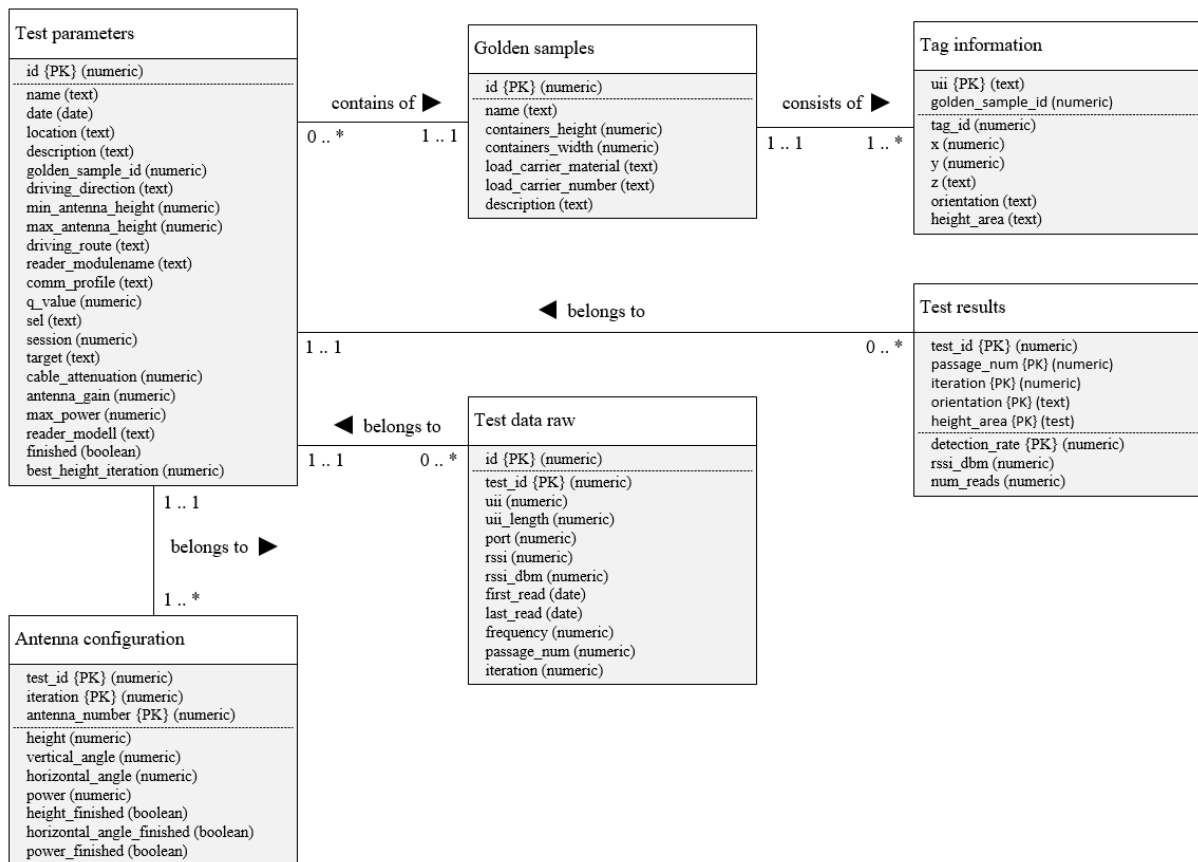


Figure 42 Entity relationship diagram of the algorithm for optimal antenna configuration

#### 4.2.2 Processing layer

The processing layer communicates with the data storage layer, and writes data to and reads data from the PostgreSQL database, but also with the visualisation layer.

The processing layer contains the algorithm, which was programmed as a REST (Representational State Transfer) web service in the Python programming language. Table 14 shows the available endpoints of the web service, as well as their description and their HTTP (Hypertext Transfer Protocol) method. The web service returns all requested data in JSON (JavaScript Object Notation) format.



Table 14 Endpoints of the REST web service

Method	Endpoint	Description
POST	/golden-sample	This reads the CSV file of the golden sample, maps each transponder to bottom, middle, top area, and then saves the golden sample with the transponder information to the database.
GET	/golden-samples	Reads the name and id of all golden samples from the database.
POST	/test-parameters	Saves the test parameters and the initial antenna configuration in the database which are transmitted in the body of the HTTP request.
GET	/test-names	Returns a list with all tests and their ids from the database.
GET	/test-parameters/{test_id}	Reads the test parameters for a test from the database.
GET	/test-results/{test_id}	Reads the test results (average detection rate and RSSI values) per iteration from the database.
GET	/test-iterations/{test-id}	Returns the number of all iterations for one test.
GET	/test-result- details/{test_id}/{iteration}	Provides the detailed test results for a test and an iteration. These include the detection rates, number of reads, RSSI values in total and per orientation and height area.
GET	/test-next- iteration/{test_id}	Determines the number of the next iteration for which the CSV files of the passes should be uploaded.
POST	/test-data-files/{test- id}/{iteration}	Stores the RFID transponder readings per test and iteration in the database, calculates the detection rate, number of reads, and RSSI values, and stores them in the database. The algorithm then runs to determine the new antenna configuration and stores the new configuration in the database.
GET	/test-antenna- config/{test_id}/{iteration}	Reads the antenna configuration of a test and iteration from the database.
GET	/test-current-antenna- config/{test_id}	Reads the antenna configuration currently set from the database of one test.
GET	/test-new-antenna- config/{test_id}	The new antenna configuration is read from the database, which should be set for one test.

### 4.2.3 Presentation layer

For the input of the parameters and files and for the visualisation of the results of the algorithm, the presentation layer is required. The user interface is realised as a web page and is programmed with the JavaScript framework Svelte because this is “*faster than any other framework like Angular or React*” (Dhaduk, 2021) and requires fewer characters of code for the same function than, for example, in React or Vue, which reduces the places where bugs can occur (Harris, 2019). The user interface communicates with the web service via REST calls. The web page has several tabs to create a golden sample, create a test, upload data with the RFID transponder readings and show the results of the algorithm, which can be seen in the Appendix in Figures 70 to 80.

### 4.3 Verification of the rule-based algorithm for optimal antenna alignment

The previously implemented OARG algorithm is verified using the case study automatic goods receipt posting with RFID gate where the antenna configuration is compared with the one from the exemplary guideline 1 because it performed better in the first verification (see Section 3.3). The verification is carried out at the RFID test centre of Mercedes-Benz AG in Böblingen, Germany.

The golden sample used for verification consists of two containers with small load carriers made of plastic and type 6429 as defined in VDA 4500 (VDA, 2015a). These load carriers contain no interfering materials. On these load carriers, 108 single-use RFID transponders of the type Confidex eKanban are attached with adhesive tape. On each outside of a small load carrier, two RFID transponders are attached above each other, as can be seen in Figures 43 and 44. The RFID reader RRU 4500, four antennas WIRA 30 and the ReaderStart software from Kathrein are used. Exemplary guideline 1 is used for the initial antenna configuration. The reader parameters can be seen in Table 9. For verification, the initial power is set to 26 dBm for all antennas, which is intentionally lower than in the exemplary guideline and corresponds to the approach of the OARG algorithm. The direction of travel is backwards and the RFID gate is passed through in the middle. A total of 15 passes through the RFID gate are made per iteration.

The results of the verification of the algorithm can be seen in Tables 16 and 17. With the initial antenna configuration according to the exemplary RFID gate guideline 1 and the power 26 dBm, an overall detection rate of 83.27 % was achieved. Here it can be seen that the middle and lower RFID transponder are read worse than the upper ones. Therefore, the OARG algorithm has determined 90 cm as the new heights for the lower antennas and 185 cm for the upper antennas. In the second iteration, the detection rate 82.78 % is obtained, which is lower than that from the first iteration. Therefore, the change in height is reversed and the horizontal angles are changed by  $\pm 20^\circ$ . As a result, a detection rate of 89.51 % is obtained. Since orthogonal transponders are read worse than parallel aligned ones, horizontal angles are set to  $\pm 40^\circ$ . In the detection rates of the fourth iteration, it can be seen that although this has improved the orthogonal detection rate by around 6 %, the parallel detection rate has deteriorated by nearly 10 %, so that the overall detection rate has also decreased. Therefore, in iteration five, the last change in horizontal angles is reversed and the power is increased. Because the increase in power leads to an increased detection rate, the power is increased again and again up to the maximum power of 30 dBm. At the end of the OARG algorithm, a total detection rate of 98.64 % was achieved.



Figure 43 Forklift with golden sample for verification



Figure 44 Passage through the RFID gate with the golden sample

Table 15 Reader parameters for verification of algorithm for antenna alignment

Parameter	Value
Communication profile	8: Tx:80kbps/Rx:320kbps/FM0
Channels	4, 7, 10, 13
Session	2

Table 16 Results of the verification of the algorithm for optimal antenna alignment – detection rates

Iteration	Total	Top	Middle	Bottom	Parallel	Orthogonal
1	83.27 %	90.74 %	88.15 %	70.93 %	99.78 %	62.64 %
2	82.78 %	84.81 %	89.26 %	74.26 %	99.55 %	61.81 %
3*	89.51 %	96.11 %	88.52 %	83.89 %	96.45 %	80.83 %
4	86.97 %	94.44 %	77.59 %	88.89 %	86.89 %	87.08 %
5	95.00 %	99.63 %	92.04 %	93.33 %	98.78 %	90.28 %
6	96.61 %	100.00 %	94.26 %	95.55 %	99.89 %	92.50 %
7	98.46 %	100.00 %	96.11 %	99.26 %	99.67 %	96.94 %
8**	98.64 %	100.00 %	96.48 %	99.44 %	99.78 %	97.22 %

\* Best iteration at a power of 26 dBm

\*\* Best iteration overall

Table 17 Results of the verification of the algorithm for optimal antenna alignment – antenna configurations

Iteration	Height bottom antennas	Height top antennas	Horizontal angle left	Horizontal angle right	Power
1	115 cm	210 cm	0 °	0 °	26 dBm
2	90 cm	185 cm	0 °	0 °	26 dBm
3	115 cm	210 cm	-20 °	20 °	26 dBm
4	115 cm	210 cm	-40 °	40 °	26 dBm
5	115 cm	210 cm	-20 °	20 °	27 dBm
6	115 cm	210 cm	-20 °	20 °	28 dBm
7	115 cm	210 cm	-20 °	20 °	29 dBm
8	115 cm	210 cm	-20 °	20 °	30 dBm

#### 4.4 Discussion of the rule-based algorithm for optimal antenna alignment

The verification showed that the detection rate was improved through the OARG algorithm compared to the exemplary guideline 1 by a full of 6.24 % without changing the power (see Table 16 iteration 1 compared to iteration 3). With the additional increase in power, an overall average detection rate of 98.64 % was achieved in iteration 8, which is 15.37 % better than the initial antenna configuration. The results of this verification proved that the OARG algorithm leads to a significant improvement in the detection rate compared to exemplary guideline 1 without testing every possible antenna configuration, and therefore hypothesis 1 is confirmed.

The newly determined antenna configuration can be used as a new guideline for RFID gates with similar widths and containers with similar heights and similar transponder positions. In addition, the implemented architecture as well as the functions for automated calculation of average detection rates, RSSI values, and number of reads can be used for every test of an RFID gate, such as RFID gate acceptance test. This saves a lot of time in the evaluation of the readings compared to manual calculations using excel.

However, there are the following limitations of the algorithm:

- 1) Not all possible antenna configurations have been tested, so it is theoretically possible that there is even a better antenna configuration.
- 2) The algorithm is developed and limited to RFID gates with four antennas, which are mounted on both sides of the gate.
- 3) The algorithm has only been verified on one RFID gate, with the direction of travel backwards, with plastic load carriers, and with one golden sample and should therefore be tested in the field in different areas in the future.
- 4) The number of RFID transponders, which are possibly in the environment and should not be read, was not considered by this algorithm, since with the application automatic goods receipt posting with RFID gate the read transponders are compared with the expected transponders in the logistics back end system. Therefore, it does not lead to material postings when unintended RFID transponders are read from the environment.
- 5) The offset caused by lifting the container was not taken into account in the golden sample or the OARG algorithm.

#### 4.5 Comparison of the three approaches to align antennas of the RFID gate

In this section, the three approaches to align the antennas of RFID gates are compared, as shown in Table 18. The first approach is to use the exemplary guideline, which specifies the number of antennas, height, vertical angles, horizontal angles, and power, and was developed based on experience and trial-and-error principle. The second approach uses the RGNP algorithm. Here, a theoretical approach with an evolutionary algorithm is used to plan the number of antennas and determine the height, vertical angles, and horizontal angles. In this approach, no specification is made about the power and the read range of the antennas, which depends on the power, must be specified as an input parameter (Knapp & Romagnoli, 2021). In the third approach, the number of antennas is taken from the exemplary guideline. For antenna alignment, the practical rule-based OARG algorithm is used, which evaluates the readings of the RFID transponders from several passes through the RFID gate and changes the antenna alignment based on this.

To evaluate the approaches with respect to the detection rate, the exemplary guideline 1 is used as a reference. The two algorithms cannot be compared directly because the verifications were performed in different environments and with different golden samples. The first verification (see Section 3.3) shows that the RGNP achieves a lower detection rate (34.23 %) than the exemplary guideline 1 (46.06 %). The second verification (see Section 4.3) shows that the OARG algorithm achieves a higher detection rate (89.51 %) than the exemplary guideline 1 (83.27 %). For this reason, the third approach is the best among these three to achieve the highest possible detection rate.

*Table 18 Comparison of the three approaches to determine antenna configuration*

	<b>Exemplary guideline 1</b>	<b>RGNP algorithm</b>	<b>OARG algorithm</b>
<b>Procedure for determining antenna configuration</b>	Experiential knowledge and trial-and-error principle	Theoretical approach with evolutionary algorithm	Practical approach with rule-based algorithm
<b>Detection rate of verification 1</b>	46.06 %	34.23 %	–
<b>Detection rate of verification 2</b>	83.27 % (26 dBm)	–	89.51 % (26 dBm) 98.64 % (30 dBm)

## 5 Test procedure to identify and reduce sources of interference










Despite optimal alignment of the RFID antennas, an RFID installation can have a worse performance, e.g., lower detection rate than an RFID installation with the same setup in a different environment due to sources of interference. This can lead to insufficient process quality, which usually results in manual rework, and in the worst case, to a non-profitable RFID installation (Knapp & Uckelmann, 2022). Therefore, it is important to systematically identify and reduce the sources of interference during a rollout, but also during operation, if the detection rate is too low. Since RFID applications are often rolled out and put into operation in places where the technology has not yet been used, the existing application experience is limited. The lack of experience and technical skills is a well-known RFID problem (Abugabah et al., 2020; Costa et al., 2017). Therefore, a test procedure is needed to systematically identify and reduce sources of interference.

### 5.1 Literature review on RFID test procedures

In this section, a literature review on RFID test procedures is first carried out to determine the state of the art and to check whether existing test procedures are suitable for identifying and reducing sources of interference. Therefore, test procedures relating to the UHF range and passive RFID transponders of the organisations ISO/IEC, VDI as well as EPCglobal and one research project were analysed. Table 19 shows an overview of the test procedures and the evaluation of their applicability for the identification and reduction of sources of interference.

Table 19 Overview and evaluation of RFID test procedures

Legend:   $\triangleq$  partially applicable;   $\triangleq$  not applicable

Test procedure	Year	Field of application	Identification / reduction of sources of interference
ISO/IEC 18046-1	2011	Test methods for system performance (ISO/IEC, 2011a)	
ISO/IEC 18046-2	2020	Test methods for interrogator performance (ISO/IEC, 2020b)	
ISO/IEC 18046-3	2020	Test methods for transponder performance (ISO/IEC, 2020a)	
ISO/IEC 18047-6	2017	Test methods for air interface communications at 860 MHz to 960 MHz (ISO/IEC, 2017)	
VDI/AIM 4472 Part 10	2008	Test methods to check the performance of transponder systems (RFID) (VDI/AIM, 2008)	
EPCglobal Dynamic Tests	2006	Conveyor Portal Test Methodology and Door Portal Test Methodology (EPCglobal, 2006a, 2006b)	
EPCglobal Tag Performance	2008	Transponder Performance Parameters and Test Methods (EPCglobal, 2008)	
EPCglobal Portal Field Strength	2009	Portal Field Strength Measurement Test Method (EPCglobal, 2009a, 2009b)	
MobiVis	2015	Mobile reading field acquisition and visualisation of UHF RFID installations (Günthner & Lechner, 2015)	

In the following, the individual test procedures are briefly described, and their evaluation with regard to their suitability for identifying and reducing sources of interference is explained.

### 5.1.1 ISO/IEC 18046-1

Part 1 of ISO/IEC 18046 (ISO/IEC, 2011a) describes the test procedure for determining the performance of an RFID system and to evaluate “*the differences between various technology providers' products in a consistent and equitable manner*” (ISO/IEC, 2011a). In this test procedure, the four scenarios mobile reader, reader with antenna(s) on one side, reader with antennas on two sides (gate) and reader with antennas on three sides (tunnel) are considered and different tests for the UHF frequency range according to ISO/IEC 18000-6 are described for each scenario. Furthermore, the arrangement of the RFID transponders is specified. The RFID transponders can be placed either linearly in a row (1D), on a plane (2D) or spatially (3D). The distances between the individual RFID transponders must also be the same. The tests shall be performed in a defined environment with a temperature of  $23\text{ °C} \pm 3\text{ °C}$  and humidity of 30 % to 60 % as well as in an RF environment where the spurious transmissions are lower than  $-80\text{ dBm}$ .

Since ISO/IEC 18046-1 is about determining performance in the defined environment without interferences, this standard is not considered suitable for identifying and reducing sources of interference.

### 5.1.2 ISO/IEC 18046-2

Part 2 of ISO/IEC 18046 (ISO/IEC, 2020b) describes tests to specify the characteristics of a reader in terms of performance. For ISO/IEC 18000-63 compliant readers, the reader sensitivity test is described. For this purpose, a transponder emulator specified according to ISO/IEC 18000-63 is positioned at a fixed distance from the reader. The backscatter power of the transponder emulator is reduced until the reader's readings of the transponder fall below the success rate. This test should also be performed in an environment with a temperature of  $23\text{ °C} \pm 3\text{ °C}$  and a humidity of 30 % to 60 % and an anechoic chamber is recommended.

Due to these characteristics, the test is considered not to be applicable for identifying and reducing sources of interference.

### 5.1.3 ISO/IEC 18046-3

The ISO/IEC 18046-3 (ISO/IEC, 2020a) describes tests to determine the performance of transponders. For ISO/IEC 18000-63 compliant transponders, the tests (i) minimum power operation threshold, (ii) sensitivity degradation, (iii) maximum operating power of transponder, (iv) survival electromagnetic power of transponder, (v) interference rejection and (vi) maximum fade rate are described. The test environment is specified the same as in ISO/IEC 18046-2. Furthermore, the tests can be performed with or without mounting material.

The tests described in ISO/IEC 18046-3 are classified as partially applicable for identifying and reducing sources of interference because when using different mounting materials, the influence and thus the interference source mounting material could be identified, but no other sources of interference or their influence can be identified and reduced by this test.

### 5.1.4 ISO/IEC 18047-6

The ISO/IEC 18047-6 (ISO/IEC, 2017) describes test procedures to ensure the compliance of RFID devices with ISO/IEC 18000-61, ISO/IEC 18000-62, ISO/IEC 18000-63, and ISO/IEC 18000-64 in the frequency range 860 – 960 MHz. The tests described therein should be performed in an environment that has a temperature of  $23^{\circ}\text{C} \pm 3^{\circ}\text{C}$  and a humidity of 40 % to 60 %. Furthermore, all measurements should be performed in an anechoic chamber.

The tests described in ISO/IEC 18047-6 are considered as not applicable for identifying and reducing sources of interference because they should be performed in an anechoic chamber.

### 5.1.5 VDI/AIM 4472 Part 10

The guideline VDI/AIM 4472 Part 10 (VDI/AIM, 2008) presents various influencing quantities, which also include ambient conditions, such as reflecting surfaces, and describes *“methods for the assessment and determination of the performance of RFID systems”* (VDI/AIM, 2008). This guideline distinguishes between three test environments: (i) favourable, (ii) moderate, and (iii) unfavourable. A favourable test environment is a *“chamber free from interferences and reflections”* (VDI/AIM, 2008). A moderate environment is characterised by *“large, open surfaces outdoors”* (VDI/AIM, 2008), and the unfavourable test environment has the real operating conditions of the RFID system. The test parameters include the transponder orientation, number and arrangement of transponders, transponder speed, and the mounting substrate of the transponders. The static test is used to verify the communication range of an RFID system or to determine the communication range. This test should be executed *“in a favourable or moderate test environment”* (VDI/AIM, 2008). For this purpose, measuring points are defined on a grid at which it is measured whether communication is successful, depending on different test parameters. The dynamic test can be performed in a moderate or unfavourable test environment. The aim is to check the bulk reading properties of an RFID system. In the process, the bulk with the transponders is moved through the communication area, e.g. a gate, over a defined measurement distance at constant speed, and then the detection rate is determined.

This guideline describes some sources of interference for RFID installations and takes into account the mounting substrate of the transponders during the tests, but it does not contain a procedure on how to identify sources of interference systematically. Therefore, this guideline can only be partially used to identify and eliminate sources of interference.

### 5.1.6 EPCglobal Dynamic Tests

EPCglobal has defined test procedures in (EPCglobal, 2006a) and (EPCglobal, 2006b) to test the performance of RFID conveyor portals and door portals (gates). The target audience are EPCglobal accredited test centres. The two test procedures describe the testing of the readability of RFID tagged boxes, pallets, or cases that are moved through door portals or conveyor belts equipped with RFID antennas. The two test procedures differ mainly in the setup of the RFID installation. The test environment for the conveyor portal test shall have an RF spectrum peak power of *“less than  $-24\text{ dBm}$  at all frequencies”* (EPCglobal, 2006a) as well as a temperature between  $10^{\circ}\text{C}$  and  $45^{\circ}\text{C}$  and humidity up to 95 %. For the door portal test, it is specified that *“no other significant radiating sources in the area where the test will take place”* (EPCglobal, 2006b) should be present and the temperature should be between  $10^{\circ}\text{C}$  and  $45^{\circ}\text{C}$  and the humidity should be between 20 % and 95 %. In the test described here for the RFID conveyor portal, the tagged housing is placed on the conveyor belt in 12 orientations and 10 times for each orientation, resulting in 120 data points. It is evaluated per iteration whether the EPC is read. Additionally, the number of reads per antenna can be recorded as well as the signal strength



per antenna and read. Furthermore, the selection of the transponders to be tested is described in the appendix, since the range can be different for transponders of the same type. The test for the RFID door portal (gate) is similar, but no number of iterations is specified (yet).

As these tests are intended for EPCglobal accredited test centres and do not describe any concrete tests or measures for the identification and reduction of interference sources, this test procedure is classified as not applicable.

### **5.1.7 EPCglobal Tag Performance**

The document “*Tag Performance Parameters and Test Methods*” (EPCglobal, 2008) from EPCglobal, describes various tests to evaluate the performance of transponders from different manufacturers. This is intended to simplify the comparison and selection of the appropriate transponders for an RFID application.

For this reason, the test procedure is considered as not suitable to identify and reduce sources of interference.

### **5.1.8 EPCglobal Portal Field Strength**

In (EPCglobal, 2009a) a draft for test procedures for measuring the electric field strength in a portal (conveyor or door) is described. However, it should be noted that this measurement method does not identify reading holes. Before the measurement is performed, external interference should be eliminated. Otherwise, no information is provided about the environmental conditions. A spectrum analyser with a calibrated dipole antenna is used to measure the field strength. During the measurement, the antenna must be fixed to a non-metallic support and specific measurement points are defined. At each measurement point, the power is measured with the antenna until all measurement points have been passed. In the draft in (EPCglobal, 2009b), recommendations are given to interpret the measurement results.

Because external interference should be eliminated before the measurement, this test procedure is considered as not applicable for identifying and reducing sources of interference.

### **5.1.9 MobiVis**

In the research report MobiVis (Günthner & Lechner, 2015) a method for measuring the electric field strength of an RFID gate is presented. For this purpose, a method with two variants (one with high-quality components and a low-cost variant) was developed, where the position of the antenna is automatically detected in parallel with the measurement. This eliminates the effort of manually positioning the antenna and makes it possible to measure the field strength at many different points in space. This makes it possible to detect reading holes and overreaches of an RFID installation. Furthermore, the measured values are displayed in 3D in the software.

Because this method identifies reading holes and overreaches that are caused by sources of interference but does not include a procedure to identify the type of sources of interference or how these can be reduced, it is classified as partially applicable.

### 5.1.10 Conclusion of the literature review

The literature review on existing RFID test procedures shows that there is no procedure to identify and reduce the sources of interference for RFID installations, which can occur in a real environment during a rollout or operation. Therefore, a new test procedure must be developed to identify and reduce sources of interference for RFID installations.

## 5.2 Literature review on sources of interference and proposed solutions

To develop a new test procedure, a systematic literature review on sources of interference for RFID installations and solutions to reduce sources of interference is first carried out. Therefore, the following three search terms were used: (i) *RFID AND Sources of interference AND Automotive industry*, (ii) *RFID “Issues OR solutions” AND installation AND “production OR logistics” AND automotive*, and (iii) *RFID AND sources of interference*. For this literature review, the databases Google Scholar, Science Direct, and ACM Digital Library were used and only publications since 2015 were taken into account. From the results, the ten most relevant sources were chosen and then filtered according to their technical relevance. Therefore, only sources, which are applicable to the production and logistics of the automotive industry, use the UHF range and passive RFID transponders, were selected. In addition, other interesting sources have been added to the results list.

Table 20 summarises the results of the literature review, where the sources of interference are clustered in the categories RFID components, electrical signals, physical environment, and environmental influences. (Knapp & Uckelmann, 2022)

Table 20 Overview of sources of interference, according to Knapp and Uckelmann (2022)

	Source of interference	Description	Proposed solutions
<b>RFID components</b>	Reader-to-transponder signal collisions	“Two readers try to read the same tag at the same time” (Knapp & Uckelmann, 2022).	<ul style="list-style-type: none"> <li>- RFID network planning algorithm</li> <li>- Shielding material</li> <li>- Change position of readers</li> <li>- Reduce power of readers</li> </ul>
	Reader-to-reader interference	Signals from an RFID reader interfere with the backscatter signal of another reader, even though their interrogation fields do not overlap.	<ul style="list-style-type: none"> <li>- Frequency-division multiple access (FDMA)</li> <li>- Time-division multiple access (TDMA)</li> <li>- Carrier-sense multiple access (CSMA)</li> <li>- Use of different times, frequencies for neighbouring readers</li> <li>- Switch not used readers off</li> <li>- Change encoding</li> <li>- Use a self-configuration method as in Windmann et al. (2017)</li> <li>- Shielding material</li> </ul>
	Transponder collisions	Several transponders send data simultaneously to the same reader, which cannot distinguish their signals.	<ul style="list-style-type: none"> <li>- Anticollision protocol, e.g., Slotted Aloha or the Q-Algorithm</li> </ul>

	Transponder-to-transponder interference	Interference can occur if there is insufficient distance between the RFID transponders.	- Experiments to place the transponders in optimal distance
<b>Electrical signals</b>	Interference from electrical devices	Electrical devices, e.g., mobile devices or electric motors, can cause electromagnetic interference for RFID installations.	- Use of an RFID system which adapts the transmission channel and power to the environment as in Windmann et al. (2017) - Change encoding from FM0 to Miller - Remove interfering devices - Use of shielding - Internal standard for device radiation and use of frequencies
	Interference from attackers	Attackers can send interference signals intentionally.	- Use of communication protocols against attacks and to detect security vulnerabilities is a proposed solution
	Reflections from the environment	Reflections from the environment are caused, for example, by metallic objects, forklifts, or cable trays, and result in reading holes or overreaches.	- Use a self-configuration method as in Windmann et al. (2017) - Remove interfering objects - Use shielding - Reduce power
<b>Physical environment</b>	Blocking by objects between the reader and transponder	Objects between the reader and the transponder made of reflecting or absorbing material can block RFID signals.	- Remove absorbing and reflecting objects - Increase power when absorbing materials are the source of interference
	Carrier material	<i>“Another source of interference are carrier objects or the contents of the object to be identified made of the materials metal, ESD (Electrostatic Discharge), glass and conductive liquids.”</i> (Knapp & Uckelmann, 2022)	- Use of suitable RFID transponder for the carrier material, e.g., on-metal-transponders - Increase the distance of carrier material and RFID transponder for example with flag-transponders - Replacement of the carrier material - Increase in reader power
	Temperature and humidity	Temperature and humidity can be a source of interference and, for example, influence the read rate.	- Environmental influences for an RFID installation should be considered during the development of the RFID application
<b>Environmental influences</b>	Salt content of the air	The salt content can also have an influence on RFID systems.	- Choose appropriate RFID transponders for the environment - Hydrophobic radome could be used against water on the transponder or antenna
	Chemical stresses	Chemical stresses include, for example, oil, alkalis, or solvents.	- Conduct experiments to determine the environmental influences

Mechanical stresses	Mechanical stresses are caused, for example, by vibration, pressure, or friction.	- Usage of a self-configuration method as described in Windmann et al. (2017)
---------------------	---	---

---

### 5.3 Test procedure to identify and reduce sources of interference

The newly developed test procedure to identify and reduce sources of interference is based on the results of the previously described literature review. The aim of the test procedure is to systematically identify and reduce sources of interference that arise during a rollout of RFID applications in a new environment. The prerequisites for carrying out the test procedure are that the RFID application has already been developed and installed, the adjustable parameters such as the number of antennas or power have been determined in a test environment, anticollision algorithms are used, and the hardware is suitable for the mechanical and chemical stresses. The start trigger for executing the test procedure can be the commissioning of a new RFID installation or changes in the environment of an existing RFID installation where the performance is not sufficient. The performance of an RFID installation is defined individually; it can be, for example, the maximum possible distance between reader and transponder or the detection rate or the reading rate per second. Figure 45 shows the test procedure, which includes the following steps:

- 1) First of all, the required performance for the process, where the RFID installation is used, must be defined, for example, detection rate of 80 %.
- 2) The second step is the measurement of the current performance of the RFID installation.
- 3) If the measured performance is too low for the process, then the questionnaire described in Section 5.3.1 must be completed. This identifies possible sources of interference and for all questions answered with “yes”, a test is given to identify the source of interference. The tests are described in Section 5.3.2.
- 4) In the fourth step, these tests must be executed one after the other. If a source of interference has been identified, the performance must be measured again. If this has not improved the performance, and further possible solutions exist, these must be applied and the performance measured again. As soon as the performance defined for the process is achieved, this test procedure is completed.
- 5) If all tests have been performed but the required performance has not been achieved, RFID experts should be contacted. (Knapp & Uckelmann, 2022)

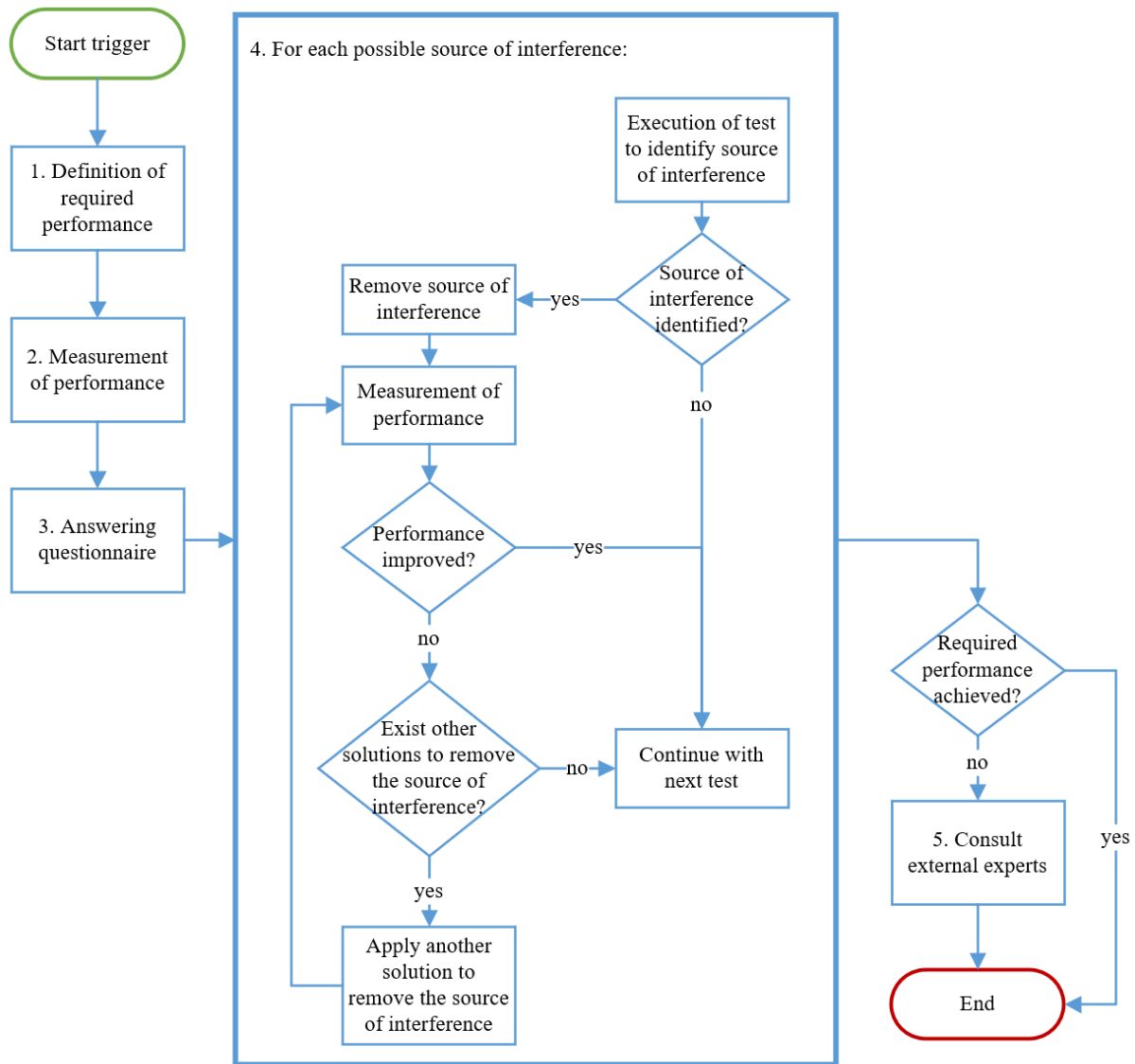


Figure 45 Test procedure to identify sources of interference, according to Knapp and Uckelmann (2022)

### 5.3.1 Questionnaire

The questionnaire is used to narrow down the sources of interference that are likely to be present. Based on the answers, different tests are proposed to identify whether this source of interference is the cause of the lower performance. The questionnaire contains the following seven questions, as described in Knapp and Uckelmann (2022):

- 1) Is the carrier object or the content of the object made of metal, ESD, glass or conductive liquids or other absorbent or reflective materials? → **Carrier material test**
- 2) Are there other electrical devices or other radio devices in the vicinity of the RFID installation or is interference by an attacker conceivable) → **Interference test**
- 3) Are there other UHF RFID readers in the vicinity? → **Reader-to-tag signal collision test and reader interference test**
- 4) Are several RFID tags placed very close to each other? → **Tag interference test**

- 5) Are there other objects between the RFID tag and the reader that are made of metal, ESD, glass or conductive liquids or other absorbent or reflective materials? → **Absorption test**
- 6) Is the RFID installation in an environment with extreme temperatures / humidity / salt content of the air or differ the environmental influences greatly from those of the test environment? → **Environmental impact test**
- 7) Is the RFID installation in a metallic environment or are there large metal objects near the RFID installation? → **Reflection test**<sup>1</sup>

### 5.3.2 Tests to identify sources of interference

The individual tests are all described in detail in Knapp and Uckelmann (2022) and summarised in the following.

The aim of the **carrier material test** is to determine the influence of the carrier material on the readability, e.g., the reading range. The environment to conduct this test should be an anechoic chamber. In addition, a network analyser optimised for RFID measurements with associated software is needed. Then the sensitivity and backscatter signal of the transponder attached to the carrier material of the RFID installation should be measured. The same measurement should be conducted with a neutral carrier material and then the measurement results must be compared. If the measurement results with neutral carrier material are much better, the carrier material of the RFID installation is a source of interference.

The **interference test** is carried out at the location of the RFID installation. First, all RFID readers must be deactivated, and then, a spectrum analyser is used to perform a frequency sweep measurement in the frequency range of the RFID installation. If the measured signals are around or lower than  $-80$  dBm, there are no interferences from other devices. This test might be carried out again at a later date, as this is only a snapshot.

The **reader-to-transponder signal collision test** is conducted in the environment of the RFID installation. First, the reader of the RFID installation should be deactivated, and then a transponder should be placed in the reading area of this RFID installation. If this transponder is read by a nearby RFID reader, the reading fields of those overlap. In this case, the nearby readers should be deactivated, and the performance of the RFID installation measured again to determine the influence of the reader collisions.

Before the **reader interference test** is carried out, reader-to-transponder signal collisions and interferences caused by other electrical devices should be excluded. The environment of this test is the RFID installation. First, the RFID reader of the installation is deactivated. Then, a frequency sweep measurement is carried out with a portable spectrum analyser in the frequency range used by the RFID installation. If the measured signal power is around  $-80$  dBm or lower, there are no interferences from other RFID readers. Otherwise, the performance of the RFID installation should be tested while the other RFID readers are deactivated to measure the influence of the reader interference.

Before carrying out the **transponder interference test**, it should be ensured that the carrier material is not a source of interference. The test should be conducted in an area without other sources of interference, such as a test centre. First, the performance of the RFID installation and the RSSI values should be measured. In the second step, the transponder distances must be increased and the performance

---

<sup>1</sup> Questionnaire is reprinted from International Journal of RF Technologies, vol. 12, no. 2, Knapp, H. & Uckelmann, D., Literature review on sources of interference and proposed solutions for RFID installations in complex production and logistics processes in the automotive industry, pp. 87-126, Copyright 2022, with permission from IOS Press

and RSSI values measured again. This can be repeated until the defined performance is reached to determine the optimal distances between the transponders.

The **absorption test** is carried out in the area of the RFID installation. Thereby, the absorbent or reflective objects between the transponders and the reader should be eliminated or replaced with neutral material. Then the performance of the RFID installation should be measured again to determine the influence of these objects.

The **environmental test** should be carried out in a climate chamber or in a location where climatic influences can be simulated. During different set climatic influences, the read rate or backscatter signal of the RFID installation should be measured. Thereby, the influence of the environment (temperature, humidity, or salt content) can be determined.

The **reflection test** is executed in the environment of the RFID installation. The reflective (metallic) objects are removed or shielded, and then, the performance of the RFID installation is measured. An improvement of the performance during shielding the reflective objects indicates that these are a source of interference.

### 5.4 Verification of the test procedure and tests

The test procedure described above is verified by simulating different sources of interference for RFID installations and applying all tests once to identify individual sources of interference.

#### 5.4.1 Verification of the carrier material test

The verification of the carrier material test is performed using the RFID application automatic material retrieval with RFID reader on the shelf (see Section 2.2.2) in the RFID test centre of Mercedes-Benz AG in Böblingen, Germany. Thereby, the source of interference is simulated by an ESD load carrier as it is known that this is a disturbing material. The start trigger for executing this test procedure could be a low detection rate. This becomes apparent when material on the assembly line is missing because when the RFID transponder is not read, no new material is ordered automatically.

- 1) As performance indicator, the number of readings is used and should be at least 20 in this verification to ensure process quality.
- 2) Then the number of readings is measured when pushing the load carrier with the RFID single-use transponder five times through the shelf. This results in an average number of reads of 13, which is lower than the defined performance indicator.
- 3) Therefore, the questionnaire is completed and the first question is answered with yes, which means that the carrier material test should be carried out.
- 4) The test is carried out at the anechoic chamber at the HFT Stuttgart, Germany, and using the Tagformance Pro Measurement System from Voyantic. The RFID transponder attached to the ESD load carrier is placed in the anechoic chamber, and the threshold measurement is executed. Then the RFID transponder is attached to a load carrier of the same size, made of plastic, which is a neutral material for RFID readings, and the threshold measurement is performed again. This determines how much reading power is needed to read the transponder and calculates the theoretical read range forward. The results show that when using the plastic load carrier, less power is needed and the theoretical read range forward is up to 5 m, whereas it is up to 3 m when using the ESD load carrier. This means that the ESD load carrier is a source of

interference. In the next step, the performance of the RFID installation is measured again using the plastic load carrier which results in an average number of reads of 38.8.

Through the application of the test procedure, the source of interference carrier material could be identified and eliminated. (Knapp & Uckelmann, 2022)

### 5.4.2 Verification of the reader interference test

The verification of the reader interference test is done by an RFID installation where the RFID reader with integrated antenna is placed at a distance of approximately 160 cm from the RFID transponder. As a performance indicator, the number of readings per second are used. The source of interference is simulated by another RFID reader, which is placed around 40 cm away from the RFID transponder. However, the interfering reader cannot read the transponder, and thereby it is ensured that the transponder is not in the reading field of this reader and reader collisions are not present. The implementation of a new RFID installation during the rollout could be the start trigger to perform this test procedure.

- 1) This RFID installation should read the transponder at least 8 times per second.
- 2) First, both readers are deactivated, and a frequency sweep measurement is carried out to ensure that there are no interferences through other electrical devices. Then the performance is measured while both RFID readers are active, which results in a reading rate per second of 7.7.
- 3) Therefore, the questionnaire is completed, which shows that the reader interference test should be conducted.
- 4) To perform this test, the RFID reader of the RFID installation is deactivated and a frequency sweep measurement with the spectrum analyser is carried out. This shows that there are signals with a power up to approximately  $-25$  dBm, indicating reader interference. After that, the performance of the RFID installation is measured again while the interfering reader is deactivated. Thereby, the performance increased to 9.2 readings per second.

This shows that the reader interference test could identify the source of interference and that performance could be improved. (Knapp & Uckelmann, 2022)

### 5.4.3 Verification of the transponder interference test

To verify the transponder interference test, the RFID application automatic material retrieval with RFID reader on the shelf was used and the test was carried out in the RFID test centre of Mercedes-Benz AG in Böblingen, Germany. To simulate the source of interference, three multi-use RFID transponders are placed next to each other on one plastic load carrier. The start trigger could be a change in transponder positioning.

- 1) This RFID installation should have a detection rate of 100 % of all RFID transponders.
- 2) The load carrier with the three transponders is pushed five times through the shelf, where the middle transponder is never read.
- 3) Due to insufficient performance, the questionnaire is completed, which shows that the transponder interference test should be carried out.
- 4) Therefore, the transponders are placed at a distance of 1 cm and the performance is measured again. This measurement results in a detection rate of 100 %.



By applying this test procedure, the source of interference (transponder interference) could be identified and eliminated, and the detection rate was increased. (Knapp & Uckelmann, 2022)

### 5.4.4 Verification of the reflection test

For the verification of the reflection test, the RFID reader with integrated antenna is placed at a distance of approximately 200 cm from the RFID single-use transponder. The source of interference is simulated by a metallic bin, placed close to the reader.

- 1) In this verification, the performance indicator read range is used and should be 190 cm.
- 2) At the beginning, the maximum read range is measured, which is 170 cm.
- 3) Answering the questionnaire identified, that the reflection test should be performed.
- 4) Thereby, the metallic object (bin) is removed, and the performance of the RFID installation is measured again. This results in a maximum read range of 200 cm.

This verification shows that the source of interference, in this case, the metallic bin, could be identified and eliminated, which significantly improved the performance. (Knapp & Uckelmann, 2022)

### 5.4.5 Verification of the absorption test

The verification of the absorption test is based on the RFID application component tagging, where individual components are tagged and read at various points in the supply chain and production (Richter, 2013). A place where these transponders are read could be the goods receipt or the automatic material retrieval with shelf. In both places, the transponders could be placed in a load carrier and read by a reader from above, as, for example, in the installation in Figure 46 where a load carrier with the components is slid under the antennas on the shelf. For this test, the reader ARU 2400 from Kathrein, which itself contains an antenna and three other external antennas and single-use Confidex eKanban transponders were used. The source of interference is simulated by an ESD lid, which is located between the RFID transponders and the reader. The start trigger could be the introduction of component tagging.

- 1) The performance indicator used is the average detection rate, which should be at least 95 %.
- 2) In the second step, the performance of the RFID installation is measured. The reader has the configuration 1 as shown in Table 21 and the small load carrier with the 4 transponders contained in it and a lid is pushed through the shelf 5 times (see Figure 46 and Figure 47). Since the detection rate is only 50 % on average, the required performance was not achieved, and this indicates the presence of a source of interference.
- 3) Since there is an absorbent material between the transponder and the reader, the question “*Are there other objects between the RFID tag and the reader that are made of metal, ESD, glass or conductive liquids or other absorbent or reflective materials?*” is answered with “yes”. The question “*Is the carrier object or the content of the object made of metal, ESD, glass or conductive liquids or other absorbent or reflective materials?*” is also answered with “yes”. Since this is about the verification of the absorption test, only this test will be performed in the following.
- 4) When performing the absorption test, the source of interference (the lid) is removed, and the performance is measured again. This leads to a significant improvement and a detection rate of 100 %. To increase the detection rate despite the source of interference and the ESD lid, the

5 Test procedure to identify and reduce sources of interference

power is increased to 14 dBm (see Table 21 configuration 2) and the test is performed again. The increase of the power leads to a detection rate of 100 % (see Table 22).

This verification showed that the absorption test was able to identify and eliminate the source of interference, thus achieving a detection rate of 100 %.



Figure 46 Setup of the RFID installation for the verification of the absorption test

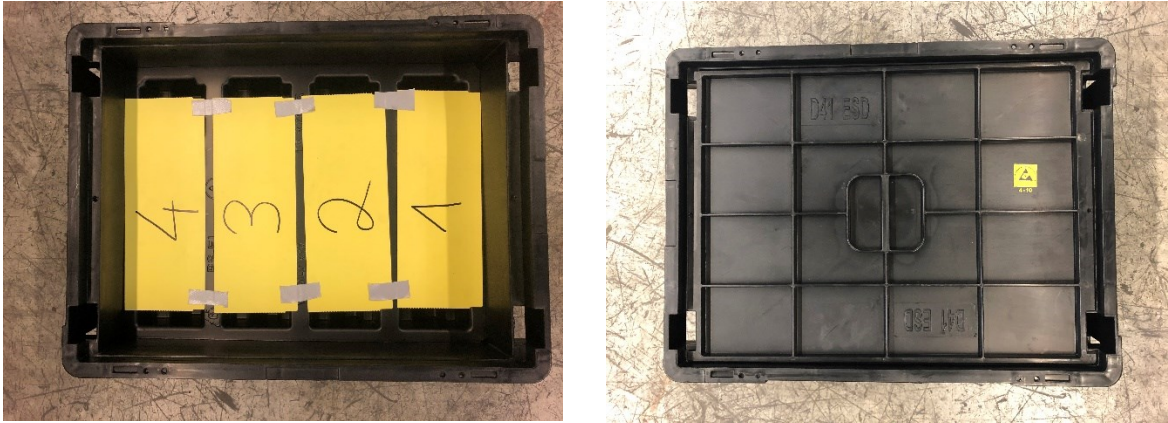


Figure 47 RFID transponders in an ESD load carrier with lid (left) and without lid (right)

Table 21 Reader parameters for the verification of the absorption test

Parameter	Value – Configuration 1	Value – Configuration 2
Power (ERP)	12.00 dBm	14.00 dBm
Communication profile	10: Tx:80kbps/Rx:80kbps/Miller4	10: Tx:80kbps/Rx:80kbps/Miller4
Channels	4, 7, 10, 13	4, 7, 10, 13
Session	0	0

Table 22 Comparison of the average detection rates of the absorption test

Lid	Power	Detection rate
With lid	12.00 dBm	50 %
Without lid	12.00 dBm	100 %
With lid	14.00 dBm	100 %

#### 5.4.6 Verification of the interference test

Figure 48 shows the setup of the RFID installation for this verification. This setup contains the RFID reader ARU 2400 from Kathrein and one RFID single-use Confidex eKanban transponder. The RFID transponder is placed at a distance of 70 cm from the RFID reader and directly next to the antenna of a LoRa (Long Range) gateway. The reader parameters used for this RFID installation are described in Table 23. The number of readings per second is used as a performance indicator, which plays a role when many transponders must be read within a short time, for example, when passing through an RFID gate. The source of interference is simulated by a LoRa gateway and the Field Test Device – LoRaWAN (Long Range Wide Area Network) Europe from Adeunis because LoRa operates in the 868 MHz frequency band in Europe (LoRa Alliance, 2015) which is also used by this RFID installation. With the Field Test Device, a signal is sent manually to the gateway by pressing a button and a confirmation is sent back from the gateway to the Field Test Device. The button is pressed repeatedly during verification to permanently simulate the source of interference. The start trigger could be the new installation of the radio technology LoRa in the vicinity of an RFID installation.

- 1) The number of readings per second is taken as the performance indicator, which should be at least 60 readings per second for this setup.
- 2) The performance is measured by recording the number of reads of the transponder for more than 3 minutes and then filtering exactly 3 minutes. The number of reads per 3 minutes is 10786 and converted this is 59.9 readings per second.
- 3) In the third step, the questionnaire is filled out, answering “yes” to the question two “*Are there other electrical devices or other radio devices in the vicinity of the RFID installation or is interference by an attacker conceivable?*”. Therefore, the interference test must be carried out.
- 4) The interference test is performed while simulating the source of interference. First, the RFID reader is deactivated. Then, a frequency sweep measurement in the frequency range of the RFID installation, which is 865.0 MHz – 868.5 MHz, is performed with the portable spectrum analyser Aaronia SPECTRAN HF-60100 until the maximum hold values no longer change. Figure 49 shows the result of this measurement, where it is clearly visible that signals with a power of up to –35 dBm are transmitted in the frequency range of the RFID installation. This means that interferences from other devices exist. The source of interference LoRa is then eliminated by no longer sending any signals from the field test device, and therefore no confirmation is sent back from the gateway. The frequency sweep measurement is repeated and shows that there are no more interferences from other devices (see Figure 50). Then the RFID reader is activated and the number of reads is measured again. The number of reads has increased to 61.82 readings per second (see Table 24).

This verification has shown that the interference test detects the source of interference simulated by the LoRa Field Test Device and gateway.

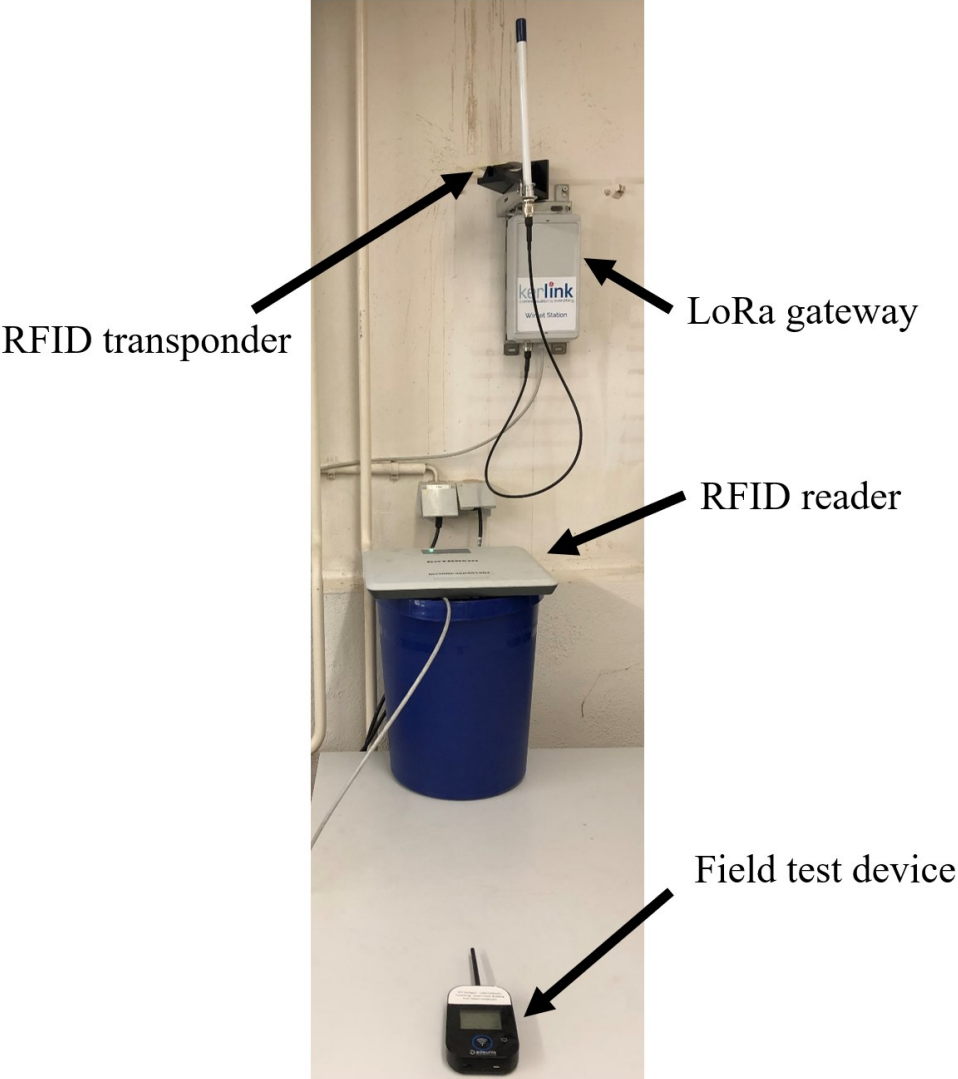


Figure 48 Setup of the RFID installation for the verification of the interference test

Table 23 Reader parameters for the verification of the interference test

Parameter	Value
Power (ERP)	12.50 dBm
Communication profile	10: Tx:80kbps/Rx:80kbps/Miller4
Channels	4, 7, 10, 13
Session	2

Table 24 Reading rate with and without LoRa signals

Number of reads	per 3 minutes	per minute	per second
With LoRa signals	10786	3595.33	59.92
Without LoRa signals	11129	3709.67	61.83

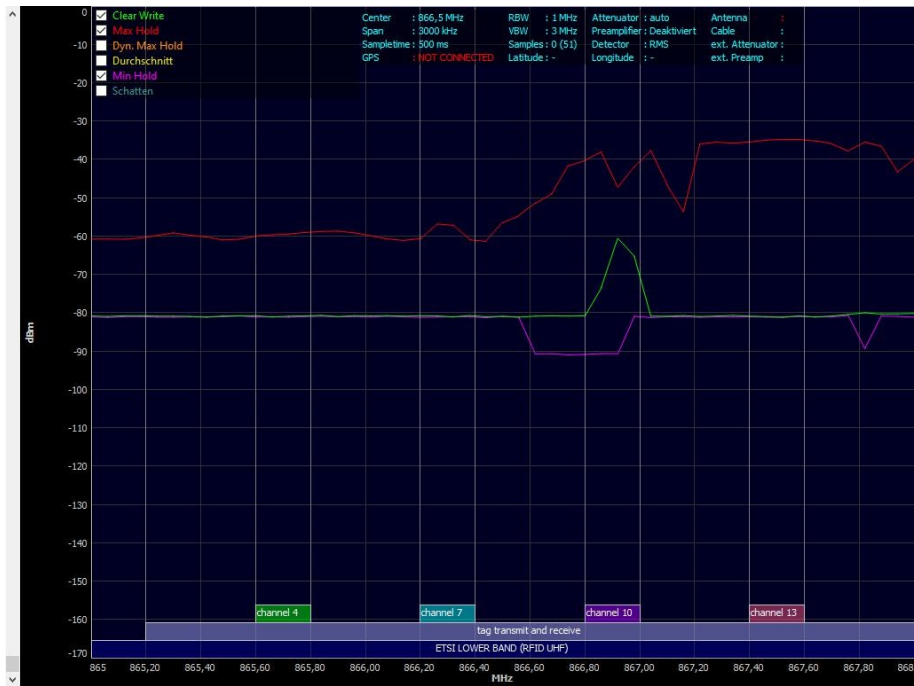


Figure 49 Frequency sweep measurement with simulated source of interference by LoRa



Figure 50 Frequency sweep measurement without simulated source of interference

### 5.4.7 Verification of the reader-to-transponder signal collision test

For this verification, the RFID application automatic goods receipt posting with RFID gate is simulated. For example, two RFID gates can be installed directly next to each other, causing the reading fields of the two readers to overlap. For this purpose, two Kathrein ARU 2400 readers are used, which contain an internal antenna, and one single-use Confidex eKanban transponder, which are set up as shown in Figure 51. The reader parameters are described in Table 25. The second RFID reader with integrated

antenna is used as the source of interference because this causes the overlap of two reading fields. The start trigger could be the installation of gates in a new hall during a rollout, where they are directly adjacent to each other due to the environment.

- 1) The number of reads per second is used as a performance indicator, which should be at least nine readings per second for this verification.
- 2) To measure performance, readings are recorded for just over 3 minutes, and then filtered for exactly 3 minutes and then converted to seconds. This results in 1610 readings per 3 minutes and 8.94 readings per second, and thus the defined performance is not achieved.
- 3) In the next step, the questionnaire is filled out and the question “*Are there other UHF RFID readers in the vicinity?*” is answered with “*yes*”. Therefore, the reader-to-transponder signal collision test is executed.
- 4) During the reader-to-transponder signal collision test, the source of interference is eliminated by deactivating the second reader and measuring the performance again. This results in a number of readings of 10 per second, and thus the required performance is achieved. To permanently eliminate the source of interference, shielding material is placed between the two readers and the performance is measured again while both readers are actively reading. This also leads to a performance of 10 readings per second (see Table 26).

This verification successfully identified and eliminated the source of interference reader-to-transponder signal collisions.



Figure 51 Setup of the RFID installation for the verification of the reader-to-transponder signal collision test

Table 25 Reader parameters for the verification of the reader-to-transponder signal collision test

Parameter	Value
Power (ERP)	26.25 dBm
Communication profile	4: Tx:40kbps/Rx:40kbps/Miller4
Channels	4, 7, 10, 13
Session	2

Table 26 Reading rate with and without both reader and shielding

Number of reads	per 3 minutes	per minute	per second
Both readers active, no shielding	1610	536.67	8.94
One reader deactivated, no shielding	1801	600.33	10.01
Both reader active, with shielding	1800	600	10

### 5.4.8 Verification of the environmental impact test

The verification of the environmental impact test is done using the setup of the RFID installation shown in Figure 52. In this setup, the ARU 2400 reader from Kathrein and the single-use Confidex eKanban transponder were used. The reader parameters can be seen in Table 27. The performance is defined by the number of reads per second. The source of interference is simulated in this verification by some water drops on the RFID transponder, as can be seen in Figure 53. In reality, this could be caused by heavy rain when the load carriers are placed in the open. The start trigger for the execution of the procedure to identify the source of interference could be, for example, low reading rates during rain in a goods receiving area where the load carriers are in the open when they are unloaded from the truck.

Before the test procedure is applied, the performance is measured without the simulated source of interference for comparison. This results in a reading rate of 3990 per minute and 66.5 per second.

- 1) The performance is the number of reads per second, which should be at least 60.
- 2) The performance is then measured under the influence of the simulated source of interference (water drops). This shows that the RFID transponder can no longer be read at all, which results in 0 readings per second.
- 3) In the third step, the questionnaire is filled out, answering “yes” to the question “*Is the RFID installation in an environment with extreme temperatures / humidity / salt content of the air or differ the environmental influences greatly from those of the test environment?*”. Therefore, the environmental test must be conducted.
- 4) Now the environmental test is carried out in a modified form as described in (Knapp & Uckelmann, 2022), as the interference source is simulated by water drops. The RFID transponder is dried to determine the influence of the water. Afterwards the read rate is measured again, and this results in 3992 readings per minute and 66.53 readings per second, and this shows that without the influence of the interference source the transponder is recognised and the number of reads corresponds to the defined performance. One measure could be to cover the area where the load carriers are unloaded from the truck.

This verification shows that the source of interference could be identified and that the elimination of the source of interference led to the RFID transponder being recognised again.

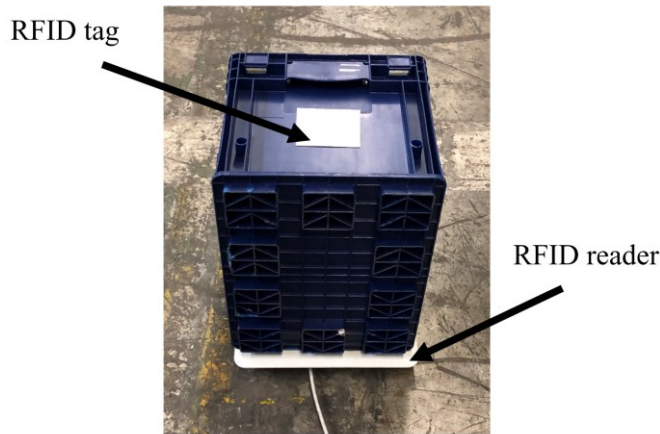


Figure 52 Setup of the RFID installation for the verification of the environmental impact test



Figure 53 RFID transponder with simulated source of interference (water)

Table 27 Reader parameters for the verification of the environmental impact test

Parameter	Value
Power (ERP)	9.00 dBm
Communication profile	10: Tx:80kbps/Rx:80kbps/Miller4
Channels	4, 7, 10, 13
Session	2

## 5.5 Discussion of the test procedure

In this chapter, a new test procedure to identify and reduce sources of interference was presented. The test procedure and the tests described to identify and reduce sources of interference were applied and verified by the simulation of eight different sources of interference. Thereby, all simulated sources of interference could be identified and reduced, leading to a significant improvement of the performance of the RFID installations, e.g., to a higher detection rate.

However, the test procedure should be subjected to a field test, and, if necessary, the feedback from the users should be implemented in a new version, which would be an additional iteration in the design cycle of the design science research methodology. If necessary, an additional training concept could be developed to train users in handling the corresponding measuring devices.

In the future, this test procedure can be used during a rollout or operation of RFID installations to systematically identify and reduce sources of interference. Subsequently, the test procedure could be anchored in a new standard such as VDI to disseminate it.



## 6 Digital twin of the RFID-enabled material flow in real time

After the antennas of the RFID installations have been optimally aligned, sources of interference have been eliminated and the installations have been put into operation; they continuously generate new data. To link these data with other data sources and to use them for further analyses and insights into the material flow, the digital twin of the RFID-enabled material flow (DTRMF) in real time is created and described in this chapter.

### 6.1 Definition and objectives of the digital twin of the RFID-enabled material flow in real time

The origins of the digital twin concept go back a long way. As early as NASA's Apollo programme, twins were used, *"where at least two identical space vehicles were built to allow mirroring the conditions of the space vehicle during the mission"* (Rosen et al., 2015). The physical twin was the vehicle that remained on earth and was used to execute simulations to support the astronauts in the space vehicle (Rosen et al., 2015).

According to Grieves and Vickers (2016) the concept of the digital twin was introduced in 2002 in a presentation of the University of Michigan to the industry. At that time, the concept was named by Grieves *"Conceptual Ideal for PLM (Product Lifecycle Management)"* but *"did have all the elements of the Digital Twin: real space, virtual space, the link for data flow from real space to virtual space, the link for information flow from virtual space to real space and virtual sub-spaces"* (Grieves & Vickers, 2016).

In 2010, the term digital twin was used by researchers at NASA (National Aeronautics and Space Administration) and defined as *"an integrated multi-physics, multi-scale, probabilistic simulation of a vehicle or system that uses the best available physical models, sensor updates, fleet history, etc., to mirror the life of its flying twin"* (Shafto et al., 2010). According to this definition, the digital twin is a highly detailed simulation of a vehicle or system and includes sensor data as well as historical data obtained with data mining and text mining. This helps to avoid possible damage and to increase the lifetime of the vehicle or system.

In the white paper from Grieves (2014) the digital twin concept is described as a model which *"contains three main parts: a) physical products in Real Space, b) virtual products in Virtual Space, and c) the connections of data and information that ties the virtual and real products together"* (Grieves, 2014).

In the meantime, there are many different definitions of the term digital twin in the literature (Al-Sehrawy & Kumar, 2021; Negri et al., 2017). Therefore, the term digital twin of the material flow in real time is defined as follows in this thesis. In this thesis, soft real time is meant by real time, which means that occasionally exceeding the set time span is accepted (Scholz, 2005). The DTRMF is a combination of a product and process twin, as it represents both the special load carriers equipped with multi-use RFID transponders and the processes of the material flow in real time. The main data source of the DTRMF are the data automatically generated by RFID installations (e.g., at the goods receipt), which are stored in the logistics back end system. However, other data from the logistics back end system and from the load carrier management system, are taken into account in the DTRMF. The data flow of the DTRMF is unidirectional, i.e., the special load carriers and processes of the real space are automatically represented in the virtual space and provided to the users who then manually intervene in the production supply. The target group of the digital twin is the production supply department of an automobile manufacturer, which is responsible for delivering the material to the production supply area on time. The goals of the DTRMF are to create transparency, identify optimisation potential in the

logistics processes, save costs, ensure production supply, ensure quality and save time. (Knapp et al., 2022)

## 6.2 Requirements of the digital twin of the RFID-enabled material flow in real time

In this section, the requirements of the above defined DTRMF in real time are described. In order to identify these requirements, various expert discussions were conducted with the future users of the DTRMF in the body shop of an international automobile car manufacturer. The requirements are divided into functional and qualitative requirements.

### 6.2.1 Functional requirements

The functional requirements define the functionalities that the DTRMF should fulfil. The general functional requirements for the DTRMF are described in the following.

- **F01:** the data from the logistics back end system and the load carrier management system must be ingested and read, because they are the data sources of the DTRMF.
- **F02:** the data from the source systems must be prepared, for example, by filtering out unnecessary data, by linking related data, and by converting the data types to ensure good data quality and the usability of the data for further analyses to generate new insights.
- **F03:** the data of the DTRMF should be logically stored in a database with a date or timestamp so that the current and historical data can be retrieved quickly and also analyses based on the historical data can be executed.
- **F04:** the data should be clearly visualised in dashboards with the possibility to filter them to provide the information to the users of the DTRMF.

In the expert discussions, five use cases of the DTRMF were identified. These use cases lead to different functional requirements. The use cases and the resulting functional requirements are described in Tables 28 – 32. For each use case, the name, goals, description, required system (logistics back end system or load carrier management system), KPIs to be calculated and the functional requirements are specified.

*Table 28 Use case 1: analysis of process times and transports between a source and a sink*

<b>Name</b>	Use case 1: analysis of process times and transports between a source and a sink
<b>Goal</b>	The goal is to create transparency about the material flow so that optimisation potential can be identified more easily.
<b>Description</b>	To identify optimisation potential, transparency about the material flow must first be created by calculating various KPIs. For this purpose, the KPIs average, minimum, and maximum transport times between a source and a sink and the number of transports between a source and a sink are needed. This can be used, for example, to identify bottlenecks between a source and a sink. However, in the logistics back end system, there are no automated analyses and visualisations regarding process times and transports between a source and a sink. The manual analysis of these KPIs by means of data exports and functions in Excel would be very time-consuming, as all the required data would first have to be exported, then linked together and

	subsequently evaluated. Moreover, this analysis would not be in real time and, therefore, would have to be carried out again and again.
<b>Required systems</b>	Logistics back end system
<b>KPIs</b>	<ul style="list-style-type: none"> <li>• Average, minimum, and maximum transport times between a source and a sink</li> <li>• Number of average transports between a source and a sink</li> </ul>
<b>Functional requirements</b>	<ul style="list-style-type: none"> <li>• <b>F1.1:</b> the DTRMF should calculate, store, and visualise the minimum, maximum, and average transport times (supply times) between a source and a sink in real time.</li> <li>• <b>F1.2:</b> the number of average transports between a source and a sink should be determined, stored, and visualised in real time.</li> </ul>

Table 29 Use case 2: analysis of the inventory of special load carriers with multi-use RFID transponders

<b>Name</b>	Use case 2: analysis of the inventory of special load carriers with multi-use RFID transponders
<b>Goals</b>	The goals of this use case are to create transparency about the inventory and load carrier circulation factor of the special load carriers with multi-use RFID transponders and to reduce costs by only procuring/reprocuring special load carriers that are really needed.
<b>Description</b>	In the automotive industry, special load carriers are used to transport special components. Due to the high costs of special load carriers, only as many as necessary should be purchased. However, if too few are purchased or replenished, this could in the worst case lead to production downtimes, as the supplier can no longer produce. The decision on the replenishment of load carriers is a challenge because transparency about the stock in circulation and the real load carrier factor is missing or very difficult to analyse. To support this decision on replenishment, the circulation stock of the special load carriers, as well as the real load carrier circulation factor, should be calculated automatically. (Knapp et al., 2023)
<b>Required systems</b>	Logistics back end system, load carrier management system
<b>KPIs</b>	<ul style="list-style-type: none"> <li>• Circulation stock</li> <li>• Real load carrier circulation factor</li> </ul>
<b>Functional requirements</b>	<ul style="list-style-type: none"> <li>• <b>F2.1:</b> the circulation stock as well as the real load carrier circulation factor of the special load carriers have to be calculated, stored, and visualised.</li> <li>• <b>F2.2:</b> data from the load carrier management system, such as demand for special load carriers for the next few months or stocks at the supplier, must be read, stored, and visualised.</li> <li>• <b>F2.3:</b> the data required for this use case from the logistics back end system and the load carrier management system should be linked with each other.</li> </ul>

Table 30 Use case 3: analysis of the best-before date for adhesive parts for a certain period of time

<b>Name</b>	Use case 3: analysis of the best-before date for adhesive parts for a certain period of time
<b>Goals</b>	The goals of this use case are to ensure production supply by determining at an early stage which adhesive parts will no longer be durable after a production break and

	have, for example, be reordered and to ensure quality by identifying adhesive parts with expired best-before dates that are already at the station at the body shop.
<b>Description</b>	Adhesive parts have a best-before date; if this is exceeded, the adhesive becomes too moist and the component must either be scrapped, brought in for testing or sent for re-drying, which, however, is time-consuming and associated with costs and is therefore only profitable for expensive components. If there are production breaks, it is difficult to determine which adhesive parts can still be used afterwards because this information is not determined and visualised in the logistics back end system. Therefore, there should be an input mask where the end of the production break is entered and an algorithm should then automatically determine whether the adhesive parts can still be used afterwards or whether they have to be ordered again or have to be dried or tested. This is important because all three processes take time and should be triggered as soon as possible. For example, it should be known at an early stage when adhesive parts have to be sent to the inspection to test if the best-before date could be extended for several days so that no bottlenecks occur there. In this way, it can be ensured that the required material is available and can be used when production is restarted after the production break. It must be taken into account that the adhesive parts have a remaining time. The remaining time describes the time that the body shop has to process the adhesive parts. Therefore, logistics can only place adhesive parts on the line (station) as long as the best-before date minus the remaining time has not been exceeded. In addition, in this use case, the number of days that an adhesive part can still be used after the production break should be calculated, because it could be that the adhesive part is not needed directly on the first day after the production break. In order to identify which adhesive parts are already at the stations, the last transfer orders to the production supply area should be identified and visualised. (Knapp et al., 2022)
<b>Required systems</b>	Logistics back end system
<b>KPIs</b>	<ul style="list-style-type: none"> <li>• Expiration date without remaining time of the adhesive parts</li> <li>• Number of days until the best-before date is reached after production break for each load carrier / adhesive part</li> </ul>
<b>Functional requirements</b>	<ul style="list-style-type: none"> <li>• <b>F3.1:</b> calculation, storage, and visualisation of the two KPIs described above.</li> <li>• <b>F3.2:</b> determination and visualisation of the last transfer orders to the production supply area.</li> </ul>

Table 31 Use case 4: analysis to determine the delayed material, the actual stock, and the expected deliveries

<b>Name</b>	Use case 4: analysis to determine the delayed material, the actual stock, and the expected deliveries
<b>Goal</b>	The goal is to save time in the analysis of delayed material by creating transparency about the delayed material, the actual stock, and expected deliveries (delivery schedules and order confirmations) for a material number.
<b>Description</b>	Production supply is responsible for ensuring that the required material is available on time at the production supply area. In the logistics back end system, all delayed materials, but also actual stocks as well as expected deliveries (delivery schedule lines and order confirmations) can be displayed via various transactions or tables. The production supply department must analyse the delayed material and assess whether manual intervention is required or whether it is not critical. To analyse the

	delayed material, it is helpful to know what the actual stock and expected deliveries are for a material number. However, in the logistics back end system, this information cannot be displayed in one overview and linking via Excel exports is time-consuming. Therefore, in this use case, the delayed materials together with the actual stock and expected deliveries should be linked and visualised on a dashboard with different filters.
<b>Required systems</b>	Logistics back end system
<b>KPIs</b>	In this use case, no additional KPIs are calculated.
<b>Functional requirements</b>	<ul style="list-style-type: none"> <li>• <b>F4.1:</b> the delayed material, expected deliveries, and the actual stock should be linked in one dashboard and clearly displayed with various filters.</li> </ul>

Table 32 Use case 5: analysis to identify open transfer orders and exceeding of the lead time

<b>Name</b>	Use case 5: analysis to identify open transfer orders and exceeding of the lead time
<b>Goal</b>	The goal is to save time when analysing open transfer orders.
<b>Description</b>	Production supply is responsible for ensuring that the required material is available on time at the production supply area. In the logistics back end system, all open transfer orders can be displayed via a transaction, and a lead time can be specified for each control cycle. This is the maximum time that should be needed to transport material from a source to a sink and thus the time in which an open transfer order should be acknowledged. However, the lead time in the logistics back end system is not automatically compared with the time that a transfer order is already open. Therefore, in this use case, this should be determined automatically and the transfer orders with exceeded lead time should be colour-coded and displayed with filters in a dashboard. This makes it easy to see which transfer orders have an exceeded lead time and to intervene at an early stage if necessary.
<b>Required systems</b>	Logistics back end system
<b>KPIs</b>	<ul style="list-style-type: none"> <li>• Exceeding of the lead time of open transfer orders</li> </ul>
<b>Functional requirements</b>	<ul style="list-style-type: none"> <li>• <b>F5.1:</b> it should be calculated whether the lead time has been exceeded in the transfer orders.</li> <li>• <b>F5.2:</b> the transfer orders should be visualised and those with exceeded lead time should be colour-coded.</li> </ul>

### 6.2.2 Qualitative requirements

The qualitative requirements are important because they form the basis of the architecture (Toth, 2015). The qualitative requirements were derived from expert discussions with future users of the DTRMF, as well as from Goll (2014) and ISO/IEC (2011b), and were already described in Knapp et al. (2022) and are summarised in the following.

- **Q1:** the DTRMF should support the execution of big data analyses on historical data by using batch jobs.
- **Q2:** the development time should be kept short and the complexity as low as possible.
- **Q3:** the maintenance and operation of the DTRMF should be easy.
- **Q4:** it should be possible to integrate a semantic data layer to ensure data interoperability.

- **Q5:** the data of the DTRMF should be processed and visualised in real time with a maximum time span of five minutes.
- **Q6:** the database of the DTRMF should support the storage, analysis, and retrieval of time series data.
- **Q7:** it should be possible to expand the DTRMF, for example, by adding further data sources.
- **Q8:** to ensure the performance, the DTRMF should be scalable, for example, when the number of users increases.
- **Q9:** occasional availability downtimes are tolerable, as the system is not production critical.
- **Q10:** company-specific guidelines should be taken into account when selecting technologies for implementation.

### 6.3 Literature review on digital twin and big data architectures

This section describes the state of the art of digital twin and big data architectures. For this purpose, a systematic literature review was conducted. This started from a Google Scholar search (freely available as opposed to commercial offerings such as Scopus) with the terms “*digital twin*” *AND architecture AND logistics* and “*digital twin*” *AND architecture*. Only references published after 2017, and other interesting papers were added to the list.<sup>2</sup>

The results of this literature review are shown in Table 33. In this table, it is analysed if the articles mentioned technologies for implementation, implemented the architecture, the level of description of the architecture, and if the requirements Q1 – Q4 (referred to R1 – R4 in this table) are met. In this evaluation, the requirements Q5 – Q10 were not included, as their fulfilment depends on the choice of technology. (Knapp et al., 2022)

---

<sup>2</sup> This paragraph is reprinted from International Journal of RF Technologies, vol. Pre-press, Knapp, H., Romagnoli, G., & Uckelmann, D., Architecture, application and implementation of a digital twin of the RFID-enabled material flow (DTRMF) in real-time for automotive intralogistics, pp. 1-32, Copyright 2022, with permission from IOS Press

## 6 Digital twin of the RFID-enabled material flow in real time

Table 33 Evaluation of the architectures from the literature review<sup>3</sup>

Legend: ●  $\triangleq$  described in detail / requirement completely fulfilled; ◐  $\triangleq$  described superficially or partially / partially fulfilled, ○  $\triangleq$  not described / not fulfilled

Architecture	Application area	Goals and key points of the architecture	Structure of the architecture	Type of data sources and data	Technologies for implementation	Implementation of architecture	Level of the description	R1: Big data analyses	R2: Development time	R3: Maintainability	R4: Data interoperability
Lambda Architecture (Marz, 2011)	Big Data	<ul style="list-style-type: none"> <li>- Architecture “beats the CAP theorem” (Marz, 2011)</li> <li>- “highly general and can be applied to any data system” (Marz, 2011)</li> </ul>	Three layers: Batch, serving and speed layer	No specific data sources / type of data	●	●	●	●	○	○	○
Kappa Architecture (Kreps, 2014)	Big Data	<ul style="list-style-type: none"> <li>- Contains no batch layer</li> <li>- Only stream processing</li> </ul>	Two layers: Speed layer (messaging system, stream processing), serving layer	No specific data sources / type of data	●	●	●	○	●	●	○
Lambda architecture for real-time IoT analytics in logistics (Haße et al., 2019)	Logistics, forklift control system	<ul style="list-style-type: none"> <li>- Integrates KPIs into the digital twin</li> <li>- Analysis and processing of real-time IoT data</li> <li>- Architecture with reference to concrete application</li> <li>- Based on lambda architecture</li> <li>- Contains a semantic layer</li> </ul>	Four layers: Data acquisition, data processing, data visualization, semantic layer	Microcontroller, sensors (e.g. position, acceleration, localization, motion)	●	●	●	●	○	○	●
Architecture for simulation-ready digital twin for realtime management of logistics systems (Korth et al., 2018)	Logistics, decision support system	<ul style="list-style-type: none"> <li>- Architecture “combines a realtime digital twin of logistics systems with simulation” (Korth et al., 2018)</li> <li>- “efficient integration of event-discrete simulation into a digital twin architecture” (Korth et al., 2018)</li> </ul>	Six components: event-controller, simulation, logbook, model, reporting, persistence	Scanners (barcode / RFID), sensors, bookings in a warehouse management system	○	●	◐	●	-	-	-
Cloud-fog-edge-based digital twin control framework (Pan et al., 2021)	Logistics	<ul style="list-style-type: none"> <li>- “multi-level cloud computing enabled digital twin system for the real-time monitor, decision and control of a synchronized production logistics system” (Pan et al., 2021)</li> <li>- edge computing, fog computing and cloud computing for different dynamics</li> <li>- synchronization mechanism</li> </ul>	Two layers: Physical layer (entity & IoT, control strategy, computing, local optimizer dimension) and virtual layer (model center, data center, synchronization control center)	“real-time data of production elements (personnel, machine tool, vehicles and cargo)” (Pan et al., 2021)	○	○	◐	●	○	○	●

<sup>3</sup> This table is reprinted from International Journal of RF Technologies, vol. Pre-press, Knapp, H., Romagnoli, G., & Uckelmann, D., Architecture, application and implementation of a digital twin of the RFID-enabled material flow (DTRMF) in real-time for automotive intralogistics, pp. 1-32, Copyright 2022, with permission from IOS Press

## 6 Digital twin of the RFID-enabled material flow in real time

Table 33 Continued

Digital twin architecture for enabling digital services (Merkle et al., 2019)	Automotive battery systems	<ul style="list-style-type: none"> <li>- reference architecture for a digital twin of manufacturing and product life cycle of a battery system to enable digital services</li> <li>- contains a UML (Unified Modeling Language) meta model</li> </ul>	Three layers: Hardware + connectivity, twin level, service level	Sensors, machinery, data loggers, manufacturing execution system, enterprise resource planning system					-	-	
Digital twin reference architecture model in industry 4.0 (Aheleroff et al., 2021)	Industry 4.0, wetland schedule maintenance	<ul style="list-style-type: none"> <li>- Reference architecture consists of three axis: Digital twin layers, agile process and digital twin integration levels</li> <li>- <i>“first attempts to build Digital Twin toward mass individualization”</i> (Aheleroff et al., 2021)</li> <li>- Digital twin as a service</li> </ul>	Five digital twin layers: physical, communication, digital, cyber, application layer	Sensor data					-	-	
Intelligent digital twin architecture (Talkhestani et al., 2019)	Production, assistance system / smart warehouse with climate control / field of metal forming	<ul style="list-style-type: none"> <li>- Intelligent Digital Twin in cyber-physical production system (CPPS)</li> <li>- Anchor-point-method for synchronization</li> <li>- Integration and precesing of the real operation data</li> <li>- Enabling co-simulation between digital twins</li> <li>- Automated control of physical assests via the digital twin</li> </ul>	Data-acquisiton interface, synchronization interface, operation data, relations, DT version management, modell, ID, organizational / technical specification, feedback interface, intelligent algorithm, service, DT model comprehension, co-simulation interface	Programmable logic controller (PLC) code of the PLC-controlled system, XML					-	-	
Architecture for a digital twin for intra-logistics process planning (Guerreiro et al., 2019)	Logistics, process planning	<ul style="list-style-type: none"> <li>- Provides a technology stack for the architecture</li> <li>- Contains information about the deployment with docker and docker swarm orchestration</li> <li>- Contains 3D visualization of the digital twin</li> </ul>	Five layers: data collection and ingestion, data storage, data processing engines, query-analytics-visualization, others (APIs, reverse proxy coordination, deployment)	Sources: services, files, RDBMS, data: manufacturing data, engineering data, produc & process data, automated storage, retrieval of parts, supply chain data					-	-	
Six layer digital twin architecture (Redelinguys et al., 2019)	Manufacturing cell	<ul style="list-style-type: none"> <li>- Architecture takes into account emulation and simulation</li> <li>- Open Platform Communications Unified Architecture (OPC UA) servers are used</li> <li>- IoT gateway (layer 4) is optional</li> </ul>	Six layers: physical devices, local controllers, local data repositories, IoT gateway, cloud based information repositories, emulation and simulation	Sensors, PLCs						-	



## 6 Digital twin of the RFID-enabled material flow in real time

Table 33 Continued

Digital twin architecture based on the industrial internet of things technologies (Souza et al., 2019)	IIoT	<ul style="list-style-type: none"> <li>- Uses OPC UA</li> <li>- Based on industrial internet of things technologies</li> <li>- Provides two views: one inside the workplace for critical processes and one outside the workplace</li> </ul>	Three components: physical twin, IIoT gateway, internal server (digital twin)	Sensors, PLCs					-	-	
Generic digital twin architecture (Steindl et al., 2020)	Industrial energy systems, thermal energy storage system	<ul style="list-style-type: none"> <li>- Technology independent architecture</li> <li>- Reference Architecture Model Industry 4.0 (RAMI4.0) was used</li> <li>- Focus on shared knowledge base and ontology concepts</li> <li>- Service oriented architecture</li> </ul>	Six layers: asset, integration, communication, information, functional, business	Sensors, events					-	-	
ISO 23247-2 – Digital twin framework for manufacturing – reference architecture (ISO, 2021)	Manufacturing	<ul style="list-style-type: none"> <li>- “reference architecture provides guidance for implementing digital twins in manufacturing” (ISO, 2021)</li> <li>- communication entity contains a device control sub-entity to control the OMEs (Observable Manufacturing Element)</li> </ul>	Four domains: observable manufacturing, device communication, digital twin, user domain	Sensors					-	-	

## 6.4 Architecture of the digital twin of the RFID-enabled material flow in real time

In this section, a new architecture for the DTRMF is presented, as the literature review revealed that the existing digital twin and big data architecture are not sufficiently described or do not fully meet the requirements of the DTRMF. The architecture consists of the following layers: (i) data ingestion layer, (ii) data processing and analyses layer, (iii) data storage layer, (iv) visualisation layer, and (v) the optional semantic layer as shown in Figure 54. To keep this architecture generic, no specific technologies are mentioned here. Each layer communicates only with the layer above and below to keep complexity low with exception of the semantic layer. (Knapp et al., 2022)

The **data ingestion layer** is about connecting the data sources and making them usable. Data sources could be, for example, databases, sensors, PLCs or files. As soon as the data are available, they are processed in the **data processing and analyses layer**. First, preprocessing is carried out, where for example the data are filtered or its format is changed. This part can be realized either as stream processing or in batch jobs, which are executed periodically in order to insure the real-time capability. The preprocessed data are then stored. The second part of this layer are the big data analyses, which are realised as batch processing and use the preprocessed and stored data. The results of the big data analyses are also stored in the database. Simulations or machine learning algorithms could also be carried out in this component. The **data storage layer** consists of the database, which saves all relevant data for the DTRMF which are the real-time data but also the historical data. In the **visualization layer**, the information of the DTRMF is visualized and thus this layer forms the interface to the users of the digital twin. The **semantic layer** is used to describe the data prepared and newly generated by the DTRMF in a uniform format and thus make the data accessible to other users and systems. Therefore, this layer has an interface to the database of the digital twin. <sup>4</sup>

---

<sup>4</sup> This paragraph is reprinted from International Journal of RF Technologies, vol. Pre-press, Knapp, H., Romagnoli, G., & Uckelmann, D., Architecture, application and implementation of a digital twin of the RFID-enabled material flow (DTRMF) in real-time for automotive intralogistics, pp. 1-32, Copyright 2022, with permission from IOS Press

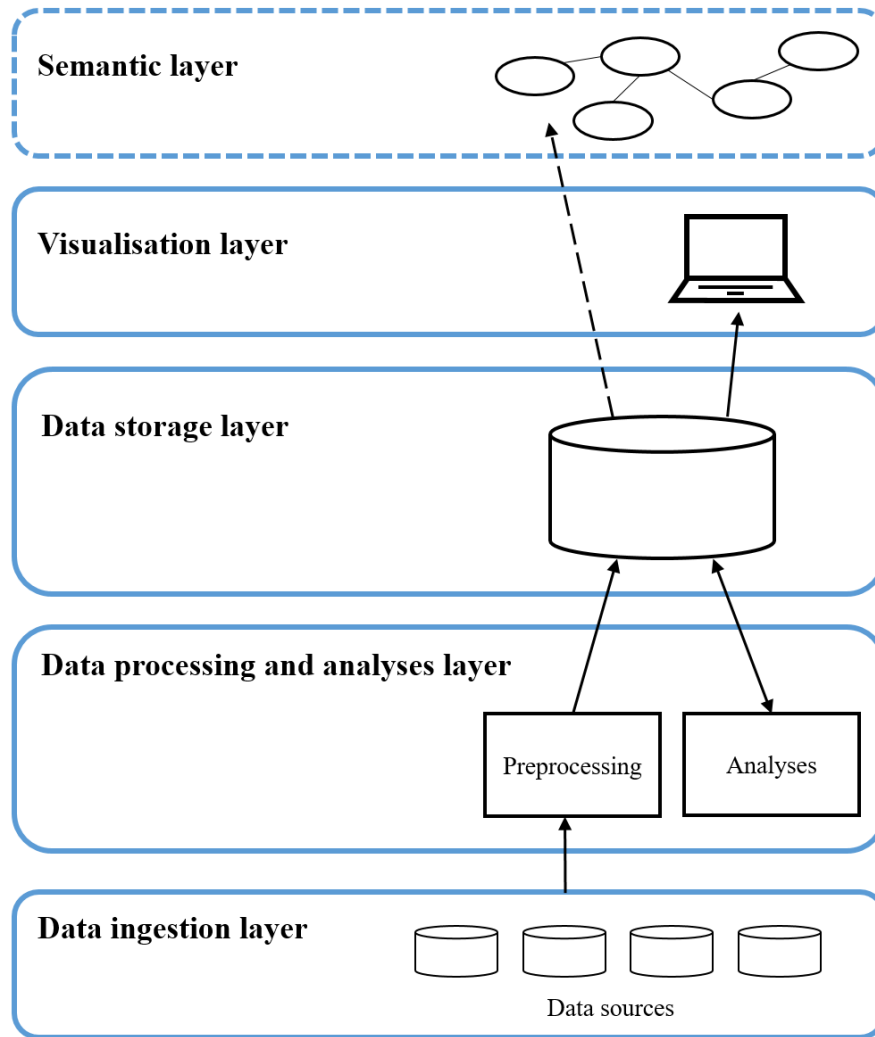


Figure 54 DTRMF architecture, according to Knapp et al. (2022)

## 6.5 Technologies for implementation of the architecture of the digital twin of the RFID-enabled material flow in real time

To implement the architecture described above, the appropriate environment and technologies must be selected. The DTRMF architecture should be implemented in a cloud environment, as this is more scalable, more flexible, no hardware needs to be procured, the infrastructure does not need to be maintained and therefore the requirements easy maintenance (Q3), scalability (Q8), and occasional non-availabilities are tolerable (Q9) are fulfilled. For the **data ingestion layer**, the software Qlik Replicate is proposed, as it supports many different source and target endpoints and it is already used in the company, thus fulfilling requirement Q10. The TimescaleDB is used as the database for the **data storage layer** because the database comparison in Knapp et al. (2022) showed that it is best suited for the requirements of the DTRMF. The **data processing and analyses layer** is realised with the programming language Python and the analyses platform Databricks. For the **visualisation layer** Databricks dashboards are used to keep development time and complexity low. The **optional semantic layer** is not considered further in this thesis, but could be realised using the Resource Description Framework (RDF) or Web Ontology Language (OWL) (see Steindl et al. (2020) and Haße et al. (2019)). But also the GS1 Core Business Vocabulary (CBV) 2.0 standard (GS1, 2022a) could be considered in this layer. (Knapp et al., 2022)

## 6.6 Implementation of the digital twin of the RFID-enabled material flow in real time by means of a case study

In order to verify the architecture of the DTRMF and to demonstrate its application with the proposed technologies, the DTRMF is implemented as a prototype in the body shop of an international car manufacturer. The requirements for this case study and the individual use cases are described in Section 6.2. The big data platform eXtollo from Mercedes-Benz Group AG (Mercedes-Benz Group AG, n.d.), which is based on the Microsoft Azure Cloud, is used as the cloud environment for the implementation.

### 6.6.1 Data ingestion layer

The basis of the DTRMF are the data. Therefore, the first step is to plan which data, data sources are needed for the implementation of the case study and how they are linked to each other. The data sources for the DTRMF are the logistics back end system and the load carrier management system. The logistics back end system in this case study is an SAP system where the data are stored in an Oracle database. The 19 database tables required for this case study from the logistics back end system are listed in Table 34. The columns used from these tables and the relations between these tables are shown in the entity relationship diagram in the Attachment 10.2.

The following data / CSV files are required for this case study from the load carrier management system for implementation of use case 2 (analysis of the inventory of special load carriers with multi-use RFID transponders).

- **Acquisition stock and open orders:** this file contains the number of procured load carriers as well as open orders per load carrier type and plant.
- **Current stock:** this contains the calculated stock of load carriers at the supplier.
- **Load carrier bookings:** the incoming and outgoing goods bookings per day and load carrier type are included here.
- **Evaluation of load carrier demands:** this contains the load carrier demands for the next weeks.

Table 34 Required tables for the case study from logistics back end system

Table	Table name
EKES	Vendor confirmations
EKET	Scheduling agreement schedule lines
EKPO	Purchasing document item
JITOCO	Call components JIT (just in time) outbound
JITOIT	Components group JIT outbound
LIKP	Sales and distribution document: delivery: header data
LIPS	Sales and distribution document: delivery: item data
LQUA	Storage quants
LTAK	Transfer order header
LTAP	Transfer order item
MAKT	Material descriptions
MARA	General material data
MARD	Storage location data for material
MCHB	Batch stocks
PABASN	Linking summarised JIT call – shipping notification

PKHD	Control loop
PVBE	Production supply area
RESB	Reservation / dependent requirements
VEKP	Handling unit header table

After planning which data and data sources are needed, they have to be ingested into the DTRMF. Due to organisational reasons, the real-time connection via Qlik Replicate of the two systems, the logistics back end system, and the load carrier management system, does not yet exist. Therefore, a simulation of these data and the real-time connection is programmed as described in Chapter 7.

### 6.6.2 Data storage layer

To realise the data storage layer, TimescaleDB was deployed in a Docker container in an Azure virtual machine and a permanent disk was attached to the virtual machine for permanent storage of the data (Knapp et al., 2022). For this purpose, the Microsoft Azure VM of the type DS5 v2 (16 VCPUs, 56 GB RAM) in the West Europe region with the operating system Linux, together with a managed disk of the type E60 (8192 GiB) were used. In addition to the physical storage of data, the data must be organised logically. When organising the data, the data should be structured in such a way that it can be accessed quickly, easily updated, linked and evaluated, but also protected from loss (Stahlknecht & Hasenkamp, 1999). The logical data organisation of the DTRMF is shown in the entity relationship diagram in Figure 55 and Figure 56 using UML. As TimescaleDB is a relational database, the data are stored in tables and each table contains a number of columns.

The materials are the central part of the material flow and the DTRMF. Each material has a material number, e.g. *A 223 630 58 01*. Then there is a language key, e.g., 'EN', which indicates the language of the material text (e.g. *SIDEWALL INR RH*). Furthermore, the remaining time and total expiration time are given for each material. The total expiration time contains the number of days from the production date to the best-before date. Furthermore, the *timestamp\_in* is saved for each material, which indicates when a material is created or changed. Thereby, the current properties of a material number can always be retrieved, but also the past states are stored and can be selected.

A control loop is identified by the control loop number and describes the assignment between a warehouse (storage location and storage type) and a production supply area. Furthermore, the control cycle contains the material number of the material that has to be transported between the specified source and sink. The supply id contains the assignment between the transfer orders that are generated for a control loop and the group of persons that carries out these transfer orders. Furthermore, the lead time for each control loop is stored. In addition, the control loop has a date from and a date until it is valid. If a control loop is changed, it is saved as a new entry in the table with the timestamp of the change. This means that the current parameters as well as past parameters of a control loop can always be selected from the database.

Each production supply area is assigned to a storage location and has a designation. A timestamp is also used here to version the changes.

When new material is needed in production, a material call-off is generated. This is uniquely identified by the part group number. Furthermore, it contains a call-off position, the control cycle number, the timestamp of the creation, the processing status, the called-off quantity as well as a delivery number and position. The timestamp *timestamp\_changed* can always be used to query the current or historical status of a material call-off.

A transfer order is uniquely identified by the transfer order number and position. The transfer order contains the load carrier type, the source storage location, the destination storage location, and other information. Furthermore, each transfer order has a creation date and time as well as an acknowledgement date and time. If a new transfer order is created, the acknowledgement date and time are initially empty. When a transfer order has been executed, the acknowledgement date and time are set by performing an UPDATE operation on the existing entry.

The stock table contains the stocks for a storage location, material number and batch. There are free usable stocks, locked stocks, stocks in quality inspection and order stocks. A new entry is created in the table with a timestamp each time it is updated and thereby, the history of the stocks is saved.

Furthermore, the stocks are stored at the level of the storage unit, which is the UII of the RFID transponder of the load carrier, in the table storage quants. The best-before date, batch, delivery, delivery position and time of removal from storage are also stored here. The time of storage of a load carrier is saved using the *timestamp\_in*.

Each goods receipt of a load carrier is stored with the timestamp of the goods receipt and the UII of the RFID transponder of the load carrier. Furthermore, the load carrier type is stored as well as the delivery number, original delivery number, the supplier, and the delivered quantity. This means that all goods receipts from each load carrier are stored as a time series in the goods receipts table.

When a supplier confirms an order, it is stored in the order confirmation table with the creation timestamp, changed timestamp and purchasing document number. The order confirmation contains the planned delivery date and time as well as the material and quantity that will be delivered. A purchasing document number is valid as long as the final delivery indicator and deletion indicator are empty.

The delivery schedule table contains the planned quantity to be delivered for each purchasing document number and day. Furthermore, the quantities already delivered are stored for each day. Here too, the history of the delivery schedule is generated by a timestamp.

In the reservations table, the material reservations are saved, which contain a unique reservation number. Furthermore, the reservation status, the material number, the validity, and the required quantity are saved. For all valid reservations, the columns *deleted* and *final issue indicator* should be empty.

The demands for load carriers are stored for the respective timespan, plant, and load carrier type as well as the date on which the demands were collected. This table is updated daily and the date could be used to determine the change in the planning of the demands or just to select the actual demands from the database.

The acquisition stock describes how many load carriers have been ordered for a plant and load carrier type and how many open orders exist. The date column contains the date on which the acquisition stock was created or updated.

The table *load carrier quantities* contains the stocks at the supplier as well as further information from the supplier, such as the city, but also the demand for load carriers at the supplier in the next few months, and the total number of load carrier booking in and out.

In the table *load carrier booking details*, the load carrier bookings in and out are stored at the load carrier type level for a supplier.

The stock in circulation and the load carrier circulation factor are calculated per day and stored together with the system stock. The system stock describes all load carriers that exist according to the logistics back end system.

## 6 Digital twin of the RFID-enabled material flow in real time

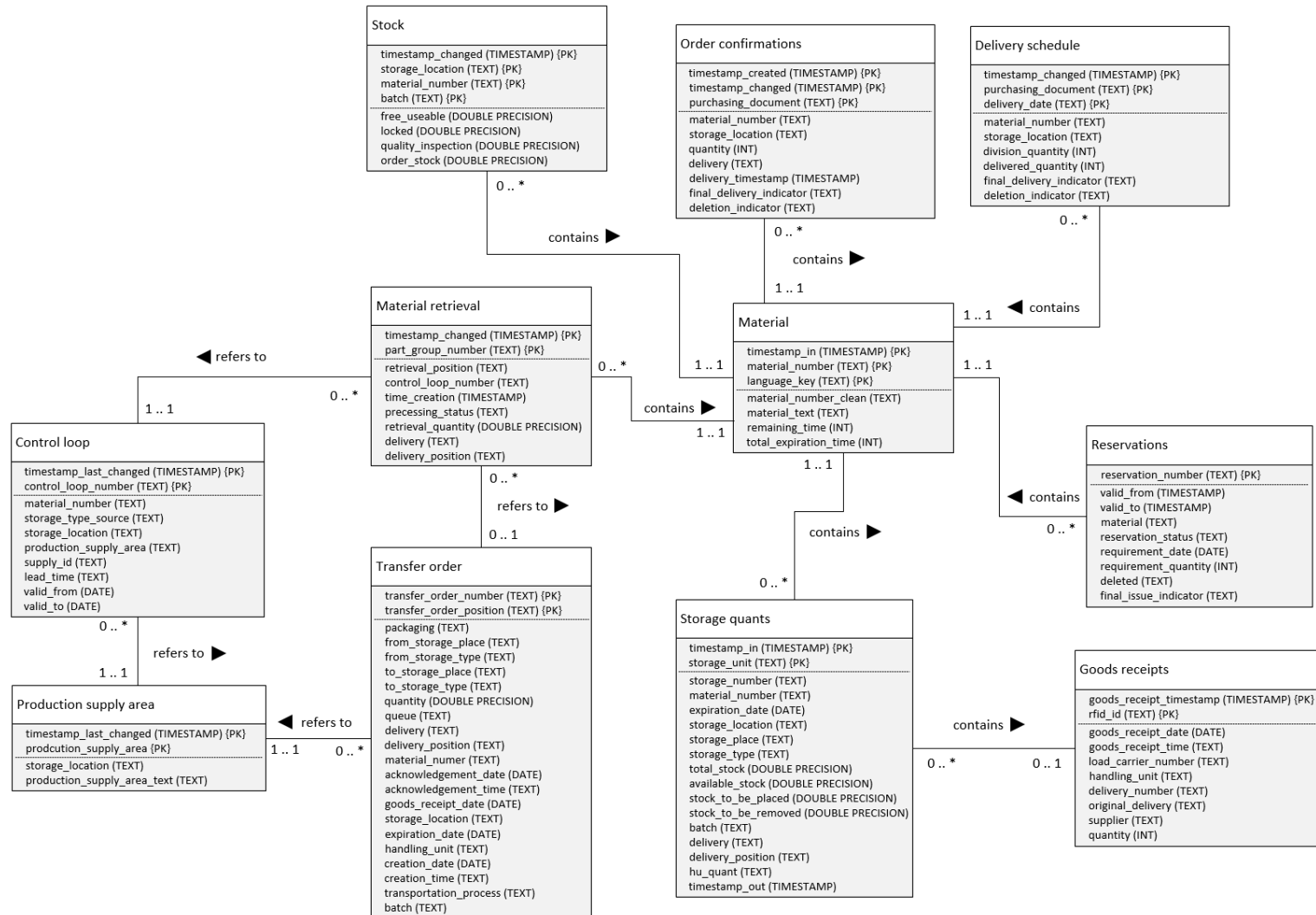


Figure 55 Entity relationship diagram of the DTRMF – part 1

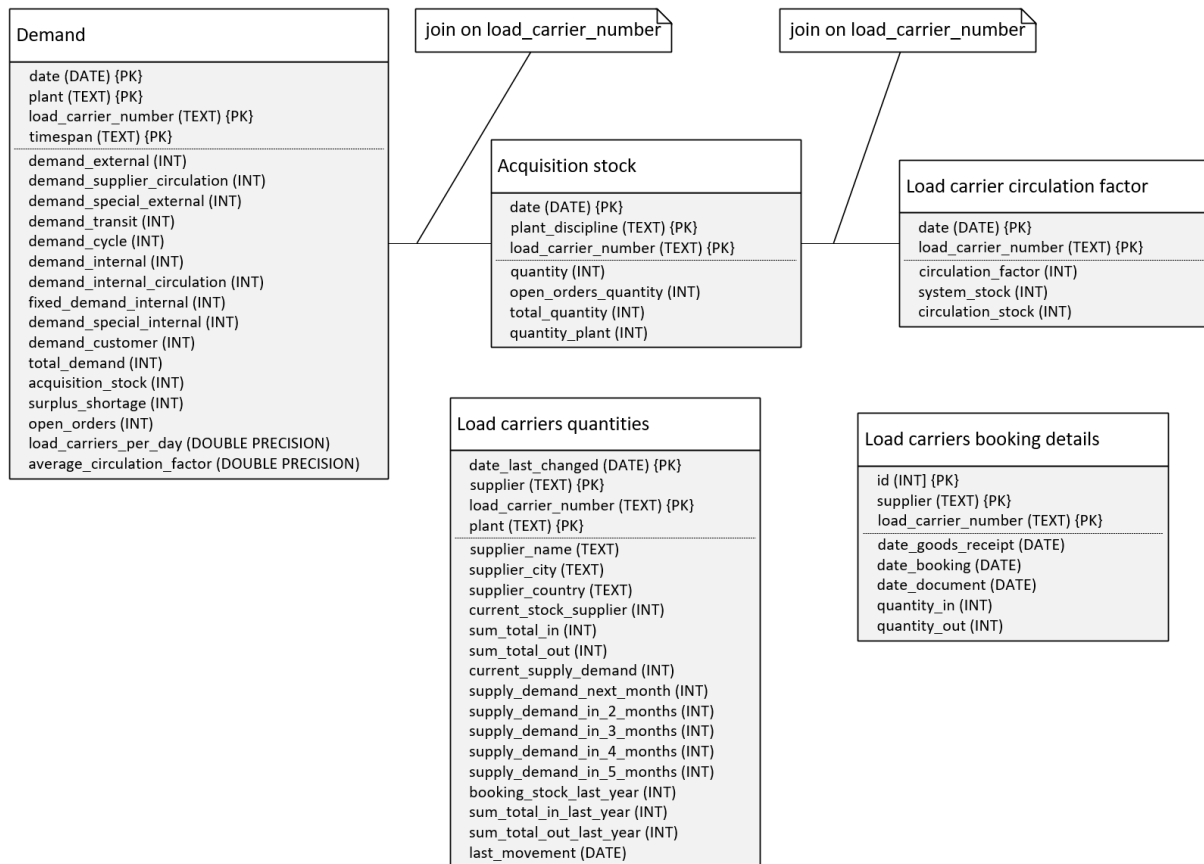


Figure 56 Entity relationship diagram of the DTRMF – part 2

### 6.6.3 Data processing and analyses layer

The data processing and analyses layer was implemented using Microsoft Azure Databricks and the programming language Python. The pre-processing is done in the following steps (similar to Knapp et al. (2022)):

1. The data for the DTRMF of each table / file from the logistics back end system and load carrier management system is stored in one folder, which contains the name *daily* in the Azure Blob Storage. The first step is to check whether there are new files from all related tables in these folders. This ensures the consistency of the data when joining multiple tables. If all contiguous tables are present, the following steps are performed in parallel in different threads to minimise the execution time. It is not necessary to go through each step for each target table of the DTRMF.
2. First, the CSV files are read from the Azure Blob Storage and stored in a PySpark DataFrame.
3. Then the columns are converted to the correct format and data type, e.g., numbers of type string are converted to type int.
4. New columns are then added, for example with calculated or transformed data.
5. Afterwards, the DataFrames are linked with each other via join operations.
6. In the sixth step, the columns of the DataFrames are renamed for better readability.
7. Then the DataFrames are stored in the DTRMF database. Here the new entries are saved with a timestamp or date for versioning so that a time series is formed, or existing entries are updated.



8. Finally, the imported CSV files are moved to the history folders of the Azure Blob Storage to archive them.

In the big data analyses for use case 2, the circulation stock and the real load carrier circulation factor are calculated. To do this, the required data are first read from the TimescaleDB using SQL (Structured Query Language) queries, then the stock in circulation and the real load carrier circulation factor are calculated and finally the results are saved in the TimescaleDB. (Knapp et al., 2023)

### **6.6.4 Visualisation layer**

The data of the DTRMF are visualised in Databricks dashboards and thus made accessible to the users. For this purpose, various SQL queries are sent to the database of the DTRMF and then, depending on the use case, further data are calculated, the columns are renamed and then visualised using widgets. The resulting dashboards are shown and described in Section 7.2 in Figure 58 to Figure 64.

## 7 Simulation of the RFID-enabled material flow and verification of the digital twin of the RFID-enabled material flow in real time

This chapter describes the simulation of the RFID-enabled material flow to verify the DTRMF. Subsequently, the results of the DTRMF and the evaluation of the requirements are presented. Furthermore, a simulative profitability analysis and a user survey are carried out.

### 7.1 Methodology and implementation of the simulation

This section describes the simulation of the RFID-enabled material flow. The simulation of the data and real-time connection is programmed in Python and is executed locally on a computer. Figure 57 shows the process of simulating the data in real time. First, the simulation is configured, then the load carrier stock at the supplier is simulated and in the third step the load carrier demands are simulated. Then the simulated data are generated for each configured load carrier type. First, initial data are generated and then the goods receipts, transfer orders and material call-offs for each day of the simulation. Finally, the data for the storage material tables are prepared and then first the initial data are uploaded in order to simulate the required data from the past and then the data of the tables are uploaded in real time to the Azure Blob Storage. The individual steps of these functions are described in detail below.

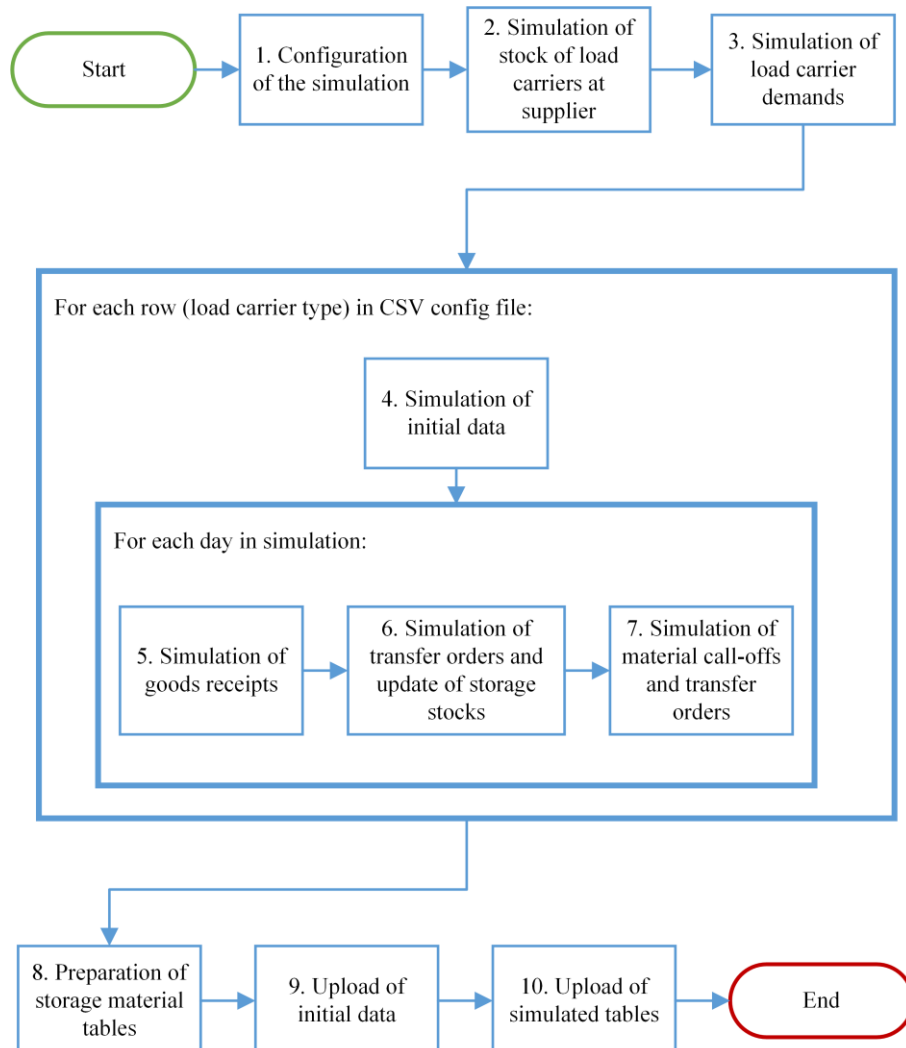


Figure 57 Flowchart of the simulation of logistics back end system and load carrier management system

### 7.1.1 Configuration of the simulation

First, the simulation is configured. For this purpose, the start date of the simulation and the number of days of the simulation are defined. For this case study the start date is set to 8<sup>th</sup> August 2022 and the number of days to 30. In addition, further input parameters for the simulation need to be defined in a CSV file (see Table 35). In the CSV file, one load carrier type and the corresponding parameters are specified for each row. For this simulation, the two load carrier types 19284 and 18681 were configured. First, the number and the name of the material in German and English that is transported in this load carrier type (e.g., 19284) are specified. Furthermore, the number of the control loop is defined. A control loop contains the relation between production supply area (sink) and the from-storage-location (source), and the way new material is retrieved. Therefore, the source storage location (e.g., H020) as well as the from-storage-type, from-storage-place, to-storage-location (sink), to-storage-type and to-storage-place are also specified. The parameter supply id specifies the assignment of a group of employees who carry out the transfer orders for one or more control loops. In addition, the validity of the control loop is specified (*valid\_from* and *valid\_to*) as well as the date and time of the last change of the control loop. Furthermore, the storage location for the quality inspection is specified. Also, the quantity present in a load carrier must be indicated as a parameter in the CSV file. Since the adhesive parts have a best-before date, the number of days until the best-before date is reached is determined as a parameter. The remaining time is also specified. This defines the number of days that the body-in-white has time to install the component until the best-before date is reached. Therefore, logistics can only place materials on the line (station) until the best-before date minus the remaining time has been reached. Another parameter of the CSV file is the number of load carriers that arrive at the goods receipt per day and the time span between two deliveries. It is also configured how many load carriers are called off per day from the plant (production supply area) and how many of these material call-offs are delayed, which means material is called off but there is no more material in the warehouse. In order to transfer the material from the warehouse to the production supply area, transfer orders are created which must be completed within a defined lead time. Therefore, the lead time and the number of transfer orders that exceed this lead time are also defined. In addition, the purchasing document number is specified, which links the vendor confirmations, scheduling agreement schedule lines and purchasing document items. Another parameter is the supplier number of the material. To simulate the circulation stock, the number of load carriers in circulation is defined. Furthermore, the path to a file containing all UIIs of the RFID transponders of the load carriers must be specified. This file was exported from the load carrier management system and saved as a CSV file for this simulation.

Table 35 Exemplary representation of the configuration file

Parameter	Example
Load carrier type	19284
Material number	A 223 630 58 01
Material name German	SEITENWAND IN RE W
Material name English	SIDEWALL INR RH
Control loop	1363406
From-storage-location	H020
From-storage-type	ÖBO
From-storage-place	020-604
To-storage-location	P020
To-storage-type	ÖP2
To-storage-place	7222_04243

## 7 Simulation of the RFID-enabled material flow and verification of the digital twin of the RFID-enabled material flow in real time

---

Supply ID	ÖVG9
Valid from	29.12.2021
Valid to	31.12.9999
Date last changed	25.01.2022
Time last changed	03:10:36
Storage location for the quality inspection	QS01
Quantity	3
Number of days until the best-before date	30
Remaining time [days]	1
Number of load carriers at goods receipt per day	7
Time span between two deliveries [hours]	1
Number of material call-offs per day	7
Number of delayed material call-offs per day	2
Lead time [minutes]	30
Number of transfer orders with exceeded lead time	3
Purchasing document number	5500252287
Supplier number	123456789
Load carriers in circulation	75
Path to file with all UIIs of the RFID transponders	VEKP_19284.csv

### 7.1.2 Simulation of stock of load carriers at supplier

In this function the stock of load carriers at the supplier is simulated, which is stored in the load carrier management system. The stock of load carriers at the supplier contains: (i) supplier number, (ii) supplier name, (iii) supplier street and street number, (iv) supplier postcode, (v) supplier city, (vi) supplier country, (vii) plant of the automotive manufacturer, (viii) load carrier type, (ix) last movement of the load carrier type, (x) current stock at supplier, (xi) current demand, (xii) planned demand next month, (xiii) planned demand in two months and further parameters. The stock at the supplier is simulated for all load carrier types at the same time and therefore the data required for this are generated in the second step of the simulation. For this purpose, a CSV data export generated from the load carrier management system is used, which contains all the parameters described above. The CSV file is first read into a Pandas DataFrame. The stocks at the supplier are not changed in this simulation, as these are not required for any further analyses of the DTRMF and it is assumed that they are inaccurate, as in some cases the stocks at the supplier are higher than the procured stocks. However, as this is only a data export, the date of the last movement must be adjusted. Therefore, a new DataFrame is generated, where all parameters for the simulation of the stock of load carriers at the supplier are stored. The adjustment of the last movement date is done in a for-loop over all days of the simulation, where the date of the last movement is replaced by the new generated timestamp and then this row is appended to the DataFrame. Finally, the column *header\_timestamp* is added to this DataFrame. This represents the timestamp at which a database operation (INSERT, UPDATE or DELETE) was performed and which would also be present in a real data connection using Qlik Replicate. Therefore, the *header\_timestamp* in this case is the timestamp of the last movement. Furthermore, this timestamp is used later to send the data to the Azure Blob Storage at the correct time.

### 7.1.3 Simulation of load carrier demands

In the third step, the data for the planned load carrier demands for the next months are simulated. These data are stored in the load carrier management system and include the following parameters: (i) load

carrier type, (ii) plant, (iii) time span, (iv) external demand, (v) supplier circulation demand, (vi) transit demand, (vii) cycle demand, (viii) internal demand, (ix) fixed demand internal, (x) special demand internal, (xi) total demand, (xii) load carrier circulation factor. For the simulation of these parameters, a data export is also used for the requirements of the current month (August) and a data export which has already been adapted in Excel to the next month (September). These data exports are first read into two Pandas DataFrames. Then a new DataFrame is created in which all simulated demands are stored. Then, in a for-loop over the number of days of the simulation depending on the current date, the DataFrame from August or September is used and added to a temporary DataFrame. Afterwards, a *header\_timestamp* with the current date of the simulation is added as a new column to this temporary DataFrame and it is attached to the DataFrame with all the simulated demands. Through this method, the parameters of the demands remain the same for each day of the simulation, but the time spans were adjusted accordingly and thus the demands were simulated sufficiently for each day.

#### 7.1.4 Simulation of initial data

If the data sources were connected using Qlik Replicate, a full load of all required database tables would be carried out at the beginning in order to transfer the data of the current state of the system and thus of the material flow to the DTRMF. Therefore, the initial data required for this are generated in the fourth step. This is done in a for-loop for each load carrier type. In addition, further individual data are generated in this step, as described below, which are then sent to the DTRMF in real time.

First, the data for the initial stocks are generated. For this purpose, the file with all existing UIIs of the RFID transponders is read into a Pandas DataFrame and columns that are not required are filtered out. This DataFrame is used to represent the initial state of the table VEKP (handling unit header table). The DataFrame is then copied into a new DataFrame that simulates and contains the circulating stock. The number of all load carriers minus the *load carriers in circulation* from the configuration file is used to calculate how many load carriers are not in circulation. Then as many rows are deleted from this DataFrame as there are load carriers that are not in circulation. This stock in circulation is used for the simulation of further data and it is assumed that these load carriers are at the supplier and are delivered to the goods receipt of the car manufacturer during the simulation.

Since there is the two-container principle in the body shop, which means that there are always two load carriers at a station (production supply area), two load carriers are placed there initially. These two load carriers are taken from the DataFrame with the circulating stock and added to a new DataFrame and further columns are added. This new DataFrame contains the columns UII, load carrier type, production supply area, material number and a timestamp at which the load carriers were placed at the production supply area.

In addition, the storage stocks are simulated. These consist of the material number, the storage location, the free usable stock, the locked stock, and the stock in quality inspection. All these stocks are set to 0 for the from-storage-location (source) and only the free usable stock at the production supply area is defined. The stock is two times the quantity per load carrier, as there are already two load carriers at the production supply area as specified before. All stocks are stored in a DataFrame and the *header\_timestamp 2022-01-01 00:00:00* and the *header\_operation INSERT* are added as columns.

Furthermore, the initial data for the table EKET (scheduling agreement schedule lines) are simulated and stored in a newly created DataFrame. The planned delivery schedule lines are already stored in the logistics back end system for approximately one year in advance. Therefore, they are initially generated for the entire period of the simulation in a for-loop over all days of the simulation. The parameters purchasing document number, quantity, and number of load carriers per day specified in the

configuration are used to generate the simulated data. The purchasing document number remains the same for each day and the expected delivery date is always the current day of the simulation. In addition, the schedule line quantity is calculated, which is the number of load carriers at goods receipt per day times the quantity. The goods receipt quantity is set to 0 because no material has been delivered yet. In addition, the timestamp *2022-01-01 00:00:00* is set as *header\_timestamp*, as the schedule line quantity is stored in the logistics back end system a long time in advance. Furthermore, the *header\_operation* INSERT is added as an additional column.

The table EKPO (purchasing document item) is then simulated. This table contains the purchasing document number, the storage location, the material number and a final delivery indicator and deletion indicator. Since it is assumed that this table changes very rarely, only the initial INSERTs into this table are simulated, but no later changes. For this purpose, the parameters purchasing document number, from-storage-location and material number from the configuration are used and the final delivery indicator and deletion indicator must be empty.

Then the material data for the tables MAKT (material descriptions) and MARA (general material data) are generated. Since it is assumed that these data rarely change, they are only generated initially during the simulation, but no changes to these two tables are simulated. For this purpose, a DataFrame is created for the MARA table and the parameters material number, remaining time, and days until the best-before date are added as columns from the configuration of the simulation. In addition, the columns *header\_operation* INSERT and the *header\_timestamp 2022-01-01 00:00:00* are added. A DataFrame is also created for the table MAKT with the material number, the material text in German, the language abbreviation 'DE' in one line and the material number, the material text in English and the language abbreviation 'EN' in a second line. In addition, the *header\_timestamp* and *header\_operation* are added as columns, as before.

Furthermore, the table PKHD (control loop) is simulated. It is assumed that this table rarely changes and therefore the data is only simulated initially. The parameters control loop number, material number, from-storage-type, to-storage-place (production supply area), supply ID, lead time, date last changed, time last changed, valid from, valid to are used from the configuration and added to a DataFrame. Furthermore, the *header\_timestamp 2022-01-01 00:00:00* and the *header\_operation* INSERT are added.

The simulation of the table PVBE (production supply area) is done analogously to the table PKHD. Here, the parameters to-storage-place and to-storage-location from the configuration file are stored in a DataFrame and the data are generated only once and then not changed during the simulation.

Finally, the initial data for the table RESB (reservation / dependent requirements) is generated. These reservations are created in the logistics back end system approximately one year in advance and are then gradually updated or deleted. Therefore, a new DataFrame is created for the initial reservations and a DataFrame where the existing reservation is then deleted daily. To do this, the number of days of the simulation is iterated over in a for-loop. In this for-loop, the reservation is first created with the parameters material number, reservation number (this is generated in ascending order), reservation status (= 'B'), the requirement date, requirement quantity, the deletion indicator (= '') and the end date (= '') as well as the *header\_operation* INSERT and the *header\_timestamp 2022-01-01 00:00:00*. The reservation status is set to 'B' because this contains the aggregated stocks which are needed for the DTRMF. Furthermore, the deletion of this reservation from the database is simulated by setting the same parameters with the *header\_operation* DELETE and the *header\_timestamp* with the date of the current day and the time 23:59:59.

Since the incoming and outgoing bookings for a load carrier type are stored in the load carrier management system, they are also simulated. To do this, it is iterated over the number of days of the simulation and two rows are created for each day. The incoming bookings of the load carriers are simulated in one row and the outgoing bookings in the second. Both rows consist of the supplier, load carrier type, automotive manufacturing plant, incoming goods receipt date, outgoing goods receipt date, date of the document, number of incoming load carriers and number of outgoing load carriers. The number of incoming / outgoing load carriers is the number of load carriers per day at the goods receipt as specified in the configuration file. The goods receipt date, the booking date, the document date, and the *header\_timestamp* are all set to the respective day of the simulation.

### 7.1.5 Simulation of goods receipts

Subsequently, further the data are simulated in a for-loop over the number of days of the simulation. First, in the fifth step of the simulation, the data for the goods receipts for the individual load carriers at the car manufacturer, the corresponding order confirmations and updates of the delivery schedule divisions are generated. Therefore, a DataFrame *df\_deliveries* is created, which contains the simulated data for the tables EKES (vendor confirmations) and EKET (scheduling agreement schedule lines) and the DataFrame *df\_goods\_receipts*, which stores the simulated data for the tables VEKP (handling unit header table), LIKP (sales and distribution document: delivery header data) and LIPS (sales and distribution document: delivery: item data). In this function, another for-loop iterates over the number of load carriers per day at goods receipt. In this for-loop, first a timestamp of the planned goods receipt / delivery is generated, which is the current date of the simulation and 07:00:00 as the time for the first load carrier per day, which is then incremented by the time span between two deliveries defined in the configuration file. Then a line for the DataFrame *df\_deliveries* is generated and added. This line contains the purchasing document number from the configuration file and the previously generated expected delivery date and time. Another parameter is the date of the order confirmation, which corresponds to the current date of the simulation, and the time of the order confirmation. The time of the order confirmation is the time of the expected delivery minus 45 minutes, as this is transmitted by the supplier in advance. The delivered quantity is set to 0, as nothing has been delivered yet at the time of the creation of the order confirmation. Furthermore, a unique delivery number is generated and the *header\_timestamp*, which is the timestamp of the order confirmation, and the *header\_operation* INSERT are added. As soon as the load carrier is at the goods receipt, this delivery is updated and therefore a new row with *header\_operation* UPDATE and *header\_timestamp* with the timestamp of the goods receipt is added to the *df\_deliveries* DataFrame. To simulate delayed material, the goods receipt timestamp of as many load carriers as were defined as delayed in the configuration file are simulated first. Therefore, 55 minutes are added to the expected timestamp of the goods receipt. If the material is not delayed, then the goods receipt timestamp is equal to that of the expected delivery. In addition, this update sets the delivered quantity to the number per load carrier defined in the configuration file. To simulate the data for the *df\_goods\_receipt*, a load carrier is removed from the DataFrame with the circulating stock and added as a new row to the DataFrame *df\_goods\_receipts*. This row contains the UII, load carrier type, handling unit and material number. Furthermore, the delivery number, external delivery number, which is generated and incremented for each load carrier, timestamp of the goods receipt, supplier and delivery quantity are added. All simulated data for the tables EKES, EKET, VEKP, LIKP and LIPS have thus been generated.

### 7.1.6 Simulation of transfer orders from the goods receipt to the warehouse and update of storage stocks

The load carriers booked at goods receipt must then be transported to the warehouse. Therefore, the transfer orders from goods receipt to the warehouse are simulated as well as the updated storage stocks.

First, the best-before date is generated for all load carriers of the current day and the batch that contains this date. In order to simulate different batches, the best-before date of the goods receipt date minus one day plus the number of days until the best-before date from the simulation is used for the first incoming load carrier per day. For all other load carriers, the goods receipt date plus the number of days until the best-before date is used as the best-before date and part of the batch.

For the simulation of the transfer orders, the DataFrame *df\_goods\_receipts* which contains all goods receipts, is iterated over. For each goods receipt, a transfer order is first created and then updated after the transfer order is acknowledged. Therefore, two rows per transfer order are added to the DataFrame *df\_transfer\_orders* with the columns described below. The transfer order number is generated in the simulation and incremented for each new transfer order. The transfer order item is always set to 1. The creation date and time are the date and time of the goods receipt. Furthermore, the parameters load carrier type, handling unit, material number, goods receipt date and quantity are taken from the *df\_goods\_receipt* DataFrame. In addition, the parameter from-storage-type is set to '902', which identifies the goods receipt area, and from-storage-place is set to 'RFID', since the transponders of the load carriers at the goods receipt are read by RFID gates and then booked automatically. The parameters to-storage-location, to-storage-type, to-storage-place describe the storage location and are stored in the configuration file as from-storage-location, from-storage-type, and from-storage-place, since the material is later transported from here to the production supply area. The queue, delivery and delivery position are empty for these transfer orders. In addition, the acknowledgement date and acknowledgement time are left empty, as these transfer orders are only created initially. The expiration date and batch generated as described above are also added as columns. The transport operation is set to the value 'TL'. In addition, the timestamp of the goods receipt is used as *header\_timestamp* and the *header\_operation* is an INSERT. The parameters for the acknowledged transfer orders are the same, except that here the goods receipt date is set as the acknowledgement date and the goods receipt time plus five minutes is set as the acknowledgement time, and the *header\_timestamp* is the timestamp of the acknowledgement timestamp and the *header\_operation* UPDATE are added. The DataFrame *df\_transfer\_order* thus contains the simulated data for the tables LTAK (transfer order header) and LTAP (transfer order item).

After the material has been placed in storage, the storage stocks must be updated accordingly. To do this, the DataFrame *df\_goods\_receipts* is copied into the DataFrame *df\_storage\_stocks*, unneeded columns are filtered out and the expiration date and batch generated as described above are set and the storage-location, storage-type, storage-place, which are defined as form-storage-location, from-storage-type, from-storage-place in the configuration file, are used. The total stock and free usable stock are both set to the delivered quantity. The stock to be stored and the stock to be removed are set to 0. The delivery position is set to 10, as the quantities of material are stored under this position. In addition, the time of storage is set, which is the timestamp of the goods receipt plus five minutes. For later functions of the simulation, the timestamp of the stock removal is set, which is empty here because the material is in the warehouse, and the reservation status is set to False. These data simulate the tables LQUA (storage quants), MARD (storage location data for material), and MCHB (batch stocks).



### 7.1.7 Simulation of material call-offs, transfer orders and update of storage stocks

In the seventh step, the material call-offs and associated transfer orders from the warehouse or, in the case of delayed material, from goods receipt to the production supply area must be simulated.

The data for this are generated in a for-loop over the number of call-offs per day, which are defined in the configuration file. First, the timestamp for the first material call-off on the day is generated, which consists of the current date of the simulation and the time 07:30:00 a.m. The timestamp of the material call-off is then always increased for the further material call-offs by the time span, e.g., 1 hour between two deliveries at the goods receipt, which is specified in the configuration file. Then it is checked whether the called-off material is available in the warehouse.

If material is available in the warehouse, a material call-off is generated with the processing status 'ZI30' and the associated transfer order. The material call-off contains a part group number that is generated and incremented with each new material call-off and then a call-off position, which is always 1. Furthermore, the control loop number, the call-off quantity, which are stored in the configuration file, are each added as a column in the DataFrame *df\_material\_call\_offs*. The timestamp at which the material call-off was created is also the timestamp of the last change to this material call-off and the *header\_timestamp*. Since the material call-off was newly created, the *header\_operation* INSERT is used. A new transfer order is then created so that the material is transported from the warehouse to the production supply area. First, the load carrier that has been in the warehouse the longest is determined from the DataFrame *df\_storage\_stocks* since it should be removed from storage first. The transfer order created for this contains a transfer order number, which is incremented for each new transfer order, and the transfer order item 2. The creation date and time are generated from the timestamp of the material call-off. In addition, the parameters material number, handling unit number, from-storage-location, from-storage-type, from-storage-place, goods receipt date, expiration date, batch and quantity are taken from the DataFrame *df\_storage\_stocks*. Furthermore, a new delivery number is created, and the delivery item is set to the value 10, which are later used for the assignment between material call-off and transfer order. As the transfer order is created, acknowledgement date and acknowledgement time are empty. For transfer orders from the warehouse to the production supply area, the transport operation is set to the value 'QB'. The *header\_timestamp* is the timestamp of the creation of the material call-off and the *header\_operation* is an INSERT. Then the confirmation of the transfer order is simulated. Transfer orders that exceed the specified lead time are also simulated. The number of transfer orders with exceeded lead time is specified in the configuration file. The first transfer orders of the day are simulated to exceed the lead time until the specified number is reached. A transfer order with exceeded lead time has the acknowledgement date of the current day of the simulation and the acknowledgement time is the time of the material call-off plus the defined lead time plus 15 minutes. For transfer orders that are acknowledged within the lead time, the acknowledgement time is the time of the material call-off plus the lead time minus 10 minutes. Otherwise, the same parameters are set as for the creation of the transfer order, only the *header\_operation* is an UPDATE and the *header\_timestamp* is the acknowledgement timestamp. After the material has been delivered to the production supply area, the material call-off is updated. To do this, a new row is created in the DataFrame *df\_material\_calls* analogous to the creation of a material call-off with the difference that the processing status is set to 'ZI99', the acknowledgement timestamp is the last changed timestamp and *header\_timestamp* and the *header\_operation* is UPDATE. The table PABASN (linking summarised JIT call – shipping notification) contains the relationship between material call-off and transfer order. To simulate this table, the part group number and call-off position from the material call-off and corresponding delivery number and position from the transfer order are added to the DataFrame *df\_pabasn* with the timestamp of the creation of the material call-off as *header\_timestamp*. Finally, it must be simulated that before a new load carrier can be placed at the production supply area, the previous one is transported away. For this purpose, the load carrier that has

already been at the production supply area the longest is transported away first since it is emptied first. The load carrier that has been transported away is then added back to the DataFrame with the circulating stock. This process is only carried out for other functions in the simulation, but in reality, it is not apparent at which point empty load carriers are transported away. However, the stock still needs to be updated because a load carrier has been removed from the warehouse. For this purpose, the UID of the transponder of the load carrier is filtered in the DataFrame *df\_storage\_stocks* and the *timestamp\_out* is set to the timestamp of the acknowledgement.

If there is no material in the warehouse, for example because the delivery has been delayed, the material call-off is generated in the same way as above, but with the processing status 'Z115'. As there is no material in the warehouse, no transfer order for material from the warehouse to the production supply area can be generated at this time. However, as soon as new material is delivered, the material call-off is set to processing status 'Z130' and a corresponding transfer order is generated. This is generated in the same way as described above with the difference that the material is transported directly from the goods receipt to the production supply area. Therefore, the variable from-storage-type is set to the value '902' and from-storage-place is 'RFID'.

The DataFrame *df\_material\_call\_offs* created in this way contains the data for the tables JITOCO (call components JIT outbound) and JITOIT (components group JIT outbound). The DataFrame *df\_transfer\_orders* later forms the tables LTAK (transfer order header) and LTAP (transfer order item). The DataFrame *df\_pabasn* represents the table PABASN and the *df\_storage\_stocks* contains the data for the tables LQUA, MARD, MCHB.

### 7.1.8 Preparation of storage material tables

After all data have been generated, the data of the warehouse stocks, which are stored in the DataFrame *df\_storage\_stocks*, must be prepared. The DataFrame can be used directly for the simulation of table LQUA, but not for tables MARD and MCHB. The DataFrame contains the storage stocks per storage location, material, batch, and load carrier (see Table 36). In table MCHB, however, the storage stocks are only stored at the level of storage location, material, and batch, and in table MARD they are only aggregated per storage location and material.

First, the DataFrame *df\_storage\_stock* is iterated over, as each row contains a *timestamp\_in* and a *timestamp\_out*. In this for loop, two rows are generated from each row and assigned to the DataFrame *df\_tmp*. One row is representing storage of the load carriers with the *header\_timestamp* equal to the *timestamp\_in* and the second representing retrieval material from the storage with the *header\_timestamp* equal to the *timestamp\_out*. The stocks, which are retrieved from the storage are also negated, as in the next step the stocks are aggregated. Table 37 shows an example of the prepared data of the DataFrame *df\_tmp*.

The variable quantity is initialised with 0, which contains the total stock of a storage location and material number. The DataFrame *df\_tmp* is iterated over and the stock of the storages and removals (which were negated before) is added up in the variable quantity. Then the storage location, the material number and the total stock is added to the DataFrame *df\_storage\_material*. Thus, the new DataFrame contains total aggregated stock, as can be seen in Table 38 as an example. The *header\_operation* is always an UPDATE.

In order to aggregate the stocks also on the batch level for the simulation of the table MCHB, a list with all existing batches is iterated over. For each batch, a variable *quantity\_batch* is first initialised with 0 and the stocks per batch are then aggregated in this variable. The aggregated stocks for a storage location, material number and batch are then added to the DataFrame *df\_storage\_batch*, as Table 39 shows as an

## 7 Simulation of the RFID-enabled material flow and verification of the digital twin of the RFID-enabled material flow in real time

example. The *header\_operation* is an INSERT the first time a new batch is present and an UPDATE otherwise.

Table 36 Exemplary representation of the stocks per storage location, material number, batch, and load carrier

Storage location	Material number	Batch	UII (shortened)	Free usable stock	Timestamp in	Timestamp out
H020	A 223 630 58 01	027296	1288376	3	2022-08-08 09:05:00	2022-08-08 10:15:00
H020	A 223 630 58 01	02720907	1288390	3	2022-08-08 10:05:00	2022-08-08 11:15:00

Table 37 Exemplary representation of the prepared stocks per storage location, material number, batch, and load carrier

Storage location	Material number	Batch	UII (shortened)	Free usable stock	Header timestamp
H020	A 223 630 58 01	027296	1288376	3	2022-08-08 09:05:00
H020	A 223 630 58 01	02720907	1288390	3	2022-08-08 10:05:00
H020	A 223 630 58 01	027296	1288376	-3	2022-08-08 10:15:00

Table 38 Exemplary representation of the stocks per storage location, and material number

Storage location	Material number	Free usable stock	Header timestamp	Header operation
H020	A 223 630 58 01	3	2022-08-08 09:05:00	UPDATE
H020	A 223 630 58 01	6	2022-08-08 10:05:00	UPDATE
H020	A 223 630 58 01	3	2022-08-08 10:15:00	UPDATE

Table 39 Exemplary representation of the stocks per storage location, material number, and batches

Storage location	Material number	Batch	Free usable stock	Header timestamp	Header operation
H020	A 223 630 58 01	027296	3	2022-08-08 09:05:00	INSERT
H020	A 223 630 58 01	02720907	3	2022-08-08 10:05:00	INSERT
H020	A 223 630 58 01	027296	0	2022-08-08 10:15:00	UPDATE

### 7.1.9 Upload of initial data

After all data for the simulation has been generated and prepared, the initial data are uploaded to the Azure Blob Storage in the ninth step. For this purpose, the previously generated DataFrames of the simulated tables are each written to a CSV file and then uploaded to the Azure Blob Storage. A separate folder was therefore created for each system and, in turn, for each table / file, a folder with the term *daily* in the name, which contains the current data, and a folder with the term *history*, for archiving the data. All simulated data are uploaded to the *daily* folders.

To simulate the procurement and open orders of load carriers, two CSV data exports from the load carrier management system are used and the files are uploaded at this point. Furthermore, a CSV data export with previous bookings of the load carriers from the load carrier management system is uploaded.

This step simulated all the required historical data for the digital twin of the RFID-enabled material flow.

### 7.1.10 Upload of simulated tables

Finally, all real-time data must be uploaded to Azure Blob Storage. As this is a simulation, all the data for one day are sent at one-minute intervals. Therefore, it is iterated over the number of days of the simulation. First, the current time is assigned to the variable *start\_time*. Then all previously generated DataFrames are filtered by their *header\_timestamp*, *timestamp\_in*, *timestamp\_out* or *goods\_receipt\_timestamp*, so that only the data of the current day are included. Then the DataFrames are prepared for the respective table to be simulated, for example by filtering them and adding a *header\_timestamp* and *header\_operation* if they do not already exist. The prepared DataFrames are then written to a CSV file for each table and uploaded to a folder in the Azure Blob Storage. After that, the current time is again assigned to the variable *end\_time* and the difference to the *start\_time* is calculated. Then this difference is subtracted from 60 seconds and the resulting time is waited for. This way, the data is uploaded approximately every minute and simulated in real time.

## 7.2 Results of the digital twin of the RFID-enabled material flow in real time

In this section, the results of the digital twin of the RFID-enabled material flow are demonstrated. On the one hand, the dashboards are described and on the other hand, the execution times of the pre-processing and updating of a dashboard are measured.

### 7.2.1 Dashboards of the digital twin of the RFID-enabled material flow in real time

The dashboard of use case 1: analysis of process times and transports between a source and a sink is shown in Figure 58 and Figure 59. It contains the filters from storage type (e.g., ÖBO) and to storage type (e.g., ÖP2) where specific sources and sinks can be entered. The filter for the timestamp is only available because simulated data were used, and this timestamp simulates a certain date and time. In the graph on the top left, the transport times between the sources and sinks are compared with each other in a heat map. In this example, the transport times between the source ÖBO and the sink ÖP2 are the largest, as the average transport time is 39 minutes and coloured in red. The average transport time between the source 902 and the sink ÖP2 is 5 minutes and thereby the lowest and coloured in light blue. The table next to the heat map visualises the average, minimum and maximum transport times as well as the number of transports and the number of transports with an exceeded lead time for each source and sink. The pie charts visualise the evaluation of the lead time for the source and sink specified in the filters. The first pie chart shows how many transfer orders were acknowledged within the lead time and how many exceeded the lead time. In this example, the lead time was exceeded for all 8 executed transfer orders, i.e., 100 %. The pie chart in the middle shows the evaluation of the previous day's transfer orders for the defined source and sink. Here, the lead time was exceeded for 24 transfer orders (75 %) and 8 transfer orders were executed within the lead time (25 %). The number of transfer orders is displayed as soon as the mouse pointer is moved over the pie chart. Finally, the third pie chart shows the evaluation of the transfer orders and their lead time of the last week. The bar chart visualises the minimum, maximum, average transport times as well as the number of transports and the number of transports with

## 7 Simulation of the RFID-enabled material flow and verification of the digital twin of the RFID-enabled material flow in real time

exceeded lead time of the last week for the source and sink specified in the filters. In the lower table, each transfer order between this source and sink is displayed with the creation date, creation time, acknowledgement date, acknowledgement time, lead time, time required until acknowledgement and whether the lead time was exceeded for this transfer order.

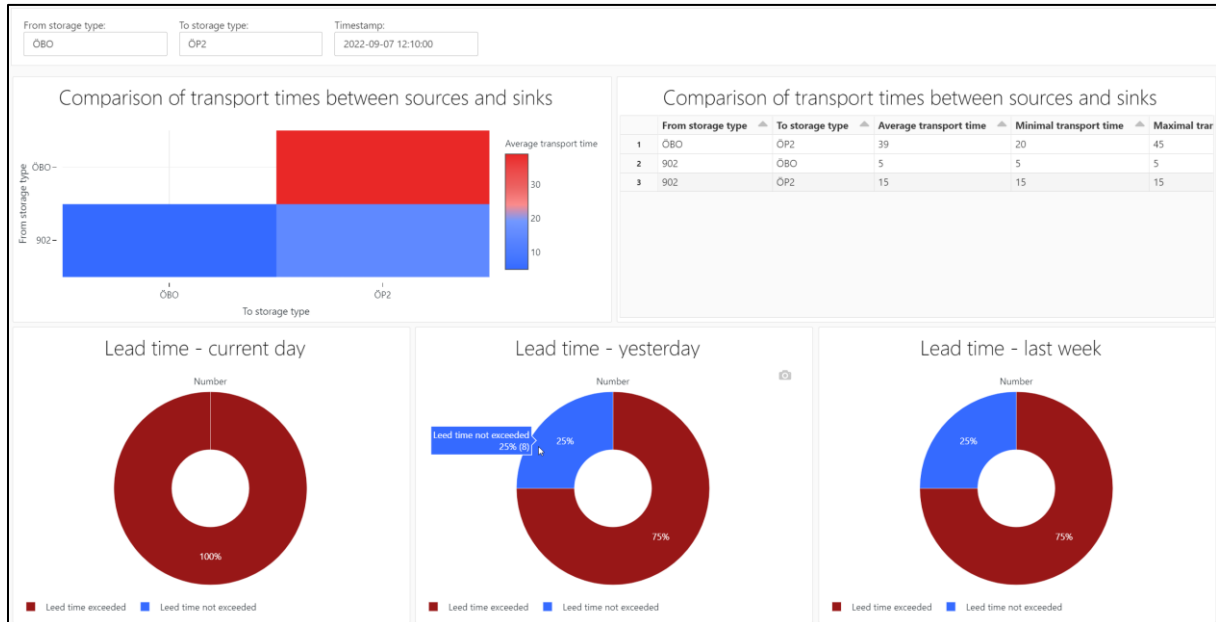


Figure 58 Dashboard of use case 1 – part 1

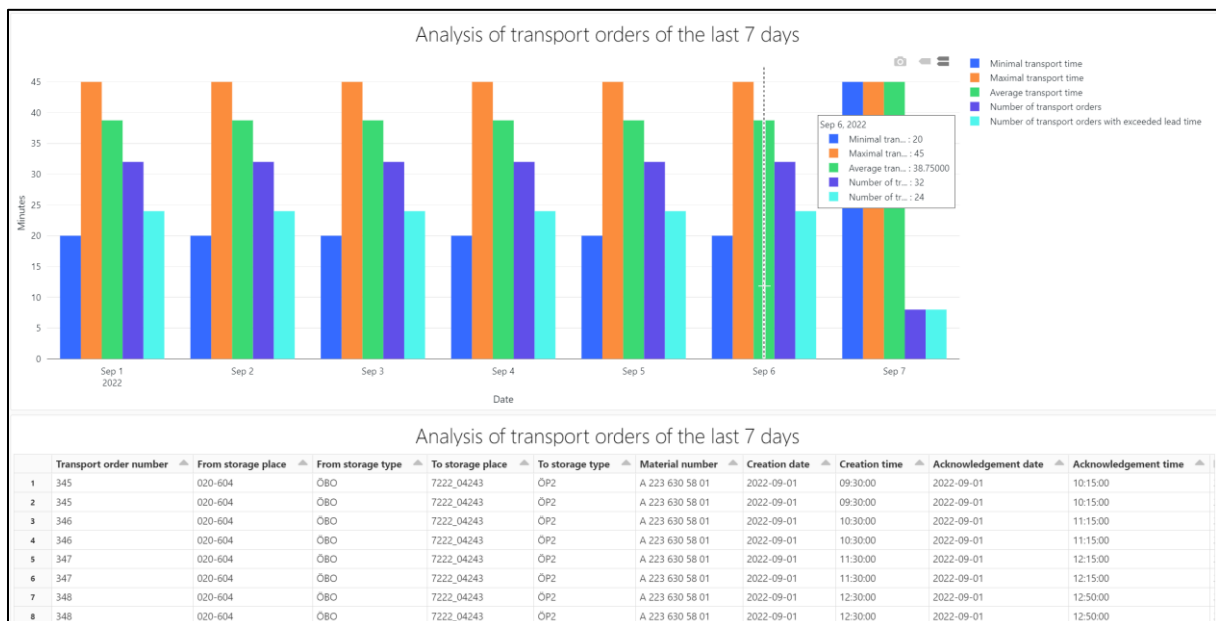


Figure 59 Dashboard of use case 1 – part 2

The dashboard of use case 2: analysis of the inventory of special load carriers with multi-use RFID transponders can be seen in Figure 60 and has the filters load carrier type and supplier. In this example, the load carrier type is 18681 and the supplier number is 123456789. The table on the top left shows the acquisition stock of the special load carriers, which is 270. There are also no open purchase orders. However, only 264 load carriers of the 270 procured are created in the logistics back end system. In this example, there are 100 load carriers in circulation and the calculated demand is 955. Thus the (simulated) data from the two systems, the load carrier management system, and the logistics back end system, were

## 7 Simulation of the RFID-enabled material flow and verification of the digital twin of the RFID-enabled material flow in real time

processed and linked together. The table on the top right shows the calculated real load carrier circulation factor and the load carrier circulation factor stored in the load carrier management system. The pie chart shows how many of the load carriers created in the logistics back end system are in circulation within the last 3 months. In this example, only 37.9 % are in circulation. The line chart shows the demands of load carriers for the current and the next months (blue line), which originate from the load carrier management system. Furthermore, the acquisition stock (green line) and the circulation stock (orange line) are shown. The table below shows the detailed demands for special load carriers, which originate from the load carrier management system. The lowest table shows information about the supplier, such as the name, location, country, and the current and future demand for load carriers at the supplier. Furthermore, the supplier's stock of special load carriers is displayed. Since this is 368 and higher than the acquisition stock, which is 270, this indicates a low data quality of this value.

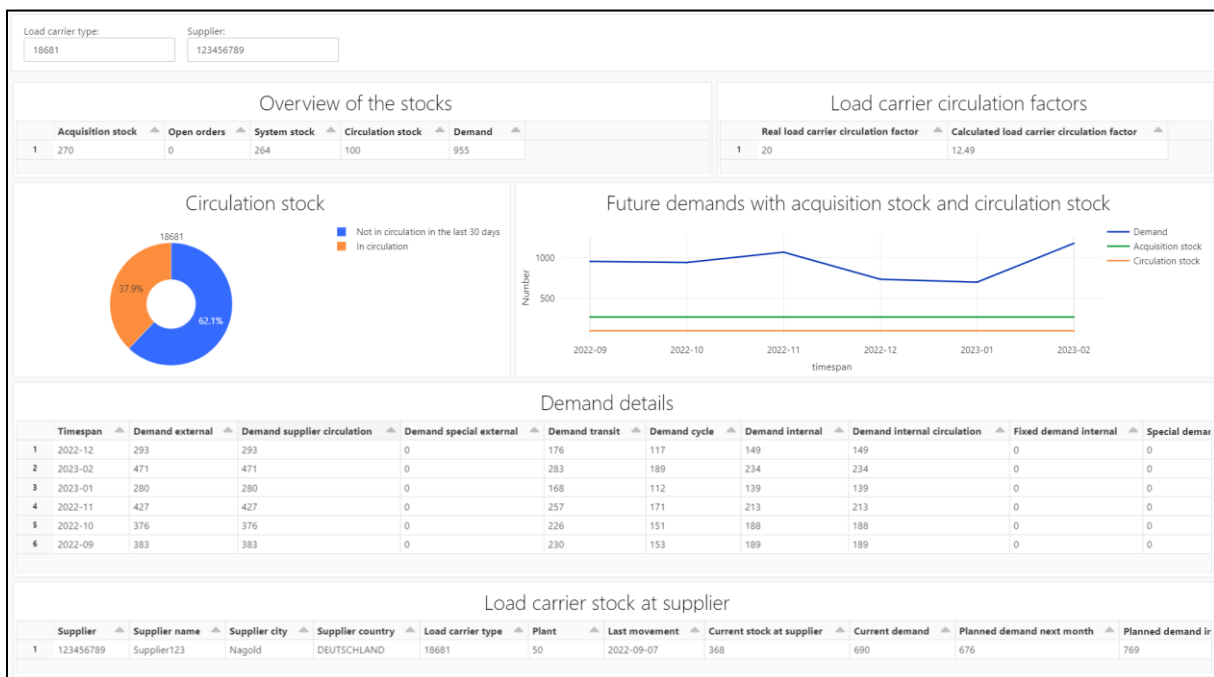


Figure 60 Dashboard of use case 2, according to Knapp et al. (2023)

Figure 61 shows the dashboard of use case 3: analysis of the best-before date for adhesive parts for a certain period of time. In the filter *expiration date*, it can be chosen if all material should be visualised or only the adhesive parts where the best-before date will be expired after the production break. Then the last day of the production break has to be entered. Furthermore, it is possible to filter according to a material number and / or a storage location. The first table shows the adhesive parts with their storage location, storage type, storage place, handling unit, Uff of the RFID transponder, the batch, the manufacturing date, the expiration date, the expiration date minus the remaining time and if the expiration date will be exceeded after the production break. Furthermore, it shows how many days the material will last after the production break. In addition, the material number, material text, remaining time and the quantity are visualised in this table. In this example, the material will expire 3 days after the production break ends (2022-09-27). In the bottom table, the last transfer orders to a production supply area are shown. These will most likely show all materials that will still be on the line (station) after the production break if the production break starts at the time this dashboard was updated and viewed. The transfer order contains the storage location, storage place, material number, material text, the acknowledgement date, acknowledgement time, the handling unit, and further parameters.

## 7 Simulation of the RFID-enabled material flow and verification of the digital twin of the RFID-enabled material flow in real time

Expiration date	Last day of the production break:	Material:	Storage location:	Timestamp:
all	2022-09-27			2022-09-01 13:06:00

RFID-ID (UII)	Charge	Manufacturing date	Expiration date	Expiration date without remaining time	Expiration date will exceed	Number of days until expiration date after production break
1 27BUN4989904418681+1319775	0272930	2022-09-01	2022-10-01	2022-09-30	no	3
2 27BUN4989904419284+1288383	02721001	2022-09-01	2022-10-01	2022-09-30	no	3

Storage location	Storage place	Material	Material text	Acknowledgement date	Acknowledgement time	Transport order number	Transport order position	Handling unit	Quantity
1 P020	7107_20193	A 223 620 17 00	RADEINBAU VST VO LI LSR2	2022-09-01	11:10:00	680	2	1285666	6
2 P020	7222_04243	A 223 630 58 01	SEITENWAND IN RE W	2022-09-01	12:50:00	348	2	1286665	3

Figure 61 Dashboard of use case 3, according to Knapp et al. (2022)

The dashboard of use case 4: analysis to determine the delayed material, the actual stock and the expected deliveries is shown in Figure 62. This contains the filters control loop number, material number (without empty spaces), part group number, processing state of the material call-off, production supply area, storage location and supply id. In the first table the delayed material is visualised with the date and time of the creation of the material call-off (e.g., 2022-09-01 08:30:00 a.m.), the part group number and position, the supply id, control loop, material number and text, the processing status (ZI15 = delayed material), the retrieval quantity, and further parameters. In the same dashboard, in the table at the bottom left, the actual stock for the selected material number, in this example A 223 630 58 01 is displayed. In this example there is no material available in the storage location H020 but at the production supply area which belongs to the storage location P020 a quantity of 6 is available. Additionally, the order stocks and assigned reservations are visualised. In the table at the middle right all order confirmations made by the supplier are visualised. In this example the current time is 08:31:00 a.m. In the simulation, the first order confirmation was created at 06:15:00 a.m. and the material has been delivered at 07:55:00 a.m. The next order confirmation was made at 07:15:00 a.m. and the expected delivery time was 08:00:00 a.m. but the material was not delivered and therefore it is delayed and the delivered quantity in this table is 0. The third order confirmation on that day was made at 08:15:00 a.m. with the expected delivery time 09:00:00 a.m. In addition, the table on the bottom right shows the delivery schedule. Here it can be seen, that in total a quantity of 21 is expected to be delivered on this day and a quantity of 3 has already been delivered. Furthermore, the storage location, material number and purchasing document number are shown.

Control loop number:	Material number:	Part group number:	Processing state:	Production supply area:	Storage location:	Supply id:
	A2236305801			all x		
Timestamp:	2022-09-01 08:31:00					

Date creation	Time creation	Part group number	Retrieval position	Supply id	Control loop	Material	Material text	Processing status	Retrieval quantity	Storage location	Produ	
1	2022-09-01	08:30:00	169	1	OVS9	1363406	A 223 630 58 01	SEITENWAND IN RE W	ZI15	3	P020	7222_1

Storage location	Material number	Charge	Free usable	Quality inspection	Locked	Order stock	Assigned reservation
	A 223 630 58 01		0	0	0	0	504
H020	A 223 630 58 01	all	0	0	0	288	0
P020	A 223 630 58 01	all	6	0	0	0	0

Creation timestamp	Delivery timestamp	Delivered quantity	Storage location	Material
1 2022-09-01T06:15:00.000+0000	2022-09-01T07:55:00.000+0000	3	H020	A 223 6
2 2022-09-01T07:15:00.000+0000	2022-09-01T08:00:00.000+0000	0	H020	A 223 6
3 2022-09-01T08:15:00.000+0000	2022-09-01T09:00:00.000+0000	0	H020	A 223 6

Delivery date	Material	Lagerort	Division quantity	Delivered quantity	Purchasing document
1 2022-09-01	A 223 630 58 01	H020	21	3	5500252287

Figure 62 Dashboard of use case 4

## 7 Simulation of the RFID-enabled material flow and verification of the digital twin of the RFID-enabled material flow in real time

The dashboard of the use case 5: analysis to identify open transfer orders and exceeding of the lead time are shown in Figure 63 and Figure 64. This dashboard contains the filter production supply area, storage location, material number, control loop number, supply id and the selection if all transfer orders or only those with an exceeded lead time should be visualised. The table shows the transfer orders with their creation date and time, retrieval position, control loop number, supply id, material, processing status, storage location and further parameters. In Figure 63 the simulated time is 10:56:00 a.m. and both transfer orders were created at 10:30:00 a.m. and have a lead time of 30 minutes. Therefore, these transfer orders have not yet exceeded the lead time. In Figure 64 the simulated time is 11:01:00 a.m. and the two transfer orders have not been acknowledged and thus the lead time was exceeded. The exceeding of the lead time is indicated by the yellow marking of the transfer orders but also shown in a column, which is just in these figures not visible because the table is scrollable. This makes it possible to see at a glance which transfer orders have an exceeded lead time.

Date creation	Time creation	Lead time	Retrieval position	Control loop	Supply id	Material	Material text	Processing status	Retrieval quantity	Storage location	Production supply area	Delivery	Delivery position	Changed on date	Changed on time	Storage type	Part group number	Transport order number	Transport order position	Packaging	Handling unit	From storage place	From storage type	To stor. place
0	2022-09-01 10:30:00	30	1	1363406	OVGV9 A	223 630 58 01	SEITENWAND IN RE W	ZI30	3	P020	7222_04243	171	10	2022-09-01 10:30:00	OBO	171	346	2	19284	1320614	020-604	OBO	7222_04	
1	2022-09-01 10:30:00	30	1	1363428	OVGV1 A	223 620 17 00	RADEINBAU VST VO LI LSR2	ZI30	6	P020	7107_20193	338	10	2022-09-01 10:55:00	OBO	338	680	2	18681	1285666	RFID	902	7107_2C	

Figure 63 Dashboard of use case 5 without exceeded lead time

Date creation	Time creation	Lead time	Retrieval position	Control loop	Supply id	Material	Material text	Processing status	Retrieval quantity	Storage location	Production supply area	Delivery	Delivery position	Changed on date	Changed on time	Storage type	Part group number	Transport order number	Transport order position	Packaging	Handling unit	From storage place	From storage type	To stor. place
0	2022-09-01 10:30:00	30	1	1363406	OVGV9 A	223 630 58 01	SEITENWAND IN RE W	ZI30	3	P020	7222_04243	171	10	2022-09-01 10:30:00	OBO	171	346	2	19284	1320614	020-604	OBO	7222_04	
1	2022-09-01 10:30:00	30	1	1363428	OVGV1 A	223 620 17 00	RADEINBAU VST VO LI LSR2	ZI30	6	P020	7107_20193	338	10	2022-09-01 10:55:00	OBO	338	680	2	18681	1285666	RFID	902	7107_2C	

Figure 64 Dashboard of use case 5 with exceeded lead time

### 7.2.2 Measurement of the execution time of the pre-processing and update of dashboards of the digital twin of the RFID-enabled material flow in real time

The execution time of the pre-processing and the updating of the dashboards is measured in this section in order to verify the requirement of processing and visualisation of the data of the DTRMF in real time. To measure the execution time, the Databricks Notebook with the pre-processing of the data from the logistics back end system was manually executed thirty times in a Databricks cluster with the following configuration:

- Databricks Runtime Version: 10.4 LTS
- 1 driver of type Standard\_DS3\_v2 with 14 GB memory, 4 cores
- 2 to 8 workers and each of type Standard\_DS3\_v2 with 14 GB memory, 4 cores

During the execution, the time was measured. For this purpose, the current time was stored in the variable *start\_time* at the beginning and after execution of the code, the current time was stored again in the variable *end\_time*. The execution time is then calculated by *end\_time* minus *start\_time*. Table 40 shows the measured execution time for 30 runs. On average, 16.24 seconds are needed to read CSV files of the simulated data, pre-process and save data to the database.

In order to automate pre-processing and big data analyses, Databricks jobs are created. One job is created for the pre-processing of the real-time data of the logistics back end system, which is scheduled to be executed every minute. Another job is created for the pre-processing of the load carrier management



system, which should be executed once a day in real operation because the data of the load carrier management system is updated once a day. For verification, the job with the pre-processing of the logistics back end system was carried out every minute while the simulation was running. Thereby the same Databricks cluster as before was used and the maximum execution was 48 seconds as shown in Figure 65.

The execution time for updating a dashboard was measured analogously to the execution time of the pre-processing using the example of dashboard from use case 1 (analysis of process times and transports between a source and a sink). The dashboard was updated 5 times manually and then the average execution time was calculated (see Table 41). On average, the execution time for one update is 3.76 seconds, which is rated as quite enough for the DTRMF.

*Table 40 Execution times of pre-processing*

		16	14.53
		17	14.79
1	17.95	18	14.44
2	23.43	19	14.78
3	16.84	20	13.62
4	16.63	21	21.62
5	15.86	22	14.50
6	20.92	23	13.56
7	15.10	24	15.15
8	15.09	25	14.32
9	14.69	26	14.14
10	15.04	27	13.59
11	21.30	28	14.74
12	18.34	29	15.20
13	14.59	30	15.97
14	14.36	<b>Average</b>	<b>16.24</b>
15	22.09		

## 7 Simulation of the RFID-enabled material flow and verification of the digital twin of the RFID-enabled material flow in real time

Start time	Run ID	Launched	Duration	Spark	Status
Dec 12 2022, 10:50 AM CET	153437	By scheduler	25s	<a href="#">Spark UI</a> / <a href="#">Logs</a> / <a href="#">Metrics</a>	✔ Succeeded
Dec 12 2022, 10:49 AM CET	152136	By scheduler	22s	<a href="#">Spark UI</a> / <a href="#">Logs</a> / <a href="#">Metrics</a>	✔ Succeeded
Dec 12 2022, 10:48 AM CET	151581	By scheduler	21s	<a href="#">Spark UI</a> / <a href="#">Logs</a> / <a href="#">Metrics</a>	✔ Succeeded
Dec 12 2022, 10:47 AM CET	150623	By scheduler	20s	<a href="#">Spark UI</a> / <a href="#">Logs</a> / <a href="#">Metrics</a>	✔ Succeeded
Dec 12 2022, 10:46 AM CET	150130	By scheduler	28s	<a href="#">Spark UI</a> / <a href="#">Logs</a> / <a href="#">Metrics</a>	✔ Succeeded
Dec 12 2022, 10:45 AM CET	149153	By scheduler	25s	<a href="#">Spark UI</a> / <a href="#">Logs</a> / <a href="#">Metrics</a>	✔ Succeeded
Dec 12 2022, 10:44 AM CET	147897	By scheduler	24s	<a href="#">Spark UI</a> / <a href="#">Logs</a> / <a href="#">Metrics</a>	✔ Succeeded
Dec 12 2022, 10:43 AM CET	146552	By scheduler	48s	<a href="#">Spark UI</a> / <a href="#">Logs</a> / <a href="#">Metrics</a>	✔ Succeeded
Dec 12 2022, 10:42 AM CET	145635	By scheduler	23s	<a href="#">Spark UI</a> / <a href="#">Logs</a> / <a href="#">Metrics</a>	✔ Succeeded
Dec 12 2022, 10:41 AM CET	144154	By scheduler	23s	<a href="#">Spark UI</a> / <a href="#">Logs</a> / <a href="#">Metrics</a>	✔ Succeeded

Figure 65 Databricks completed runs

Table 41 Execution times of dashboard update

Run	Execution time [s]
1	3.81
2	4.33
3	3.90
4	3.57
5	3.21
<b>Average</b>	<b>3.76</b>

### 7.3 Evaluation of the requirements of the digital twin of the RFID-enabled material flow in real time

This section evaluates which functional and qualitative requirements for the prototype of the DTRMF have been met.

#### 7.3.1 Evaluation of the functional requirements

Through the implementation of the DTRMF, all functional requirements were met, as described below.

- **F01 and F02:** the functional requirements F01 and F02 were fulfilled because the data from the logistics back end system and the load carrier management system are ingested by the simulation and read in and prepared during pre-processing using Databricks (see Section 6.6.3).
- **F03:** the data are all stored with a date or timestamp so that always the current but also the historical data of the DTRMF can be retrieved, as described in Section 6.6.2 and therefore functional requirement F03 has been met.

- **F04:** the data are clearly visualised in several dashboards with different filters and therefore requirement F04 was fulfilled.
- **F1.1:** the dashboard of use case 1 shows the minimum, maximum and average transport times (supply times) between a source and a sink (see Figure 58) and thus this requirement has been fulfilled.
- **F1.2:** the number of average transports between a source and a sink are determined and visualised in the dashboard of the first use case (see Figure 59), thus fulfilling requirement F1.2.
- **F2.1, F2.2 and F2.3:** the KPIs circulation stock and real load carrier circulation factor were calculated and visualised in the dashboard of use case 2 (see Figure 60). Other data from the load carrier management system, such as demands of load carriers for the next months and supplier stocks, are also displayed in this dashboard and linked with the data from the logistics back end system. Thus, the requirements F2.1, F2.2 and F2.3 were fulfilled.
- **F3.1 and F3.2:** the KPIs expiration date without remaining time and the number of days until the best-before date is reached after production break for each load carrier were calculated and visualised in the dashboard of use case 3 (see Figure 61). In addition, the last transfer orders to the production supply area were determined and visualised in this dashboard. Therefore, the requirements F3.1 and F3.2 were fulfilled.
- **F4.1:** in the dashboard of use case 4 (see Figure 62), the delayed material, expected deliveries and the actual stock are linked and clearly visualised with filters, thus fulfilling the requirement F4.1.
- **F5.1:** it is calculated whether the lead time is exceeded in the transfer orders and all transfer orders are visualised in the dashboard of use case 5 (see Figure 63 and Figure 64). The transfer orders with exceeded lead time are marked yellow, thus fulfilling the requirements F5.1 and F5.2.

### 7.3.2 Evaluation of the qualitative requirements

The qualitative requirements for the DTRMF were all met as described in the following (see also Knapp et al. (2022)).

- **Q1:** the architecture of the DTRMF contains the processing and analyses layer. In use case 2: analysis of the inventory of special load carriers with multi-use RFID transponders a big data analysis was implemented to calculate the circulation stock and real load carrier factor using historical data. The chosen technology Databricks has proven to be well suited for carrying out **big data analyses** and therefore this requirement has been fulfilled.
- **Q2:** the architecture of the DTRMF as well as the programming of the pre-processing and big data analyses and the creation of the dashboards could be realised within a few months and thus the requirement **short development** time was fulfilled.
- **Q3:** requirement Q3 **maintenance and operation** has been met, as the virtual machine and Databricks are running in the Microsoft Azure Cloud and do not need to be maintained and therefore only the TimescaleDB needs to be maintained, which is considered to be easy. Since the pre-processing and the data analyses were implemented in one system (Databricks), it is assumed that the operation is also simple.

- **Q4:** the semantic layer has not been implemented because at the point of development it was not required but the architecture provides an optional semantic layer and therefore the requirement Q4 **data interoperability** was fulfilled.
- **Q5:** the execution time of the pre-processing and update of dashboard takes together less than one minute (see Section 7.2.2) and therefore, the requirement processing and visualisation in **real time** with a maximum time span of 5 minutes is met.
- **Q6:** the TimescaleDB supports the storage, analyses, and retrieval of **time series data** and thus the requirement Q6 is met.
- **Q7:** the implementation of different use cases and connection of two data sources have shown that the DTRMF is **extensible** and therefore requirement Q7 was fulfilled.
- **Q8:** requirement Q8 **performance scalability** was met by using the Microsoft Azure Cloud and the chosen technologies, such as Databricks.
- **Q9:** the **availability** of the selected Microsoft Azure Cloud environment is sufficient because the DTRMF is not production-critical.
- **Q10:** the requirement Q10 was also met because internal **company guidelines** were taken into account in the selection of environment and technologies, such as the choice of the eXtollo platform and Databricks.

## 7.4 Simulative profitability analysis and user survey

In order to demonstrate the economic viability and the need for the DTRMF, a simulative profitability analysis and a user survey are carried out in this section.

### 7.4.1 Simulative profitability analysis

The simulative profitability analysis in this thesis is carried out using the example of use case 2: analysis of the inventory of special load carriers with multi-use RFID transponders. This analysis supports the users from the production supply department by automatically calculating the circulation stock and the real load carrier circulation factor to support the decision whether additional special load carriers have to be procured.

#### 7.4.1.1 Methodology

First, a literature review is conducted to investigate how economic analyses have been done for other digital twins. For this purpose, the term “*digital twin*” *economic analysis* was searched for in the title of the article in the google scholar database. This search has resulted in only two hits. Both the paper “*Urban Air Mobility (UAM) and Total Mobility Innovation Framework and Analysis Case Study: Boston Area Digital Twin and Economic Analysis*” (Tuchen et al., 2022) and “*Health Economic Analysis of Digital Twin Technology for Remission of Diabetes - Initial Insights From the Prospective Randomised Controlled Clinical Trial*” (Shah et al., 2021) are not about a digital twin of RFID-enabled material flow in the automotive industry and therefore not applicable. The results of this literature review show that there is very limited literature on the economic analysis of digital twins. Therefore, further literature in the field of container management was consulted. Sydow (2017) has developed a concept

for dynamic container logistics using Bluetooth Low Energy technology. However, no detailed economic analysis is carried out where, for example, the costs for the IT system are taken into account.

In Zeiler (2022), an architecture for the container management of intelligent, modular special load carriers was developed and the added values were determined by means of a user survey. However, no profitability analysis was carried out in this dissertation. In Graßl et al. (2021), a cost-benefit assessment of the use of intelligent, modular special load carriers is carried out. However, no concrete development costs for the system are listed here.

In Uckelmann (2012) different performance measurement methods are presented and compared to measure RFID performance. Since each method has its advantages and disadvantages, only the savings potential through the DTRMF is calculated here by comparing the expenditure without the DTRMF with the expenditure with the DTRMF. In this profitability analysis, it is assumed that exactly the required number of special load carriers can be procured/reprocured by using the DTRMF. The simulative profitability analysis is carried out for the use of the DTRMF in one plant, the rollout in another plant and the use of the DTRMF in a total of five plants. Hereby, it is assumed that the DTRMF will be in operation for five years. Therefore, in this case there are no unnecessary costs due to excessively procured special load carriers, but also no costs due to production downtimes at the supplier or the car manufacturer. To calculate the expenses with and without the DTRMF, the costs for the development as well as the operation of the DTRMF, special load carriers and production downtimes are estimated first. Then six different scenarios are defined where too many or too few special load carriers were procured and their impact on costs for unnecessarily procured special load carriers as well as production downtimes caused. In this simulative profitability analysis, the advantages such as an automated inventory of special load carriers, possible reduction of storage spaces, savings in labour costs, as no manual evaluation of the circulation stock and real load carrier circulation factor must be carried out, are not taken into account.

#### 7.4.1.2 Estimated costs

##### Costs for the DTRMF

Table 42 shows the costs to develop and operate the DTRMF. The development costs, maintenance and support costs have been estimated by the author based on the costs of another internal big data project as no information on this was provided in the literature described above. The one-off development costs for the DTRMF for one plant are estimated to be € 300,000. It is assumed that the adaptation of the existing code to an additional plant will require significantly fewer working hours than a new development and therefore this is estimated to be € 75,000. The maintenance and support costs for the DTRMF for one plant are assumed to be € 70,000 per year. The DTRMF is running in the Microsoft Azure Cloud and therefore, the costs for the infrastructure were calculated using the Microsoft Azure Calculator and based on the technologies used in the prototype of the DTRMF. The database TimescaleDB is running in a virtual machine with a managed disk. It is assumed that a Microsoft Azure VM of the type DS5 v2 (16 VCPUs, 56 GB RAM) is used in the West Europe region with the operating system Linux, together with a managed disk of the type E60 (8192 GiB) and a reservation over 3 years. This results in monthly costs of € 943.33 which were rounded to 940 €. The pre-processing, analyses and dashboards are executed in Databricks. It is assumed that a general purpose instance of type DS4 v2 is used. The costs for the DBUs (Databricks Units) are therefore € 602.40 per month and for the VM with reservation over three years € 766.44 per month. These were added up and rounded for better readability and thus result in € 1,370 per month. The total costs of the DTRMF for a plant consist of the one-off development costs ( $d_{costs}$ ), the maintenance and support costs over 5 years ( $m_{costs}$ ) and the

infrastructure costs for 5 years ( $i_{costs}$ ). Since only one use case out of a total of five is considered in this profitability analysis, these costs are divided by 5. This results in total costs of € 157,720 for the DTRMF in one plant as shown in Eq. 13. The total costs for the use of the DTRMF in another plant is calculated by the additional one-off development costs ( $d_{costs\_a}$ ), the maintenance and support costs ( $m_{costs\_a}$ ) for one addition plant and the infrastructure costs for 5 years ( $i_{costs}$ ) divided by five (see Eq. 14). Therefore, the total costs of the DTRMF in one additional plan are € 112,720.

$$\begin{aligned} total\ costs\ in\ one\ plant &= \frac{1}{5} * (d_{costs} + m_{costs} + i_{costs}) && Eq. 13 \\ &= \frac{1}{5} * (300,000 + 350,000 + 138,600) = € 157,720 \end{aligned}$$

$$\begin{aligned} total\ costs\ in\ one\ additional\ plant &= \frac{1}{5} * (d_{costs\_a} + m_{costs\_a} + i_{costs}) && Eq. 14 \\ &= \frac{1}{5} * (75,000 + 350,000 + 138,600) = € 112,720 \end{aligned}$$

Table 42 Costs for the DTRMF, load carriers and production downtime

<b>Costs of the DTRMF</b>	
One-off development costs for the DTRMF for one plant [EUR]	300,000
One-off development costs for adapting the DTRMF to one additional plant [EUR]	75,000
Maintenance and support costs for the DTRMF for one plant per year [EUR]	70,000
Maintenance and support costs for the DTRMF for one plant over five years [EUR]	350,000
Costs for the Microsoft Azure VM with managed disk per month [EUR]	940
Costs for the Microsoft Azure Databricks Cluster per month [EUR]	1,370
Infrastructure costs of the DTRMF per plant per year [EUR]	27,720
Infrastructure costs of the DTRMF over five years per plant [EUR]	138,600
<b>Total costs of the DTRMF per use case over five years [EUR]</b>	<b>157,720</b>
<b>Total costs of the DTRMF per use case over five years for one additional plant [EUR]</b>	<b>112,720</b>

### Costs for special load carriers

The special load carriers are made in the automotive industry for the transport of special components and are therefore very expensive (Bertagnolli, 2022; Scholz-Reiter et al., 2011). In Cobb (2016) a model is presented where “the inventory levels for used, inspected, repaired (serviceable), and purchased containers are explicitly modeled and the holding costs are accounted for in the models based on the average inventory levels” (Cobb, 2016). This model was applied in a case study in a major brewery in the United Kingdom. In this model, many parameters must first be known, such as the demand per unit of time or expected value of fraction of repairable fraction. In use case 2, many different load carriers are used, which circulate between the car manufacturer and different suppliers. To the best of the author's knowledge, there is therefore not enough data to apply the model described above, as these parameters vary for each type of load carrier, the demand changes dynamically and it would probably be very costly and take a long time to collect these data. Therefore, only the costs of procuring special load carriers are considered in this simulative profitability analysis and the costs for storage, inspection and repair are neglected. The average costs of a special load carrier are estimated to be € 1,250. In Graßl et al. (2021) it is assumed that the development and manufacturing costs of a special load carrier amount to € 1,253 which confirms this estimation.

### Costs for production downtimes

The costs of a production downtime at the supplier, which can occur if not enough load carriers are in circulation, are estimated to be € 500,000, because in the report from riskmethods and BME (2018) it is

written that damages from every 5th supply chain interruption amount to between € 250,000 to € 500,000. The costs of a production downtime at the car manufacturer, which could occur if the supplier cannot produce new material due to missing special load carriers, are estimated by the author to be higher than at the supplier and therefore amount to € 1 million in this simulative profitability analysis. It should be noted that these costs are a gross simplification of reality, as the costs of a production downtime depend on the duration of the production downtime and are usually difficult to predict.

#### **7.4.1.3 Scenarios and profitability analysis**

In this section, six different scenarios are defined and their impact on the costs and savings for too many or too few procured special load carriers are determined (see Table 43). For this purpose, it was simulated how many special load carriers are needed, how many are procured and how many production downtimes occur due to missing load carriers. The parameters and calculations are described in the following on the example of scenario 1 and 6.

In scenario 1, 40 % too many special load carriers are considered. In total 16,800 load carriers were procured but only 12,000 are required. That means 4,800 too many load carriers were procured. In this scenario, there is no production downtime due to lack of material because too many load carriers were procured. First the costs for the procured load carriers are calculated which are € 21,000,000 and the costs for the too many procured load carriers are € 6,000,000. The total costs without the DTRMF are composed of the costs for the procured special load carriers and the total costs for the production downtimes, which are in this scenario € 21,000,000. The assumption is made here that with the DTRMF only the number of special load carriers required is procured and that there are no production downtimes due to too few special load carriers being procured. The costs with the DTRMF are the total costs for the development and operation of the DTRMF plus the costs for the required number of special load carriers, which are € 15,157,720 in scenario 1. This leads to cost savings of € 5,842,280 through the DTRMF in one plant over five years. If the DTRMF is rolled out to a further plant, additional € 5,887,280 can be saved and, if the DTRMF is used in a total of five plants, even € 29,391,400 can be saved in scenario 1.

In scenario 6, 40 % too few special load carriers are procured. That means only 7,200 of the required 12,000 load carriers were procured and 4,800 are missing. Due to the missing load carriers, it is assumed that within five years 13 production downtimes are caused at the supplier and 4 at the car manufacturer. Compared to scenario 1 the costs of € 9,000,000 for the procurement of the load carriers are lower. The additionally required load carriers would cost € 6,000,000. The total costs for the production downtimes at the supplier and the car manufacturer amount € 10,500,000. The total costs without the DTRMF in one plant consist of the costs for the special load carriers and the costs for the production downtimes and result in € 19,500,000. When using the DTRMF the costs for the production downtimes are omitted but the costs for additionally required load carriers and the costs of the DTRMF are added, which results in total costs of € 15,157,720. This leads to cost savings of € 4,342,280, which are 22 % of the total costs for procuring special load carriers and production downtimes without the DTRMF. When the DTRMF is rolled out into one additional plant further € 4,387,280 can be saved. A usage of the DTRMF in five plants leads in this scenario to cost savings of € 21,891,400.

The simulative profitability analysis shows that under the assumptions made, the DTRMF can save 5 – 28 % of the total costs which would arise without the DTRMF for procuring special load carriers and production downtimes in the various scenarios. Due to these cost savings, the DTRMF has a high profitability.

## 7 Simulation of the RFID-enabled material flow and verification of the digital twin of the RFID-enabled material flow in real time

Table 43 Costs and savings of different scenarios

Scenarios	Scenario 1	Scenario 2	Scenario 3	Scenario 4	Scenario 5	Scenario 6
Description of the scenarios	40 % too many special load carriers procured	20 % too many special load carriers procured	10 % too many special load carriers procured	10 % too few special load carriers procured	20 % too few special load carriers procured	40 % too few special load carriers procured
<b>Parameters</b>						
Number of special load carriers required per plant	12,000	12,000	12,000	12,000	12,000	12,000
Number of special load carriers procured per plant	16,800	14,400	13,200	10,800	9,600	7,200
Number of special load carriers not required per plant	4,800	2,400	1,200	0	0	0
Number of under-procured special load carriers per plant	0	0	0	1,200	2,400	4,800
Number of production downtimes caused at the supplier due to missing special load carriers within 5 years per plant	0	0	0	5	9	13
Number of production downtimes caused at the car manufacturer due to missing special load carriers within 5 years per plant	0	0	0	0	2	4
<b>Costs and savings through the digital twin in one plant</b>						
Costs for procured special load carriers per plant [EUR]	21,000,000	18,000,000	16,500,000	13,500,000	12,000,000	9,000,000
Costs for too many special load carriers procured per plant [EUR]	6,000,000	3,000,000	1,500,000	0	0	0
Costs for additionally required special load carriers per plant [EUR]	0	0	0	1,500,000	3,000,000	6,000,000
Costs for caused production downtimes at the supplier [EUR]	0	0	0	2,500,000	4,500,000	6,500,000
Costs for caused production downtimes at the car manufacturer [EUR]	0	0	0	0	2,000,000	4,000,000
Total costs for caused production downtimes [EUR]	0	0	0	2,500,000	6,500,000	10,500,000
Total costs without the digital twin in one plant [EUR]	21,000,000	18,000,000	16,500,000	16,000,000	18,500,000	19,500,000
Total costs with the digital twin in one plant [EUR]	15,157,720	15,157,720	15,157,720	15,157,720	15,157,720	15,157,720
<b>Cost savings with the digital twin in one plant [EUR]</b>	<b>5,842,280</b>	<b>2,842,280</b>	<b>1,342,280</b>	<b>842,280</b>	<b>3,342,280</b>	<b>4,342,280</b>
<b>Cost savings with the digital twin in one plant [%]</b>	<b>28 %</b>	<b>16 %</b>	<b>8 %</b>	<b>5 %</b>	<b>18 %</b>	<b>22 %</b>
<b>Costs and savings when the digital twin is rolled out in another plant</b>						
Total costs without the digital twin in one additional plant [EUR]	21,000,000	18,000,000	16,500,000	16,000,000	18,500,000	19,500,000
Total costs with the digital twin in one additional plant [EUR]	15,112,720	15,112,720	15,112,720	15,112,720	15,112,720	15,112,720
<b>Cost savings with the digital twin in one additional plant [EUR]</b>	<b>5,887,280</b>	<b>2,887,280</b>	<b>1,387,280</b>	<b>887,280</b>	<b>3,387,280</b>	<b>4,387,280</b>
<b>Cost savings with the digital twin in one additional plant [%]</b>	<b>28 %</b>	<b>16 %</b>	<b>8 %</b>	<b>6 %</b>	<b>18 %</b>	<b>22 %</b>
<b>Costs and savings when using the digital twin in five plants</b>						
Total costs without the digital twin in five plants [EUR]	105,000,000	90,000,000	82,500,000	80,000,000	92,500,000	97,500,000



## 7 Simulation of the RFID-enabled material flow and verification of the digital twin of the RFID-enabled material flow in real time

Total costs with the digital twin in five plants [EUR]	75,608,600	75,608,600	75,608,600	75,608,600	75,608,600	75,608,600
<b>Cost savings with the digital twin in five plants [EUR]</b>	<b>29,391,400</b>	<b>14,391,400</b>	<b>6,891,400</b>	<b>4,391,400</b>	<b>16,891,400</b>	<b>21,891,400</b>
<b>Cost savings with the digital twin in five plants [%]</b>	<b>28 %</b>	<b>16 %</b>	<b>8 %</b>	<b>5 %</b>	<b>18 %</b>	<b>22 %</b>

### 7.4.2 User survey to identify the need of the DTRMF

In order to determine the needs of the DTRMF, a user survey was conducted after the implementation of the prototype in addition to the profitability analysis. A questionnaire with five questions was developed for this purpose and eleven future users of the DTRMF were interviewed. These users are production engineers, foremen as well as people from the control and steering stations from production supply. First, the dashboards of the DTRMF were presented and then each user completed the questionnaire (see Figure 66).

The five questions of the questionnaire are described in the following. In order to determine the current effort required to obtain the information from the DTRMF, the first question is *“How difficult is it to obtain the information provided by the digital twin using the logistics back end system, load carrier management system and evaluations in Excel?”*. The users could answer on a Likert-scale from 1 = very easy to 5 = very complicated.

The second question serves to quantify the need for a DTRMF and is: *“How great is the need for a digital twin that calculates new KPIs and clearly presents information about the material flow in order to optimise the production supply processes?”*. This could be answered on a Likert-scale from 1 = no need to 5 = great need.

The third question intended to determine the usefulness of the DTRMF and is *“How useful is the information provided by the digital twin of the material flow in the body shop?”*. The users could answer on a Likert-scale from 1 = useless to 5 = very helpful.

In order to determine the greatest advantages of the DTRMF for the users, the fourth question is: *“What are the greatest advantages of the digital twin of the material flow in the body shop in real time?”*. The answer to the question is open.

The fifth question identified which information or KPIs would be additionally relevant to present in the DTRMF and therefore this is *“Which information / KPIs should be provided additionally in the digital twin of the material flow in the body shop in order to optimise the material flow?”*. This question was asked openly.



The advantages mentioned in the answers of the fourth question are faster transparency / overview, faster and easier access to data, clearer presentation, better filtering options, comparison of past values, time savings, faster reaction, and the merging of several databases.

In the answers of the fifth question, the integration of further systems and databases was mentioned, such as the high bay warehouse system or the vehicle production programme. In addition, the calculation and display of further KPIs, such as the exceeding of set shortages in the warehouse or the warehouse utilisation were stated in the answers.

The user survey shows that the DTRMF is needed to optimise the production supply processes.

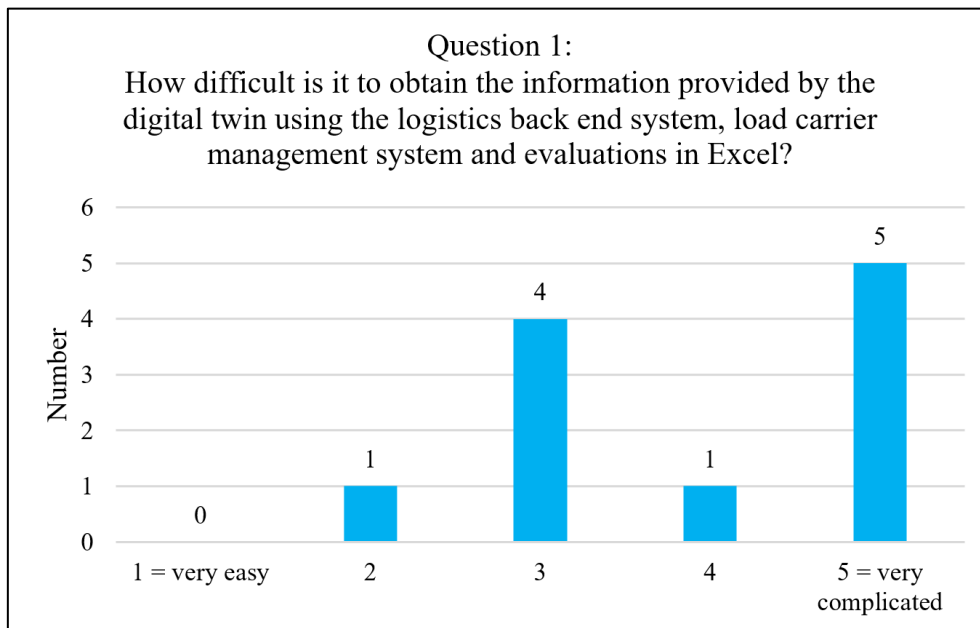


Figure 67 Results of question 1 of the user survey (n = 11)

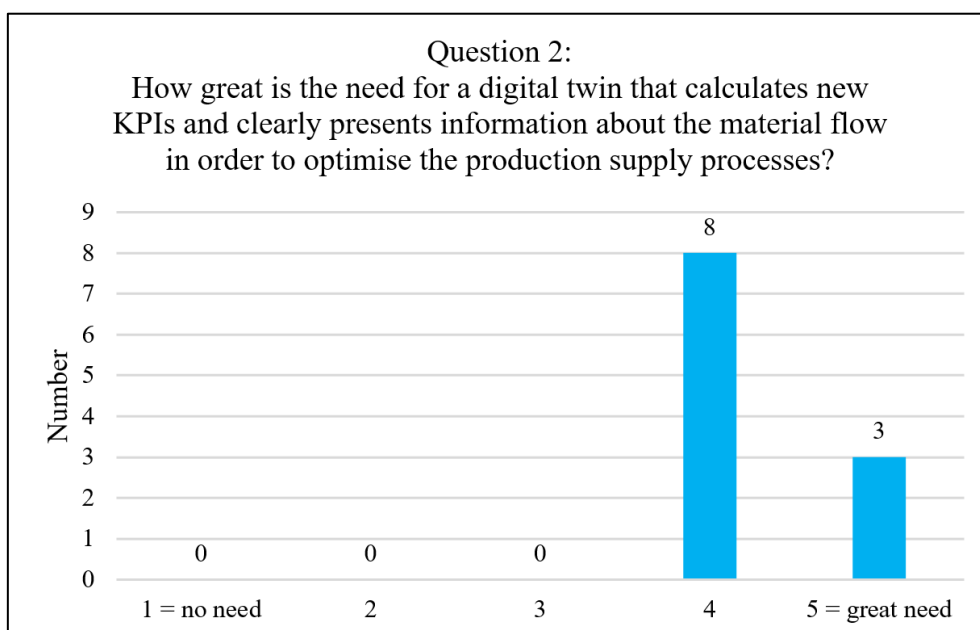


Figure 68 Results of question 2 of the user survey (n = 11)

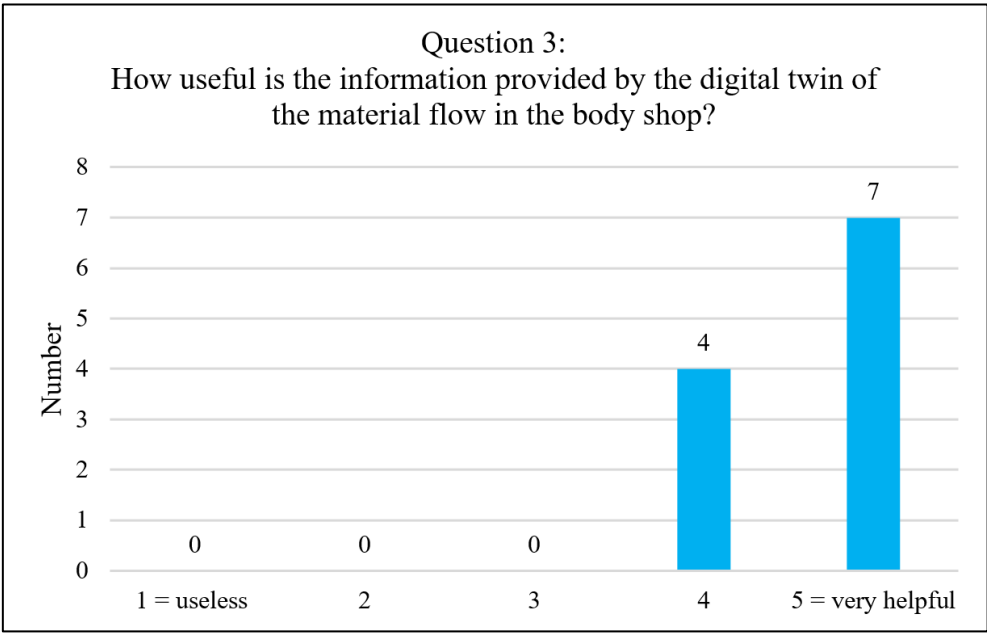


Figure 69 Results of question 3 of the user survey (n = 11)

### 7.5 Discussion of the digital twin of the RFID-enabled material flow in real time

In Chapter 6, a new architecture for DTRMF in real time was proposed and implemented by means of a case study in the body shop of a car manufacturer. At the beginning of this chapter, the simulation of the material flow in real time was programmed to verify the DTRMF architecture. To the best of the author’s knowledge, it is the first time that such a simulation of the material flow has been programmed. The ingestion of the simulated data into the DTRMF and the resulting dashboards proof the suitability of the new architecture of the DTRMF. In the dashboard for the first use case the analysis of the process times and transports are visualised. The dashboard for use case 2 displays the calculated circulation stock and the real load carrier circulation factor as well as further information about the stocks and demands of special load carriers from the logistics back end system and load carrier management system. The analysis of the best-before date for adhesive parts after a production break is shown in the dashboard of use case 3. The dashboard of use case 4 shows the analysis of delayed material, actual stock and expected deliveries. The transfer orders and the analysis of the exceeding of the lead time is visualised in the dashboard of use case 5. This demonstrated how the data of the RID-enabled material flow can be used to gain new insights into the material flow.

However, it must be taken into account that the architecture of the DTRMF was developed based on the requirements of an automobile manufacturer and therefore needs to be adjusted to requirements in other industries to optimise the material flow.

The verification of processing and visualisation in real time was carried out by means of a simulation and the measurement of the execution times. However, this is only an approximation to reality because, for example, only two load carrier types were simulated and therefore the data volume is lower than in reality. Nevertheless, it is assumed that even with an increased data volume, the architecture is optimally suited because the Databricks cluster is scalable. In addition, the time needed to read CSV files is omitted when the data are transferred via the software Qlik Replicate. Another limitation is that the latency caused by the network during data transfer was not measured. However, it is assumed that these latencies

are in the millisecond range and can therefore be ignored because a timespan of maximum 5 minutes is required to ensure real time.

The data of the DTRMF are stored as time series in the TimescaleDB. This means that both current and historical data can be retrieved at any time. However, over time, the storage of all historical data creates large amounts of data and a concept with rules should be developed to first compress or aggregate old data and automatically delete data that are no longer needed. This ensures the performance of SQL queries and saves costs, as no unnecessary storage space has to be paid for.

In addition, a simulative profitability analysis was carried out with six different scenarios, which showed that the DTRMF can save an enormous amount of costs. However, the profitability analysis was carried out using some assumptions and would need to be calculated accurately in the future using real internal company data. Furthermore, the analysis was only carried out for one use case as an example but should be calculated for all others as well, because another use case could achieve greater or smaller cost savings.

The user survey showed that the DTRMF is needed to optimise the material flow and that the DTRMF brings many advantages, such as better transparency, time savings and the possibility to compare past data.

## 8 Conclusions and outlook

The rollout and operation of RFID applications in the automotive industry pose several challenges. Low detection rates are a major problem for RFID installations. During a rollout, the antennas of an RFID gate must be optimally aligned, because the positioning and orientation between RFID transponders and antennas influence the detection rate. The alignment and positioning are a major challenge due to the many possible mounting heights and angles of the antennas of an RFID gate. Until now, the most common approaches were exemplary guidelines based on expert knowledge and the trial-and-error principle, which lead to the hypothesis that there is a better approach to align and position the antennas of an RFID gate. Therefore, in this thesis, a new RFID network planning algorithm was developed as well as the algorithm for optimal alignment of the antennas of the RFID gate. Then all three approaches were compared with each other. Despite it has a coverage rate of 99 % of the transponder area and minimised overlapping of the antenna fields, the RFID network planning algorithm led to a lower detection rate than the exemplary guideline 1. However, the detection rate of the algorithm for optimal alignment of the antennas of the RFID gate was 6.24 % higher than using the exemplary guideline 1 at the same reading power (26 dBm). Therefore, the best approach is to use the algorithm for optimal alignment of the antennas of the RFID gate, which answered the **RQ1** and fulfils the objective **O1**. The verification and comparison of the three approaches also confirmed the hypothesis **H1**. The antenna configuration determined by the algorithm for optimal alignment of the antennas of the RFID gate can be used as a new guideline for RFID gates in the automotive industry. In addition, this algorithm could be further developed and adapted for similar RFID applications in other areas.

Another problem with the rollout of RFID applications are the sources of interference. During a rollout, the RFID installation is set up and put into operation in a new environment. The different environmental influences lead to different sources of interference, which have a negative effect on the performance, such as the detection rate, and thus reduce the process quality. Due to the lack of application experience, it is a challenge to systematically identify and reduce these sources of interference, because there are no test procedures or guidelines for this. Therefore, in this thesis, a new test procedure was developed to systematically identify and eliminate sources of interference, thus answering research question **RQ2** and fulfilling objective **O2**. In addition, the test procedure was verified by simulating different sources of interference and applying it to RFID installations. This verification showed that by applying the test procedure all simulated sources of interference could be eliminated and thus the performance could be improved enormously. This verification shows that with a test procedure it is possible to systematically identify and eliminate the sources of interference for RFID installations and thus confirms hypothesis **H2**. The developed test procedure to identify and reduce sources of interference should be tested in practice and adapted if necessary and could then be anchored in a new standard such as VDI in the future.

After the RFID installations have been put into operation and the sources of interference have been eliminated, the RFID installations continuously generate data. However, these data are often used for the automation of individual processes and not for analyses to optimise the material flow. This choice, however, could help to solve the general problem of the low-cost efficiency of RFID technology, because big data analyses can, for example, reduce costs by only procuring the special load carriers that are really needed. Therefore, the architecture of the digital twin of the RFID-enabled material flow in real time was developed in this thesis and the implementation was described by means of a case study. Furthermore, a simulation of the material flow in real time was programmed and the architecture was verified using this simulation. The evaluation of the functional and qualitative requirements of the digital twin of the RFID-enabled material flow in real time showed that all could be fulfilled.

The implementation and verification of the digital twin showed how the data of the RFID-enabled material flow can be used for further analyses and findings to optimise the material flow and thus **RQ3**

was answered and objective **O3** fulfilled. Furthermore, a simulative profitability analysis was carried out on the example of one use case, which clearly shows the enormous cost savings and profitability of the digital twin of the RFID-enabled material flow in real time in different scenarios because from € 842,280 up to € 29 million that is 28 % of the total cost for procuring special load carriers and covering production downtimes could be saved by using the digital twin. In addition, a user survey was conducted to determine the current effort of information gathering and the need for the digital twin of the RFID-enabled material flow in real time. The results show that the digital twin of the RFID-enabled material flow in real time is very helpful and is needed to optimise the material flow and thus confirms hypothesis **H3**. The next step is to realise the data connection of the logistics back end system and the load carrier management system in real time. Despite a concept to first compress or aggregate old data and automatically delete data that are no longer needed in order to save storage should be developed. After that, the digital twin of the RFID-enabled material flow should be validated in the field and industrialised. Thereby, further systems could be connected to the digital twin and even more data analyses and dashboards could be created. In addition, a semantic layer could be implemented in the future to make the data of the digital twin of the RFID-enabled material flow available to other users and applications.

In summary, the following contributions for rollouts of RFID applications were made in this thesis:

- A new approach and algorithm for optimal antenna configuration of RFID gates were developed which do not require expert knowledge and are not based on the trial-and-error principle.
- A new test procedure to identify and reduce sources of interference was developed and verified by simulations which did not exist before in the analysed RFID test procedures.
- A new architecture for the digital twin of the RFID-enabled material flow was developed, implemented, and verified by simulating the material flow which did not exist before in the analysed literature.

Through the algorithms, test procedures and digital twin developed in this thesis, the author has shown a way to improve the detection rate of RFID installations, reduce sources of interference and optimise the RFID-enabled material flow. The author is convinced that the results presented in this work could bring closer a full deployment of RFID in the automotive logistic.

## 9 References

- Abugabah, A., Nizamuddin, N., & Abuqabbeh, A. (2020). A review of challenges and barriers implementing RFID technology in the Healthcare sector. *Procedia Computer Science*, 170, 1003–1010. <https://doi.org/10.1016/j.procs.2020.03.094>
- Aheleroff, S., Xu, X., Zhong, R. Y., & Lu, Y. (2021). Digital Twin as a Service (DTaaS) in Industry 4.0: An Architecture Reference Model. *Advanced Engineering Informatics*, 47, 101225. <https://doi.org/10.1016/j.aei.2020.101225>
- Al-Sehrawy, R., & Kumar, B. (2021). Digital Twins in Architecture, Engineering, Construction and Operations. A Brief Review and Analysis. In E. Toledo Santos & S. Scheer (Eds.), *Proceedings of the 18th International Conference on Computing in Civil and Building Engineering: ICCCBE 2020. Lecture Notes in Civil Engineering* (Vol. 98, pp. 924–939). Springer, Cham. [https://doi.org/10.1007/978-3-030-51295-8\\_64](https://doi.org/10.1007/978-3-030-51295-8_64)
- Amerland, A. (2015). *Die Potenziale von Big-Data-Analysen sind enorm*. <https://www.springerprofessional.de/marktforschung/die-potenziale-von-big-data-analysen-sind-enorm/6597426>
- Azizi, A. (2019). *Applications of Artificial Intelligence Techniques in Industry 4.0. SpringerBriefs in Applied Sciences and Technology*. Springer Singapore. <https://doi.org/10.1007/978-981-13-2640-0>
- Azizi, A., Vatankhah Barenji, A., & Hashmipour, M. (2016). Optimizing radio frequency identification network planning through ring probabilistic logic neurons. *Advances in Mechanical Engineering*, 8(8), 168781401666347. <https://doi.org/10.1177/1687814016663476>
- Bacanin, N., Tuba, M., & Strumberger, I. (2015). RFID Network Planning by ABC Algorithm Hybridized with Heuristic for Initial Number and Locations of Readers. In *2015 17th UKSim-AMSS International Conference on Modelling and Simulation (UKSim)* (pp. 39–44). IEEE. <https://doi.org/10.1109/UKSim.2015.83>
- Bartneck, N., Klaas, V., & Schönherr, H. (Eds.). (2008). *Prozesse optimieren mit RFID und Auto-ID: Grundlagen, Problemlösungen und Anwendungsbeispiele*. Publicis Corporate Publishing, Erlangen.
- Bertagnolli, F. (2022). Supply Chain. In *Lean Management: Introduction and In-Depth Study of Japanese Management Philosophy* (pp. 279–294). Springer, Wiesbaden. [https://doi.org/10.1007/978-3-658-36087-0\\_21](https://doi.org/10.1007/978-3-658-36087-0_21)
- Brunner, B., Peiffer, F., Finkenzeller, K., & Biebl, E. (2015). Impact of GSM Interference on passive UHF RFIDs. *European Conference on Smart Objects, Systems, and Technologies, June 16-17, 2015 in Aachen, Germany*, 259.
- Bundesnetzagentur. (n.d.). *RFID, das kontaktlose Informationssystem*. Retrieved July 13, 2021, from <https://docplayer.org/9114224-Rfid-das-kontaktlose-informationssystem.html>
- Chen, M., & Chen, S. (2016). *Rfid Technologies for Internet of Things. Wireless Networks*. Springer International Publishing. <https://doi.org/10.1007/978-3-319-47355-0>
- Ciftler, B. S., Kadri, A., & Guvenc, I. (2015). Experimental performance evaluation of passive UHF RFID systems under interference. In *2015 IEEE International Conference on RFID Technology and Applications (RFID-TA)* (pp. 81–86). IEEE. <https://doi.org/10.1109/RFID-TA.2015.7379802>
- Cobb, B. R. (2016). Inventory control for returnable transport items in a closed-loop supply chain. *Transportation Research Part E: Logistics and Transportation Review*, 86, 53–68. <https://doi.org/10.1016/j.tre.2015.12.010>



- Costa, F., do Sameiro Carvalho, M., Fernandes, J. M., Alves, A. C., & Silva, P. (2017). Improving visibility using RFID – the case of a company in the automotive sector. *Procedia Manufacturing, 13*, 1261–1268. <https://doi.org/10.1016/j.promfg.2017.09.048>
- Dhaduk, H. (2021). *Best Frontend Frameworks of 2021 for Web Development*. <https://www.simform.com/best-frontend-frameworks/#section9>
- Ebrahimi-Asl, S., Ghasr, M. T. A., & Zawodniok, M. J. (2017). A Solution to Low Read Rate Problem in RFID Scattering Networks. *IEEE Journal of Radio Frequency Identification, 1*(2), 176–184. <https://doi.org/10.1109/JRFID.2017.2768546>
- EHI Retail Institute. (2021). *EHI-Studie „Technologie-Trends im Handel 2021“*. <https://www.handelsdaten.de/deutschsprachiger-einzelhandel/einsatz-von-rfid-im-handel-2021>
- EPCglobal (2006a). *Dynamic Test: Conveyor Portal Test Methodology: For Applied Tag Performance Testing (Rev 1.1.4)*.
- EPCglobal (2006b). *Dynamic Test: Door Portal Test Methodology: For Applied Tag Performance Dynamic Testing (Rev 1.0.9)*.
- EPCglobal (2008). *Tag Performance Parameters and Test Methods (Version 1.1.3)*.
- EPCglobal (2009a). *Portal Field Strength Measurement Test Method (Draft): For Applied Tag Performance Testing (Rev 1.2)*.
- EPCglobal (2009b). *Portal Field Strength Measurement Test Method Evaluation and Minimum Performance Recommendation (Draft) (Version 1.0.0)*.
- Esposito, E., Romagnoli, G., Sandri, S., & Villani, L. (2015). Deploying RFID in the fashion and apparel sector: an "in the field" analysis to understand where the technology is going to. *XX Summer School "F. Turco", Industrial Mechanical Plants*. [http://summerschool-aidi.it/edition-2015/images/Naples2015/proceed/02\\_romagnoli\\_02.pdf](http://summerschool-aidi.it/edition-2015/images/Naples2015/proceed/02_romagnoli_02.pdf)
- ETSI (2020). EN 302 208 V3.3.1: Radio Frequency Identification Equipment operating in the band 865 MHz to 868 MHz with power levels up to 2 W and in the band 915 MHz to 921 MHz with power levels up to 4 W.
- Finkenzeller, K. (2015). *RFID-Handbuch: Grundlagen und praktische Anwendungen von Transpondern, kontaktlosen Chipkarten und NFC (7., aktualisierte und erweiterte Auflage)*. Carl Hanser Verlag GmbH Co KG.
- Fleisch, E., & Mattern, F. (Eds.). (2005). *Das Internet der Dinge: Ubiquitous Computing und RFID in der Praxis: Visionen, Technologien, Anwendungen, Handlungsanleitungen*. Springer Berlin Heidelberg.
- Franke, W., & Dangelmaier, W. (Eds.). (2006). *RFID-Leitfaden für die Logistik: Anwendungsgebiete, Einsatzmöglichkeiten, Integration, Praxisbeispiele*. Gabler Verlag.
- Goll, J. (2014). *Architektur- und Entwurfsmuster der Softwaretechnik*. Springer Fachmedien Wiesbaden. <https://doi.org/10.1007/978-3-658-05532-5>
- Graßl, M., Falter, L., Harth, A., Naumann, V., Zink, M., Fottner, J., Zeiler, J., Meißner, S., Romer, M., Schlittenbauer, S., Seitz, R., & Voigt, G. (2021). Netzwerk für intelligente, modulare Sonderladungsträger: Schlussbericht iSLT.NET.
- Greis, N. P., Nogueira, M. L., & Rohde, W. (2021). Digital Twin Framework for Machine Learning-Enabled Integrated Production and Logistics Processes. In A. Dolgui, A. Bernard, D. Lemoine, G. von Cieminski, & D. Romero (Eds.), *Advances in Production Management Systems: Artificial Intelligence for Sustainable and Resilient Production Systems* (Vol. 630, pp. 218–227). Springer, Cham. [https://doi.org/10.1007/978-3-030-85874-2\\_23](https://doi.org/10.1007/978-3-030-85874-2_23)
- Grieves, M. (2014). Digital Twin: Manufacturing Excellence through Virtual Factory Replication. <https://www.3ds.com/fileadmin/PRODUCTS-SERVICES/DELMIA/PDF/Whitepaper/DELMIA-APRISO-Digital-Twin-Whitepaper.pdf>
- Grieves, M., & Vickers, J. (2016). Origins of the Digital Twin Concept. Advance online publication. <https://doi.org/10.13140/RG.2.2.26367.61609>

- GS1 (2019). *EPC Tag Data Standard* (Release 1.13).
- GS1 (2022a). *Core Business Vocabulary (CBV) Standard* (Release 2.0).  
<https://ref.gs1.org/standards/cbv/>
- GS1 (2022b). *Overview of UHF frequency allocations (860 to 960 MHz) for RAIN RFID*.  
[https://www.gs1.org/docs/epc/uhf\\_regulations.pdf](https://www.gs1.org/docs/epc/uhf_regulations.pdf)
- Guerreiro, G., Figueiras, P., Costa, R., Marques, M., Graça, D., Garcia, G., & Jardim-Gonçalves, R. (2019). A Digital Twin for Intra-Logistics Process Planning for the Automotive Sector Supported by Big Data Analytics. In *ASME International Mechanical Engineering Congress and Exposition* (Volume 2B: Advanced Manufacturing). ASME.  
<https://doi.org/10.1115/IMECE2019-11362>
- Günther, W.A., Atz, T., Klaubert, C., & Salfer, M. (2011). *RFID-MachLog: Methodik für UHF-RFID-Machbarkeitsstudien. Forschungsbericht*. Lehrstuhl für Fördertechnik Materialfluss Logistik (fml), Technische Universität München.
- Günthner, W. A., & Lechner, J. (2015). *RFID-MobiVis - Mobile Lesefelderfassung und -visualisierung von UHF-RFID-Installationen: Forschungsbericht zu dem IGF-Vorhaben 17390 N/1 der Forschungsstelle Lehrstuhl für Fördertechnik Materialfluss Logistik, Technische Universität München*. Lehrstuhl für Fördertechnik Materialfluss Logistik (fml), Technische Universität München.
- Günthner, W. A., Meißner, S., Conze, M., & Fischer, R. (2010). *Stand und Entwicklung des RFID-Einsatzes in der Automobillogistik: Ergebnisse einer empirischen Studie*. Lehrstuhl für Fördertechnik Materialfluss Logistik (fml), Technische Universität München.
- Harris, R. (2019). *Write less code*. <https://svelte.dev/blog/write-less-code>
- Haße, H., Li, B., Weißenberg, N., Cirullies, J., & Otto, B. (2019). Digital twin for real-time data processing in logistics. In *Artificial Intelligence and Digital Transformation in Supply Chain Management. Proceedings of the Hamburg International Conference of Logistics (HICL)* (Vol. 27, pp. 3–28). Berlin: epubli. <https://doi.org/10.15480/882.2462>
- Hevner, A., & Chatterjee, S. (2010). *Design research in information systems: Theory and practice. Integrated series in information systems: Vol. 22*. Springer.
- Hevner, A., March, S. T., Park, J., & Ram, S. (2004). Design Science in Information Systems Research. *MIS Quarterly*, 28(1), 75–105. <https://doi.org/10.2307/25148625>
- Hur, S. M., Jeong, S., & Suh, S.-H. (2009). An experimental approach to RFID system performance prediction model. *International Journal of Computer Integrated Manufacturing*, 22(7), 686–697. <https://doi.org/10.1080/09511920903068775>
- Ident (2022). *ident Jahrbuch*. Ident Verlag & Service GmbH.  
[https://www.ident.de/sites/default/files/Heftarchiv/ident\\_2022/ident\\_2022\\_Jahrbuch\\_Web.pdf](https://www.ident.de/sites/default/files/Heftarchiv/ident_2022/ident_2022_Jahrbuch_Web.pdf)
- ISO (2021). *Automation systems and integration - Digital twin framework - Part 2: Reference architecture for manufacturing* (ISO 23247-2:2021(E)).
- ISO/IEC (2011a). *Information technology - Radio frequency identification device performance test methods: Test methods for system performance* (ISO/IEC 18046-1:2011).
- ISO/IEC (2011b). *Systems and software engineering - Systems and software Quality Requirements and Evaluation (SQuaRE) - System and software quality models* (ISO/IEC 25010:2011).
- ISO/IEC (2015). *Information technology - Radio frequency identification for item management: Parameters for air interface communications at 860 MHz to 960 MHz Type C* (ISO/IEC 18000-63:2015).
- ISO/IEC (2017). *Information technology - Radio frequency identification device conformance test methods: Test methods for air interface communications at 860 MHz to 960 MHz* (ISO/IEC 18047-6:2017).
- ISO/IEC (2020a). *Information technology - Radio frequency identification device performance test methods: Test methods for tag performance* (ISO/IEC 18046-3:2020).

- ISO/IEC (2020b). *ISO/IEC 18046-2:2020*: Test methods for interrogator performance.
- Jaballah, A., & Meddeb, A. (2019). A new variant of cuckoo search algorithm with self adaptive parameters to solve complex RFID network planning problem. *Wireless Networks*, 25(4), 1585–1604. <https://doi.org/10.1007/s11276-017-1616-9>
- Jamwal, A., Agrawal, R., Sharma, M., & Pratap, S. (2021). Industry 4.0: An Indian Perspective. In A. Dolgui, A. Bernard, D. Lemoine, G. von Cieminski, & D. Romero (Eds.), *Advances in Production Management Systems: Artificial Intelligence for Sustainable and Resilient Production Systems* (pp. 113–123). Springer, Cham.
- Kathrein Solutions GmbH. (2011). *Wide Range RFID UHF Antenna: WIRA 30 Circular Antenna Unit*. [https://www.kathrein-solutions.com/files/db\\_52010086\\_52010087.pdf](https://www.kathrein-solutions.com/files/db_52010086_52010087.pdf)
- Kathrein Solutions GmbH. (2017). *Configuration Manual Reader for Kathrein RFID UHF Readers - Version 3.00*.
- Kirch, M., Poenicke, O., & Richter, K. (2017). RFID in Logistics and Production – Applications, Research and Visions for Smart Logistics Zones. *Procedia Engineering*, 178, 526–533. <https://doi.org/10.1016/j.proeng.2017.01.101>
- Klein, D., Tran-Gia, P., & Hartmann, M. (2013). Big Data. *Informatik-Spektrum*, 36(3), 319–323. <https://doi.org/10.1007/s00287-013-0702-3>
- Kleist, R. A. (2004). *Rfid labeling: Smart labeling concepts & applications for the consumer packaged goods supply chain* (1. ed., August). Printronix.
- Knapp, H., & Romagnoli, G. (2021). RFID systems optimisation through the use of a new RFID network planning algorithm to support the design of receiving gates. *Journal of Intelligent Manufacturing*. Advance online publication. <https://doi.org/10.1007/s10845-021-01858-0>
- Knapp, H., Romagnoli, G., & Uckelmann, D. (2022). Architecture, application and implementation of a digital twin of the RFID-enabled material flow (DTRMF) in real-time for automotive intralogistics. *International Journal of RF Technologies*, vol. Pre-press, 1–32. <https://doi.org/10.3233/RFT-221513>
- Knapp, H., Romagnoli, G., & Uckelmann, D. (2023). A case study for a digital twin of the material flow for automated inventory of load carriers with RFID. *Accepted in 12TH International Conference on Industrial Technology and Management*.
- Knapp, H., & Uckelmann, D. (2022). Literature review on sources of interference and proposed solutions for RFID installations in complex production and logistics processes in the automotive industry. *International Journal of RF Technologies*, 12(2), 87–126. <https://doi.org/10.3233/RFT-210312>
- Korth, B., Schwede, C., & Zajac, M. (2018). Simulation-ready digital twin for realtime management of logistics systems. In *2018 IEEE international conference on big data (big data)* (pp. 4194–4201). <https://doi.org/10.1109/BigData.2018.8622160>
- Kreps, J. (2014). *Questioning the Lambda Architecture: The Lambda Architecture has its merits, but alternatives are worth exploring*. <https://www.oreilly.com/radar/questioning-the-lambda-architecture/>
- Lechner, J. K. (2020). *Messkonzept zur Analyse und Bewertung von passiven UHF-RFID-Installationen*. Doctoral dissertation, Lehrstuhl für Fördertechnik Materialfluss Logistik (fml), Technische Universität München.
- Li, J., & Tan, Y. (2020). A Comprehensive Review of the Fireworks Algorithm. *ACM Computing Surveys*, 52(6), 1–28. <https://doi.org/10.1145/3362788>
- Lietaert, P., Meyers, B., van Noten, J., Sips, J., & Gadeyne, K. (2021). Knowledge Graphs in Digital Twins for AI in Production. In A. Dolgui, A. Bernard, D. Lemoine, G. von Cieminski, & D. Romero (Eds.), *Advances in Production Management Systems: Artificial Intelligence for Sustainable and Resilient Production Systems* (pp. 249–257). Springer, Cham.

- LoRa Alliance (2015). White Paper: A technical overview of LoRa and LoRaWAN.  
<https://www.tuv.com/content-media-files/master-content/services/products/1555-tuv-rheinland-lora-alliance-certification/tuv-rheinland-lora-alliance-certification-overview-lora-and-lorawan-en.pdf>
- Luh, Y.-P., & Liu, Y.-C. (2011). Reading Rate Improvement for UHF RFID Systems with Massive Tags by the Q Parameter. *Wireless Personal Communications*, 59(1), 147–157.  
<https://doi.org/10.1007/s11277-010-0198-y>
- Marz, N. (2011). *How to beat the CAP theorem*. <http://nathanmarz.com/blog/how-to-beat-the-cap-theorem.html>
- Mercedes-Benz AG. (2019). *Readiness-Check RFID@MO SC: Internal document*.
- Mercedes-Benz Group AG. (n.d.). *eXtollo Our Big Data Platform*. Retrieved June 7, 2022, from <https://group.mercedes-benz.com/careers/about-us/artificial-intelligence/community-and-tools/extollo.html>
- Merkle, L., Segura, A. S., Grummel, J. T., & Lienkamp, M. (2019). Architecture of a Digital Twin for Enabling Digital Services for Battery Systems. In *2019 IEEE International Conference on Industrial Cyber Physical Systems (ICPS)* (pp. 155–160). IEEE.  
<https://doi.org/10.1109/ICPHYS.2019.8780347>
- Moretti, E. d. A., Anholon, R., Rampasso, I. S., Silva, D., Santa-Eulalia, L. A., & Ignácio, P. S. d. A. (2019). Main difficulties during RFID implementation: an exploratory factor analysis approach. *Technology Analysis & Strategic Management*, 31(8), 943–956.  
<https://doi.org/10.1080/09537325.2019.1575351>
- Negri, E., Fumagalli, L., & Macchi, M. (2017). A Review of the Roles of Digital Twin in CPS-based Production Systems. *Procedia Manufacturing*, 11, 939–948.  
<https://doi.org/10.1016/j.promfg.2017.07.198>
- Pan, Y. H., Qu, T., Wu, N. Q., Khalgui, M., & Huang, G. Q. (2021). Digital Twin Based Real-time Production Logistics Synchronization System in a Multi-level Computing Architecture. *Journal of Manufacturing Systems*, 58, 246–260. <https://doi.org/10.1016/j.jmsy.2020.10.015>
- Redelinghuys, A., Basson, A., & Kruger, K. (2019). A Six-Layer Digital Twin Architecture for a Manufacturing Cell. In T. Borangiu, D. Trentesaux, A. Thomas, & S. Cavalieri (Eds.), *Service Orientation in Holonic and Multi-Agent Manufacturing* (Vol. 803, pp. 412–423). Springer International Publishing. [https://doi.org/10.1007/978-3-030-03003-2\\_32](https://doi.org/10.1007/978-3-030-03003-2_32)
- Richter, M. (2013). *Nutzenoptimierter RFID-Einsatz in der Logistik: Eine Handlungsempfehlung zur Lokalisierung und Bewertung der Nutzenpotenziale von RFID-Anwendungen*. Schriftenreihe Logistik der Technischen Universität Berlin: Vol. 23. Universitätsverlag der TU Berlin.
- riskmethods, & BME (2018). Supply Chain Risk Management: Herausforderungen und Status Quo 2020: Ergebnisse einer gemeinsamen Umfrage von riskmethods und dem Bundesverband für Materialwirtschaft, Einkauf und Logistik.  
<http://assets.bme.de/public/uploads/d104a7387f471e7bdcf2e761598ee5a3215c114e356f4f7d8cf33ed6954e>
- Rosen, R., Wichert, G. von, Lo, G., & Bettenhausen, K. D. (2015). About The Importance of Autonomy and Digital Twins for the Future of Manufacturing. *IFAC-PapersOnLine*, 48(3), 567–572. <https://doi.org/10.1016/j.ifacol.2015.06.141>
- Russell, H. (2018). *RSSI's Role in RFID*. <https://www.atlasrfidstore.com/rfid-insider/rssi-role-rfid>
- Sachan, S., Jangra, H., & Kumar, V. (2021). *RFID Market Outlook - 2030*.  
<https://www.alliedmarketresearch.com/rfid-market-A14522>
- Salayong, K., Phaebua, K., Lertwiriayaprapa, T., Boonpoonga, A., Chaiyasang, L., & Kumjinda, A. (2019). Linen Laundry Management System in Hospital by Using UHF-RFID. In *Research, Invention, and Innovation Congress (RI2C)* (pp. 1–4). IEEE.  
<https://doi.org/10.1109/RI2C48728.2019.8999948>

- Schmidt, M., Thoroe, L., Doerrheide, D., & Schumann, M. (2011). Managing the complexity of large-scale RFID rollout projects in logistics. *ECIS 2011 Proceedings*, 168. <https://aisel.aisnet.org/ecis2011/168>
- Scholz, P. (2005). *Softwareentwicklung eingebetteter Systeme: Grundlagen, Modellierung, Qualitätssicherung*. Springer Berlin Heidelberg.
- Scholz-Reiter, B., Lappe, D., & Werthmann, D. (2011). Sonderladungsträgermanagement in der Automobilindustrie. *Industrie Management*, 27, 77–81.
- Shafto, M., Conroy, M., Doyle, R., Glaessgen, E., Kemp, C., LeMoigne, J., & Wang, L. (2010). *DRAFT Modeling, Simulation, Information Technology & Processing Roadmap*. Technology Area 11.
- Shah, L., Joshi, S., Dharmalingam, M., Shamanna, P., Vadavi, A., Mohammed, J., Mohamed, M., Poon, T., Keshavamurthy, A., Thajudeen, M., Bhonsley, S., & Willis, B. (2021). Abstract #1088834: Health Economic Analysis of Digital Twin Technology for Remission of Diabetes - Initial Insights From the Prospective Randomised Controlled Clinical Trial. *Endocrine Practice*, 27(12), S7. <https://doi.org/10.1016/j.eprac.2021.08.025>
- Souza, V., Cruz, R., Silva, W., Lins, S., & Lucena, V. (2019). A Digital Twin Architecture Based on the Industrial Internet of Things Technologies. In *2019 IEEE International Conference on Consumer Electronics (ICCE)* (pp. 1–2). IEEE. <https://doi.org/10.1109/ICCE.2019.8662081>
- Stahlknecht, P., & Hasenkamp, U. (1999). *Einführung in die Wirtschaftsinformatik* (Neunte, vollständig überarbeitete Auflage). *Springer-Lehrbuch*. Springer Berlin Heidelberg.
- Steindl, G., Stagl, M., Kasper, L., Kastner, W., & Hofmann, R. (2020). Generic Digital Twin Architecture for Industrial Energy Systems. *Applied Sciences*, 10(24), 8903. <https://doi.org/10.3390/app10248903>
- Strumberger, I., Tuba, E., Bacanin, N., Beko, M., & Tuba, M. (2018a). Bare Bones Fireworks Algorithm for the RFID Network Planning Problem. In *2018 IEEE Congress on Evolutionary Computation (CEC)* (pp. 1–8). IEEE. <https://doi.org/10.1109/CEC.2018.8477990>
- Strumberger, I., Tuba, E., Bacanin, N., Beko, M., & Tuba, M. (2018b). Modified Monarch Butterfly Optimization Algorithm for RFID Network Planning. In *Proceedings of 2018 6th International Conference on Multimedia Computing and Systems (ICMCS)* (pp. 1–6). IEEE. <https://doi.org/10.1109/ICMCS.2018.8525930>
- Sydow, A. (2017). *Dynamische Behälterlogistik: Konzeption eines IT-gestützten Management- und Entscheidungsunterstützungssystems für automobiler Mehrwegbehälterkreisläufe*. Doctoral dissertation, Shaker Verlag GmbH.
- Talkhestani, B. A., Jung, T., Lindemann, B., Sahlab, N., Jazdi, N., Schloegl, W., & Weyrich, M. (2019). An architecture of an Intelligent Digital Twin in a Cyber-Physical Production System. *At - Automatisierungstechnik*, 67(9), 762–782. <https://doi.org/10.1515/auto-2019-0039>
- Tamm, G., & Tribowski, C. (2010). *RFID. Informatik im Fokus*. Springer Berlin, Heidelberg.
- Tao, F., Zhang, H., Liu, A., & Nee, A. Y. C. (2019). Digital Twin in Industry: State-of-the-Art. *IEEE Transactions on Industrial Informatics*, 15(4), 2405–2415. <https://doi.org/10.1109/TII.2018.2873186>
- Toth, S. (2015). *Vorgehensmuster für Softwarearchitektur: Kombinierbare Praktiken in Zeiten von Agile und Lean* (2., aktualisierte und erw. Aufl.). Carl Hanser Verlag GmbH & Co. KG.
- Tuba, M., Bacanin, N., & Beko, M. (2015). Fireworks algorithm for RFID network planning problem. In *2015 25th International Conference Radioelektronika (RADIOELEKTRONIKA)* (pp. 440–444). IEEE. <https://doi.org/10.1109/RADIOELEK.2015.7129049>
- Tuba, V., Alihodzic, A., & Tuba, M. (2017). Multi-objective RFID network planning with probabilistic coverage model by guided fireworks algorithm. In *2017 10th International Symposium on Advanced Topics in Electrical Engineering (ATEE)* (pp. 882–887). IEEE. <https://doi.org/10.1109/ATEE.2017.7905125>

- Tuchen, S., LaFrance-Linden, D., Hanley, B., Lu, J., McGovern, S., & Litvack-Winkler, M. (2022). Urban Air Mobility (UAM) and Total Mobility Innovation Framework and Analysis Case Study: Boston Area Digital Twin and Economic Analysis. In *2022 IEEE/AIAA 41st Digital Avionics Systems Conference (DASC)* (pp. 1–14). IEEE.  
<https://doi.org/10.1109/DASC55683.2022.9925865>
- Uckelmann, D. (2012). *Quantifying the Value of RFID and the EPCglobal Architecture Framework in Logistics*. Springer Berlin Heidelberg.
- Uckelmann, D., Gimber, N., & Krug, T. (2018). Logistikunternehmen sollten auf Big Data setzen. *Big Data Insider*. <https://www.bigdata-insider.de/logistikunternehmen-sollten-auf-big-data-setzen-a-729489/>
- Uckelmann, D., Harrison, M., & Michahelles, F. (2011). An Architectural Approach towards the Future Internet of Things. In D. Uckelmann, M. Harrison, & F. Michahelles (Eds.), *Architecting the Internet of Things* (pp. 1–24). Berlin: Springer.
- van Hoek, R. (2019). Exploring blockchain implementation in the supply chain: Learning from pioneers and RFID research. *International Journal of Operations & Production Management*, 39(6/7/8), 829–859. <https://doi.org/10.1108/IJOPM-01-2019-0022>
- VDA (2015a). *VDA 4500: Kleinladungsträger (KLT)-System Teil 1*. Verband der Automobilindustrie.
- VDA (2015b). *VDA 5500: Grundlagen zum RFID-Einsatz in der Automobilindustrie*. Verband der Automobilindustrie.
- VDA (2016). *VDA 5501: RFID im Behältermanagement der Supply Chain*. Verband der Automobilindustrie.
- VDA (2022). *VDA 4994 - Global Transport Label*. Verband der Automobilindustrie.
- VDI (2006). *Anforderungen an Transpondersysteme zum Einsatz in der Supply Chain: Allgemeiner Teil (VDI 4472 Blatt 1 / Part 1)*. Düsseldorf.
- VDI/AIM (2008). *Anforderungen an Transpondersysteme zum Einsatz in der Supply Chain: Testverfahren zur Überprüfung der Leistungsfähigkeit von Transpondersystemen (RFID) (VDI/AIM 4472 Blatt 10 / Part 10)*. Düsseldorf.
- Wagner, J. (2009). *Technische Konzepte zur RFID-gestützten Bauzustandsdokumentation in der Automobilindustrie*. Doctoral dissertation, Lehrstuhl für Fördertechnik Materialfluss Logistik, Technische Universität München.
- Wang, J. (2017). *Indoor Localization using Augmented UHF RFID System for the Internet-of-Things*. Doctoral dissertation, University of Ottawa.
- Wang, X., Yang, L. T., Li, H., Lin, M., Han, J., & Apduhan, B. O. (2019). NQA: A Nested Anti-collision Algorithm for RFID Systems. *ACM Transactions on Embedded Computing Systems*, 18(4), 1–21. <https://doi.org/10.1145/3330139>
- Weicker, N., Szabo, G., Weicker, K., & Widmayer, P. (2003). Evolutionary multiobjective optimization for base station transmitter placement with frequency assignment. *IEEE Transactions on Evolutionary Computation*, 7(2), 189–203.  
<https://doi.org/10.1109/TEVC.2003.810760>
- Whitney, A., Fessler, J., Parker, J., & Jacobs, N. (2014). Received signal strength indication signature for passive UHF tags. In *2014 IEEE/ASME International Conference on Advanced Intelligent Mechatronics* (pp. 1183–1187). IEEE. <https://doi.org/10.1109/AIM.2014.6878242>
- Windmann, S., Niggemann, O., Ruwe, H., & Becker, F. (2017). A novel self-configuration method for RFID systems in industrial production environments. In *2017 22nd IEEE International Conference on Emerging Technologies and Factory Automation (ETFA)* (pp. 1–5). IEEE.  
<https://doi.org/10.1109/ETFA.2017.8247774>
- Yuan, C., Hanning, C., Shen, J., Lin, N., Su, W., Liu, F., & Liang, X. (2019). Indicator-based multi-objective adaptive bacterial foraging algorithm for RFID network planning. *Cluster Computing*, 22(S5), 12649–12657. <https://doi.org/10.1007/s10586-018-1715-0>

- Zeiler, J. R. (2022). *Architektur für ein unternehmensübergreifendes Service-System mit intelligenten, modularen Sonderladungsträgern*. Doctoral dissertation, Lehrstuhl für Fördertechnik Materialfluss Logistik (fml), Technische Universität München, München.
- Zhang, T., & Liu, J. (2017). An efficient and fast kinematics-based algorithm for RFID network planning. *Computer Networks*, *121*, 13–24. <https://doi.org/10.1016/j.comnet.2017.04.035>
- Zhao, C., Wu, C., Chai, J., Wang, X., Yang, X., Lee, J.-M., & Kim, M. J. (2017). Decomposition-based multi-objective firefly algorithm for RFID network planning with uncertainty. *Applied Soft Computing*, *55*, 549–564. <https://doi.org/10.1016/j.asoc.2017.02.009>
- Zhu, X., Mukhopadhyay, S. K., & Kurata, H. (2012). A review of RFID technology and its managerial applications in different industries. *Journal of Engineering and Technology Management*, *29*(1), 152–167. <https://doi.org/10.1016/j.jengtecman.2011.09.011>

## 10 Appendix

### 10.1 User interface of the algorithm for the optimal alignment of the antennas of the RFID gate

The screenshot shows a web interface for creating a golden sample. At the top, there are navigation tabs: 'Description', 'Create Golden Sample' (which is active and underlined), 'Create Test', 'Upload Data', and 'Show results'. Below the tabs, the form consists of several input fields and a file upload button:

- Golden Sample Name:** A text input field containing 'Golden sample for verification'.
- Golden Sample Description:** A text area containing 'The golden sample consists of 6 containers with load carriers made of plastic and 104 single-use RFID tags.' with a small edit icon on the right.
- Load Carriers Number (T5-Number):** A text input field containing '6429'.
- Load Carriers Material:** A text input field containing 'plastic'.
- Golden Sample Height:** A text input field containing '200'.
- Golden Sample Width:** A text input field containing '100'.
- Upload the tag positions for this golden sample:** A file upload button labeled 'Datei auswählen' with the text 'Keine Datei ausgewählt' next to it.
- Save Golden Sample:** A prominent red button at the bottom center with a mouse cursor pointing to it.

Figure 70 User interface to create a golden sample



Description   Create Golden Sample   Create Test   Upload Data   Show results

Test name:

Test Description:

Location:

Date:

Golden Sample:

Driving direction:

Driving route:

Figure 71 User interface to create a test – part 1

**Antenna parameters**

antenna	height [cm]	vertical angle [°]	horizontal angle [°]	power [dBm]
1	<input type="text" value="115"/>	<input type="text" value="0"/>	<input type="text" value="0"/>	<input type="text" value="26"/>
2	<input type="text" value="210"/>	<input type="text" value="0"/>	<input type="text" value="0"/>	<input type="text" value="26"/>
3	<input type="text" value="115"/>	<input type="text" value="0"/>	<input type="text" value="0"/>	<input type="text" value="26"/>
4	<input type="text" value="210"/>	<input type="text" value="0"/>	<input type="text" value="0"/>	<input type="text" value="26"/>

Minimal possible antenna height:

Maximal possible antenna height:

Maximal possible power:

Figure 72 User interface to create a test – part 2

**Reader Parameter**

Reader Modulname:

Reader Modell:

Communication Profile:

Initial Q-value:

Sel:

Session:

Target:

Cable Attenuation:

Antenna Gain:

Figure 73 User interface to create a test – part 3

Description   Create Golden Sample   Create Test   [Upload Data](#)

Verification of algorithm (id: 93)

Iteration: 1

Upload the test data files for this iteration:

Keine Datei ausgewählt

Figure 74 User interface to upload data with RFID readings

[Description](#)   [Create Golden Sample](#)   [Create Test](#)   [Upload Data](#)   [Show results](#)

### Optimization Algorithm Results

Verification of algorithm (id: 93) Load test results

**Test parameters:**

Test Name: Verification of algorithm

Description: In this test the algorithm for optimal alignment of the antennas is tested.

Date: 2021-07-01

Location: Curt Georgi, Böblingen

Golden Sample: 11

Driving Direction: backward

Driving Route: center straight

Minimal Antenna Height: 60

Maximal Antenna Height: 300

**Reader parameters:**

Reader Modulname: M050RF36G000005

Reader Modell: RRU 4500 ETSI

Communication Profile: 8: Tx80kbps/Rx:320kbps/FMO

Initial Q-value: 3

Sel: All

Session: 1

Target: A

Cable Attenuation: 2 dB

Antenna Gain: 11 dBiC

Max Power: 30 dBm

Figure 75 User interface to show the test results – part 1

Algorithm finished! Best iteration: 8

**Best Antenna Parameters:**

antenna	height	vertical angle	horizontal angle	power
1	115	0 °	-20 °	30 dBm
2	210	0 °	-20 °	30 dBm
3	115	0 °	20 °	30 dBm
4	210	0 °	20 °	30 dBm

Figure 76 User interface to show the test results – part 2

Detection rates and RSSI values		
iteration	total detection rate	rss
8	98.64 %	-81.2
7	98.46 %	-81.12
6	96.61 %	-80.83
5	95 %	-80.44
4	86.97 %	-80.47
3	89.51 %	-80.09
2	82.78 %	-79.6
1	83.27 %	-79.78

Figure 77 User interface to show the test results – part 3

Details					
select the iteration					
7	Load test result details				
8					
7	Antenna parameters:				
6					
5					
4	antenna	height	vertical angle	horizontal angle	power
3					
2		115 cm	0 °	-20 °	30 dBm
1					
	2	210 cm	0 °	-20 °	30 dBm
	3	115 cm	0 °	20 °	30 dBm
	4	210 cm	0 °	20 °	30 dBm

Figure 78 User interface to show the test results – part 4

<p><b>Detection rates</b></p> <table border="1"> <tr><td>detection rate</td><td>98.64 %</td></tr> <tr><td>detection rate parallel tags</td><td>99.78 %</td></tr> <tr><td>detection rate orthogonal tags</td><td>97.22 %</td></tr> <tr><td>detection rate bottom</td><td>99.44 %</td></tr> <tr><td>detection rate middle</td><td>96.48 %</td></tr> <tr><td>detection rate top</td><td>100 %</td></tr> </table>	detection rate	98.64 %	detection rate parallel tags	99.78 %	detection rate orthogonal tags	97.22 %	detection rate bottom	99.44 %	detection rate middle	96.48 %	detection rate top	100 %	<p><b>Number of reads</b></p> <table border="1"> <tr><td>number of reads</td><td>9.39</td></tr> <tr><td>number of reads parallel tags</td><td>9.74</td></tr> <tr><td>number of reads orthogonal tags</td><td>8.96</td></tr> <tr><td>number of reads bottom</td><td>9.13</td></tr> <tr><td>number of reads middle</td><td>9.41</td></tr> <tr><td>number of reads top</td><td>9.63</td></tr> </table>	number of reads	9.39	number of reads parallel tags	9.74	number of reads orthogonal tags	8.96	number of reads bottom	9.13	number of reads middle	9.41	number of reads top	9.63																				
detection rate	98.64 %																																												
detection rate parallel tags	99.78 %																																												
detection rate orthogonal tags	97.22 %																																												
detection rate bottom	99.44 %																																												
detection rate middle	96.48 %																																												
detection rate top	100 %																																												
number of reads	9.39																																												
number of reads parallel tags	9.74																																												
number of reads orthogonal tags	8.96																																												
number of reads bottom	9.13																																												
number of reads middle	9.41																																												
number of reads top	9.63																																												
<p><b>RSSI values</b></p> <table border="1"> <tr><td>RSSI</td><td>-81.2</td></tr> <tr><td>RSSI parallel tags</td><td>-80.64</td></tr> <tr><td>RSSI orthogonal tags</td><td>-81.92</td></tr> <tr><td>RSSI bottom</td><td>-81.54</td></tr> <tr><td>RSSI middle</td><td>-80.94</td></tr> <tr><td>RSSI top</td><td>-81.1</td></tr> </table>	RSSI	-81.2	RSSI parallel tags	-80.64	RSSI orthogonal tags	-81.92	RSSI bottom	-81.54	RSSI middle	-80.94	RSSI top	-81.1	<p><b>Detection rates per passage</b></p> <table border="1"> <thead> <tr> <th>passage</th> <th>detection rate</th> <th>number of reads</th> <th>rss</th> </tr> </thead> <tbody> <tr><td>1</td><td>99.07</td><td>10.89</td><td>-81.15</td></tr> <tr><td>2</td><td>98.15</td><td>8.64</td><td>-81.22</td></tr> <tr><td>3</td><td>99.07</td><td>9.46</td><td>-81.17</td></tr> <tr><td>4</td><td>98.15</td><td>9.94</td><td>-81.49</td></tr> <tr><td>5</td><td>99.07</td><td>10.02</td><td>-81.28</td></tr> <tr><td>6</td><td>99.07</td><td>9.55</td><td>-81.27</td></tr> <tr><td>7</td><td>97.22</td><td>9.21</td><td>-81.1</td></tr> </tbody> </table>	passage	detection rate	number of reads	rss	1	99.07	10.89	-81.15	2	98.15	8.64	-81.22	3	99.07	9.46	-81.17	4	98.15	9.94	-81.49	5	99.07	10.02	-81.28	6	99.07	9.55	-81.27	7	97.22	9.21	-81.1
RSSI	-81.2																																												
RSSI parallel tags	-80.64																																												
RSSI orthogonal tags	-81.92																																												
RSSI bottom	-81.54																																												
RSSI middle	-80.94																																												
RSSI top	-81.1																																												
passage	detection rate	number of reads	rss																																										
1	99.07	10.89	-81.15																																										
2	98.15	8.64	-81.22																																										
3	99.07	9.46	-81.17																																										
4	98.15	9.94	-81.49																																										
5	99.07	10.02	-81.28																																										
6	99.07	9.55	-81.27																																										
7	97.22	9.21	-81.1																																										

Figure 79 User interface to show the test results – part 5

Tag details			
tag id	detection rate	rss	num reads
1	100	-80.18	3.93
2	100	-80.52	8.67
3	100	-80.59	3.13
4	100	-83.47	5.07
5	100	-80.85	16
6	100	-81.54	10.6
7	100	-82.88	4.13
8	100	-80.78	11.87
9	100	-82.12	5
10	87	-82.61	1.8
11	100	-80.38	11

Figure 80 User interface to show the test results – part 6

## 10.2 Entity relationship diagram of the tables from the logistics back end system

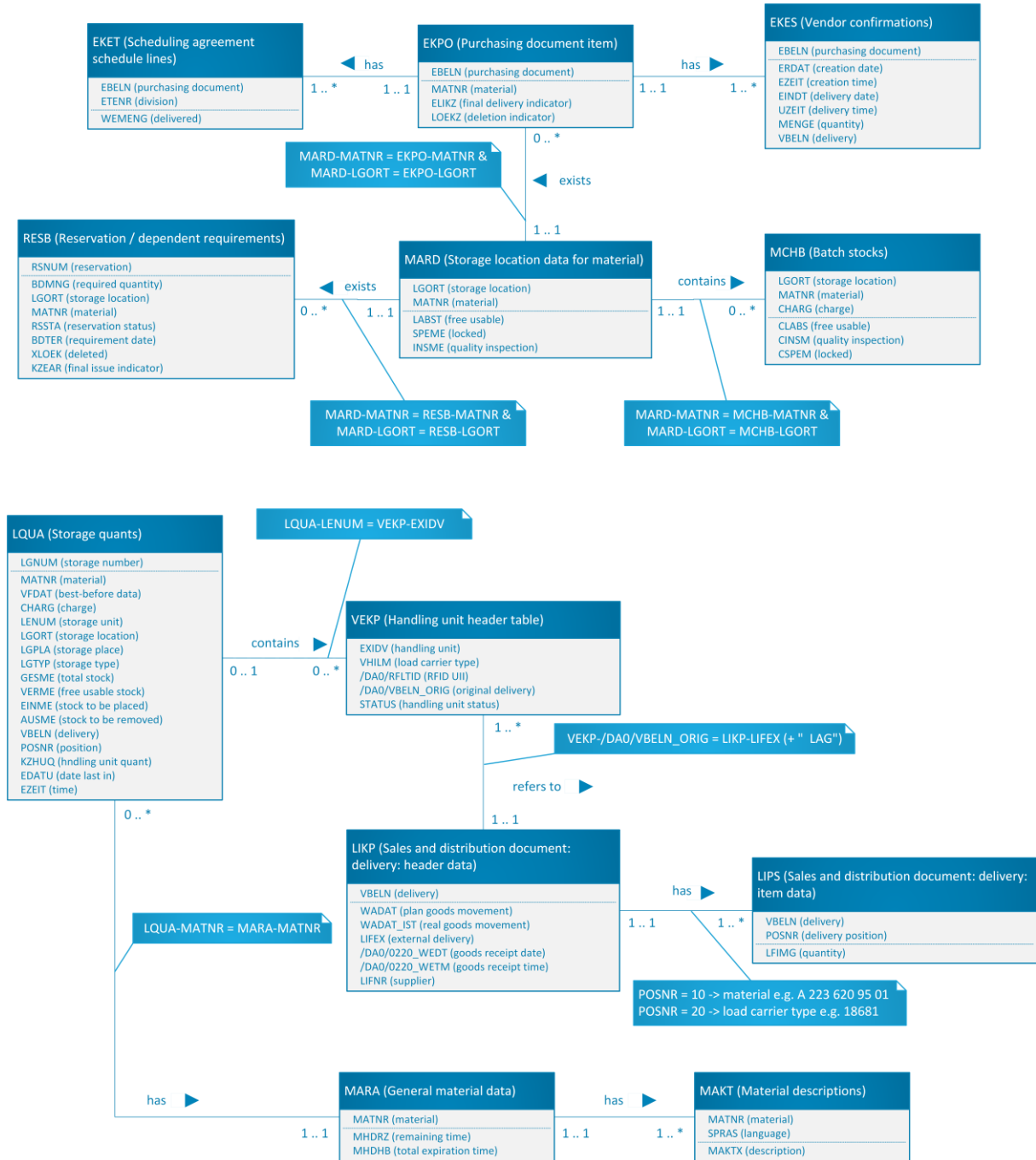


Figure 81 Entity relationship diagram of the logistics back end system – part 1

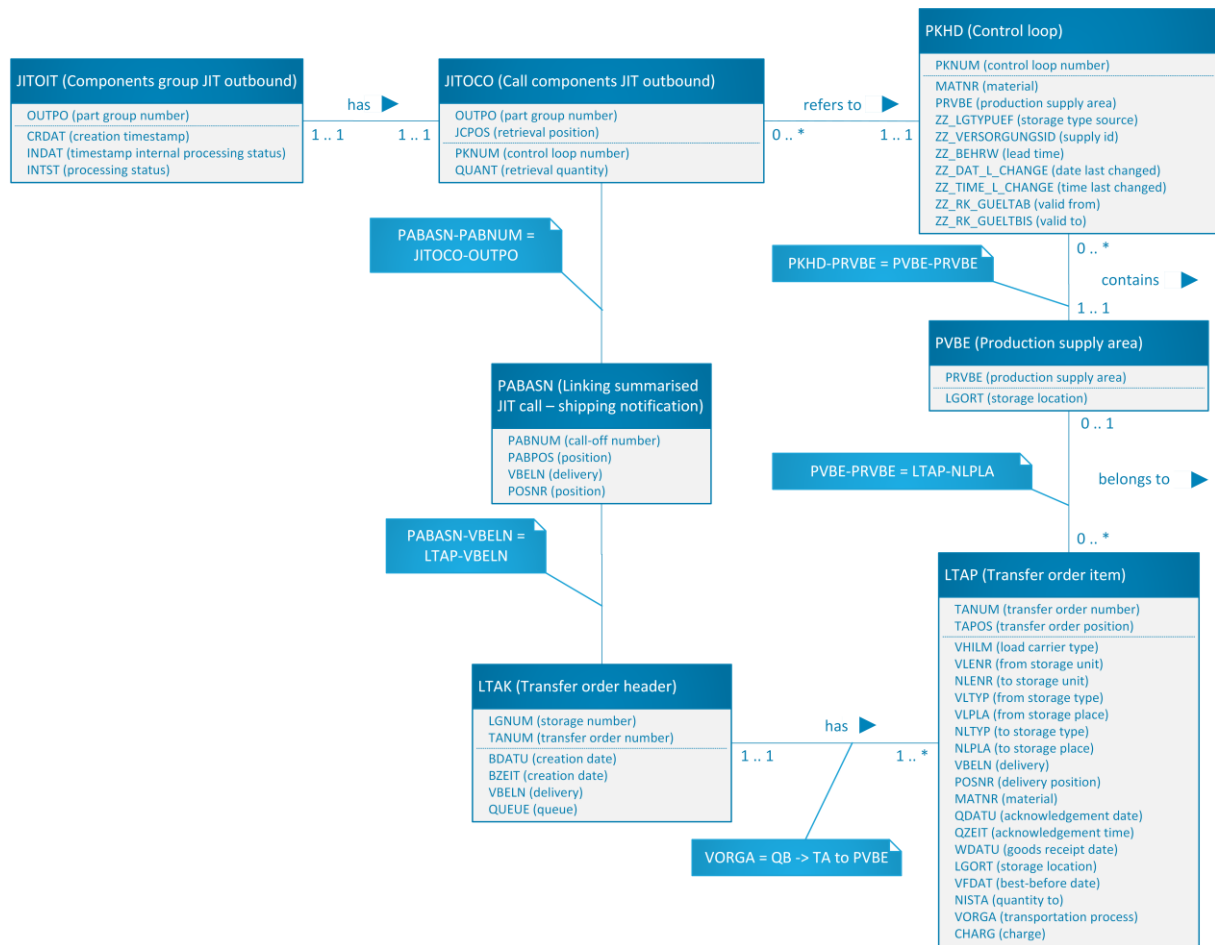


Figure 82 Entity relationship diagram of the logistics back end system – part 2